



T.R.
EGE UNIVERSITY
Graduate School of Applied and Natural Science



**THERMODYNAMIC AND EXERGO-ECONOMIC
ANALYSIS OF A SOLAR-BIOMASS HYBRID POWER
PLANT FOR MULTI-ENERGY GENERATION**

PhD Thesis

Alain Christian BIBOUM BIBOUM

Solar Energy

Izmir

2019

T.R.
EGE UNIVERSITY
Graduate School of Applied and Natural Science

**THERMODYNAMIC AND EXERGO-ECONOMIC
ANALYSIS OF A SOLAR-BIOMASS HYBRID POWER
PLANT FOR MULTI-ENERGY GENERATION**



Alain Christian BIBOUM BIBOUM

Supervisor: Asst. Prof. Dr. Ahmet YILANCI

Solar Energy Branch
Energy Program

Izmir
2019

Alain Christian BIBOUM BIBOUM tarafından Doktora Tezi olarak sunulan “Çoklu Enerji Üretimi için Bir Güneş-Biyokütle Hibrid Güç Santralının Termodinamik ve Eksergo-Ekonomik Analizi (Thermodynamic and Exergo-Economic Analysis of a Solar-Biomass Hybrid Power Plant for Multi-Energy Generation)” başlıklı bu çalışma EÜ Lisansüstü Eğitim ve Öğretim Yönetmeliği ile EÜ Fen Bilimleri Enstitüsü Eğitim ve Öğretim Yönergesi'nin ilgili hükümleri uyarınca tarafımızdan değerlendirilerek savunmaya değer bulunmuş ve 19.08.2019 tarihinde yapılan tez savunma sınavında aday oybirliği/oyçokluğu ile başarılı bulunmuştur.

Jüri Üyeleri:

Jüri Başkanı : Dr. Öğr. Üyesi Ahmet YILANCI

Raportör Üye : Doç. Dr. Orhan EKREN

Üye : Dr. Öğr. Üyesi Öner ATALAY

Üye : Prof. Dr. Mustafa GÜNEŞ

Üye : Doç. Dr. Alpaslan TURGUT

İmza

.....

.....

.....

.....

.....

EGE ÜNİVERSİTESİ FEN BİLİMLERİ ENSTİTÜSÜ

ETİK KURALLARA UYGUNLUK BEYANI

EÜ Lisansüstü Eğitim ve Öğretim Yönetmeliğinin ilgili hükümleri uyarınca Doktora Lisans Tezi olarak sunduğum “Çoklu Enerji Üretimi için Bir Güneş-Biyokütle Hibrid Güç Santralinin Termodinamik ve Eksergo-Ekonomik Analizi” başlıklı bu tezin kendi çalışmam olduğunu, sunduğum tüm sonuç, doküman, bilgi ve belgeleri bizzat ve bu tez çalışması kapsamında elde ettiğimi, bu tez çalışmasıyla elde edilmeyen bütün bilgi ve yorumlara atıf yaptığımı ve bunları kaynaklar listesinde usulüne uygun olarak verdiğimi, tez çalışması ve yazımı sırasında patent ve telif haklarını ihlal edici bir davranışımın olmadığını, bu tezin herhangi bir bölümünü bu üniversite veya diğer bir üniversitede başka bir tez çalışması içinde sunmadığımı, bu tezin planlanmasından yazımına kadar bütün safhalarda bilimsel etik kurallarına uygun olarak davrandığımı ve aksinin ortaya çıkması durumunda her türlü yasal sonucu kabul edeceğimi beyan ederim.

19 / 08 / 2019

Alain Christian BIBOUM BIBOUM

ÖZET**ÇOKLU ENERJİ ÜRETİMİ İÇİN BİR GÜNEŞ-BİYOKÜTLE
HİBRİD GÜÇ SANTRALİNİN TERMODİNAMİK VE EKSERGO-
EKONOMİK ANALİZİ**

BIBOUM BIBOUM, Alain Christian

Doktora Tezi, Güneş Enerjisi Anabilim Dalı
Tez Danışmanı: Dr. Öğr. Üyesi Ahmet YILANCI

Ağustos 2019, 343 sayfa

Orta Afrika'nın batı bölgesinde yer alan Kamerun, biyokütle kaynakları ve güneş enerjisi potansiyeli bakımından iyi bir coğrafi konumdadır. Ancak, Kamerun'un halen ticari enerjiye erişimi olmayan bazı bölgeleri, özellikle ülkenin kuzey kesiminde, bulunmaktadır. Biyokütle ve güneş enerjisi kaynaklarını birlikte kullanmak, kesintisiz enerji temini sağlamak için en uygun seçeneklerden biri olarak değerlendirilebilir. Kamerun'un kuzey kesimi için bu kaynakların potansiyeli enerji üretimi bakımından yeterli durumdadır. Ayrıca, enerji kaynaklarının hibrid kullanımı güç sistemlerinin dönüşüm verim arttıran umut verici bir alternatif, enerji talebinin düşük maliyetle karşılanmasını sağlayabilen cazip bir özelliktir.

Bu çalışmada, üç farklı Yoğunlaştırılmalı Güneş Enerjisi (CSP) teknolojisinin, Biyokütle yakma (BF) teknolojiyle birleşimi olan güneş biyokütle hibrid enerji sistemleri incelenmiştir. Güneş enerjisinin dönüşümünde, Parabolik Oluklu Kollektör (PTC), Doğrusal Fresnel Yansıtıcı (LFR) ve Güneş Kulesi (ST), CSP teknolojileri olarak seçilmiştir. 5 MWe kurulu güce sahip her bir hibrid sistem için dört alt sistem, güneş ve biyokütle sahası, güç bloğu, ısı geri kazanımlı buhar üretimi (HRSG) ve absorpsiyonlu soğutma ve kurutma sistemlerini içeren çoklu üretim enerji sistemi tasarlanmış ve analiz edilmiştir. Her sistem ve bileşenleri için enerji, ekserji, ve eksergoekonomik yönlerden kapsamlı

ekonomik ve termodinamik analizler, maliyetin en aza indirilmesi ve performansın artırılması amacıyla yapılmıştır.

PTC, ST ve LFR'ye dayalı hibrid enerji sistemlerinin ihtiyaç duyduğu ilk yatırım maliyetleri sırasıyla 38.47 Milyon ABD Doları, 51.47 Milyon ABD Doları ve 25.23 milyon ABD Doları olarak elde edilmiştir. Hibrid enerji sistemlerinin tekno-ekonomik değerlendirmelerinden, LFR-BF için 76.4 ile 143.4 USD/MWh arasında değişen seviyelendirilmiş elektrik maliyeti değerlerinin en düşük olduğu bulunmuştur. Geri ödeme süresine göre, LFR-BF, 8.4 yıl ile en kısa bir yatırım dönüş süresine sahiptir, ardından 10.62 yıl ile PTC-BF gelmektedir; ST-BF ise 14.71 yıl ile en yüksek geri ödeme süresine sahip olmaktadır. Ayrıca, PTC-BF, ST-BF ve LFR-BF için sırasıyla %13.79, %12.64 ve %16.49 olan iç karlılık oranlarına göre LFR-BF bu üç hibrid enerji sistemi arasında en karlı yatırım gibi görünmektedir.

Üç hibrid enerji sistemin ileri ekserji analizinden, tek başına güneş sahasındaki ekserji yıkımının (PTC-BF için %86.3, ST-BF için %92.2 ve LFR-BF için %85.4) tüm ekserji yıkımlarının büyük kısmından sorumlu olduğu görülmektedir. PTC-BF için, eksergoekonomik analizden rejeneratör 1, güç bloğuna bağlı ara ısı değiştiricisi ve buhar türbinlerinin kaçınılabılır-iç ekserji yıkımları ile ilgili toplam maliyet değerlerinin sırasıyla 7.33 USD/saat, 4.17 USD/saat ve 4.49 USD/saat olduğu belirlenmiştir. ST-BF için kaçınılabılır-iç ekserji yıkımları ile ilgili toplam maliyet değerlerinin rejeneratör 1, güç bloğuna bağlı volümetrik alıcı ve buhar türbinleri için sırasıyla 3.87 USD/saat, 84.75 USD/saat and 3.94 USD/saat olarak bulunmuştur. LFR-BF için kaçınılabılır-iç ekserji yıkımları ile ilgili toplam maliyet değerlerinin rejeneratör 1, güç bloğuna bağlı ara ısı değiştiricisi ve buhar türbinleri için sırasıyla 4.11 USD/saat, 1.76 USD/saat and 2.84 USD/saat olarak hesaplanmıştır. PTC-BF, ST-BF ve LFR-BF için önlenebilir iç ekserji yıkımları ile ilgili toplam maliyetler, sistem optimizasyonu için gerekli toplam maliyetlerin sırasıyla %21.7'si, % 26'sı ve % 24.5'i civarındadır.

Bu çalışmada, üç hibrid enerji sistemini iyileştirmek için gereken aylık harcamalar da incelenmiştir. PTC-BF sisteminde güneş sahası için 41553.30 USD,

güç bloğu için 1715.28 USD ve HRSG için 2997.41 USD; ST-BF sisteminde güneş sahası için 24695.10 USD, güç bloğu için 1362.57 USD ve HRSG için 1230.32 USD; LFR-BF sisteminde güneş sahası için 18987.90 USD, güç bloğu için 926.60 USD ve HRSG için 1218.34 USD olarak bulunmuştur.

İleri ekserji ve eksergoekonomik analiz sonuçları, hibrid enerji sistemlerinin genel verimliliğini arttırmak için kaçınılmaz olarak iç ekserjiyi geri kazanmanın gerekli olduğunu ortaya koymaktadır. Çalışmanın ana bulgularına göre, LFR'ye dayanan hibrid enerji sisteminin en iyi tekno-ekonomik sonuçları sunduğu ve bunu PTC'ye dayalı sistemin izlediği söylenebilmektedir.

Anahtar sözcükler: Hibrid enerji sistemi, Güneş enerjisi, Biyokütle, İleri ekserji analizi, Eksergoekonomik analiz.

ABSTRACT**THERMODYNAMIC AND EXERGO-ECONOMIC ANALYSIS OF A
SOLAR-BIOMASS HYBRID POWER PLANT FOR MULTI-
ENERGY GENERATION**

BIBOUM BIBOUM, Alain Christian

Ph.D. Thesis, Solar Energy Branch

Supervisor: Assist. Prof. Dr. Ahmet YILANCI

August 2019, 343 pages

Cameroon, is located in the western part of Central Africa, has a good geographical position in terms of the potential of biomass sources and solar energy. However, there are still some regions in Cameroon without access to commercial electricity, especially in the northern part of the country. Using biomass and solar energy sources together can be considered as one of the most suitable options to provide uninterrupted energy supply. Potentials of these sources are sufficient to generate energy for the northern part of Cameroon. The hybridization of energy sources is a promising alternative to increase the conversion efficiency of the power system, constitutes an attractive option which can ensure low cost of energy demand.

In this study, solar-biomass hybrid energy systems, which are combinations of three different Concentrating Solar Power (CSP) technologies with biomass-fired (BF) technology, are investigated. Parabolic Trough Collector (PTC), Linear Fresnel Reflector (LFR) and Solar Tower (ST) are selected for solar energy conversion as CSP technologies. For each hybrid system with an installed capacity of 5 MWe and which contains four subsystems, solar and biomass field, power block, heat recovery steam generation (HRSG) and multigeneration energy system using absorption refrigeration and drying systems, are configured and analyzed. Comprehensive economic and thermodynamic analyses in terms of

energetic, exergetic and exergoeconomic analyses for each system and its components are conducted to minimize the cost and increase the performance.

Initial investment costs required for the hybrid energy systems based on PTC, ST and LFR are obtained to be 38.47 Million USD, 51.47 Million USD and 25.23 million USD, respectively. From the techno-economic evaluations of the hybrid energy systems, levelized cost of electricity values for LFR-BF are found to be the lowest varying from 76.4 to 143.4 USD/MWh. According to the payback period, LFR-BF has a short return on investment with 8.4 years, followed by PTC-BF having 10.62 years while ST-BF has the highest payback period of 14.71 years. Also, LFR-BF seems to be the most profitable investment among three hybrid energy systems based on internal rate of return values for PTC-BF, ST-BF, and LFR-BF which are 13.79%, 12.64%, and 16.49%, respectively.

It is found from the advanced exergy analysis of the hybrid energy systems that exergy destruction from the solar field alone (86.3% for PTC-BF, 92.2% for ST-BF and 85.4% for LFR-BF) is responsible for the most of all exergy destructions. For PTC-BF, it is obtained from exergoeconomic analysis that the value of the total cost associated with the avoidable-endogenous exergy destruction of the regenerator 1, the intermediate heat exchanger connected to power block and the steam turbines are 7.33 USD/hour, 4.17 USD/hour and 4.49 USD/hour, respectively. For ST-BF, the value of cost associated with the avoidable-endogenous exergy destruction of the regenerator 1, the volumetric receiver connected to power block and the steam turbines are found to be 3.87 USD/hour, 84.75 USD/hour and 3.94 USD/hour, respectively. For LFR-BF, the value of cost associated with the avoidable-endogenous exergy destruction of regenerator 1, the intermediate heat exchanger connected to power block and steam turbines are calculated as 4.11 USD/hour, 1.76 USD/hour and 2.84 USD/hour, respectively. Total costs associated with avoidable-endogenous exergy destructions for PTC-BF, ST-BF, and LFR-BF are around 21.7%, 26% and 24.5% of the total cost required for system optimization, respectively.

In this study, the maximum monthly expenditures required to optimize three hybrid energy systems are also investigated. They are found to be 41553.30 USD

for the solar field, 1715.28 USD for the power block and 2997.41 USD for the HRSG in PTC-BF system; 24695.10 USD for the solar field, 1362.57 USD for the power block and 1230.32 USD for the HRSG in ST-BF system, and 18987.90 USD for the solar field, 926.60 USD for the power block and 1218.34 USD for the HRSG in LFR-BF system.

The results of the advanced exergy and exergoeconomic analysis reveal that it is essential to recover endogenous-avoidable exergy to improve the overall efficiency of the hybrid energy systems. According to the main findings of the study, it can be said that the hybrid energy system based on LFR presents the best techno-economic results and it is followed by the system based on PTC.

Keywords: Hybrid energy system, Solar energy, Biomass, Advanced exergy analysis, Exergoeconomic analysis.

PREFACE

This thesis is submitted for the degree of Doctor of Philosophy at Ege University. It is focused on thermodynamic and exergo-economic analysis of solar-biomass hybrid energy systems for my country, Cameroon, located in the Sub-Saharan region, which has an important solar potential and biomass residues. Three different Concentrating Solar Power (CSP) technologies hybridizing with Biomass-fired (BF) technology for multi-energy production are investigated. Therefore, performance evaluations of these hybrid energy systems, in terms of technically and economically, are proposed.

I hope that this study will be followed up by many others, and it would be useful for the future studies on solar-biomass hybrid energy systems.

IZMIR

19 / 08 / 2019

Alain Christian BIBOUM BIBOUM

CONTENTS

	<u>Page</u>
İÇ KAPAK	ii
KABUL ONAY SAYFASI	iii
ETİK KURALLARA UYGUNLUK BEYANI.....	v
ÖZET	vii
ABSTRACT	xi
PREFACE.....	xv
CONTENTS	xvii
LIST OF TABLES.....	xxii
LIST OF FIGURES	xxx
NOMENCLATURE	xxxvi
1. INTRODUCTION.....	1
1.1 Importance of Renewable Energy Systems	1
1.2 Current Status of Renewable Energy Systems in the World	7
1.3 Energy Outlook of Cameroon.....	12

CONTENTS (continued)

	<u>Page</u>
1.4 Prime Movers.....	19
1.4.1 Solar thermal power plants	19
1.4.2 Biomass based power system.....	35
1.5 Solar-Biomass Hybrid Energy Systems for Multi-energy Generation	40
2. LITERATURE REVIEW	43
2.1 Introduction.....	43
2.2 Combined Cycles and Multigeneration Energy Systems.....	47
2.3 Solar Thermal Power Systems	50
2.4 Biomass-Fired Based Power Systems.....	52
2.5 Solar-Biomass Hybrid Energy Systems	54
2.6 Aims, Objectives and Motivations of the Thesis	60
2.6.1 Motivations	60
2.6.2 Aims and objectives.....	62
2.7 Outline of the Thesis	65
3. DESIGN AND DESCRIPTIONS OF SOLAR-BIOMASS HYBRID ENERGY SYSTEMS	67

CONTENTS (continued)

	<u>Page</u>
3.1 Introduction.....	67
3.2 Descriptions of the Systems	69
3.2.1 Case 1: Parabolic trough collector/Biomass – fired system	71
3.2.2 Case 2: Solar tower/Biomass-fired system	74
3.2.3 Case 3: Linear Fresnel reflector/Biomass-fired system.....	76
3.3 Thermodynamic Properties of the Hybrid Energy Systems	77
4. ENERGY, EXERGY AND EXERGOECONOMIC ANALYSIS.....	82
4.1 Introduction.....	82
4.2 Exergoeconomic	87
4.3 Advanced Exergoeconomic Method.....	90
4.4 Advanced Exergoeconomic for System Optimization	93
5. ANALYSES OF THE HYBRID ENERGY SYSTEMS.....	99
5.1 Thermodynamic Analysis of the Hybrid Energy Systems	99
5.1.1 Thermodynamic analysis of the prime movers.....	99
5.1.2 Thermodynamic analysis of the power block subsystem	108
5.1.3 Thermodynamic analysis of the absorption refrigeration subsystem	108

CONTENTS (continued)

	<u>Page</u>
5.1.4 Thermodynamic analysis of the drying subsystem	115
5.2 Exergoeconomic Analysis of the Hybrid Energy Systems	116
5.2.1 Exergoeconomic analysis of the prime movers	116
5.2.2 Exergoeconomic analysis of the power block and HRSG subsystem	118
5.2.3 Exergoeconomic analysis of the absorption refrigeration subsystem	125
5.2.4 Exergoeconomic analysis of the drying subsystem	128
5.3 Advanced Exergoeconomic Analysis of the Hybrid Energy Systems	129
5.3.1 Advanced exergoeconomic analysis of the prime movers	129
5.3.2 Advanced exergoeconomic analysis of the power block subsystem	134
5.3.3 Advanced exergoeconomic analysis of the HRSG subsystem.....	139
5.3.4 Advanced exergoeconomic analysis of the absorption refrigeration subsystem.....	142
5.3.5 Advanced exergoeconomic analysis of the drying subsystem.....	145
6. RESULTS AND DISCUSSION.....	146
6.1 Conventional Exergy and Cost Analysis of the Systems	146
6.2 Conventional Exergoeconomic and Techno-economic	164

CONTENTS (continued)

	<u>Page</u>
6.3 Advanced Exergy Analysis.....	169
6.4 Economic Analysis	194
6.5 Advanced Exergy and Exergoeconomic Analysis.....	199
6.5.1 Advanced exergy and exergoeconomic analysis of solar power system using parabolic trough collector technology	199
6.5.2 Advanced exergy and exergoeconomic analysis of solar power system using solar tower technology.....	209
6.5.3 Advanced exergy and exergoeconomic analysis of solar power system using linear Fresnel reflector technology	217
6.5.4 Advanced exergy and exergoeconomic analysis of biomass - fired technology.....	225
7. CONCLUSION	233
7.1 Summary of the Results.....	233
7.2 Future Works and Recommendations.....	237
REFERENCES	233
APPENDIX	263
ACKNOWLEDGEMENT	293
CURRICULUM VITAE.....	294

LIST OF TABLES

Table	Page
1.1. On-grid renewable energy capacity in the world	10
1.2. Off-grid renewable energy capacity in the world.....	12
1.3. Installed power plants in Cameroon.....	18
1.4. Power station installed (outstanding) and available in Cameroon	18
1.5. CSP technology using parabolic trough collector technology	24
1.6. CSP technology using solar tower technology.....	26
1.7. CSP technology using solar tower and linear Fresnel technology	28
1.8. Comparative analysis of biomass power technologies based on plant operational conditions and techno-economic criteria.....	38
1.9. Comparative analysis of biomass power technologies based on environmental and social criteria.	39
2.1. Recent studies on hybrid (solar-biomass) energy system using CSP and combustion technology.....	45
3.1. Meteorological data of Garoua, Faro-Poli.....	67
3.2. Main crop residues in Cameroon	68
4.1. Exergy rates associated with the fuel and product for key components at a steady-state.....	86

LIST OF TABLES (continued)

<u>Table</u>	<u>Page</u>
4.2. Cost rates associated with the fuel and product as well as auxiliary exergoeconomic relations at steady-state.....	89
4.3. Exergoeconomic methods and analysis.....	96
5.1. Correlation used to determine PEC and levelized costs of the main component used for the power block.....	103
5.2. Efficiencies of heliostat field.....	104
5.3. Correlation used to determine PEC and breakdown costs of the absorption refrigeration cycle.....	114
5.4. Input data for the drying system (DFC).....	116
5.5. Main parameters of the prime mover subsystem used for advanced exergoeconomic analysis real conditions (RC), unavoidable thermodynamic inefficiency (UTI), unavoidable investment cost.....	134
5.6. Main parameters of the power block subsystem used for advanced exergoeconomic analysis real conditions (RC), unavoidable thermodynamic inefficiency (UTI), unavoidable investment cost.....	139
5.7. Main parameters of the HRSG subsystem used for advanced exergoeconomic analysis real conditions (RC), unavoidable thermodynamic inefficiency (UTI), unavoidable investment cost.....	142

LIST OF TABLES (continued)

<u>Table</u>	<u>Page</u>
5.8. Main parameters of the absorption refrigeration systems used for advanced exergoeconomic analysis real conditions (RC), unavoidable thermodynamic inefficiency (UTI), unavoidable investment cost (UIC)	145
5.9. Main parameters of the drying subsystem used for advanced exergoeconomic analysis real conditions (RC), unavoidable thermodynamic inefficiency (UTI), unavoidable investment cost (UIC)	145
6.1. Properties of sorghum stalk and technical characteristic of the boiler - grate stocker furnace.....	147
6.2. Energy analysis of the steam generation process in the grate stocker furnace (boiler) for the biomass-fired power system.	147
6.3. Exergy analysis of the steam generation process in the grate stocker furnace (boiler) for the biomass-fired power system.	148
6.4. First and second law analysis of the steam generation process in the grate stocker furnace (boiler) for the biomass-fired power system.....	148
6.5. Properties and technical characteristics of the parabolic trough collector technology-LS3/PTR80 solar field.....	149
6.6. Energy analysis of the steam generation process in the PTC-solar field.....	149

LIST OF TABLES (continued)

<u>Table</u>	<u>Page</u>
6.7. Exergy analysis of the steam generation process in the PTC-solar field.	150
6.8. First and second law analysis of the steam generation process PTC-solar field.	150
6.9. Major purchased equipment cost of a hybrid energy system based on PTC-BF technology	151
6.10. Properties and technical characteristics of the solar tower technology-solar field	153
6.11. Energy analysis of the steam generation process of the ST-solar field.	153
6.12. Exergy analysis of the steam generation process of the ST-solar field.	154
6.13. First and second law analysis of the steam generation process of the ST-solar field.	154
6.14. Major purchased equipment cost of a hybrid energy system based on ST-BF technology.....	155
6.15. Properties and technical characteristics of the linear Fresnel reflector-solar field	157
6.16. Energy analysis of the steam generation process of the LFR-solar field.	157

LIST OF TABLES (continued)

<u>Table</u>	<u>Page</u>
6.17. Exergy analysis of the LFR-solar field.....	158
6.18. First and second law analysis of the LFR-solar field.	158
6.19. Major purchased equipment cost of a hybrid energy system based on LFR-BF technology.....	159
6.20. Thermodynamic analysis of the power block system according to the prime movers.....	161
6.21. Thermodynamic analysis of the HRSG system according to the prime movers.....	161
6.22. Absorption refrigeration system (LiBr/Water) connected to the HRSG of the power system based on PTC technology.....	162
6.23. Absorption refrigeration system (LiBr/Water) connected to the HRSG of the power system based on ST technology.	164
6.24. Absorption refrigeration system (LiBr/Water) connected to the HRSG of the power system based on LFR technology.....	163
6.25. Absorption refrigeration system (LiBr/Water) connected to the HRSG of the power system based on BF technology..	163
6.26. The average cost per exergy unit and levelized cost rate of product for subsystems containing in standalone power systems	167
6.27. Techno-economic analysis of hybrid energy system based on the PTC and BF technology	195

LIST OF TABLES (continued)

<u>Table</u>	<u>Page</u>
6.28. Techno-economic analysis of hybrid energy system based on the ST and BF technology	196
6.29. Techno-economic analysis of hybrid energy system based on the LFR and BF technology.....	197
6.30. Advanced exergy analysis of the power system based on PTC technology.....	201
6.31. Advanced exergoeconomic analysis of the power system based on PTC technology	204
6.32. Advanced analysis of the total cost associated with exergy destruction of components used for the power system based on PTC technology	206
6.33. Endogenous avoidable exergy cost analysis of component used for the power system based on PTC technology	207
6.34. Data obtained from avoidable cost rates of exergy destruction analysis in the power system based on PTC technology	208
6.35. Advanced exergy analysis of the power system based on ST technology.....	218
6.36. Advanced exergoeconomic analysis of the power system based on ST technology	221

LIST OF TABLES (continued)

<u>Table</u>	<u>Page</u>
6.37. Advanced analysis of the total cost associated with exergy destruction of components used for the power system based on ST technology	223
6.38. Endogenous avoidable exergy cost analysis of component used for power system based on ST technology	224
6.39. Data obtained from avoidable cost rates of exergy destruction analysis in the power system based on ST technology	225
6.40. Advanced exergy analysis of the power system based on LFR technology	211
6.41. Advanced exergoeconomic analysis of the power system based on LFR technology.....	213
6.42. Advanced analysis of the total cost associated with exergy destruction of components used for the power system based on LFR technology.....	214
6.43. Endogenous avoidable exergy cost analysis of component used for power system based on LFR technology	215
6.44. Data obtained from avoidable cost rates of exergy destruction analysis in the power system based on LFR technology.....	217
6.45. Advanced exergy analysis of the power system based on BF technology	227

LIST OF TABLES (continued)

<u>Table</u>	<u>Page</u>
6.46. Advanced exergoeconomic analysis of the power system based on BF technology.....	229
6.47. Advanced analysis of the total cost associated with exergy destruction of the components used in the power system based on BF technology.....	230
6.48. Endogenous avoidable exergy cost analysis of component used for power system based on BF technology.....	231
6.49. Data to choose the corresponding approach for reducing avoidable cost rates of exergy destruction in the power system based on BF technology.....	232

LIST OF FIGURES

<u>Figure</u>	<u>Page</u>
1.1. Concentrating solar power technologies	20
1.2. Analytical structure of the technical phases involved in the selection of suitable biomass-fired technology for the electricity generation.....	37
1.3. Description of the power block system used in the hybrid (solar– biomass) energy system.	41
1.4. a) Schematic view of heat recovery steam generator (HRSG) system of the hybrid power system based on ST - BF technology (b) Heat recovery steam generator (HRSG) system of hybrid energy system based on PTC or LFR – BF technology..	42
3.1. Case study I - schematic diagram of a hybrid biomass-solar power system based on parabolic trough collector..	72
3.2. (a) Drying system (b) Single – effect absorption system.....	75
3.3. Case study II - schematic diagram of a hybrid biomass-solar power system based on the solar tower.....	73
3.4. Case study III - schematic diagram of a hybrid biomass-solar power system based on linear Fresnel reflectors.....	73
3.5. T – s diagram of the steam Rankine cycle based on (a) PTC and LFR technologies, (b) ST and BF technologies..	78

LIST OF FIGURES (continued)

<u>Figure</u>	<u>Page</u>
3.6. T – s diagram of the organic Rankine cycle based on (a) parabolic trough collector and linear Fresnel reflector technologies. (b) solar tower and biomass-fired technologies.	79
3.7. T-s diagram of lithium bromide/water of an absorption refrigeration cycle (cooling generation side).	80
4.1. One-outlet, one-exit control volume	82
4.2. Complete splits of the exergy destruction in an advanced exergetic analysis.....	91
4.3. Overview of the modeling steps in advanced exergoeconomic optimization.	98
5.1. Turbines of the power block system used in the hybrid (solar-biomass) energy system.	108
6.1. Major cost breakdown for the hybrid energy system based on PTC-BF.....	152
6.2. Major cost breakdown for the hybrid energy system based on ST-BF.....	156
6.3. Major cost breakdown for the hybrid energy system based on LFR-BF.....	160
6.4. Cost per exergy unit of the absorption refrigeration unit.....	168

LIST OF FIGURES (continued)

<u>Figure</u>	<u>Page</u>
6.5. Cost per exergy unit of main components of the organic Rankine cycle.	169
6.6. Monthly exergy production capacity of the solar field based on PTC technology.....	171
6.7. Distribution of the exergy destruction forms present in the intermediate heat exchanger of the PTC solar field.	172
6.8. Exergy produced and destroyed in the HRSG of the power system based on PTC technology.....	173
6.9. Distribution of Exergy destruction forms in the HRSG of the solar power system based on PTC technology.....	173
6.10. Repartition of exergy destruction forms in the regenerator 1 of the HRSG system connected to the solar power system based on PTC technology.	174
6.11. Repartition of exergy destruction forms in the regenerator 2 of the HRSG system connected to the solar power system based on PTC technology.	175
6.12. Repartition of exergy destruction in the regenerator 3 of the HRSG system of the power system based on the PTC technology.	176
6.13. Monthly exergy production capacity of the solar field based on ST..	177
6.14. Distribution of the exergy destruction forms present in the intermediate heat exchanger of the ST-solar field.	178

LIST OF FIGURES (continued)

<u>Figure</u>	<u>Page</u>
6.15. Exergy produced and destroyed in the HRSG of the power system based on ST technology.....	179
6.16. Distribution of exergy destruction forms in the HRSG of the solar power system based on ST technology.....	180
6.17. Repartition of exergy destruction forms in the regenerator 1 of the HRSG system connected to the solar power system based on ST technology.....	181
6.18. Repartition of exergy destruction forms in the regenerator 2 of the HRSG system connected to the solar power system based on solar tower technology.....	181
6.19. Repartition of exergy destruction forms in the regenerator 3 of the HRSG system connected to the solar power system based on solar tower technology.....	182
6.20. Repartition of exergy destruction forms in the regenerator 4 of the HRSG system connected to the solar power system based on solar tower technology.....	182
6.21. Repartition of exergy destruction forms in the regenerator 5 of the HRSG system connected to the solar power system based on solar tower technology.....	183
6.22. Monthly exergy production capacity of the solar field based on LFR. technology.....	184

LIST OF FIGURES (continued)

<u>Figure</u>	<u>Page</u>
6.23. Distribution of the exergy destruction forms present in the intermediate heat exchanger of the LFR - solar field.....	184
6.24. Exergy produced and destroyed in the HRSG of the power system based on LFR technology.....	185
6.25. Distribution of Exergy destruction forms in the HRSG of the solar power system based on LFR technology.	186
6.26. Repartition of exergy destruction forms in the regenerator 1 of the HRSG system connected to the solar power system based on LFR technology.	186
6.27. Repartition of exergy destruction forms in the regenerator 2 of the HRSG system connected to the solar power system based on LFR technology.....	187
6.28. Repartition of exergy destruction forms in the regenerator 3 of the HRSG system connected to the solar power system based on linear Fresnel reflector technology.....	188
6.29. Monthly exergy produced the capacity of the power system based on BF technology.	189
6.30. Distribution of the exergy destruction forms present in the intermediate heat exchanger of the BF technology.....	189
6.31. Exergy produced and destroyed in the HRSG of the power system based on BF.....	190

LIST OF FIGURES (continued)

<u>Figure</u>	<u>Page</u>
6.32. Distribution of Exergy destruction forms in the HRSG of the power system based on BF technology.....	190
6.33. Repartition of exergy destruction forms in the regenerator 1 of the HRSG system connected to the power system based on BF technology.....	191
6.34. Repartition of exergy destruction forms in the regenerator 2 of the HRSG system connected to the power system based on BF technology.....	192
6.35. Repartition of exergy destruction forms in the regenerator 3 of the HRSG system connected to the power system based on BF technology.....	192
6.36. Exergy destruction forms in the regenerator 4 of the HRSG system of the power system based on BF technology.	193
6.37. Exergy destruction forms in the regenerator 5 of the HRSG system of the power system based on BF technology.	193

NOMENCLATURE

<u>Preferred name</u>	<u>Symbol</u>	<u>Unit</u>
Absorbed energy input	$\dot{Q}_{use,in}$	kW
Active area	A_{act}	m^2
Ambient temperaure	T_a	K
Aperture area	A_{ap}	m^2
Area	A	m^2
Area of individual heliostat	AH	m^2
Avoidable exergy destruction	$\dot{E}_{D,k}^{AV}$	kW
Capital investment/levelized cost rate	\dot{Z}	USDcent/s
Cost per unit exergy	c	USD/GJ
Cost	C	USD
Cost rate associated	\dot{C}	USDcent/s
Efficiency factor of collector	F'	-
Endogenous exergy destruction	$\dot{E}_{D,k}^{EN}$	kW
Enthalpy	h	kJ/kg
Exergoeconomic factor	f_k	-
Exergy	E	kW

NOMENCLATURE (continued)

<u>Preferred name</u>	<u>Symbol</u>	<u>Unit</u>
Exergy loss	\dot{E}_q	kW
Exogenous exergy destruction	$\dot{E}_{D,k}^{EX}$	kW
Fuel	F	-
Fuel cost	FC	USD
Geometric factor	R_b	-
Gravity	g	m/s ²
Heat losses coefficient	U_L	W/m ² K
Higher heating value	HHV	MJ/kg
Internal energy	U	kJ/kg
Kinetic energy	KE	kJ/kg
Length of collector	L	m
Levelized cost of energy	LCOE	USD/MWh
Log means temperature	LMTD	-
Lower heating value	LHV	MJ
Net rates of work transfer	W	kJ/kg

NOMENCLATURE (continued)

<u>Preferred name</u>	<u>Symbol</u>	<u>Unit</u>
Net rates of heat transfer	Q	kJ/kg
Number of pieces	N	-
Optical efficiency	η_o	%
Overall heat transfer	U_o	W/m ² K
Potential energy	PE	kJ/kg
Product	P	-
Purchased equipment cost	PEC	USD
Rate of entropy transfer	m.s	kJ/K
Rate of exergy destruction	T.s	kJ/kg
Receiver temperature	Tr	K
Reference temperature	To	K
Relative cost difference	r_k	%
Solar field	SF	-
Solar intensity	I	W/ m ²
Solar power input	\dot{Q}_{solar}	kWth
Sun temperature	Tsun	K

NOMENCLATURE (continued)

<u>Preferred name</u>	<u>Symbol</u>	<u>Unit</u>
Sunshine duration	ΔTh	K
Sustainable extraction	S_{ext}	%
Unavoidable exergy destruction	$\dot{E}_{D,k}^{UN}$	kW
Useful energy output	\dot{Q}_{abs}	kWth
Velocity	V	m/s
Yearly operation	YOP	hour

Subscripts

<u>Preferred name</u>	<u>Symbols</u>
Absorber	ab
Air compression	ac
Avoidable	AV
Biomass	b
Capital Investment	CI
Condenser	cond
Control volume	cv

NOMENCLATURE (continued)

<u>Preferred name</u>	<u>Symbols</u>
Destruction	D, d
Endogenous	EN
Evaporator	ev
Exit	e
Exogenous	EX
Extraction	ext
Generator	g
Heat exchanger	hx
High	h
Inlet	in
Intermediate heat exchanger	ihe
Isentropy	is
k th component, incidence angle modified	k
Loss, Low	L
Mass	m
Optical	opt

NOMENCLATURE (continued)

<u>Preferred name</u>	<u>Symbols</u>
Outlet	out
Pump	p
Solar	s
Solution	sp
System	sys
Therminol VP – 1	th
Total	tot
Turbine	t
Unavoidable	un
Width	w

Greek symbols

<u>Name</u>	<u>Symbols</u>
Absorptivity	α
Atmospheric attenuation efficiency	η_{att}
Collector efficiency	η

NOMENCLATURE (continued)

<u>Name</u>	<u>Symbols</u>
Cosine effect efficiency	η_{cos}
Efficiency of exchanger	π
Efficiency of the LFR	ε_c
Energetic efficiency	η_{th}
Exergetic efficiency	η_{ex}
Heliostat field efficiency	η_t
Intercept efficiency	η_{int}
Intercept factor	δ
Optical efficiency	η_o
Primary emittance	ρ_1
Reflectivity	ρ
Reflectivity efficiency	η_{ref}
Secondary emittance	ρ_2
Shading and blocking efficiency	$\eta_{S\&B}$
Transmissivity	τ
Win efficiency	η_{win}

NOMENCLATURE (continued)***Abbreviations***

<u>Terms</u>	<u>Abbreviation</u>
Absorption Refrigeration System	ARS
Advanced Exergoeconomic Analysis	AEEA
Annual Operating Expenses	AOE
Biomass Thermal Power Plants	BTPP
Cameroon Development Corporation	CDC
Capital Cost	ICC
Capital Expenditure	CAPEX
Central Receiver	CR
Certified Tax Carbon	CER/TAX
Chemical Engineering Cost Index	CECI
Combined Cycles Power Plant	CCPP
Combined Cooling Heat and Power	CCHP
Combined Heat and Power	CHP
Combined Rankine Cycles	CRC
Concentrating Solar Power	CSP

NOMENCLATURE (continued)

<u>Terms</u>	<u>Abbreviation</u>
Direct Normal Irradiation	DNI
Direct Steam Generation	DSG
Drying Food Conservation	DFC
Earning after Interest and Tax	EAIT
Earnings before Interest and Tax	EBIT
Environmental and Social Impact Assessment	ESIA
Exergoeconomic Analysis	EEA
Feed in Tariff	FiT
Heat Recovery Steam Generation	HRSG
Heat Transfer Fluid	HTF
Indirect Steam Generation	ISG
Initial Investment	IT
Integrated Solar Combined Cycles System	ISCCS
Intermediate Heat Exchanger	IHE
Internal Rate Return	IRR
Linear Fresnel Reflector	LFR

NOMENCLATURE (continued)

<u>Terms</u>	<u>Abbreviation</u>
Marshall and Swift Index	MSI
National Renewable Energy Laboratory	NREL
Net Present Value	NPV
Operating Expenditure	OPEX
Organic Rankine Cycle	ORC
Parabolic Trough Collectors	PTC
Payback Period	PBP
Required Cost for Optimization	RCO
System Advisor Model	SAM
Solar collector assemblies	SCA
Solar Double – Chimney Power Plant	SDCPP
Solar electricity generating System	SEGS
Solar Field	SF
Solar Multiple	SM
Solar Power Plant	SPP
Solar Tower	ST

NOMENCLATURE (continued)

<u>Terms</u>	<u>Abbreviation</u>
Solar Tower Power Plant	STPP
Steam Rankine Cycle	SRC
Slopped Solar Chimney Power Plant	SSCPP
Thermal Energy Storage	TES
Total Direct Cost	TDC
Total Installed Cost	TIC

1. INTRODUCTION

1.1 Importance of Renewable Energy Systems

In the past decades, several major changes have been observed in the production and consumption pattern of energy for the non-industrialized countries across the globe, and the majority of these changes have been observed in the Sub-Saharan region. Major attentions of this region have been given to projects that will contribute directly to their industrialization such as extension of electricity networks, construction of new power plants that reinforce the energy autonomy of the nations with accompanying measures promoting the liberalization of the energy sector. Implementation of the decentralization power plants for electricity production has been the major target to increase the accessibility of electricity in rural areas. However, given the complexity that lies in the protection of public electrical installations, the question of liberalization distribution has occupied the mind of many economic actors. To cope with this situation, the majority of the countries having centralized management, the answers are on the same ones but remained identical on the bottom. Thus, in this new decade, it is possible to develop available energy resources that remain untapped for a long time when considering the decentralized system. On the other hand, programs and seminars are organized by the regulators of the electrification sector to raise awareness among consumers, economic players and potential investors in the energy sector. The results are considered for countries in the Sub-Saharan region, which have experienced a continuous increase in electrification, employment and share of renewable energies in national energy mix over the past few years.

Nevertheless, it is essential to take into account the challenges associated with implementing energy policy suitable for new energy production measures and processes that will no longer be limited to only electricity production for local or region use, but also consider the rational use of renewable energies to support social, environmental and economic aspects.

The use of renewable energies in the national or regional electricity production shows its importance through:

- The growth of cogeneration energy systems for domestic use in urban areas and industrial projects;
- The energy independence of households and private companies;
- The reduction of greenhouse gases in large cities;
- The renewal or hybridization of the power plants for the national utility company;
- The reduction of the use of fossil fuels in electricity production;
- Better access to electricity by proposing a very competitive cost per kWh.

Many countries are updating energy policies by adopting the use of renewable energies, and introducing programs that encourage the development of efficient energy systems to achieve their social, environmental, energy and economic goals. These energy policies consist of eradicating the growing energy insecurity in Sub-Saharan countries. Nowadays, more than 50% of the population in Sub-Saharan region still have no access to modern energy services to meet their daily needs such as lighting, cooking, heating, cooling, and conservation of medical products and foodstuffs in rural areas. This leads to a low consumption per capita, paradoxically a significant waste of energy recorded in the public services. However, the inadequacy of electricity production has remained the main reason for increasing inaccessibility to energy by the majority of households. This low production affects economic growth due to lack of access to modern energy services for industrialization. For a long time, many Sub-Saharan countries had resorted to the usage of fossil fuel such as diesel, coal, and gas, hence the cost of energy has continued to rise as the fossil resources are becoming increasingly scarce as well as due to increasing energy demand. Fortunately, renewable

energies are the best alternative solutions to curb several scourges constituting an obstacle to public health and social development. Renewable energies offer efficient decentralized alternatives that are adapted to protect the environment.

Although not fully within the reach of the poorest populations, many still believe that they have major assets to sustainably meet the energy needs of centralized production. This is illustrated by the fact that many Sub-Saharan countries have introduced regional policies and national programs which promote the implementation of projects based on renewable energy technologies such as hydro, solar, wind or biomass power plants that use agricultural or forestry residues. Moreover, the potential in terms of implementation of micro-hydroelectric projects in Central Africa is enormous and almost unexploited. The hydropower resource is the best-exploited renewable energy source on the continent, with 10% being economically exploitable. The total hydropower reserves are estimated at 1100 TWh, but only 8% has been exploited. In the western sub-Saharan region, only 16% of the estimated 25,000 MW have been implemented. The equatorial region has the greatest potential which is still underexploited. In the field of geothermal energy, less than 1% of the capacity of the Rift Valley is exploited, only 54 MW is being extracted from the potential of about 9 GW. Most countries in the sub-Saharan region have an average solar flux potential of about 5 to 6 kWh/m² /day. The lack of access to modern energy services in rural areas has contributed to the uncontrolled consumption of forest resources such as trees, wood, etc. leading to the acceleration of the phenomenon of desertification.

As of the beginning of 2019, three-quarters of sub-Saharan countries are implementing energy policies which may lead to a rapid expansion of renewable energy projects. These policies include programs to promote the sustainable development of renewable energy power plants, mandatory or voluntary renewable portfolio and energy efficiency resources standards and financial incentives which will lead to a better understanding of the environmental protection, high energy efficiency, and economic performance. Furthermore, these policies will contribute to the quality of life by improving public health through

the reduction of harmful air pollutants, reasonable energy costs, increase in employment rate and the reliability of the country's energy sector.

Renewable energies have to be converted into fuel that can be used to generate electricity, heat, and fuel for engines. The conversion process is often achieved through a combination of specific processes like thermal, thermochemical, mechanical, and chemical. There is a variety of renewable energy resources to which at least one of the above conversion processes for electricity generation could be applied. The choice of the industrial process is related to the nature of the available resource, the efficiency of the energy system, some aspects related to the environmental and social impacts, the financial subsidies during initial investment phase and the annual production of the system that supports the implementation of renewable energy technologies. During the analysis of the processes that accompany the production of energy, it has been noticed that the control of the use of renewable energy resources contribute to the growth of the technical capacities, a better control of the mechanisms of financing in this sector, an energy independence that relies on the energy mix, the control of the quality of its production, and a rational use of available renewable energy resources.

- The mastery of technical ways resides on the ability to make energy systems more efficient while supporting the environment. Hence, a balance between quality and quantity of production should be determined. The hybridization of energy systems is at the center of the themes that govern the use of renewable energies by combining the cost of selling energy with the quality of production. The complexity of its implementation is gradually being conducted by institutions which protect the environment and combat climate change through financing or supporting research work and implementation of pilot projects.
- Renewable energies project funding mechanisms has been used for a long time to make technologies mature in an economic region and within a specific number of actions. Thus, these projects create many opportunities for investment. This cannot be a definite success for both

the government and the investors if the financing mechanisms remain unacknowledged by the state institutions responsible for setting up renewable energy projects. In this regard, many countries in the Sub-Saharan region do not have a regulatory policy to accommodate certain hybrid projects.

- Mix and energy independence, energy demand is steadily increasing in many countries across the globe, while the use of renewable energy sources has generally remained low in many sub-Saharan countries for a long time. However, nowadays several technologies allowing their exploitation are now considered to be mature. Thus, present an important part in the production of energies by considerably their ability in reducing dependency on fossil fuel sources.
- Sustainable use of renewable energy resources, it is closely linked to the control of technologies, optimal use of available resources and the diversification of the existing power system for a better national energy mix.

The sustainable use of renewable energy resources ensures management of available resources by controlling the use of available energy sources in sub-Saharan countries which is a way to meet existing energy needs. This has remained a crucial step to reach the phase of maturation that will justify the multiple technological advances in the energy sector. So far, the expertise of the renewable energy technology field has remained and is being controlled by big multinationals companies from developed or developing countries. For sub-Saharan countries, this is an opportunity that will allow them to align with an international energy policy in which they can decide how much leeway they have to give to international partners. Thus, many institutions have been created for better monitoring of progress in the sector at regional and international level. These have contributed to increasing the share of renewable energy in the energy mix of many sub-Saharan countries.

The use of renewable energy systems have many benefits such as job creation for both skilled and unskilled person, a higher plant efficiency, acceptable level of maturity, less optimization needs in term of waste heat recovery system, low operating cost, less pollution in term of greenhouse gas emissions, better use of resources, easy to hybridize, multiple generation options, low cost of energy, increased reliability and less grid failure due to short transmission lines and fewer distribution network.

The use of renewable energy technologies can improve the overall efficiency of hybridizing and standalone systems, including the ability to reduce operating costs compared to the conventional power plants that use fossil fuel with a single prime mover. The hybridization of renewable energy sources may lead to a full electricity production without any important heat waste. Thus, the overall efficiency of hybridized or standalone thermal power systems using renewable energies to produce electricity and heat separately is above 60%. Many renewable energy systems can be used to generate more than one form of energy by adding various subsystems. Generally, in these case, part of the input energy and /or the waste heat from the power production are used to operate the cooling and heating systems without the need for external energy sources.

Thus, a renewable energy system uses cheap fuel cost compared to the conventional power system to generate the same output energy. Therefore, the energy produced by using renewable energy sources reduces greenhouse gas (GHG) emissions with a lower cost of energy and a higher payback period due to high initial investment. Renewable energy systems can be developed close to electricity transmission lines and distribution units to reduce grid installation cost and energy losses. These systems compared to conventional systems can be exposed to the environment. The electricity, produced from them needs to be transferred through short or medium transmission lines and fewer distribution units.

The advantages presented above have encouraged many governments, investors, and institutions to invest in the use of renewable energy sources. It is important to notice that, several power plants using renewable energies have been

developed since the beginning of this decade. Furthermore, the assessments and component costs contribute to select the renewable energy technology of a plant, using parameters such as the onsite, offsite cost and operation expenditures.

1.2 Current Status of Renewable Energy Systems in the World

In the past decades, the electricity generation sector has experienced a fast and unprecedented change by adding the use of renewable energies. This change is closely related to the maturity of renewable energy (RE) technologies used for electricity generation, the strong competitiveness of power plant equipment manufacturing sector, and the reduction in the initial investment cost. Table 1.1 shows the installed renewable energy capacity and shares of used renewable energy technologies between 2008 and 2017 in the world. The total RE capacity installed as of the end of 2011, is less than two-thirds of the total RE capacity installed in the world as of 2017 as shown in Table 1.1. At the end of 2017, the total RE installed capacity exceeded 2179 GW, which is to conclude that the global installation of RE technologies has doubled in a decade (IRENA, 2018b). The total RE installed capacity between 2016 and 2017 had reached 166.7 GW, a breakdown defined as 22 GW of new hydroelectric capacity, 0.005 GW of energy marine, 46.7 GW of wind energy, 93.7 GW of solar energy, 5 GW of biomass energy and 0.650 GW of geothermal energy. The cumulative production capacity of solar energy estimated at 93.7 GW is distributed as follows: 0.1 GW as a capacity of concentrating solar power (CSP) technologies and 93.6 GW solar photovoltaic systems. It is important to note that nearly 99% of the world's production is directly connected to the electricity grid.

The growth recorded follows similar proportions, as the acceleration of the deployment of RE technologies has increased, especially for solar and wind energy in Africa, America, Caribbean, and Pacific regions. Forecasting on global solar and wind installed capacity in 2017, with little contribution from the above-mentioned regions had set a new record year for the deployment of RE installations. As presented in the previous section, electricity generation through the use of RE presents a favorable ecological environment, in which political actors lean in their favor for energy policy for their country to accelerate their

deployment, improvements and cost reductions. Thereby reducing the cost of electricity and better protection of the environment benefit for the population living in rural areas. These RE technologies are supporting the energy policies development in many countries and their adoption is experiencing unprecedented growth in the strategic energy deployment programs.

As of 2017, the vast majority of regions around the world using RE technologies such as solar, hydropower, biomass, wind, and onshore geothermal for electricity generation have provided competitive levelized cost of energy (LCOE) compared to other technologies using fossil fuels without any financial support. This change marked the beginning of a new period of centralized/decentralized production, which until now had resisted the advancement of renewable energies. It is important to note that this change is still subject to significant resistance, essentially the hydrocarbon producing countries. Some of these countries are not benefiting from large renewable energy sources, including the mastery of new technologies, which have not reached the maturity stage. The growth of RE technologies for electricity generation and subsidiaries using solar and wind energies have increased installed capacity to record levels equaling hydropower plants. As a result, these RE technologies have recorded low LCOE in centralized systems, for example, the LCOE of solar photovoltaic technology has dropped by 73% between 2010 and 2017, making it very competitive for commercial application in almost all countries. These technological and economic improvements marked by the reduction of direct-indirect costs for the implementation of the projects have affected the RE technologies such as solar PV and wind turbines. Thus, raising them at the top of the most competitive technologies for the production of electricity by the new energies. However, it is essential to state that this rapid maturity of these aforementioned RE technologies presents for some experts a major disadvantage within the large family of RE technologies. Since these alone constitute more than 85% of the global market in the RE technology production as of 2017. Besides, these technologies are experiencing explosive growth, as the contribution to the use of RE technologies for global electricity production has increased from 52.5% in 2008 to 83.38% in 2017. The consequences are immediate, a significant decline was noticed in the market of hydroelectric dams estimated at 35.67% between

2008 and 2017. The contribution of hydropower technologies in the global electricity generation using RE technologies decreases from 42.32% in 2008 to 13.19% in 2017 as shown in Table 1.1. Like hydropower, a significant decline in the CSP technologies and solid biofuels market was also noticed estimated at 17.51% between 2008 and 2017. Moreover, its contribution to the world production of electricity compared to other RE technologies is decreasing, which was recorded at nearly 6.85% in 2008 while 2.74% in 2017 (IRENA, 2018a).



Table 1.1. On-grid renewable energy capacity in the world (IRENA, 2018a).

RE World Capacity (Year)	2008	2009	2010	2011	2012	2013	2014	2015	2016	2017
Total installed RE capacity– [GW]	1057.9	1138.7	1225.7	1329.3	1443.8	1564.6	1692.0	1848.7	2012.4	2179.1
Hydropower (including mixed plants) – [GW]	960.6	994.8	1028.9	1059.5	1092.6	1137.1	1175.4	1210.2	1248.1	1270.1
Renewable hydropower	864.4	894.2	928.3	955.7	986.4	1029.7	1066.4	1098.8	1131.3	1151.9
Pure pumped storage	96.1	100.6	100.5	103.8	106.1	107.4	109.05	111.4	116.8	118.6
Marine energy – [GW]	0.245	0.246	0.249	0.503	0.509	0.509	0.512	0.515	0.525	0.529
Wind energy – [GW]	114.79	150.09	180.71	220.01	269.64	301.55	349.18	416.79	467.25	513.93
Onshore wind energy	113.35	147.96	177.66	216.24	264.31	294.38	340.69	405.08	452.87	494.66
Offshore wind energy	1.44	2.13	3.05	3.77	5.33	7.17	8.49	11.71	14.35	19.27
Solar– [GW]	15.16	23.21	39.84	70.49	98.42	137.10	174.36	224.34	296.87	390.62
Solar photovoltaic	14.63	22.44	38.57	68.78	95.85	133.26	169.86	219.59	292.02	385.67
CSP*	0.54	0.76	1.27	1.71	2.57	3.84	4.50	4.75	4.85	4.95
Bioenergy – [GW]	53.86	61.14	66.46	72.60	78.38	85.00	90.36	96.49	104.27	109.21
Solid biofuels and waste	45.96	51.28	55.23	59.39	63.20	69.10	45.96	78.60	85.52	89.99
Bagasse – [GW]	7.60	8.11	10.42	11.54	12.65	14.45	15.50	16.84	17.60	17.94
Renewable Mun. Waste. – [GW]	4.91	5.19	7.03	7.09	7.51	8.56	8.82	9.92	10.67	11.54
Other solid biofuels	33.45	37.98	37.77	40.76	43.04	46.09	48.86	51.84	57.25	60.51
Liquid biofuels– [GW]	1.19	1.61	1.76	1.85	2.04	2.02	2.29	2.41	2.31	2.30
Biogas – [GW]	6.70	8.24	9.47	11.36	13.14	13.87	14.88	15.48	16.44	16.91
Geothermal energy	9.45	9.90	10.12	10.01	10.47	10.74	11.19	11.79	12.25	12.90

Although CSP technology is not widely used, it has seen a decrease in the total installation cost. Market studies between 2016 and 2017 show that, despite the absence of financial support, this technology will be able to compete with fossil fuels from the beginning of the next decade if an appropriate energy policy for their implementation is developed. These policies will either contribute to reducing the levelized cost of energy (LCOE) through clean production subsidies or by reducing or removing taxes on manufacturing and trading from equipment aimed directly at reducing the cost of installation. Such incentives will open the market for the manufacturing of CSP technology equipment in most countries. These will also help to make manufacturing more competitive by having a direct implication on improving the performance of existing technologies. It is, therefore, always expected that there will be a gradual reduction in the cost of CSP technology (IRENA, 2012;2018b). The gradual evolution of global renewable energy production shows that this sector is proving itself in terms of maturity and cost reduction. This progress has been achieved through huge investments in more efficient manufacturing processes by reducing costs in the supply chain and also through improved efficiency of technologies as compared to other contemporary mature technologies. The results of the share of growth in the world energy production market between 2008 and 2017 support the above results. It should be noted that the construction of Giga-farms with a record of 70 USD per MWh prices for solar photovoltaic and CSP electricity production was achieved in Abu Dhabi, Turkey, Chile, Dubai, Mexico, Peru, and Saudi Arabia. The cost of project installations using wind and CSP commissioned from 2018 will be lower than the costs of many of the fuel generators already installed around the world. Still unknown to the general public in some parts of the world RE technologies continues to suffer from an outdated perception according to which renewable energies are considered as an alternative solution to the production of electricity. Thus, they hardly contribute to the energy mix of certain countries.

The statistical report of IRENA (2018a) shows that the general assumption, electricity generated from RE technologies is more expensive, is not true because they produce more and more electricity with competitive costs, almost less than

fossil fuels. Table 1.2 shows the off-grid installed capacity using RE technologies (hydropower, solar PV, and others) to generate electricity.

Table 1.2. Off-grid renewable energy capacity in the world (IRENA, 2018a).

World Capacity	2008	2009	2010	2011	2012	2013	2014	2015	2016	2017
Total RE inst. (MW)	1909.7	2638.6	2890	3680.1	4027.2	4143.1	4764.2	5197.5	5956.2	6574.6
Hydropower (MW)	412.7	415.1	417.7	422.01	447.81	465.36	470.37	498.57	503.98	508.93
Solar PV (MW)	248.8	291.9	379.6	572.8	719.51	938.09	1235.9	1530.4	2162.4	2742.9
Other RE inst. (MW)	1248.1	1931.6	2092	2685.3	2859.8	2739.6	3057.8	3168.4	3289.7	3322.6

1.3 Energy Outlook of Cameroon

Cameroon is located in the western part of the Central Africa region at the bottom of the Gulf of Guinea between the latitudes of 1°40' and 13°05' North of the Equator and longitudes of 8°30' and 16°10' East of the Meridian. It is bordered with Nigeria to the North-West, Chad to the North-East, the Central African Republic to the East, Equatorial Guinea, Gabon and Congo to the South, and the Atlantic Ocean to the south-west. It has 402 km coastline, with 475,440 km² surface area which is divided into 10 regions. According to topographic and climatic information, the country can be divided into three climatic regions, Sahara dry climate, Savannah, and dry tropical (FAO, 2018). The Northern regions are mainly influenced by Saharan dry climate, with diminishing precipitation and vegetation changes from dense rain forest to savannah. This part of the country is characterized by dry tropical with arid periods that can last up to nine months and average precipitation varies from 300 to 900 mm per year. It contains two main lowlands, the Benue depression and the plains along Lake Chad.

Cameroon's biomass is resulting from various sources such as forest residues, wood waste, domestic and agricultural waste. This enormous biomass potential has is sufficient capacity for producing electricity. Hence, this renewable source could contribute about 40% of the total electricity demand in Cameroon

(Ackom et al., 2013). Other renewable energy sources such as solar energy have the largest potential estimated at 3491 hours per year with annual radiation of about 2045 kWh. m^{-2}/yr . in the far north region of the country (Fotsing et al., 2015). Furthermore, the annual average of global energy production from the solar energy source is estimated at 2327.5 TWh, which is about 20 times the hydropower potential of Cameroon (MINEE, 1990).

The current energy situation of Cameroon is characterized by an imbalance between demand and supply. In the 2000s, Cameroon faced an electricity crisis. From 2000 to 2006, the total installed hydropower plant capacity has been constant at 719 MW with an annual energy production of 3892 GWh as of 2006. In the same period between 2003 and 2006 a new thermal power plant was built in Limbe with a nameplate capacity of 85 MW, this increased the existing power station capacities for power plants located in Oyombang I and Logbaba. In 2006, the global capacity of thermal power plants installed by national utility company was 206 MW with an annual energy production of 255 GWh. The Kribi Gas-fired plant with 216 MW capacity was introduced to the network in 2013. However, in the past decades, the electricity generating systems in Cameroon exploits mostly non-renewable energy sources to overcome the national energy demand, which has serious impacts on the environment and public health, currently in Cameroon, there is no commercial thermal power plant which uses biomass waste to produce electricity. Only some isolated biomass thermal power plants (BTPP) have been developed by agro-industries such as SOCAPALM, SODECOTON, Cameroon Development Corporation (CDC), MAISCAM, FERME Suisse and SOSUCAM using palm-oil, cotton, maize, animal waste and sugar cane (Africa-EU Energy Partnership, 2014). Also, currently the country is not involved in research programs for the promotion of these renewable energies. This can be witnessed due to lack of official renewable energy policy in the country which can promote the use of these sources for a national program in the electricity production (Engelken et al., 2016; Abanda, 2012).

The challenges related to climate change, access to energy and the energy deficit in the sub-Saharan countries including the management of available energy sources are the major drivers for urgency to develop an energy policy program

which will help direct the future developments in the energy production sustainably. As a result, it is paramount important to set new targets to meet the energy demand of the population and the industrial sector. The economic boom of the countries is closely linked to progress in the energy sector. The issue of the management and use of decentralized power generation systems plays a key role, as there are so far many untapped or improperly exploited primary sources, despite the increase in the energy demand over the years. Cameroon's energy consumption increased from 2,697 to 6,922 TWh between 1990 and 2014, which corresponds to a growth of +157%. Despite the efforts made, such as the liberalization of the sector through the construction of new natural gas thermal and the heavy fuel oil power plants, to offset the existing energy demand, the country has continued experiencing energy deficit.

The usage of rural mini-power plants for the production of electricity and other forms of energy for industrial processes (drying and chilled water) contribute to improving the overall efficiency of the electricity sector and RE technologies. Hence, it is very important to identify these issues for better planning of Cameroon's energy policy in the renewable energy sector. The efficiency of conventional power plants using fossil fuel as a primary energy source is generally less than 39%. Therefore, much of the energy is lost as heat during the conversion process. This is the main reason integrated subsystems producing heat and cold have significantly increased the efficiency of combined plants by more than 40% (IEA 2008; Kerr, 2008). The units of the multi-generative small-scale systems, have an overall efficiency greater than 85%, with the capital expenditure (CAPEX) and the operating expenditure (OPEX) that have competitive cost compared to those of large power plants (Hinrichs, 2004; Onovwiona and Ugursal, 2006). Moreover, with the availability of new RE technologies, it is possible to optimize systems regardless of size. Therefore, for future problems, the following issues require special attention:

- Existing infrastructure should be used as long as possible to meet demand. One of the most effective ways of using existing infrastructures is to consider them as an integrated system in the planning and the

operations of the distribution system. If the infrastructures are integrated correctly, they can be implemented and managed sustainably.

- To make the systems more efficient, the newly installed plants must use the latest technologies that offer better technical and economic characteristics, while preserving the environment.

The power conversion between the different energy carriers establishes a coupling that corresponds to the economic and technical interactions resulting from the power flow. Thus, research on the implications of these economic and technical interactions on multi-generative and hybrid systems should cover all work related to the transport of energy. To date, there are several software being used for recent energy infrastructures installed across the globe for industry distribution systems (IRENA, 2012).

In 1998, the energy sector in Cameroon was liberalized for the benefit of energy end-users and independent power producer. The national electricity network of Cameroon is composed of three separate electricity networks – The South Interconnected Network (SIN), The North Interconnected Network (NIN), and The East Interconnected Network (EIN) mostly supplied by a thermal power plant. In 2008, the total electricity capacity of Cameroon infrastructures was 1413 MW which produced total annual electricity of 5552 GWh (Africa-EU energy partnership, 2012). The transport sector consumes around 7% of petroleum products and approximately 12% of the total energy consumption of the country (IEA Statistics, 2009). In 2009, Cameroon's government had initiated the emergency thermal program to reinforce the Southern Interconnected Network capacity with an additional of 100 MW in addition to a gas power plant at Kribi with a capacity of 216 MW which was expanded to 330 MW. In 2010, the total annual electricity production increased to 5834 GWh with an installed plants capacity of around 1925.86 MW. Cameroon has an on-grid total installed capacity of about 1324 MW, of which approximately two-thirds is hydropower and the rest is thermal (Nfah et al., 2008, 2009).

Currently, Cameroon has three main hydropower production dams, namely Songloulou with an installed capacity of 387 MW, Edea with an installed capacity of 263 MW and Lagdo on the Benue River has an installed capacity of 72 MW with three other dams devoted to reinforce the Edea and Songloulou power plants (SIE-Cameroun, 2011; Africa-EU energy partnership, 2012). The three remaining dams are respectively, Mbakaou constructed on Djerem River, the Bamendjin on Noun River and the Mape on Mbam River. Unfortunately, hydropower plant operates with a low production rate of 55%, especially during the dry season (Tamo et al., 2010). The rural areas and some districts in urban areas of the capitals cities are usually powered by isolated mini-grids of 24 kW to 6.4 MW, while the larger areas which include the regional and divisional capitals in the north, south, and east, are electrified using the three separate grids (Nfah et al., 2008, 2009). For example, the northern regions in Cameroon are electrified through the Northern Interconnected Grid (NIG) from the Lagdo hydropower dam and more than 14 MW thermal power plant. The Eastern Isolated Grid (EIG) is served generally by thermal units with a capacity of 24 MW (CEIP, 2013). The south, which includes large cities is powered by the Southern Interconnected Grid (SIG). There are approximately 26 isolated thermal units with a total installed capacity of 15.3 MW and total power output as of 2011 of 42,765 GWh. Currently, the government plans to lease some micro and Pico-hydropower projects to private investors to increase the share of hydropower for an equitable, integrated and sustainable development (ADEID). The rural population represents the majority of the population in Cameroon without access to electricity. The energy demand in Cameroon has continued remained unsatisfied by the utility company with the access rate to modern energy services remaining very low. Access to modern energy is represented by an average rate of 15% for electricity and 18% for domestic gas (IFC and WB, 2012; Abanda, 2012). Furthermore, the access to electricity is about less than 50% in urban areas against less than 10% in rural areas, which is a significant threat to the economy and improving the standard of living for the populations. The regions that suffer more from a lack of electrification are, the Adamaoua, East, Extreme North, North, North-West, and South-West, where the average rate of electricity access is 10% among the poor and 33% among non-poor populations (Africa-EU energy partnership, 2012).

- Low-energy households, mostly in the rural area requiring less than 70 kWh/yr. for lighting and radio communications,
- Medium-energy households requiring more than 80 kWh/yr. but less than 250 kWh/yr. for lighting, radio communications and television viewing,
- High-energy households, mostly in the urban area requiring more than 300 kWh/yr. due to television, network devices, computer, and other loads, such as refrigerator, water heaters, electric fans, etc. (Nfah et al., 2007).

The governmental documents intended for the implementation of energy policy in Cameroon does not indicate the provisions related to promoting renewable energies development. The legal and regulatory framework for renewable energies is essentially apprehended through the different texts of legislation relating to the electricity sector and their implementation decrees. Furthermore, there is a tendency to reduce energy to the exclusive notion of electricity, which does not include the regulations on the renewables energies sector. Despite the evolutions contained in the 2011 law governing the electricity sector, which devotes one section to renewable energies, the implementing legislation is still expected (Loi N° 2011/022, 2011). This law provides in the conditional tense the creation of an agency in charge of renewable energy promotion. Overall, the country's energy policy does not take into consideration the use of biomass and other abundant renewable energies (Tchatat, 2012). Hence, a lack of coordination among Cameroon's regulating bodies is the main obstacle concerning decisions and actions in this sector. Investigation of modern off-grid lighting technologies by Ngnikam, (2009) was found that PV products are largely absent in most of the market of Cameroon (Ngnikam, 2009). This is due to the weak development of this market, in both rural and urban areas, where there exists greater purchasing power. Most of the modern renewable products are imported from Asia, especially from China. Energy consumption in the rural areas is thus essentially structured around solid biomass technologies coupled with less efficiency and having high risks on human health (WHO, 2006). The government predicts the production of 2500 MWe by the use of hydroelectric power stations

and other forms of renewable energy, for the period 2012 to 2020. Table 1.3 presents Cameroon's installed capacity of power plants based on hydropower, biomass, biofuel and fossil in 2016.

Table 1.3. Installed power plants in Cameroon (Africa-EU Energy Partnership, 2014; IEA, 2016).

Project name	Project manager	Primary sources	Locaciton	Project capacity	Grid type
KPDC	Globeleq Energy hold.	Natural gas	Kribi	216.0 MWe	On-grid
DPDC	Globeleq Energy hold.	Heavy-fuel	Dibamba	86.0 MWe	On grid
MBANG / CHP	ROUGIER -CDM	Wood waste	Mbang/East	1.5 MWe	Off grid
	AES- sonel	Hydropower	Edea	263.0 MWe	On grid
	AES- sonel	Hydropower	Songloulou	388.0 MWe	On grid
	AES- sonel	Hydropower	Lagdo	72.0 MWe	On grid
	HYSACAM	Landfill	Douala/Ydé	60.0 MWe	-
	Others companies	Biomass	-	535.0 MWe	Self-grid
	Other IPP	Diesel/ Biomass	-	15.3 MWe	Off grid

Table 1.4 shows the current status of power station installed, it should be noticed that the hydropower will increase its capacity through the construction of Nachtigal and Mekin hydropower plant with a capacity of about 420 MW and 15 MW, respectively. At the end of 2020, the total capacity of hydropower is expected to increase to approximately 1230 MW, which is around 49.2% of the predicted capacity.

Table 1.4. Power station installed (outstanding) and available in Cameroon (Africa-EU Energy Partnership, 2014; IEA, 2016 and IEA, 2018).

Plant Type	Owner	Southern Interconnected Grid (MWe)		Northern Interconnected Grid (MWe)		Eastern Isolated Grid (MWe)		Total (MWe)	
		Installed capacity	Available capacity	Installed capacity	Available capacity	Installed capacity	Available capacity	Installed capacity	Available capacity
Thermal plant	AES-Sonel	308	254	29	26	12	10	349	290
Thermal plant	IPP	503	413	21	17	73	61	597	491
Hydro-power	AES-Sonel	687- 1668	599	72	61	0	0	759- 1740	660
Hydro-power	AES-Sonel underconst	420	0.0	0.0	0.0	15	0.0	435	0.0
Biomass	AES-Sonel	0.0	0.0	0.0	0.0	0.0	0.0	0.0	0.0
Biomass	IPP	0.0	0.0	0.0	0.0	0.0	0.0	0.0	0.0
Solar	AES-Sonel	0.0	0.0	0.0	0.0	0.0	0.0	0.0	0.0
Solar	IPP	0.0	0.0	0.0	0.0	0.0	0.0	0.0	0.0
Total		1321.0	1090.0	112.0	94.0	72.0	58.0	1505.0	1441.0
Demand			-		-		-		1611.0

To overcome the predicted energy deficit, the government announced the launch of thermal power plants construction for electricity generation using renewable energy sources as a raw material for the largest part. These recent technologies will be designed to integrate additive units for heating and cooling. These integrated systems will contribute to significantly increase the efficiency of the thermal power stations. Presently, the annual energy production has certainly evolved but the proportions and the quality of the production have not seen any real improvement. Thus, it is necessary and urgent for the government and the people living in the eastern and northern regions of Cameroon to develop alternative and sustainable solutions to contribute to sustainable development and rural socio-economic development.

1.4 Prime Movers

Thermal power plants can be classified according to type of prime movers (primary energy sources used for producing thermal energy). The biggest difference between thermal power plants lies in the technology of electricity production because it defines several parameters such as the overall efficiency of the system through the electrical efficiency and the output temperature of the residual fluids of the system. The technology selection generally depends on ecological and economic parameters as well as topographical and demographic site parameters.

1.4.1 Solar thermal power plants

A. Concentrating solar power technologies

Solar energy is the most abundant source of energy that can be implemented as a suitable alternative to fossil energy. It can be converted to electricity using two main technologies: photovoltaic (PV) and Concentrating Solar Power (CSP) which uses the thermodynamic cycles. However, the lifespan and efficiency of solar PV technology are less than for CSP technologies. Figure 1.1 shows a schematic of four main CSP technologies: Parabolic Dish (PD), Parabolic Trough Collector (PTC), Solar Tower (ST) and Linear Fresnel Reflector (LFR). However,

this study focuses on three common technologies as PTC, Solar Tower ST and Linear Fresnel LFR.

The first CSP technology was installed in the USA in 1982; after this first experience, there has been a rapid expansion worldwide. Currently, more than 100 CSP plants are operating across the globe. Many studies on the CSP technology announced a rapid development of this technology over the world, especially in Asia, Southern African countries and the Middle East and North Africa (MENA) regions.

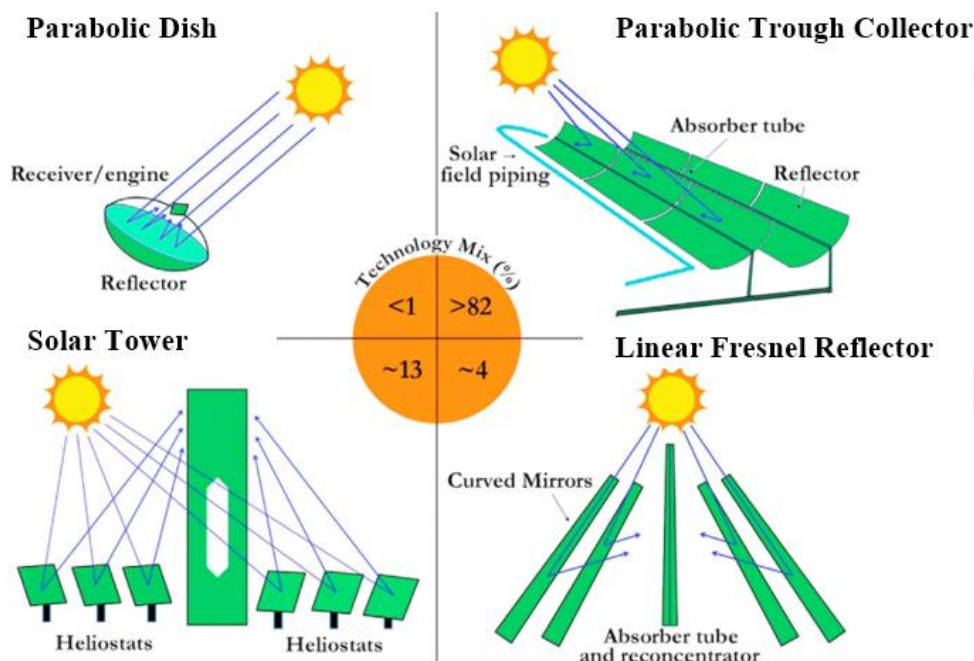


Figure 1.1. Concentrating solar power technologies (Xu et al., 2016).

The CSP technology is an ideal technology to produce electricity directly or to hybridize with existing thermal power plants presenting different types and levels of synergy depending on the hybridized energy source, the location of the plant, the thermal power technology used and plant configuration. Many parameters such as daily solar availability, water resource for cleaning, cooling, easy operation, and land are crucial for CSP plants development. For an economic analysis of the technologies used for CSP plant development a range of costs including capital cost, O&M costs, cost of land area, cost of water volume required and others are assessed during these studies. The LCOE of CSP plants is

an important factor to determine the suitable technology for an available direct normal irradiation in the location and a required investment cost which is approximately four-fifths of the total cost. The rest is the cost for operation and maintenance of the plant and others. Compared to other RE - thermal technologies, CSP has a high initial investment cost according to the specific technology used. This factor is closely related to the economic lifetime, the capital cost, the meteorological data, the plant's capacity factor, efficiency, O&M costs, and insurance. The minimum range can be achieved by varying the use of the thermal energy storage capacity and solar multiple values. Furthermore, according to recent research, the LCOE of RE technologies, in general, depends on the technology used, the renewable energy source availability and the country's energy policies. The CSP technologies can be classified into one or two-axis tracking system. However, this study focuses on only the three common technologies in this field: Parabolic Trough Collectors (PTC), Solar Tower (ST) and Linear Fresnel Reflectors (LFR) technology. The PTC consist of solar collectors (mirrors) with receivers and support structures. The parabolic-shaped mirrors are constructed by forming a sheet of reflective material into a parabolic shape that concentrates incoming sunlight onto a central receiver tube at the focal line of the collector. The arrays of mirrors can be 100 meters or more, with the curved aperture of 5 m to 6 m. A single-axis tracking mechanism is used to orient both solar collectors and heat receivers toward the solar trajectory.

For all the technologies, the solar radiation, land and water requirement were found to be 2045 kWh/m², 5–7 acres/MW and 4 m³/MWh, respectively. The PTC and LFR technologies are suitable for commercial power generation capacities between 10 and 200 MW and ST technology for capacities from 10 MW to 150MW (Ahmadi et al., 2018). Furthermore, both PTC and ST are mature technologies for electricity production, but PTC is the most proven mature technology used in the CSP power plant projects. The LFR is in the demonstration stage due to its lower utilization despite a low installation cost compared to other technologies. The ST is regarded as the most efficient technology used for commercial CSP plants; it is expected to reach a 50% better efficiency than other technologies.

The PTC is one of the CSP technologies containing a large number of mirrors used to reflect solar radiation. The collector field contains loops with more than one solar collector assemblies (SCA) each, and are placed in parallel rows aligned on a north-south axis to track the sun as it moves from east to west to maximize the collected thermal energy. The tracking system aims is to ensure that the solar radiation is continuously focused on the absorber pipes located in the receiver. The receiver or absorber tube has to achieve the maximum absorbed solar irradiation and reduce the heat losses in the receiver during this process to transfer a significant amount of heat to the heat transfer fluid (HTF) which move through the receiver. The HTF is circulated through the absorber tubes to collect the solar energy and transfers it to the steam generator or the heat storage system. However, depending on the type of steam generation systems and thermodynamic cycle used to generate electricity, the heat transfer fluid can be water, Thermal oil, Diphenyl oxide, Therminol VP-1, Xcelterm-MK1, Molten salt and other HTFs which are a kind of mixture with different percentage.

The absorber has to be designed with a high absorption coefficient through its focal line, to ensure an efficient heating process of the working fluid. Contrary to the output heating value of the HTF which depends on the parameters like a local direct normal irradiation (DNI), absorption and emittance coefficient and others, its output temperature value is related to the type of thermal oil used for the heat transfer process. The solar-to-electric efficiency depends on the amount of annual energy production, the field layout and the local DNI value which is generally around 15% for the CSP system using PTC technology while the power block efficiency depends on the output temperature of heat transfer fluid (Fernández-García et al., 2010).

When the solar field system is integrated with a steam turbine power plant, the process is called direct steam generation (DSG) technology and uses water/steam as a heat transfer fluid. Otherwise, if the transfer fluid is not water and an intermediate heat transfer system is used to connect the solar field and the power block, the technology is called indirect steam generation (ISG) using water as working fluid (IEA, 2010; Philibert, 2010). The biggest advantages of the ISG system are that the heat transfer fluid such as molten salt can be stored and used during periods of less availability of sunlight. The thermal energy storage system

can be built anytime to generate electricity during the night whereas the operation and maintenance works can be done in a short period without a negative impact in energy production. The major disadvantage is its initial investment and O&M cost, which are influenced by the use of the IHE and thermal energy storage system. PTC technology is the most widely used for CSP power projects. The technology was developed in 1912 in Egypt, and the first commercial CSP plant using PTC was installed in Grenada, 2008 named Andasol-1 (Ummadisingu and Soni, 2011). Table 1.5 presents some characteristics such as capacity, power cycle, steam generation technology, heat transfer fluid, thermal energy storage, total investment, annual energy production, aperture area of solar field, number of loops, number of solar collector assembly per loop, type of collector used for the installed concentrating solar power plants based on PTC.

Most existing PTC technologies use synthetic oils as heat transfer fluid which are stable up to 400°C. New plants under demonstration use molten salt at 540°C either for heat transfer and/or as the thermal storage medium. High-temperature molten salt may considerably improve the thermal storage performance. The solar field is by far the largest cost component and accounts for between 35% and 49% of the total installed costs of the projects evaluated. The price of a solar collector is mainly determined by the cost of the metal support structure (10.7% of the total plant cost), the receiver (7.1%), the mirrors (6.4%), the heat transfer system (5.4%) and the heat transfer fluid (2.1%). The use of PTC in a thermal power plant without thermal energy storage (TES) has an installation cost per kW as low as 4 600 USD/kW, but with a low capacity factor between 0.2 and 0.25. Once six (6) hours of TES system are added, the installation cost per kW increases considerably and it is ranged between 7100 USD/kW and 9800 USD/kW, which allows capacity factors to be doubled. The lower cost of energy for solar thermal power plant using a PTC technology today lies in the range of 0.20 USD/kWh to 0.36 USD/kWh, but this depends on the area where the plant will be developed, because a site with excellent solar energy sources could contribute to decreasing the LCOE as low as USD 0.14 USD/kWh to 0.18 USD/kWh (IRENA, 2012).

Table 1.5. CSP technology using parabolic trough collector technology (NREL, 2019).

Power Plant Name	Country, date	Capacity (MW)	An. energy prod. (GWh) Yearly DNI	Area aperture, m ²	Number of loop (SC)	Collector technology (length)	Power Cycle	Heat Transfer fluid	TES system (HTF)	Investment cost. Million	Cost per kW installed
Xina Solar 1	South Africa, 2018	100	400	-	-	-	ISG-SRC	-	5.5hr. M-S	880M. USD Operational	8800
Shams 1	UAE, 2013	100	210 (1934)	630000	192(4)/12mod	Euro Trough	ISG-SRC(400-300C, 100bar)	Therminol VP-1	None	600M. USD operational	6000
Kaxu solar one	South Africa, 2015	100.0	300	800 000	300(4)/10mod	Sener Trough	ISG-SRC(393-293C, 100bar)	Thermal Oil	2.5 hr. M-S	860M USD Operational	8600
Termosol 50	Spain, 2011	50.0	175 (2097)	510 120 (817)	156 (4)	Sener Trough	ISG-SRC(393 - 293C, 100bar)	Diphenyl oxide	7.5 hr. M-S	270M Euros Operational	6300
Shagaya	Kuwait, 2017	50.0	180	-	-	-	-	-	10 hr. M-S	385M Euros Underconst.	9400
Acrosol	Spain, 2011	49.9	175 (2097)	510 120 (817)	156 (4)	Sener Trough	ISG-SRC(393-293C, 100bar)	Diphenyl oxide	7.5 hr. M-S	270M Euros Operational	6700
Bokport	South Africa	50.0	230	588 600	-	Sener Trough	ISG-SRC(393-293C, 100bar)	Dowtherm A	9.3 hr. M-S	565M. USD Operational	11 300
Olivenza	Spain	50.0	100	402 200 (545)	123 (6)	(Sunfield) Siemens	ISG-SRC (393-293C)	Thermal Oil	None	264M Euros Operational	6970
Orellana	Spain	50.0	118	405 500	124 (4)	Sener Trough	ISG-SRC (393-293C)	Thermal Oil	None	240M Euros Operational	6050
Moron	Spain	50.0	100	380 000	116 (4)	-	ISG-SRC (393 - 293C, 100bar)	Thermal Oil	None	265 M.USD Operational	5300
Megha Solar plant La Africana	India	50.0	110	366 240 (817)	112 (4)	Euro Trough	ISG-SRC (393-293C)	Xceltherm MK1	None	285M USD Operational	5700
Andasol 1,2,3	Spain	50.0	175 (2 200)	510 120 (817)	156(4)/12mod	AT 150	ISG-SRC(393 - 293C,100bar)	Dowtherm A	7.5 hr. M-S	315M Euros Operational	6300
Agua Prieta II	Mexico	12.0 (14 .0)	34	85 000 (817)	26(4)/ 12mod	Euro Trough	-	Thermal Oil	None	- Operational	-
Archimede	Italy	4.72 (5.0)	9.20 (1936)	31 860	9(6)/ 8mod	Luz LS-3	ISG-SRC (550 -C, 98bar)	Molten salt	8 hr. M-S	- Operational	-
Thai solar energy	Thailand	5.0	8	45 000	19 (4)	Sky fuel sky-Tr.	ISG-SRC(340 - 210C, 30bar)	Water/steam	None	- Operational	-

The ST technology is one of the most used technologies for the CSP Plant which use a ground-based field of mirrors to focus direct solar irradiation onto a receiver mounted high on a central tower where the light is captured and converted into heat. The heat drives a thermodynamic cycle, in most cases a water-steam cycle, to generate electric power. The solar field consists of a large number of computer-controlled mirrors, called heliostats that track the sun individually in two axes. These mirrors reflect sunlight onto the central receiver where a fluid is heated up. ST technologies can achieve higher temperatures than PTC and LFR technologies because more sunlight can be concentrated on a single receiver and the heat losses at that point can be minimized. This is the main reason that made it popular in the thermochemical process. The receiver uses various types of materials such as ceramics and metals which are the most known in these areas to generate high temperature.

Table 1.6 presents characteristics of the installed concentrating solar power plants based on ST technology such as capacity, location, power cycle properties, heat transfer fluid, thermal energy storage, total investment, annual energy production, aperture area of solar field, number of heliostats installed, tower height and type of receiver.

To operate efficiently, the heat transfer fluid or working fluid used to run the power block should receive an average solar flux between 200 kW/m^2 and 1000 kW/m^2 impinging receiver through a glass (Benoit et al., 2016). Furthermore, ST technologies are flexible for electricity generation; a commercial Solar Tower Power Plant (STPP) can use both direct and indirect steam generation system. Generally, fluids as Helium, Water/steam, and air can be used for DSG system and others like molten salt, Water/steam and thermal oil can be used for ISG system (Alexopoulos, 2010). According to data recorded by the National Renewable Energy Laboratory (NREL), commercial STPP uses mostly for their power block a steam Rankine-cycle to generate electricity due to its maturity in term of application. Thus, solar towers use water, air or molten salt to transport the heat to the power block system.

Table 1.6. CSP technology using solar tower technology (NREL, 2019).

Name	Country, Date	Capacity (MWe)	Annual energy production (GWh) and Yearly DNI (kWh/m ²)	Area aperture (m ²) and Tower height (m)	Number of heliostats	Receiver type	Power cycle	Heat transfer fluid	TES system (HTF)	Investment cost (Million)	Cost per installed kW (USD/kW)
Golmud	China, 2018	200.0	1120 (2158)	-	-	-	-	Molten salt	15hr. M-S	839 MUSD Underconst.	4200
Ivanpah	USA, 2014	377.0	1079 (2717)	2600000 (140)	173500	- 140 m	SR (1050-480F, 160 bar)	Water / Steam	None	2.2 BUSD Operational	5835
Crescent Dunes Solar	USA, 2015	110.0	500 (2685)	1197180 (195)	10347	External cylindrical	SR (1050 -550F, 115 bar)	Molten salt	10 hr. M-S	- Operational	-
Ashalim	Israel, 2017	121.0	175 (250)	1052480 (250)	50600	-	-	Water / Steam	None	- Operational	-
Khi Solar One	South Africa, 2016	50.0	180	576 800 (200)	4120	-	SR	Water / Steam	2 hr. M-S	- Operational	-
SupCon Solar	China, 2018	50.0	120	434880 (80)	217440	-	SR	Molten salt	6 hr. M-S	270 MUSD Underconst.	5400
Gema solar	Spain, 2011	20.0	80 (2100)	304000 (140)	2650	Cavity140 m	SR (595 – 290)	Molten salt	15 hr. M-S	230 MUSD Operational	11500
Shouhang Dunhuang	China, 2016	10.0	100	175375 (138)	11525	-	SR	Molten salt	15 hr. M-S	68 MUSD Operational	6800
Planta Solar	Spain, 2007	11.0	23.4 (2012)	75000 (115)	624	Cavity	SR (595 – 290°C,45 bar)	Water / Steam	1 hr. M-S	- Operational	-
Sierra Sun Tower	USA, 2009	5.0	2629	27670	24360	Dual cavity	SR (440 - 218°C)	Water / Steam	None	- Operational	-

Depending on the receiver design and the type of working fluid, the upper working temperatures are expected to range from 250°C to 1000°C for future plants, although temperatures of around 600°C are the norm with current molten salt technology.

Due to the high operating temperature, the annual solar-to-electric efficiency of solar tower power plant varies from 20% to 35% (Müller-Steinhagen and Trieb, 2004). This efficiency depends on the mirror's tracking system accuracy, optical characteristics of heliostat and the cleanliness of the mirror. Many research findings highlight that for ST technology to be economically viable and profitable, it must be built in a large size. However, in terms of hybridization, it is the major technology for a large conventional thermal plant as a coal-fired plant. The typical size of today's solar tower plants ranges from 10 MW to 50 MW and can be extended according to project size. However, increasing the solar field size leads to a greater distance between the receiver and the outer mirrors of the solar field. Solar towers have some potential advantages such as the higher temperatures operating which allow greater efficiency of the steam cycle and reduce water consumption for cooling the condenser.

Solar towers might become the technology of choice in the future because they can achieve very high temperatures with manageable losses by using molten salt as a heat transfer fluid. Thermal plants using this technology can cost between 6300 and 10500 USD/kW when energy storage is between 6 and 15 hours. These plants can achieve capacity factors of 0.40 to as high as 0.80 (IRENA, 2012). Table 1.7 summarizes some characteristics of the installed concentrating solar power plants based on LFR technology such as capacity, location, power cycle, heat transfer fluid, thermal energy storage, total investment, annual energy produced, aperture area of solar field, number of installed loops, number of solar lines assembly per loops, the type of linear reflector.

Table 1.7. CSP technology using linear Fresnel reflector technology (NREL, 2019).

Name	Country, Date	Capacity (MWe)	Annual energy production (GWh) and Yearly DNI (kWh/m ²)	Area aperture (m ²)	Number of liines	Linear reflector (length)	Power cycle	Heat transfer fluid	Thermal energy storage system	Investment cost and Status	Cost per installed kW (USD/kW)
Dadri ISSC plant	India, 2017	14.0	-	33000	-	-	DSG-SRC (250 C -)	Water	None	- Operational	-
eLLo Solar	France, 2018	9.0	20.2	153000	27	(340m,14m)	SRC (285 -190C, 70bar)	Water	1 hours Molten salt	- Operational	-
Kimberlina	USA, 2008	5.0	500 (2685)	26000	3	Compact LF (385m,2m)	SR (300C, 40bar)	Water	none	- Operational	-
Dhursar	India, 2014	125.0	280	-	-	-	-	-	None	316 M USD Operational	2525 USD/kW
IRESEN	Morocco, 2016	1.0	1.7	11400	-	-	ISG-ORC (300-180C)	Mineral Oil	0.33 hr. Molten-salt	6.42 M USD Operational	6420 USD/kW

LFR technology is similar to PTC consisting of an array of linear mirrors in series of long flat or slightly curved placed at different angles, with a tracking system, process and instrumentation system, receivers and metallic structure to concentrate the sunlight on either side of a fixed receiver. Each line of mirrors is equipped with a single-axis tracking system and is optimized individually to ensure that sunlight is always concentrated on the fixed receiver. The receiver consists of a long, selectively-coated absorber tube.

Unlike PTC, the focal line of LFR collectors is distorted by astigmatism. Moreover, the mechanism of reflectors is the same as that used for a Fresnel lens. The sun's rays are reflected by a Fresnel lens on a linear receiver supported by metallic structures. The linear receiver shaped like a long cylinder which contains many tubes filled with heat transfer fluid. But, its annual solar-to electricity efficiency is between 8 and 10% lower than parabolic trough collectors.

Comparing to other CSP technologies LFR presents an advantage in terms of initial investment cost due to the possibility of using very cheaper flat glass mirrors, less steel, and concrete, as the metal support structure is lighter. Furthermore, the cost of mirror area per receiver is cheaper in PTCs than in LFRs, given that the receiver is the most expensive component in both PTC and LFRs. The wind loads on linear Fresnel technology are smaller, resulting in better structural stability which affects the system efficiency and O&M expenditure through the reduction of optical losses, less mirror-glass breakage, and an easier assembly process. The cost per kW for LFR installation is lower than PTC and ST technologies, but the technology is less mature compared to others. The largest CSP plant using LFR technology with a capacity of 125 MW and an annual energy production of 280 GWh is in India.

B. Heat transfer fluids

The heat transfer fluids can be classified using their original states of matter at normal operating conditions. Generally, there exist three groups of HTF corresponding to the standards states (gaseous, solid and liquid) that can undergo a phase change or supercritical fluids during thermal operating processes. The

HTF is a key component of STPP because it determines the suitable cycle used for power block and TES technology that must be used to increase their performances.

Tony (2009) and Heller (2013) presented the main factors required for consideration in the heat HTFs selection as follow:

- Excellent thermal stability and resistance to degradation due to excessive temperature
- Good relationship (established by a well-known correlation) between vapor pressure and temperature
- High availability and low cost
- Able to operate at low pressures
- Enable to use as working fluid
- Enable to use for TES system with high density and heat capacity decreased
- Low freezing point (low temperature for solidification)
- Low corrosivity (Compatibility with the materials of construction)
- Low viscosity and high specific heat capacity (for vapor systems a high latent heat capacity) that allows a suitable work of pumps and other components used in the HTF system.
- Friendly environmental characteristics (low toxicity, flammability, explosivity, and environmental hazard)
- higher temperature limitation (evaporation temperature/thermal stability limit)

The liquid heat transfer fluids family that is commonly used in CSP technologies include thermal synthetic oil, water-steam, molten salts, and liquid metals. This family contains the heat transfer and working fluids used by existing commercial CSP power plants. Almost all commercial STPP working with the parabolic trough collector as solar concentrating technology of solar field use thermal oil as heat transfer fluid. Whereas the STPP working with Heliostats field use molten salts or water-steam steam as HTF. Therefore, it is important to mention that, water as a working fluid is generally selected for power generation independently to CSP technology (NREL, 2018).

The use of gaseous and solids materials as heat transfer fluids are in the experiment stage. However, many studies have been conducted including their utilization as a key component of improving power cycle efficient. The gaseous family can be classified as, supercritical fluids (Air, CO₂, He, H₂) and pressurized gas (s-CO₂, s-H₂O). The solid particles suspension used as heat transfer media in the pressurized volumetric receiver of Solar Tower technology is considered as a type of solid heat transfer (BAUD, 2011). An investigation on the usage of HTF in solar fields' forms has been conducted by Benoit et Al. (2016), to determine the suitable HTF according to the cycle efficiency range. The authors concluded that, between 35% and 40%, current liquid and two-phase HTFs can be used. However, considering cycle efficiency above or equal to 50% for new HTFs that may be stable at temperatures above 700°C there is a need for further investigation. Supercritical water, carbon dioxide, pressurized gas, liquid metals, and new molten salts are some of the new potential heat transfer fluids. To increase the Steam Rankine Cycle efficiency for a solar thermal power plant using PTC, many studies suggest the usage of molten salts instead of synthetic oil which has a limitation in temperature. In 2012, Yu-Ting et Al. (2012), did an investigation on the use of molten salts to obtain its behavior during an experiment to create a forced convective heat transfer in a circular tube. The research was conducted to obtain a convective heat transfer coefficient of the studied molten salt mixture (53wt% KNO₃ -7wt% NaNO₃ - 40wt%NaNO₂) commercially named HITEC for turbulent and transition flow at high temperature. The study concluded that existing correlation can be applied to molten salts at high temperatures to determine convective heat transfer key values. In a similar work, the assessment

of heat transfer fluids was carried out to determine the suitable fluid for each plant according to CSP technology (Becker, 1980). During the experiment, typical HTF such as HITEC molten salt mixture, Thermal oil, Air, Water-steam, Hydrogen, and Helium were assessed to determine their thermal and transport properties such as convective heat transfer coefficients, Nusselt's number times thermal conductivity ($Nu.\lambda$) and volumetric heat capacities.

- **Synthetic thermal oil**

The HTF is an essential component in a solar thermal power plant because it has a direct impact on the efficiency of the receiver tube. It is also important because it is applied in the selection of the thermodynamic cycle, the storage technology and the determination of the performances that could be acquired. The operating temperature of a solar thermal plant is mainly limited by the stability of the thermophysical properties of the HTF in the receiver tube. The synthetic thermal oil, commonly used in the receiver tube comes in various mixture types. These are generally known under the following brand names, Therminol VP-1, Therminol D-12 and Dowtherm A (Evangelos et al, 2017; Malika et al., 2013). The synthetic thermal oil is a very proven HTF used in factories and some commercial facilities such as the SEGS plant in California, which for two decades have been operating without any major problems. However, many anomalies such as hydrogen build up in the vacuum of the glass cover, usually increases the heat losses of the tube receivers which were discovered in many absorber tubes of the SEGS plant. When the synthetic thermal oil reaches temperatures above 400 ° C, the hydrocarbons decompose rapidly and produce hydrogen, which would reduce the lifetime of the HTF and cause the accumulation of sludge and other byproducts that decrease the efficiency of heat transfer of the system and increasing maintenance costs (Benoit et al., 2016; Guo et al., 2016). It should be noted that the adoption of synthetic thermal oil as HTF limits the upper temperature of the thermodynamic cycle to 400°C, such that the expected efficiency is limited to about 38%.

- **Water and steam**

For higher operating temperatures requirements, conventional HTF such as molten salt or synthetic oil require replacements. In addition to the high temperature which leads to frequent replacement of synthetic oil, the following three other major issues must be considered for the research and development industries working on the HTF for the CSP plants;

- Simple operation and security,
- A simple storage concept,
- A low cost without toxins.

The steam Rankine cycle (SRC) is used mostly by commercial solar power plants. In this technology, water is used as a transfer fluid that passes inside a tube or volumetric receiver according to concentrating solar power (CSP) technology used. During this process, water evaporates directly into the receiver to produce steam (Giglio et al., 2017). During the operation process, the water in its liquid state flows through the cylindrical tube or volumetric receiver, absorbs the concentrating solar rays from the solar field (active area), and then this water undergoes a gradual phase change from liquid-vapor to saturated vapor and finally to superheated steam. The direct steam generation (DSG) system continues to be extensively researched in many European countries due to the various advantages this technology offers for electricity generation (Lüpfert et al., 2006). DSG systems are characterized by the simultaneous use of water as a transfer and working fluid. Its advantages compared to existing commercial facilities that adopt synthetic thermal oil as a transfer fluid lies in the fact that, it can reach very high temperatures, thus allowing high thermal efficiencies in the power block (Abengoa Solar, 2018). The CSP plant using PTC technology has been developed at the Solucar platform by Abengoa Solar since 2009 to experiment the use of the DSG system.

- **Molten salt**

Many studies have been conducted to improve HTF to reach higher operating temperatures and reduce the cost related to their application in solar thermal power plants. Several studies have been conducted by researchers and industrialists on the development of advanced fluids that could operate at temperatures higher than the current fluids levels, the studies were aimed at increasing the cycle efficiency without sacrificing other parameters such as cost reduction or energy production quality (Hofmann et al., 2016). Molten salts are mixtures of salts, which are used as HTF in solar thermal applications because of their chemical characteristics. Sodium-potassium nitrate is widely used in CSP technology for both heat transfer and thermal energy storage, their composition is expressed in mass fractions: 60-50% by weight of NaNO_3 + 40-50% by weight of KNO_3 (Taylor et al. 2011). It is important to note that the composition of molten salts impacts the characteristics of its heat transfer capability (Nunes et al., 2016).

Pacheco et al, (2002) exploited the main challenge of molten salt for its application in STTP using PTC technology, to help increase the operating temperature and decreasing of the solar field's size (Pacheco et al., 2002). To evaluate the feasibility of using molten salt as HTF in a tube receiver, an experimental scale was set up in Italy (Richert et al., 2015). The conducted experiments have shown that it is convenient to use molten salt as an HTF for a CSP plant using Parabolic Trough Collector (PTC) technology.

However, it is important to consider sophisticated approaches to prevent molten salts from freezing inside receiver tubes. Also, several kinds of research were initiated by Abengoa Solar's company to develop a test loop for the evaluation of certain molten salts as heat transfer fluids (HTF), which can allow the CSP plant using PTC technology to operate at temperatures of about 500°C (Zarza et al., 2004). Another study which was conducted by Du et al. (2016) has shown that molten salts exhibit higher thermophysical properties at higher temperatures: very low vapor pressure, high thermal stability, high density, and large specific heat capacity. Also, molten salts have other advantages which makes it economically viable and environmental friendly HTF. These advantages

include abundant of resources at low cost, pollution-free and non-flammable compared to synthetic thermal oils (Pramod et al., 2016). The main disadvantage of molten salts lays in its high melting point which results in operating and maintenance costs for frost protection. The synthetic thermal oils used in commercial solar power plants freeze at about 15°C, while the ternary and binary molten salts freeze at a temperature range between 100°C and 230°C (Ren et al., 2016).

With regards to maintenance and operations O&M expenditures, it is important that operators ensure that freezing molten salt does not occur in a solar field, because this situation can cause a severe damage to a fluid transport system's component such as receivers, valves, ball joints and pumps (Coscia et al., 2013).

1.4.2 Biomass based power system

Tables 1.8 and 1.9 present comparisons of some biomass technologies such as gasification, combustion and co-firing, which use various prime movers or combined prime movers for electricity generation. Gasification is the most recent technology in terms of biomass conversion to energy. This technology has the particularity to add some complexity to the traditional Combustion system, making it more expensive. The process consists of burning the wood feedstock in an environment with less oxygen to create volatile pyrolysis gases, such as hydrogen and carbon monoxide. These gases are then released into the gasification chamber. The resulting gas is called syngas, after the fuel is fed into the gasification chamber, a gasifying agent is introduced into the system. The syngas is released from the gasification chamber after an interaction between the fuel and gasifying agent. The syngas can be treated in two different processes. The first treatment consists of mixing the syngas with pure oxygen gas or air to produce heat through combustion. The produced heat can be distributed externally or sent to a boiler to produce energy for distribution. The second treatment is to cool the syngas to filter and purify it, during this process tar and particles can be removed as much as possible, then it can be used as fuel for gas turbines and combustion engines. Hence, the formation process of the syngas has remained the

same. The main types of gasifier reactors can be classified as, fluidized bed, fixed bed, entrained flow, and a rotary kiln. Each type has its requirements set in terms of thermodynamic properties and gasifying agents. Furthermore, these reactors vary also with a process consisting of the way used to introduce the gasification agent in the fuel, but the output is generally the same. Gasification plants can vary in capacity with the boiler's sizes, hence for commercial utilization capacities often vary approximately between 20 MW and 50 MW. Although small sizes with a capacity of 30 kW exist. The combustion and combined heat and power (CHP) is the most used technologies to generate electricity from biomass using conventional boilers. These boilers can burn waste wood products from agriculture and wood-processing industries. Often the raw materials are transported using augers or conveyor belts to the combustor. The heat created during combustion is transferred to the boiler which contains water, the generated steam water is converted to electrical power by steam turbines. CHP is used to capture the heat that would otherwise be wasted as hot water and non-saturated steam during the electricity generation process and used for space heating, cooling, and industrial purposes. CHP technologies can be classified into two main categories: "topping cycle" and "bottoming cycle." The common type of CHP is the "topping cycle," where fuel is firstly used to generate electricity and a part of the waste heat is used to provide useful thermal energy.

According to the existing commercial plant with prime movers such as steam turbines, gas turbines, reciprocating engines, microturbines, and fuel cells can also be classified. The co-firing technology can be used for biomass thermal plant, it replaces a portion of the fuel in coal-fired boilers with biomass. This technology has been successfully used in most boiler types, including cyclone, spreader stoker units, pulverized coal, and fluidized bed. The particularity of co-firing is low consumption of raw material during the conversion of biomass to electricity by adding biomass as a partial substitute fuel to coal boilers. Figure 1.2 presents a diagram of multi-criteria method for the biomass technology selection.

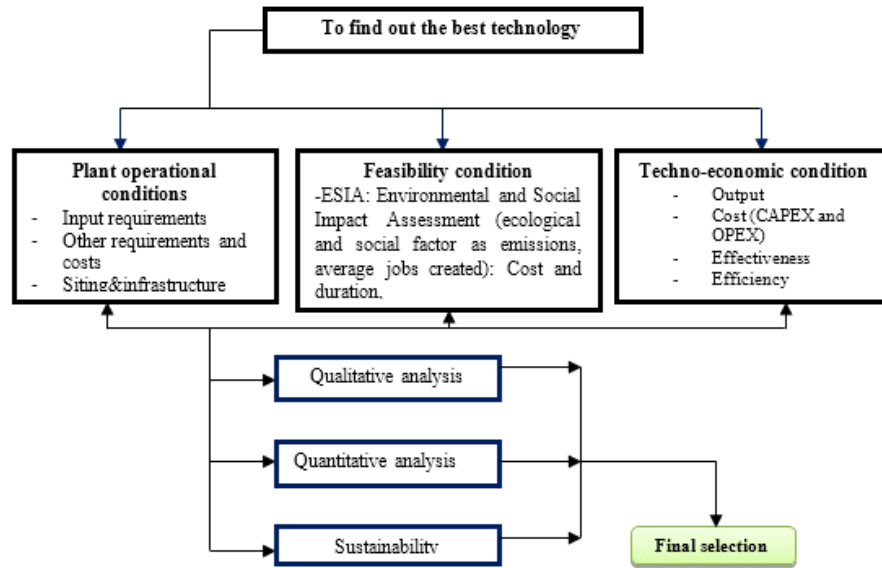


Figure 1.2. Analytical structure of the technical phases involved in the selection of suitable biomass-fired technology for the electricity generation.

Table 1.8. Comparative analysis of biomass power technologies based on plant operational conditions and techno-economic criteria.

Technologies	Combustion	CHP	Gasification	Co-firing
Input requirements	Woodchips < 20% moisture, and agricultural waste	Woodchips and agricultural waste	Woodchips, logwood, wood pellets or oven-dry wood< 30% moisture with best results at lowest moisture	Greenwood and dry sawdust (<2'' diameter)
Output	Steam, electricity	Steam, electricity	Gas ¹	Electricity
Prime mover for electricity generation	Turbine	Turbine	Engine (less than 10MW) Turbine (up to 10MW)	
Efficient	20 -25% ²	75-80% ³	15 - 45%	33-37%
Waste	Bio-char, particular matter, CO2 and tar at certain temperatures. ⁴	Bio-char, particular matter, CO2 and tar	Biochar, tar, particular matter, CO2, ammonia, sulphuric/hydro chloric acid, water/condensate	Particular matter, CO2, sulphur dioxide, nitrogen oxides.
Requirements and costs	cost of a Combustion system is the least expensive among other biomass conversion technologies -Investment cost can be between \$1,800 and \$4,200/kW	cost of a CHP system depends on the complexity of prime movers (heat recovery or emissions monitoring systems) - Investment costs are typically in the range of \$3,500 - \$6,800/kW. The economic viability of CHP depends on their safety level and ability to reliably ⁵	more expensive than combustion boilers; fixed and fluidized bed gasifiers require - investment costs of \$2,140-\$5,700/kW, which can be anywhere from \$1,200 to \$3,800/kW more than combustion boilers	Fuel supply is the most important cost factor. Investment cost depends on location, power plant type, and the availability of low-cost biomass fuels. If wood needs to be dried, size needs to be reduced, or the boiler requires a separate feeder cost can be increased significantly (\$150 to \$300/kW) of biomass generation system. Cyclone boilers technology offer the lowest cost \$50 per kW
Incentives	- Investment tax credit of up to 17% -Production tax credit: Yes	- Investment tax credit of up to 23%. -Production tax credit: Yes	- Investment tax credit of up to <15%. -Production tax credit: No	- Investment tax credit of up to <%. -Production tax credit: No

¹ US EPA, 1997,

² US EPA, 2018

³ Subpart 201-3. Permit Exempt and Trivial Activities. Subchapter 201-3.2 Exempt Activities.

⁴ Partnership for Policy Integrity, 2014

⁵ IRENA, 2012

Table 1.9. Comparative analysis of biomass power technologies based on environmental and social criteria.

Technologies	COMBUSTION	CHP	GASIFICATION	CO-FIRING
Environmental Utilization of woody biomass as a feedstock produces many types of emissions, dominant among them are CO ₂ and PM. [1]	To prevent contamination of the surrounding environment, we have to add that: Combustion and CHP technologies deal with waste steam water.	Requires the least complex pollution control equipment. The use of enhanced combustion air systems decreases considerably air pollutant.	Produces tar in addition to ash. But tar is difficult to prevent and even more difficult to discard properly. Furthermore, it produces numerous air pollutants, including nitrogen oxides, and carbon monoxide in addition to PM and CO ₂ .	The amount of CO ₂ emitted per unit of energy generation depends on the efficiency of the BPP and the amount of feedstock.
Policy-based incentives Ownership type Eligibility criteria others	-	-	-	-
Social Health Safety Job creation Others	higher air pollution potential and higher traffic hazards associated due to increased movement of trucks due to the BPP efficiency.	Movement of trucks increases the risk of accident in the region. The number of jobs created depends on the type technology used and operating cost of the plant (transportation, O&M, and feedstock treatment). approximately 2 jobs for each 1 MW	Problems related to health issues can arise considerably from PM emissions and other pollutants generated during the plant's operations	Job creation in the locality depends on local human resource and preferred skills (skilled and semiskilled jobs). Otherwise, CHP and Combustion created a higher number of unskilled or semiskilled jobs.
Siting and infrastructures Site requirements Land use Water use	Combustion and gasification plants require easy connectivity to local grid for electricity offtake along with a good transportation network for raw material	Requires a good quality of connectivity to the local grid for electricity offtake as well as the appropriate infrastructure to distribute the heat and transportation network for raw material. the water supplied for district heating as steam is not recovered completely	The boiler feed water of Combustion and gasification plants can be recovered and recycled to an extent of more than 95%	
Plant operational The efficiency of the plant is closely linked to the feedstock requirement	The amount of feedstock used for running a plant is inversely proportional to the BPP's efficiency.	CHP is a very efficient and competitive technology because it requires less feedstock and	Gasification and co-firing exert a considerable amount of stress on the surrounding forests.	-

1.5 Solar-Biomass Hybrid Energy Systems for Multi-energy Generation

A solar – biomass hybrid energy system combined with multi-energy generation for numerous purposes refers to the use of two sources of input energy. Mostly electricity, cooling, heating are the main purposes and can be accompanied by other purposes such as freshwater, hot water, and air. Multi-energy generation purposes match with a power plant, residential application and industrial processes where various energy outputs are required. The needs and requirements of the location have to be known before any work related to modeling, analyzing and optimization of the hybrid solar – biomass systems. Currently, there are few studies on modeling, analyzing and optimization of combined solar – biomass hybrid energy system with multi-energy generation. These systems may contribute to the rational usage of available energy source and present a major solution for the global warming problems.

For a better understanding of the proposed solar – biomass hybrid energy system for multi-energy generation, it is essential to highlight the main different technology adopted for the hybridization of primary energy sources. It is also essential to describe the different methods used to achieve the proposed multi-energy generation system. Figures 1.3 and 1.4 present the schematic of solar – biomass hybrid energy system using combined Rankine cycles (CRC) and multi-energy generation system which provides cooling, heating, and water, based on the heat recovery steam generation (HRSG) system. The HRSG system is connected to power block and considered as a dispatching point of heat required for additive subsystems able to respond to a specific purpose. This system contributes to increasing temperature and produces a phase change of the high-pressure water to non-saturated steam water ready to be transferred to a boiler or an intermediate heat exchanger (IHE). The low – pressure steam water from HRSG system is transferred as an input into the generator of a single effect absorption chiller, which is working with lithium bromide/water (LiBr/H₂O) to produce the required cooling. The other part of this low – pressure non-saturated steam coming from the HRSG system is transferred as an input into an exchanger of drying system to produce hot air for food conservation and hot water for

domestic purposes. Compared to the CHP standard, the studied system presents a better efficiency because the waste from the standard CHP is used to produce cooling and heating applications for food conservation and domestic purposes. The energy efficiency of these kinds of the combined system is higher than 70% (Ahmadi, 2013).

Figure 1.3 presents a combined Rankine cycle (CRC) used as a power block of the Hybrid solar – biomass power system. This helps to evaluate each subsystem contained in the proposed hybrid system to select the better combination of renewable energy technologies.

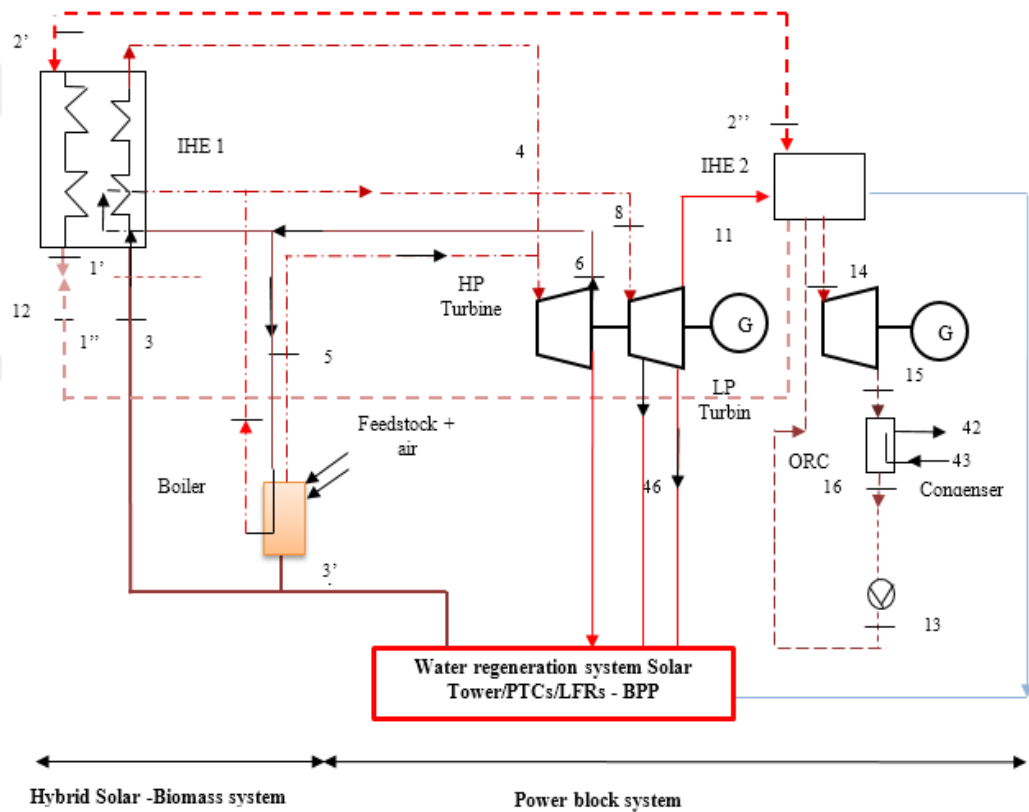
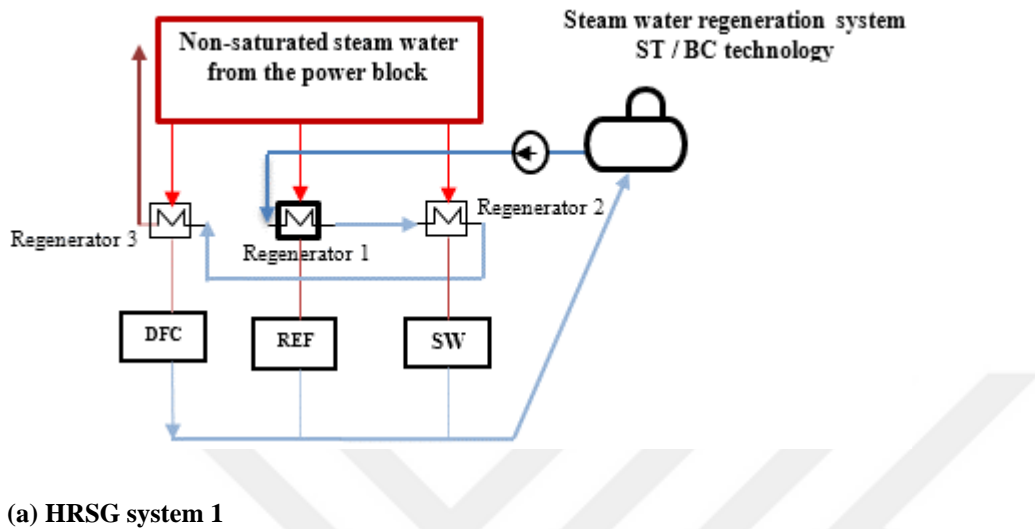


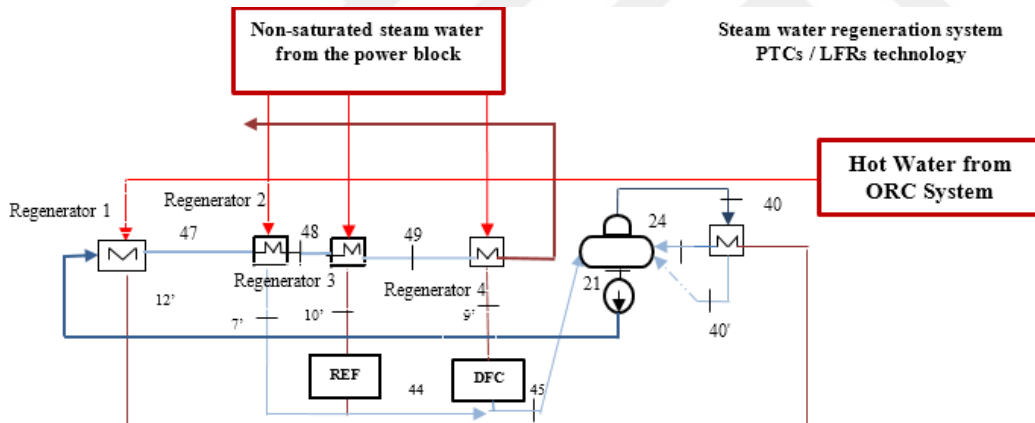
Figure 1.3. Description of the power block system used in the hybrid (solar–biomass) energy system.

It is necessary to notice that, various solar thermal technology such as parabolic trough collector (PTC), linear Fresnel reflectors (LFR) and solar tower (ST) are used for hybrid system simulation during this study, while a single biomass-fired technology has been adopted for the proposed hybrid system. Figure 1.4 presents a HRSG system connected with an additive block to produce

cooling, heating and hot water for domestic purposes. This system comprises of three subsystems, a single - effect absorption chiller, drying system, and hot water production system.



(a) HRSG system 1



(b) HRSG system 2

Figure 1.4. a) Schematic view of heat recovery steam generator (HRSG) system of the hybrid power system based on ST - BF technology (b) Heat recovery steam generator (HRSG) system of hybrid energy system based on PTC or LFR – BF technology.

2. LITERATURE REVIEW

2.1 Introduction

There is a lack of literature on the solar-biomass hybrid energy systems combined with multi-energy generation system due to the complexity of the topic. Hence, the literature review has been conducted separately for different design models, technologies and evaluation methods used for system performance related to the studied hybrid system. This comprised of a review of topics related to; concentrating solar power technologies, biomass-fired technologies, the thermal hybrid solar–biomass power systems and multi-energy generation system. The research on thermal hybrid energy systems has gained interest in the past few decades due to increased energy needs and global warming problems. Despite increased interest in the system only one commercial hybrid solar-biomass power system using biomass-fired technology has been implemented across the globe. Hence, this highlight the relevance of this research using combined thermal technologies. However, several studies have been conducted to improve the prime movers of the system. Table 2.1 presents analysis methods, steam generation systems and brief results of the studied system in the literature. Most recent studies related to the above topics based on the following factors have been also conducted:

- a) **A socio-political factor** can be determined according to the level of risk for stakeholders, the level of facilities and civil infrastructure (roads, bridges, supply points, and others) security, the acceptance of plant technology by the local population and country governance.
- b) **Environmental and socio-economic factor** relies primarily on human rights, the right to work for the local population, the creation of decent jobs, the health and safety of people living near the facilities or civil infrastructure that will be required during its exploitation period and the risks related to the frequency use of the vital resources intended for the populations use such as: the water, the forest, the farms and some agricultural waste.

- c) **The technical factor** can be determined from the technical characteristics of the thermal power plant such as efficiencies, performance ratio, capacity factor, Ingress Protection (IP) and system maturity.
- d) **Financial Factor** gives a clear insight into the nature of the investment, as well as the bankability and feasibility of the plant development. As a result, it is evaluated according to the possibility of contracting funds in the form of loans by the stakeholders to a financial institution to share the risks on the initial investment. This generally includes incentives, subsidies, exonerations, the life cycle assessment of the project, some clauses of the power purchase agreement (duration and an approximate Feed-in-Tariff price) and a detailed financial analysis able to bring out the levelized cost of electricity and the return on investment.

This section presents the literature regarding the analysis methods which can be classified as; thermodynamic modeling and performances analysis. Exergoeconomic and techno-economic analysis and optimization of a multi-energy generation system. These methods are used to analyze many subsystems able to generate various forms of energy based on solar and biomass energy resource. The energy efficiency, the environment protection, robustness, the initial investment cost and the levelized low cost of energy are the major factors driving the utilization of renewable energy resources. Therefore, it is essential to analyze renewable energy technologies for the exploitation of these renewable energy sources. Table 2.1 below presents the categorization of the main power cycles used in the development of hybrid solar-biomass and standalone power systems. These categories are used to establish the maturity, advantages, and disadvantages of these technologies and their use in different plants. Table 2.1 also presents the main types of power block connected with HRSG systems such as Brayton-Joule cycles, Rankine cycles, combined cycles (open or closed) using steam turbines, gas turbines, micro-turbines, and fuel cells.

Table 2.1. Recent studies on hybrid (solar-biomass) energy system using CSP and combustion technology.

Type of hybrid system	Capacity (MW)	Country, state	Primer movers	Description of the analysis	Approach/Analysis	Authors, Date
PT (ISG) + TES + (wheat straw /wood pellets)	50 88-12%	Spain, Ciudad Real	Steam turbines	The environmental performance of CSP plant hybridized with renewable fuels (wheat straw, wood pellets and biogas) using a LCA method: 37.5-34.2 kg CO ₂ eq/MW h	Life Cycle Assessment and inventory (LCA +LCI)	B. Corona, G. San Miguel (2015)
Forestry residues + PT (ISG)	10 MW (SM:1.2)	Australia	Combined steam turbines (P. Block efficiency: 27.2%) boiler eff.: 90.7%	Conversion rates: 1.30 MWh/t Fuel CV (dry): 19.0 MJ/kg Max. steam temperature: 540 C Specific investment: 7.0 AU\$m/MWe	Techno-economic approach	Juergen H. Peterseim et Al. (2014)
(jurema-preta) Biomass fill fraction (BFF) + PT (ISG) [65]	30 MW (SM : 1.2) 46.4 -53.6%	Bom J3sus da Lapa-Bahia, Brazil	Combined steam turbines (ISG)	LCOE: 11.4 cent USD/kWh Capacity factor: 51.4% BFF Fuel CV (dry): 20.45 MJ/kg Price per volume: 9 USD/m ³	Techno-economic approach	Rafael Soria et Al. (2015)
Biomass (cotton stalk) + ST (DSG)	50 MW	Yanqi, - Xinjiang, China	Combined cycles using gas and steam turbines (based on Brayton cycle)	Thermodynamic optimization has been used to compare solar gasification combined cycles (SGCC) and solar hybrid combined cycles (SHCC). System efficiency: 29.4% and 18.5%	Thermodynamic optimization approach.	Qibin Liu et Al. (2016)
Biomass +TES (3h) ST (ISG using Molten salt)	30 MW 50 - 50%	Griffith, New South Wales, Australia	Steam turbine P. Block eff.: 33.4% (30.2) full load	The techno-economic analysis using specific data such as straw supply per hr., operating duration, DNI, and initial investment helped to carry out the LCOE (155 AU\$)	Techno-economic approach	Juergen H. Peterseim et Al. (2014)
Biomass (Rice husk+ Sugarcane bagasse/ straw) +ST (ISG using air)	200 MW	WNT, Indonesia. Backlands, Brazil.	steam cycle (steam turbine)	The authors combined LCA and Techno-economic method to carry out the LCOE: LCOE (Backlands, Brazil) = 0.23 USD/kWh LCOE (WNT, Indonesia) = 0.60 USD/kWh	Life Cycle Assessment (LCA)+ Techno-economic approach.	M. Borges da Fonseca et Al. (2014)
Biomass (Rice husk/ Coconut shell) +LFR (DSG)	2-10MW (SM: 1-2.5)	Gujarat and Tamilnadu, India	Steam turbines	The use of exergoeconomic approach to evaluate Financial, Technical and environmental criteria for biomass selection.	Exergoeconomic and Optimization approach.	J.D. Nixon et Al. (2012)

Table 2.1. (Continued)

CST (DSG)		-	Hybridizing with the steam Rankine cycle and Brayton cycle (Gas turbine)	Technical compatibility (temperature and availability)	Investigation	G.J. Nathan et Al. (2018)
Biomass +TES (1.3–5.0 h)+ PT (ISG using Molten salt)	2.1-MW	Priolo Gargallo - Siracusa, Italy,	a combined cycle: Externally Fired Gas-Turbine (EFGT) and bottoming ORC: 66 - 33%	thermodynamic performance analysis of hybrid biomass – solar with CHP technology to find out: The available thermal power output of CHP LCOE (100 Eur/MWh to above 220 Eur/MWh)	Thermo-economic approach	Antonio M. Pantaleo et Al (2017)
Biomass (willow pellet) +TES (0.5m ³) +PT (ISG using Therminol VP-1)	8.2 kW	-	organic Rankine cycle and a vapor compression cycle	A thermo-economic analysis of a polygeneration system which is driven by solar energy and a biomass boiler to determine, yearly energetic and exergetic efficiency of the system are 51.26% and 21.77%	Thermo-economic approach	Evangelos Bellos et Al. (2018)
Biomass (rice husk) + PT (DSG) [68]	0.8 MW 50-100% (50-0) %	DNI:960W/m ² with a beam component of 700 W/m ²	Regenerative steam Rankine cycle.	Performance characteristics of solar–biomass hybrid power plant have been determined using the thermodynamic analysis. Rice husk HHV: 11.75 MJ/kg) Fuel efficiency (hybrid thermal efficiency) vary as follows: 15% to 32% (15% to11%).	Thermodynamic and optimization approach	T. Srinivas and B.V. Reddy [2014)
Biomass + ST (ISG)	14 MW 47 – 53%	Kerman, IRAN	Solar-biomass-based GT combined cycle (Brayton Joule and ORC): Cycle-I, II & III:	The exergoeconomic approach allows the determination of the most effective investment costs among the components of the combined cycle.	Exergoeconomic and environmental approach.	Simin Anvariet A. (2018)
Biomass + PT (ISG)	2923 kW VAR : 7278 kW Des.: 4405 kW		Steam cycle combined with absorption and desalination cycle.	Optimization of hybrid solar- biomass using the objective functions as the decision Variables and constraints led to the utilization of the genetic algorithm in EES software for polygeneration.	Exergoeconomic and optimization approach.	U. Sahoo et Al. (2018)

This chapter outline detailed literature review for the aforementioned CSP technologies; hence it provides a summary of the literature review of solar-biomass thermal power plants. The literature review is organized as follows: the first section provides the brief examination of combined cycles and multi-energy generation system followed by concentrating solar power and biomass-fired technologies used for the commercial plants associated with thermodynamic cycles involving steam turbines. The second section presents the preview of previous research conducted on combine power solar-biomass systems for the production of electricity with a separate or combined power cycle. Finally, the overall energy efficiency and analyze of multi-energy generation system of hybrid systems is presented in chapter 6. A synthesis of the studies carried out in the literature will highlight the use of the studied systems compared to standalone systems or similar systems without multi-energy generation system.

2.2 Combined Cycles and Multigeneration Energy Systems

Many innovative cycles have been proposed to recover the low temperature which may be converted into electricity. Organic Rankine cycle, Kalina cycle and the cycle developed in other researches are some of the cycle models (Kalina, 2017a; 2017b). All these cycles have one thing in common, the use of a gas turbine to generate electricity. Many studies considered the combined power cycles which use at least one gas turbine to generate electricity and uses the heat generated by superheated steam water. Cao et al. (2004) designed a combined power cycle using gas cycle and organic Rankine cycle (ORC) able to recover heat released by the top cycle. In their study, authors carried out thermodynamic performance analysis, to highlight the impact of the bottom cycle (ORC) on the overall power block system. In the same study, the combination of a gas turbine and steam turbine as a prime mover of the bottoming cycle was conducted. The results showed a better energy efficient conversion compared to standalone power block using gas turbine technologies. These gas turbine technologies, despite having low conversion efficiency is being used in other countries where natural gas is cheaply and abundantly available for electricity generation. The efficiency of combined cycles depends generally on the gas topping cycle parameters such as the exhaust temperature of burned gas, relative humidity of compressed inlet air,

thermal efficiency of intermediate heat exchanger, gas turbine inlet temperature and gas cycle pressure ratio (Guoqiang et al., 2016). Table 2.1 shows that all commercial solar thermal power plants independently of the technology used in the system, the turbines are employed to generate electricity, which varies in size, as well as in the primary energy sources. Many studies show that the characteristics of the combustion chamber and the heat source that feeds the turbine directly are the main parameters that influence the thermal power plant efficiencies. Research and development work carried out has provided innovative solutions to improve the performance of the combined cycle used for the CCHP system following social and environmental impacts, sustainable development and the improvement of standard living. Many methods have been developed to recover exhaust heat which proceeds by utilization of another bottoming cycle. In the first method, the recovered heat can be used to supply end-users directly whereas in the second method the exhaust gas of the main power cycle can be used as a heat source for bottoming cycles, depending on the value of exit temperature. Mohammadi et al. (2017) studied, the performance of a small CCHP system able to produce 30 kWe power, 8 kW cooling and almost 7.2 ton of hot water. The studied system included a combined gas turbine using fuel gas as working fluid and ORC using Toluene as working fluid with an efficiency of 67.6%. A similar study was conducted by Kumar (2016), the study investigated the performances of power block using a Brayton-Rankine combined cycle to generate electricity. Zare and Hasanzadeh (2016) studied a complete thermodynamic of a closed Brayton cycle combined with ORCs. The authors used concentrating solar power technology to generate the required heat for the power block. During this work, authors combined Brayton-Joule cycle using Helium as working fluid and two ORCs that use R123 as working fluid to increase the amount of electricity generated. In the combined Brayton-Rankine cycle, usually, the Rankine cycle (SRC/ORC) use the exhaust gas from the Brayton open cycle to heat the working fluid. This conversion process contributes to the increasing of the electricity generated and the overall efficiency of the power cycle.

A multi-energy generation system is defined as any system containing more than three different useful outputs for industrial or domestic purposes. Generally, the main outputs are electricity, heating, and cooling which are mostly

accompanied by other subsystems to meet some purposes such as domestic hot or freshwater and industrial drying system. Al – Sulaiman et al. (2012), studied a thermodynamic analysis of biomass prime movers using an organic Rankine cycle for multigeneration purposes. The results of the study led to the increase of power efficiency from 12% to 88% for trigeneration system. In a comparative analysis conducted by Eshoul et al., (2015), for a standalone combined cycle power plant (CCPP) and a combined cycle power plant connected with multi-energy generation system using single effect desalination and thermal vapor desalination as additives subsystems, the results show that, the standalone CCPP has a better overall exergy efficiency. An assessment of solar tower power system combined with coal gasification for industrial purposes conducted by Öztürk and Dinçer (2013) in order to evaluate thermodynamic efficiencies of each subsystem, the authors added five subsystems to the power system and concluded that, the energy and exergy efficiencies of each subsystem including power block ranged between 19.43 – 46.05% and 14.41 – 46.14% respectively. The above studies showed the importance of a HRSG system in the power plant containing a multi-energy generation system. Cihan et al. (2006) studied combined power cycle performances using gas turbines to improve its overall efficiency. During their research, it was found that more than 85% of the overall exergy loss is produced by the combustion chamber, turbines, and HRSG system. In another study conducted by Woudstra et al., (2010) the evaluation of HRSG performance at different pressure levels showed the advantages of using HRSG in combined cycles. In the work conducted by Yilmazoglu et al. (2010) the combustion chamber was shown as being a key component responsible for exergy destruction in the power plant with an estimated value of 54.41% of the total exergy destroyed. In a similar work based on multi-objective method conducted by Ahmadi et al., (2011), the results revealed that combustion chamber of combined power plant presents the highest exergy destruction. Besides, the results showed that increasing the inlet temperature inside of gas turbine leads to the decreasing of exergy destruction cost related to the combined power cycles plant (Ahmadi et al., 2011).

2.3 Solar Thermal Power Systems

In 2016, a study conducted by Ehtiweth et al. (2016), consisted of life cycle assessment of 50 MWe parabolic trough plant with the main objectives of creating the relation between weather, environmental pollution, and cost of electricity generation. The researchers used thermo-economic analysis to present these outcomes. The results showed that considering all the materials used in CSP plants, molten salt, and synthetic oil are the major contributors to environmental impact. The impact on human health presented approximately 70%, followed by the impact on resources with 25%. The highest exergy demand falls in line with the price and volume of steel manufacturing. The results furthermore show that the solar field presents the largest value of cost rate followed by boiler and condenser. Li et al. (2017), analyzed a hybridized existing geothermal power plant and solar-powered system using steam-Rankine topping cycle. During this study, the authors carried out energetic, exergetic and economic performance analysis. The results presented shows that, solar efficiency of 12.2% and consumption of up to 17% less than the standalone geothermal plant could be achieved.

Adibathla and Kaushick (2014) in their research integrated a solar aided system to the existing 500 MWe coal-fired thermal power plant. The study was conducted to elaborate an exergoeconomic analysis of 500 MWe thermal power plant. The results showed that the solar field and boiler have the maximum exergy destruction ratios of 78.90% and 56.52%, respectively. Seif et al. (2018) studied molten salt utilization as a heat transfer fluid for dry cooled solar thermal power plants, to minimize water consumption in the arid region. The study investigated the effects of heat transfer fluid utilization instead of synthetic oil. It also considered an optimization of a solar parabolic trough power plant coupled with a dry cooling system. The results showed that the levelized cost of electricity is better when the power plant uses molten salt as a heat transfer fluid. Ahmadzadeh et al. (2017), studied thermodynamic performance and thermo-economic analysis of the studied system, to develop a genetic algorithm optimization. This algorithm was conducted to improve thermal energy by 25%, 21.3% in exergy efficiency by 21.3% and 7.7% reduction in the total cost of the proposed system. Deepak and Sudhakar (2012), evaluated the thermal performance of 100 MWe linear Fresnel

reflector with solar thermal power plant technology using SAM Software. The studied plant included 16 modules per solar collector assembly. The results showed that the capacity utilization of the plant represents 30.2%, the plant efficiency for an annual electricity generation close to 263.973.360 kWh.

The solar thermal power plant studies were focused on solar chimney utilization with height chimney as the main focus. However, there are few studies which contribute to optimize the height of the chimney. The solar double-chimney power plant is a new model developed by Cao et al. (2017), to optimize the power productivity of STTP. The authors used the method to compare the named sloped solar chimney power plant (SSCPP) and a solar chimney power plant (SCPP) technology. The results showed that the productivity of solar thermal tower using the solar double-chimney power plant is 1.59 times larger than SCPP technology and 2.77 times larger than the SSCPP technology. Bakir (2017) proposed a new methodology for optimizing STTP using the techno-economic parameters. The optimization was evaluated according to the collector area and the height of the chimney. The results showed that, at the same solar irradiation and electricity price, the simple payback period for 200 MWe with sloped collector design would have a simple payback period similar to a 5 MW with floating chimney design. Zhu et al. (2016) conducted works to achieve exergy distribution of 1 GWe of solar thermal aided coal-fired power generation system, including exergy efficiency and exergy destruction of each component. The authors proposed that, before optimizing the solar power plant integration, boiler and solar field arrangement has to be analyzed carefully. Bonyadi et al. (2018), studied a hybridization of the existing geothermal power plant and solar-powered using steam–Rankine topping cycle. During the study, the authors conducted energetic, exergetic and economic performance analysis. Concentrating solar thermal power using parabolic trough collector technology represents one of the most promising options among available CSP technologies for generating electricity at utility-scale. Munoz et al. (2017), studied an unconventional thermodynamic cycle intended for integration into solar thermal power plants using parabolic trough collector with a maximum temperature of heat carrier equal to 670 K. The results revealed that propane and R125 are the most suitable working fluids for the studied cycle. Furthermore, the results showed that propane

can be considered as the best option with a moderate design point pressure ratio equal to 14:1 and cycle efficiency range for the annual operation was found to be in the ranges of 30.2% - 41.4%. Shahnazari and Lari (2017) studied standalone solar electricity generating systems (SEGS) integrating solar combined cycle system (ISCCS). The authors used various methods to compare these configurations. The results showed that ISCCS increase the net production capacity from 331 to 398 MWe according to calculation.

2.4 Biomass-Fired Based Power Systems

An investigation of rice straw potential for electricity generation in Egypt was conducted by Abdelhady et al. (2014). The results indicated that with 3.1 Million tons/Years of rice straw they can provide 2,447 GWh as annual net output electricity which can contribute to decreasing CO₂ emission, approximately 1.2 million tons CO₂ per year. Krywik and Swaja (2017), presented results on the fermentation process of putrid potatoes, which are not used as food, by applying the biomass to biogas conversion technology. It was found that the use of biogas from fermented potatoes in comparison to maize is lower by approximately 35%. The putrid potatoes are not good as compared to maize for biogas generation in the agriculture biomass to biogas power. Soares and Oliviera (2017) conducted a numerical simulation of a hybrid concentrating solar power to drive an organic Rankine cycle. The studied system was working with parabolic trough collector and a biogas boiler as a backup. The results showed that the annual yield is significantly improved with hybridization from 3.4 to 9.6%. Nunes et al. (2017) conducted out an investigation on current difficulties related to the biomass utilization from residual forest stemming for forestry activities and wood waste of industrial process for the thermal power plants.

Kalina (2017a) studied the concept of a small-scale combined cycle system and Organic Rankine cycle, integrated with thermal gasification of biomass. The author developed models of the system that gives an estimated value of power and energy efficiency of the proposed setup. Furthermore, in another research conducted by Kalina (2017b), the author examined different configurations of the heat recovery process in a combined cycle power plant. In 2018, Abdelhady et

al., (2018) used SAM software for modeling of biomass thermal power plant fed with rice straw. The results showed that the average nominal and average real LCOE of the power plant were 10.55 and 6.33 USD cents/kWh respectively. Furthermore, it was found that LCOE was highly sensitive to feedstock price and discount. Malek et al. (2017) did an investigation of a biomass power plant for suitable and secure energy. The authors analyzed 10 MW biomass power plant using fruit bunch, mesocarp fiber, oil palm frond, oil palm trunk, and palm kernel shell while considering the net present values, internal rate of return, payback period and system efficiencies. Sahoo et al. (2016), presented work including general aspects associated with hybrid biomass-solar power plant using parabolic trough collector (PTC). During the study, the authors carried out the thermodynamic evaluation of the hybrid thermal plant to determine the most suitable parametric values of steam superheated and plant layout design. Performance analysis of the two powers plant configuration with 100 kWe capacity was conducted by Perna et al. (2015) to optimize system efficiencies. During the, study the authors developed numerical models using both thermodynamic and thermochemical equations. Grebreegziabher et al. (2014), proposed a thermodynamic analysis of a biomass thermal power plant using empty fruit brunches as a primary energy source. The results of this study showed that with a drying and heat integrated unit the overall efficiency of the studied biomass power plant can be improved.

Nixon et al. (2012) conducted an assessment study of hybrid trigeneration thermal power plant in India using solar and biomass as primary energy sources. The authors used technical, financial and environmental criteria to identify and select the best investment scenario. The comparison between biomass standalone and hybrid plant showed that the operations save up to 29% of biomass and land. Sampim et al. (2017) presented a method that could reduce the risks stemming from biomass price fluctuation using Fuel Switching Flexibility method. The used models' increased financial values considerably. Cheng et al. (2014) developed a methodology able to analyze the agriculture biomass potential in the country, to develop a biomass thermal power plant. The developed methodology uses local condition, the demand of multi-duties agricultural residues and logistics, which led to a sensitivity analysis. Milani et al. (2017), analyzed a series design, parallel

design, and steam extraction design configurations of a hybridized power plant using CSP technology and biomass through SAM software as the main software for simulation. The results showed that the series design configuration had the lowest leveled cost of electricity while the parallel design presented the highest installed capacity.

2.5 Solar-Biomass Hybrid Energy Systems

A solar – biomass hybrid energy system is a multipurpose system that uses two sources of input energies, i. e. solar and biomass sources. Several studies have been conducted with hybrid systems using various CSP and biomass-fired technology as main parts of the studied system to generate electricity. The multi-energy generation system is a system based on electricity, cooling, heating as main useful output and can be accompanied with other subsystems such as freshwater, hot water, and air to meet domestic and industrial purposes. These subsystems contributed to the increase of power plant overall efficiencies where various energy outputs are needed. For an excellent understanding of the hybrid energy system selection process, it is important to determine keys parameters and main criteria which need to be examined to select a suitable hybridized system. The main criteria commonly used for selecting the most suitable hybridized system can be classified as environmental, social, technical, techno-economic and financial. Each of these criteria requires that the key parameters are considered according to their weight during the selection process without any interaction considerations. Furthermore, the requirements of location have to be known before any work related to the modeling, analyzing and optimization of multi-energy generation system and hybrid solar – biomass systems separately. The environmental impact of the solar-biomass hybridized system has been frequently assessed in the past decade to improve the power production, rational usage of energies resources and reducing of greenhouse gas emission. Recently a study conducted by Corona and Miguel (2015) presented an assessment of environmental performance of 50 MW concentrated power plant using parabolic trough collectors, synthetic oil as heat transfer fluid as key parameters of solar field which had to feed both heat exchanger of ISG system and the 7.5 hours storage system working with molten salt. During the study, the authors worked on

the hybridization of solar power by integrating successively the following fossil fuels natural gas, coal, and fuel oil. In the first step, the wheat straw was considered, wood pellets and biogas as renewable energy fuels were considered in the second step. Then, a life cycle assessment methodology was used to compare their environmental and economic impact in the sustainability of the project and to determine the most suitable fuel type for the hybridization. The cumulative energy demand of the solar standalone system was estimated at 1158 MJ/MWh at a payback period of 1.44 years, while the hybridized system using wheat straw and pellets had a cumulative energy demand between 2779.2 and 3126.6 MJ/MWh with a payback period varying in a range of 1.72-1.83 years with the lowest CO₂ emission between 37.5 – 34.9 kgCO₂eq. In a similar study, an exergoeconomic and environmental analysis of a hybrid system using solar-biomass energy resources for power generation has been carried out by Simin et al. (2018). During the study, the authors assessed various costs, impacts and sustainability criteria related to the power production, the environment protection and viability of such project through the amount of CO₂ emission generated per year. The authors concluded that the use of solar power system added as an integrated unit to the biomass plant present a positive impact because it contributes to the decreasing of CO₂ by 22% and a considerable increase in the annual energy production by 30%. The application of hybrid systems in the manufacturing industrial process contributes to reducing the amount of CO₂ produced by the existing plant. Nathan et al. (2018) conducted research to contribute to a better environmentally friendly. In the study conducted by Nathan et al. (2018) several main advantages related to the hybridization of concentrating solar power with biomass combustion systems to provide at the same time, a firm supply and cost-effective CO₂ mitigation were studied. During the study, the authors analyzed hybridization of the solar-fossil fuel system which does not use the carbon capture technology with lower potential usage, while they offer a potential low-cost carbon-negative or carbon-neutral energy in the longer term. The authors presented oxy-fuel and chemical looping combustion as a potential technology for the power plant which can be used as an integrated system or storage. This technology has the potential to the cost reduction in the hybrid system. Furthermore, the results show that this technology has the potential to the decreasing of carbon-negative energy which leads to a low cost of energy.

Nevertheless, there are several studies which have been conducted on solar-biomass hybrid energy system projects, however, very few numbers of these projects have been realized around the world. In 2017, Iftekhar et al (2017), conducted technology assessment for different biomass-solar hybrid power generating system in Europe. This was done to highlight the potential of the CSP-biomass hybrid system for commercial usage. The authors highlighted that by 2017 there was only one concentrating solar power – biomass power plant in Europe. The power plant is located in Les Borges Blanques-Lleida, Spain. It uses the most proven CSP technology. The Termosolar Borges plant started to operate in 2012 with a capacity of 22.5 MW and using parabolic trough collectors as a CSP technology. Before the implementation of the Termosolar's project, many studies have been carried out to present the feasibility of such kind of system in many countries. Examples of such research were conducted by Peterseim et al. (2014a), in Australia. The research was aimed at identifying the best biomass energy source which can be used with the concentrating solar power plant hybridization by using annual energy produced as the main criterion. During the research, the authors assessed energy from biomass using waste such as forestry residues, bagasse, stubble, wood waste and residues derived fuels to determine the suitable solution. The results presented that forestry residues were the suitable fuel that can be used as a raw material in biomass combustion system integrated to CSP plant. This was mainly due to specific data such as the investment cost, the conversion rates, and the net cycle efficiencies for different capacities of the hybridized power plant. With the technical support from some manufacturing companies, several studies have been conducted for both solar and biomass technologies as prototype and project concept by using CSP and biomass technology to highlight the commercial use of the hybrid system. A study conducted by Da Fonseca et al. (2014), is a perfect illustration of pre-implementation project, in the study, the authors assessed the environmental and economic impacts of the multi-pulverized biomass fuel and solar tower hybrid energy system called SolComBio. In the study, land availability, meteorological conditions, civil infrastructure, and feedstock markets were considered as main parameters to contribute to the SolComBio project's success. The authors noted that it was important to add economic data to the project development studies to establish their feasibility. Nixon et al. (2012) analyzed various case studies with

peak capacities between 2 MW and 10 MW using simulation models developed in TRNSYS. During the evaluation of environmental, financial and technical criteria authors carried out a suitable solar multiple based on the trade-offs with a size between 1 and 2.5. The high variation factor of feedstock price used in the simulation and the hybrid system size remained competitive compared to standalone CSP system. The results show that its operation contributed to saving up to 29% biomass and land with an increase of the cost of exergy loss between 8.3 and 28.4 USD/GJ/a and a levelized cost of energy between 1.8 and 5.2 USD cents/kWh. In the same period, many studies have been carried out by several researchers to value the use of thermal energy produced that cannot be used to produce electricity. Some authors such as Pantaleo et al. (2017) realized a techno-economic analysis of a small hybrid energy system using solar and biomass energy resource with an integrated subsystem called combined heat and power able to generate 960 kWt and 2.1 MWe by using a combined cycle for flexible power generation. The concentrating solar power system was based on the use of the parabolic trough collectors with molten salt as heat transfer. It was found that a levelized cost of energy between 100 Euro/MWh and 220 Euro/MWh could be achieved for an investment cost range between 4.3 and 9.5 Million Euros. The results indicated low economic profitability of the hybridized system compared to a standalone biomass plant due to a high investment cost. In 2014, Peterseim et al. (2014b) assessed the development of a 30 MW hybrid power plant using concentrating solar power and biomass system in Australia. The authors used a central receiver as concentrating solar power technology with a 3 hours storage system using molten salt as heat transfer fluid. The techno-economic analysis of the hybrid system leads to the annual energy production of 160.3 GWh, with a levelized cost of energy of 155 AU\$/MWh and reduction cost of 43% compared to a standalone solar tower power plant. Soria et al. (2015) conducted a socio-economic assessment of a 30 MW hybrid CSP-biomass systems in a semiarid region due to the high cost installation of standalone CSP plant. During the economic analysis, authors introduced a biomass system using biomass fraction fill as raw material available in Brazil's semiarid north region. This was to assess a low-cost of the energy of the system was estimated at 114 USD/MWh. The results showed a positive social impact of the Hybrid plant development through the creation of 760 jobs during the plant construction phase estimated at 2 years and

70 jobs related to the operation and maintenance of power plant which could contribute to the employment rate in the region. In other work conducted by Tanaka et al. (2015), the possibility to hybridize power generation system using solar and biomass considering the pinch temperature as the key parameter in the selection of the suitable size of the hybrid system was studied. In this study, Syngas was used to run a gas turbine in the top cycle, while a steam Rankine cycle constituted another part of power block which generated electricity. During the analysis of the proposed system, it was found that concentrating solar thermal plant with a small capacity below 5 MW has the utility pinch equal to a temperature corresponding to the evaporation pressure level of the steam Rankine cycle. Despite the importance given to environmental and socio-economic studies, the fact remains that, the rational use of available resources is a major concern because of the experience that was once lived in the past. This reason has led to the establishment of very high energy-efficient hybrid systems. Thus, studies such as those conducted by Peterseim et al. (2014c) which comprised of the comparison of hybrid combinations have allowed the determination of the efficient design without considering the financial and environmental criteria. This study revealed that Solar Tower technology combined with biomass combustion system presents the best peak efficiency around 33% when working as direct steam generation system. Whereas, an indirect steam generation system integrated to CSP technology using parabolic trough collectors combined with biomass combustion system has an efficiency of around 29.5% for an output temperature of 380°C. Srinivas and Reddy (2014), conducted the participation level analysis participation of a solar and biomass system in the hybrid power plant without energy storage. During this study, the authors established a relation between the share of energy sources and plant efficiency. The study concluded that when the solar participation level is between 10% and 50% the energy efficiency increases from 16% to 29%. To carry out specific parameters of technical criteria of a polygeneration hybrid energy system using solar-biomass resources, a Thermo-economic and optimization analysis was conducted using thermodynamic laws and economic data (Sahoo et al., 2018). The optimized values found were the efficiencies and the output data of integrated cooling, desalination, power block and the global system. The study concluded that the studied hybrid system had energy and exergy efficiency of 49.85% and 20.94%, respectively. Liu et al.

(2016) conducted a thermodynamic analysis of two hybridization scenarios to determine the overall energy efficiency and solar-to-electric efficiency of the hybrid system. The studied system was a solar tower power plant with an integrated biomass system. The biomass system considered, was a thermochemical gasification system and a thermal biomass system which affected the overall efficiencies of the power block. During the simulation, the system overall energy and solar-to-electric efficiency reached 29.36% and 18.49% respectively with an integrated thermochemical process of 28.03% and 15.13% for a hybrid plant with thermal biomass concept developed. To increase the overall efficiency of a Solar-Biomass hybrid system, Evangelos et al. (2018) carried out the performance evaluation of the system by integrating vapor compression and organic Rankine cycle. During the optimization analysis, the authors optimized a suitable design in dynamic conditions for one year. The results showed that the annual energetic and exergetic efficiency of the system was 51.26% and 21.77% respectively. Furthermore, the techno-economic analysis of the system provided a payback period of 5.13 years with an internal rate of return of 21.26%. Karellas and Braimakis (2015) investigated the trigeneration and cogeneration system based on solar – biomass hybrid thermal power system using an organic Rankine cycle as a power block system. During this work, the authors found an exergy efficiency of organic Rankine cycle system around 7%. In the similar study based on Hybrid solar-biomass power system combined with multi-energy generation system was conducted by Khaliq et al. (2015) to determine the thermodynamic efficiencies of the overall system. The energy and exergy efficiency of the studied system was found to be 66.5% and 39.7%, respectively.

The reviewed literature as presented above suggests that hybrid solar – biomass power system combined with multi-energy generation system is the best alternative option for rational use of renewable energy resource and a mitigated solution for global warming due to the improved overall system efficiency. Therefore, the modeling, analysis, and optimization of integrated subsystems in the hybrid solar – biomass power system is paramount importance in this thesis due to lack of research in this research area. Hence, the present study contributes to learning more about the origin and share of exergy destruction inside of each

subsystem. These results may contribute to improving the use of these technologies for hybrid thermal power system by increasing both exergy and energy efficiencies of the overall system.

2.6 Aims, Objectives and Motivations of the Thesis

2.6.1 Motivations

Energy plays a key role in the socio-economic development of countries. Moreover, it is essential and indispensable for sustainable development and improving the standard of living for the population. For the past decade, energy demand has been growing so rapidly, leading to several industrial and domestic challenges that drive people to seek alternative solutions to meet their daily energy needs. Since these energy needs will continue growing, it is now urgent to propose energy production systems that are efficient, sustainable, economically attractive and above all environmentally friendly. To do this, renewable energies such as solar, wind, geothermal, hydropower and biomass are positioned as alternatives to the use of fossil and nuclear energy.

The use of natural resources is limited by the volume available, the accessibility and the means required for their exploration and exploitation. Several energy production systems and international conventions have been developed, tested and signed to provide an effective response to climate change and accompanying measures for countries wishing to implement international energy policies. To do this, the use of renewable energies for power generation, the integration of multi-energy generation system to optimize the efficiency of systems and the installation of control instruments for greenhouse gas emissions are strongly encouraged. It is important to note that, the capacity of renewable energies available on earth is sufficient to meet the needs of the populations. The reviewed literature presents a multi-energy generation system of energy as a solution to the rational use of energy resources. Besides, these technologies offer better advantage since they help to reduce the tons of CO₂ produced per unit of Megawatt hour (MWh) generated and also helps to increase the thermal efficiency of the facilities without affecting the investment cost.

The depletion of fossil fuels and climate change has helped to change the behavior of both energy consumers and producers, hence leading to the use of renewable energies. It has also contributed to the hybridization of existing energy systems. Integrated multi-energy generation system is considered as an essential technology to optimize the thermal efficiency of the power block, and the production of existing or under-construction thermal power plants. A multi-energy generation system can produce various forms of energy that can meet the needs of the industry or community. This can be done through the use of one or more primary energy sources. The main application of these systems is in thermal systems to increase the amount of energy generated and thermal efficiency, reduce greenhouse gas emissions and promote the rational use of the available resources to support a sustainable environment. Some people are tempted to think that the multi-energy generation system does not find their application in renewable energy plants because they believe that renewable energies already contribute to the reduction of environmental impact and sustainability. However, it is important to note that the efficiency of thermal power plants using available biomass and solar energy shows a low energy efficiency for a considerable investment cost. As a result, the integration of the multi-energy generation system and the hybridization of renewable energy sources provide a better position as an integrated solution for the implementation of renewable energy projects.

The literature review on hybrid power plants shows that there is not enough study integrating the use of a multi-energy generation system. Studies show that the integration of these systems helps to increase the thermal energy efficiency of the overall system. According to a study conducted by Ahmadi, (2013) integration of a multi-energy generation system contributes to reaching an overall yield of 70%. Therefore, application of a multi-energy generation system to a hybrid (solar-biomass) power plants presents an interesting line of research for the energy industry. Moreover, considering the existing literature, it was noticed that there are few studies on the exergoeconomic analysis of a hybrid power plant combined with an integrated multi-energy generation system.

2.6.2 Aims and objectives

The aims of this research are determination effectiveness and the relevance of the hybrid energy system using sustainable energy technologies for thermal power plant development in the sub-Saharan region. This research, therefore, presents an approach for determining the technical and economic viability of hybrid system based on concentrating solar power and biomass-fired technologies by considering the socio-economic, environmental, and technical criteria both qualitative and quantitative in the determination of the most optimal hybrid system. To conduct the analyses, the practical and essential data for implementation of large scales solar-biomass hybrid systems such as CSP and biomass-fired technology parameters including the availability of primary energy sources and local area geographical characteristics were considered. The expected results of this study were further verified and solidified by existing literature and data from similar commercial facilities (NREL, 2019). The comparative study of the results allows the validation of the specific objectives that were to achieve the main research objective.

To achieve the main objective of the research, the following specific objectives have been set:

- To provide a general overview of the literature on similar work and the technologies that make up the hybrid (solar-biomass) power system to have an important database that will allow us to:
 - To evaluate the maturity of the renewable energy technologies considered for hybridization and develop models for simulation,
 - To conduct a comparative study between existing models and mathematical models based on exergoeconomic and techno-economic analysis.

- To elaborate a preliminary study that will corroborate the report of the environmental and social impact assessment (ESIA) of the selected site.
- To propose a conceptual model of a 5 MW capacity hybrid system that will take into account the specificities of concentrating solar technologies which will interact with a biomass-fired technology for energy produced. Thus, combinations of the following technology that ensure the multi-energy generation system have been considered for the hybrid energy systems:
 - Parabolic Trough Collector/Biomass-fired technologies (PTC-BF),
 - Solar Tower/Biomass-fired technologies (ST-BF),
 - Linear Fresnel Reflector/Biomass-fired technologies (LFR-BF).
- To elaborate the techno-economic analysis of the studied system that allows determination of the investment cost required by taking into account the direct and indirect costs, the purchased equipment cost and contingency that constitute to the input variables with the following output variables;
 - The levelized cost of energy,
 - The return on investment,
 - The net present value,
 - The payback period and
 - The internal rate of the return.

The analysis of this study introduces the exergoeconomic analysis and its optimization since it also indicates the annual expenditures related to the operation and maintenance.

- To develop a mathematical model that uses the thermodynamics laws combined with economic concepts:
 - To determine the exergy destruction associated with costs for the main equipment of the hybrid system.
 - To propose an optimized model that combines the intrinsic data of hybrid systems equipment and the parameters from the techno-economic and advanced exergoeconomic analysis.

Considering these models, the following are the expected results:

- The economic impact of the global systems' exergy destruction.
- The exergy and exergoeconomic performance of each subsystem that constitutes the power block of the hybrid system
- The distribution of exergy destruction forms that are attributed to each subsystem and equipment.
- The impact of the exergetic destruction on the performance of the hybrid system.
- The impact of the exergoeconomic of these equipment's on the quality of the production, O&M expenditures.

The structure of the specific objectives presents, the framework of this research that was set to achieve the final objective.

2.7 Outline of the Thesis

The thesis report is divided into six chapters which are organized as summarized below:

Chapter 1: This chapter presents the overview of the energy market and general information of Cameroon.

Chapter 2: This chapter presents the literature review of similar studies recently conducted across the globe including the results obtained in those studies. This allows the contextualizing of our study and set objectives that respect the originality of the thesis.

Chapter 3: This chapter presents the design and description of hybrid (solar-biomass) power system combined with multi-energy generation system. Hence, it deals with the hybrid system design approach and presents the subsystems that need to be integrated. It also establishes the thermal processes and thermophysical conditions that govern energy production. Finally, it establishes the relationship between technical analysis and the economic concept.

Chapter 4: The chapter presents the energy, exergy and exergoeconomic analysis. It deals with the modeling of different subsystems that contribute to make the hybrid system and power. Besides, it presents the structure of the optimized model based on the criteria that are used for the selection of the optimal hybrid system among the three types that have been conducted in the study.

Chapter 5: In this chapter, the research results and discussion are illustrated in detail, thus, the chapter presents all the results obtained during the study and describes their relevance to the body of knowledge. Also, it helps to better understand the results by comparing them with those of similar studies.

Chapter 6: This chapter contains results; hence it concludes the thesis results by summarizing and discussing the most important results achieved.

Chapter 7: In this chapter, the research conclusion and recommendations are presented, hence this chapter concludes the thesis findings by summarizing and discussing the most important results achieved and suggesting future work to perfect this study.



3. DESIGN AND DESCRIPTIONS OF SOLAR-BIOMASS HYBRID ENERGY SYSTEMS

3.1 Introduction

This chapter presents three different hybrids (solar-biomass) power system combined with multi-energy generation system for industrial and domestic purposes. The study was conducted in the city of Faro-Poli, located in the district of Faro, province of Garoua, North region of Cameroon with geographical coordinates of 8° 29' 0" North, 13° 15' 0" East. Solar irradiation is estimated at 2140 kWh /m² /year. Table 3.1 presents the meteorological data of the region.

Table 3.1. Meteorological data of Garoua, Faro-Poli (Meteonorm 7.0, 2019).

Months	Monthly global solar radiation (kWh/m ²)	Daily sunshine duration (h)	Av. solar radiation during sunshine hours (W/m ²)	Ambient temperature (°C)	Wind speed (m/s)
January	191	9.2	692.1	22.9	1.8
February	176	9.1	690.7	25.5	2.1
March	190	7.7	796	27.2	2.2
April	175	6.8	857.8	27.0	2.5
May	172	6.4	866.9	25.7	2.4
June	156	5.5	945.4	23.4	2.1
July	145	4.3	1087.8	22.1	1.9
August	158	4.3	1185.3	21.7	1.8
September	146	5.1	954.2	22.1	1.7
October	161	5.9	880.3	22.9	1.6
November	183	8.9	685.4	23.5	1.6
December	185	9.4	635.4	22.8	1.7
Av. values	2040	6,9	856,4	23,9	2,0

This region has a significant pastoral activity and ranks second in terms of productivity because of cereals products especially maize, sorghum, and cotton. The most important part of cereal production is based in the northern regions of Cameroon. Table 3.2 presents the energy potential and the volume of various agriculture residues as of 2018. The potential of waste residues (straw, stalk and other) from sorghum in the named localities can be estimated at 1.13 TWh per annum

Table 3.2. Main crop residues in Cameroon (FAO data, 2018).

Agricultural crops	Production	Residue type	Residue of products ratio	Residue	Moisture	Residues	Sustainable extraction	Lower heating value	Energy potential	Potential MWh (annual energy production) AEP		The capacity of the biomass power plant	
										M x 0.278 x LVH x E		C = AEP/ Y.O.T (hours)	
										E: 15 %	E: 40%	YOT : 5000 – 6000 hrs	
tons	n/a	n/a	Tons	%	Tons	Tons	MJ/kg	GJ	MWh	MWh	MW	MW	
Maize	2.16E +06	stalk	1.5	3.24E +06	15	2.75E +06	5.5E +05	15.48	8.51E +06	3.55E +05	9.46E +05	71 – 59.1	189.2 - 158
Sorghum	1.34E +06	stalk	2.62	3.51E +06	15	2.98E +06	6.0E +05	17	10.1E +06	4.23E +05	1.13E +06	84.6 - 70.5	226 – 188.3
Rice, paddy	3.59E +05	straw	1.5	5.38E +05	15	4.57E +05	9.1E +04	15.56	14.2E +05	5.93E +04	1.58E +05	11.9 – 9.8	31.6 – 26.3
Millet	1.00E +05	stalk	3	3.00E +05	15	2.55E +05	5.1E +04	15.52	7.91E +05	3.31E +04	8.80E +04	6.62 – 5.51	17.6 – 14.6
Sugar cane	1.29E +06	bagasse	0.3	3.87E +05	75	9.67E +04	1.9E +04	13.38	2.59E +05	1.08E +04	2.88E +04	2.16 – 1.8	5.76 – 4.8
Cocoa, beans	2.92E +05	Pods, husk	1	2.92E +05	15	2.48E +05	4.9E +04	15.48	7.68E +05	3.20E +04	8.54 E +04	6.4 – 5.3	17.1 – 14.2
Coconut	5.25E +03	shell	0.6	3.15E +03	10	2.83E +03	5.67E +02	10.61	6.01E +03	2.51E +02	6.68E +02	0.05 – 0.41	0.13 – 0.11
		EFB ⁶⁷	0.25	6.75E +05	65	2.36E +05	4.72E +04	17.65	8.33E +05				
		K. shell ⁶⁷	0.08	2.16E +05	10	1.94E +05	3.88E +04	20.1	7.80E +05	9.79E +04	2.61E +05	19.6 – 16.3	52.2 - 43.5
Oil, palm fruit	2.70E +06	P. Fiber ⁶⁷	0.122	3.29E +05	40	1.97E +05	3.94E +04	18.7	7.36E +05				
		husk	2.1	6.84E +04	15	5.82E +04	1.16E +04	12.56	1.46E +05	6.09E +03	1.62E +04	1.2 - 1	3.25 – 2.71
Coffee, green	3.26E +04	straw	1.2	1.02E +03	15	8.72E +02	1.74E +02	15.60	2.72E +03	1.13E +02	3.02E +02	0.02 – 0.01	0.06 – 0.05
Wheat	8.55E +02	Aerial p. ⁸	3.52	8.76E +05	41.5	5.13E +05	1.02E +05	18.8	1.92E +06	8.04E +04	2.14E +05	16.1 – 13.4	42.8 – 35.6
Seed cotton	2.49E +05	Shell ⁹	0.477	3.56E +05	8.2	3.27E +05	6.55E +04	15.66	1.02E +06	4.25E +04	1.13E +05	8.5 – 7.1	22.6 – 18.8
Groundnut (shell)	7.48E +05												

⁶ LVH and moisture values of Palm oil residue were respectively based on published information (Chua, 1991; Husain et al., 2003; Yusoff, 2006 and Chuah et al., 2006),

⁷ The residue of product ratio (RPR) values were based on published information (Prasertsan and Prasertsan, 1996)

⁸ LVH and moisture values of seed cotton residue were respectively based on published information (Hiloidhari and Burah, 2011)

⁹ RPR, LVH and moisture values of groundnut residue were respectively based on published information (Lim et al., 2012)

3.2 Descriptions of the Systems

The systems in this study are combinations of the concentrating solar power and biomass-fired technologies using solar and sorghum residues as primary energy sources for electricity generation. The HRSG configuration varies according to operating conditions of the combined power cycles. During the research, three cases were modeled, analyzed and optimized for a 5 MWe hybrid (solar- biomass) power plant for electricity, heating, cooling, and hot water generation. These hybrid systems use parabolic trough collectors, solar tower and linear Fresnel reflectors among other concentrating solar technologies combined with biomass-fired technology.

The hybrid system includes biomass-fired technology using feedstock from sorghum stalk and concentrating solar power technology that uses solar irradiation. The hybrid system operates continuously with the biomass-fired technology covering the long periods of unavailability of solar energy, while the CSP technology work during daytime. The agriculture residues from sorghum harvesting are used as a feedstock, its pre-treatment processes were not considered during the study. Nevertheless, the volume and properties of the feedstock were determined by taking into account the capacity of the system, annual production of electricity, system operating time and boiler efficiency. Besides, the characteristics of the equipment that contribute to the production of thermal energy have also been studied which included the components of the system and the regeneration of steam water. The evaporation process of water occurred inside of the heat recovery steam system. The steam generation circuit of the power system is based on five regenerators that help to produce the phase change of the water and raise its temperature from 87°C to 319.4°C at 10.5 MPa. This regeneration process contributes enormously to the energy production and efficiency of the studied system by increasing the mass flow rate of the steam entering the boiler. Thus, the heat recovery steam generation system is of a key subsystem for thermal power system design, since it is impacting the capacity of the system and the volume of feedstock used to generate the required thermal energy. Furthermore, it also makes possible the connection of additive units for

multi-energy generation purposes such as heating, cooling and producing hot water for domestic activities.

A good hybridization of the power system using concentrating solar power technologies requires an assessment of the existing systems that match with the study cases. Each technology assessed leads to the determination of their characteristics that are related to the performance of the designed solar field, the power block capacity and the amount of heat waste that can be recovered. In general, the solar tower is considered as a most flexible CSP technology. Due to the use of water as a fluid transfer in the solar field as well as the working fluid in the power block. This particularity can be seen as an advantage in term of complexity level for the operating condition. Thus, the steam generation process is considered as a direct process which makes easy the combination of the solar tower and the biomass-fired technology in the hybrid system. According to this, a unique design of the heat recovery steam generation system is required. Moreover, this hybrid system does not require an intermediate heat exchanger due to (DSG process. The combined Rankine cycles used in the power block has similar operating conditions for both biomass-fired and solar tower technologies. Since the disposal of the additive units for multi-energy generation system are similar, this leads to reduced cost of the hybridized system in this case. The design of the solar field is the main task of this research. On other hands, it is essential to note that, the operational characteristics of the power block of a STTP using PTC or LFR technology are identical, because of the Therminol VP-1 that has been used as the heat transfer fluid. The steam water is generated through an ISG process leading to the use of an intermediate heat exchanger. The Therminol VP - 1 used as transfer fluid circulates in a closed loop between the points 1 - 2 - 2' - 1' and the 1 - 2 - 2'' - 1'' to ensure that the thermal energy required for the power block of the hybrid system remains available for multi-energy purposes. The annual thermal energy output of studied solar technologies depends on the inherent intrinsic parameters such as, mirror design, concentrating ratio, optical loss of receivers, the efficiency solar - to - electricity and others. It is important to notice that, the operating conditions of the power block affect the HRSG system. Therefore, these two solar technologies adopt a particular design of the steam regeneration system containing three (3) generators which contribute to produce the phase change of

the water and raise its temperature from 87°C to 267.8°C at 5MPa. On the other hand, given the importance of the ORC in the studied system, part of the heat transported by the Therminol VP-1 has been transferred to the heat exchanger of the closed ORC system.

3.2.1 Case 1: Parabolic trough collector/Biomass – fired system

Parabolic Trough Collector is considered as a mature concentrating solar technology used for commercial thermal power plant construction as discussed in the literature. This technology has been experimented in many existing power plants and has presented better results. Therefore, this technology combined with biomass-fired technology using solid fuel from sorghum stack has been used during the study. The schematic view of the proposed Hybrid biomass-fired/parabolic trough collector power system as shown in Figure 3.1 is divided into three subsystems namely; solar–biomass field system, power block system, and HRSG system. The first subsystem contains a solar field consisting of an arrangement of collector's assembly interconnected, piping system, intermediate heat exchanger and other control devices. The solar radiation is concentrated into a Schott PTR80's receiver by using LUZ S-3 collectors arranged in 20 loops each containing 4 solar collector assemblies with 48 modules. The Therminol VP–1 goes through each loop and heat transfer circuit to transport the thermal energy generated by a solar field that needed to be transferred to the power block system by using the intermediate heat exchanger. The total land occupied by the solar field is estimated at 100936 m² where only 43.19% represents the active area covered by 960 modules with a length and an aperture width of 8.33m and 5.75 m respectively. The area occupied by the biomass-fired system, feedstock processes, and storage with a yearly capacity of 28152 dry tons is estimated at less than 5% of the total land occupied by a hybrid power plant. The solar multiple (SM) of the solar field used for the proposed hybrid energy system has been chosen equal to 1 (SAM 17.9.5, NREL software). The indirect steam generation process has been adopted for the power block due to the use of Therminol VP – 1 as the heat transfer fluid. The steam generation process can be considered as direct when biomass solid fuels are burned inside of the boiler. It is essential to mention that; the variation of the steam generation process affects the operation conditions of

The combined power cycles used to produce electricity is a combination of steam Rankine turbines cycle and an organic Rankine cycle. The HRSG described above contains many units which are considered as one multi-energy generation system. The heat recovered from the power cycles is used to feed the generator of this unit to produce the energy required for domestic and industrial purpose. The usage of this multi-energy generation system contributes to improving the rational use of thermal energy generated during conversion of renewable energy sources. Figure 3.2 presents absorption refrigeration and a drying unit integrated into the HRSG system connected to the power block.

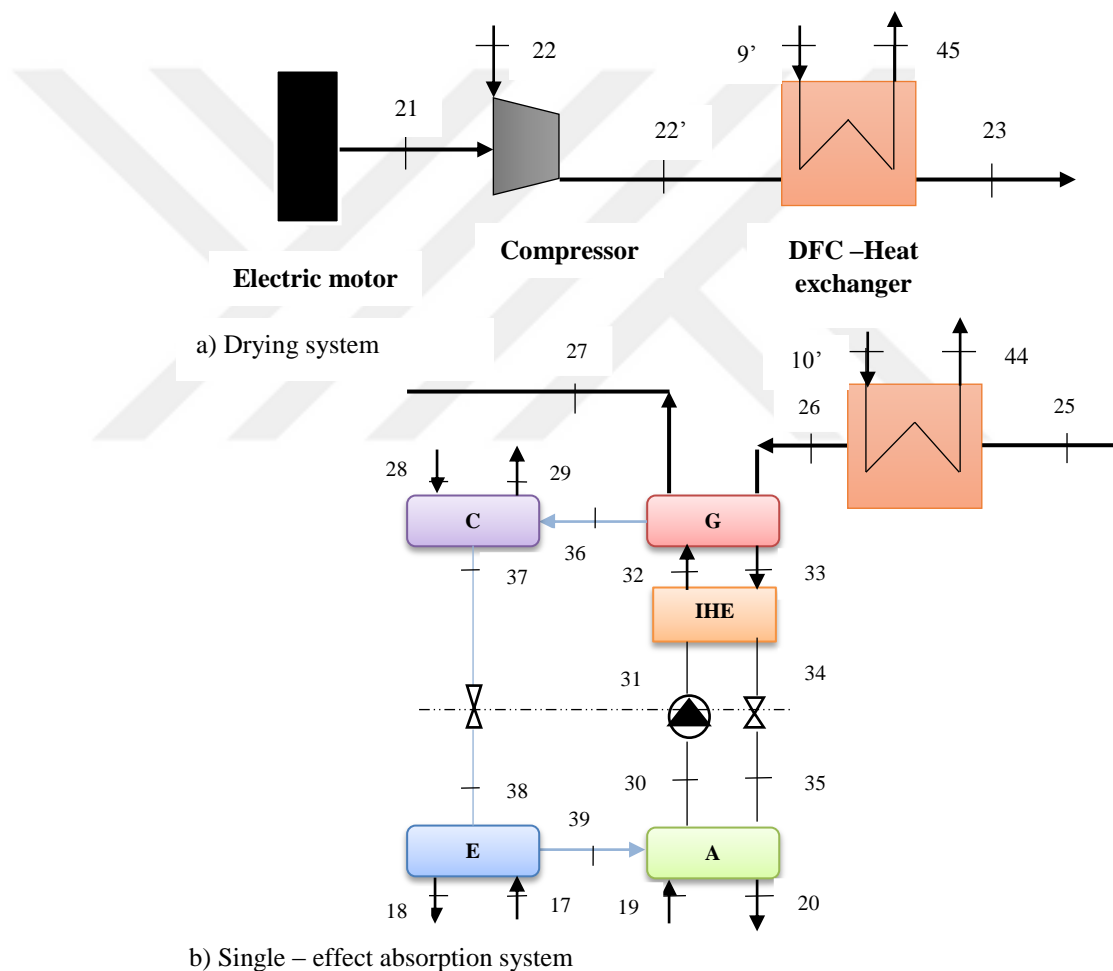


Figure 3.2. (a) Drying system (b) Single-effect absorption system.

3.2.2 Case 2: Solar tower/Biomass-fired system

Solar tower technology is also considered as a mature technology compared to the linear Fresnel reflectors and parabolic dishes technology. Because of its high operating conditions, the solar tower is a better option for combining with a thermal power plant in a hybridized system. Hence, many commercial solar thermal power plants have been built using them as CSP technology. In this study solar tower and biomass-fired technology have been combined to hybridize the primary energy input sources. The design presented in Figure 3.3 is completely different from the hybrid systems considering other CSP technologies due to the use of water as a heat transfer fluid in the solar field. The proposed hybrid energy system based on biomass-fired and solar tower technology does not use the intermediate heat exchanger. Hence, the combined power cycle works at a single – operating conditions between 314.9°C-541°C for an inlet pressure of 10.5 MPa and a mass flow rate which varies between 8.39 and 8.66 kg/s according to the thermal energy generated. The exhaust heat of the low – pressure steam turbine is used to feed the heat exchanger of the ORC system. The circuit of the HRSG system does not influence the operation process of electricity generation. These affect the overall proposed hybrid energy system performance and leads to a cost reduction due to the usage of standalone combined power cycles and heat recovery steam generation system.

The active land of the solar field covered an area estimated at 50667.1 m² which contains 351 heliostats with a specific area of 144 m². The solar field of ST technology is one of the most difficult tasks during the design of the system configuration because of its particular arrangement and some parameters such as: the distance from the tower, the height ratio of tower and heliostat that are required to be carefully determined. The proposed hybrid energy system considered a tower with a height of 37.65 m and receiver with, height and diameter of 4.93 m and 5.39m where the coating emittance and absorptance are 0.88 and 0.94, respectively. Other parameters related to the boiler, superheater, and reheaters such as tube diameter, thickness, the material used for manufacturing and heat losses have been determined. Furthermore, the solar multiple has been taken equal to 1.4.

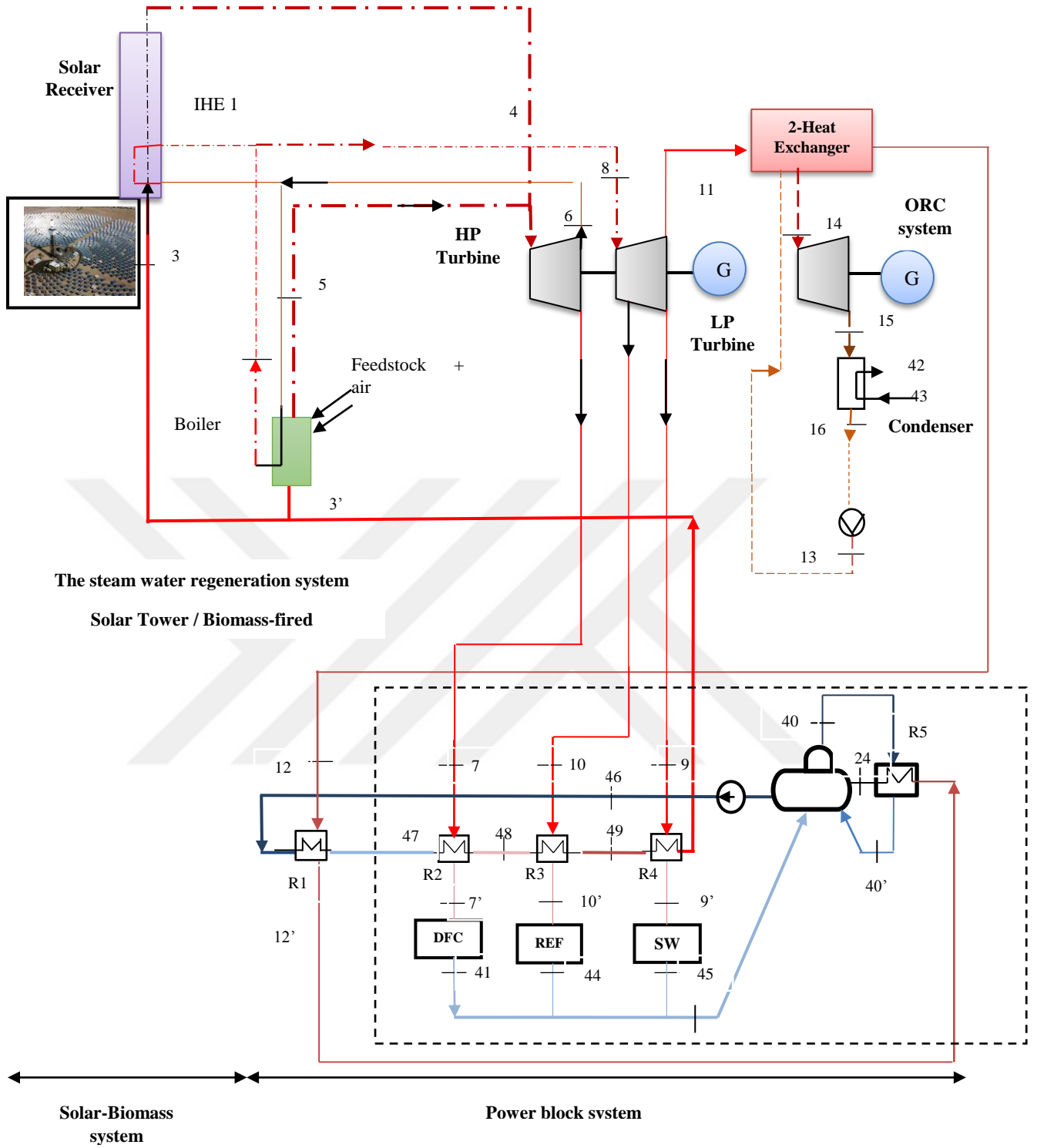


Figure 3.3. Case study II - schematic diagram of a hybrid biomass-solar power system based on the solar tower.

3.2.3 Case 3: Linear Fresnel reflector/Biomass-fired system

Figure 3.4 presents a hybrid energy system based on biomass-fired and linear Fresnel reflectors which is not yet considered as a mature technology due to its less use for commercial thermal power plants. This creates a challenge in the design of its solar field based on its previous effectiveness in other studies and projects.

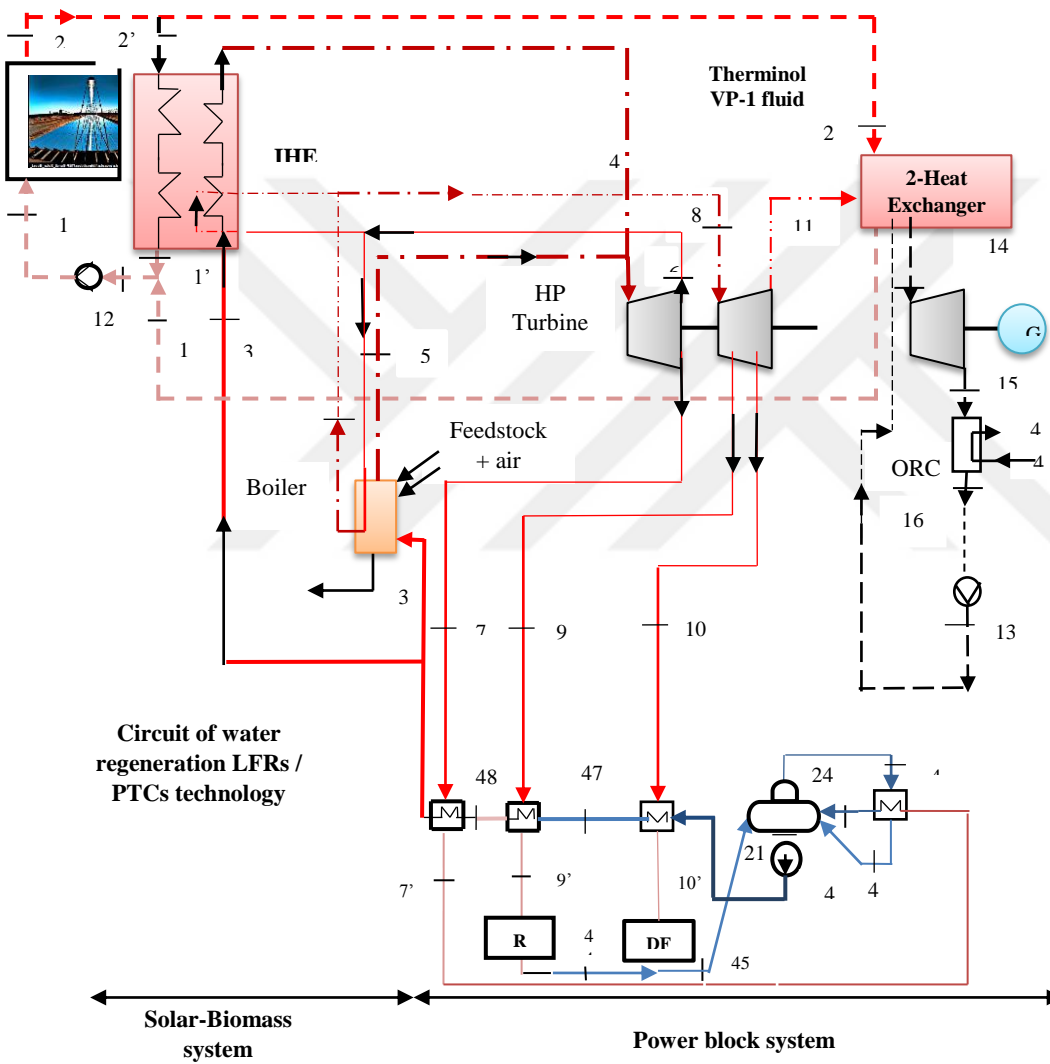


Figure 3.4. Case study III - schematic diagram of a hybrid biomass-solar power system based on linear Fresnel reflectors.

Therefore, the design of the solar field developed for the hybrid energy system based on LFRs technology which is similar to the power system based on PTCs technology taken as a reference to the design. The schematic view of the

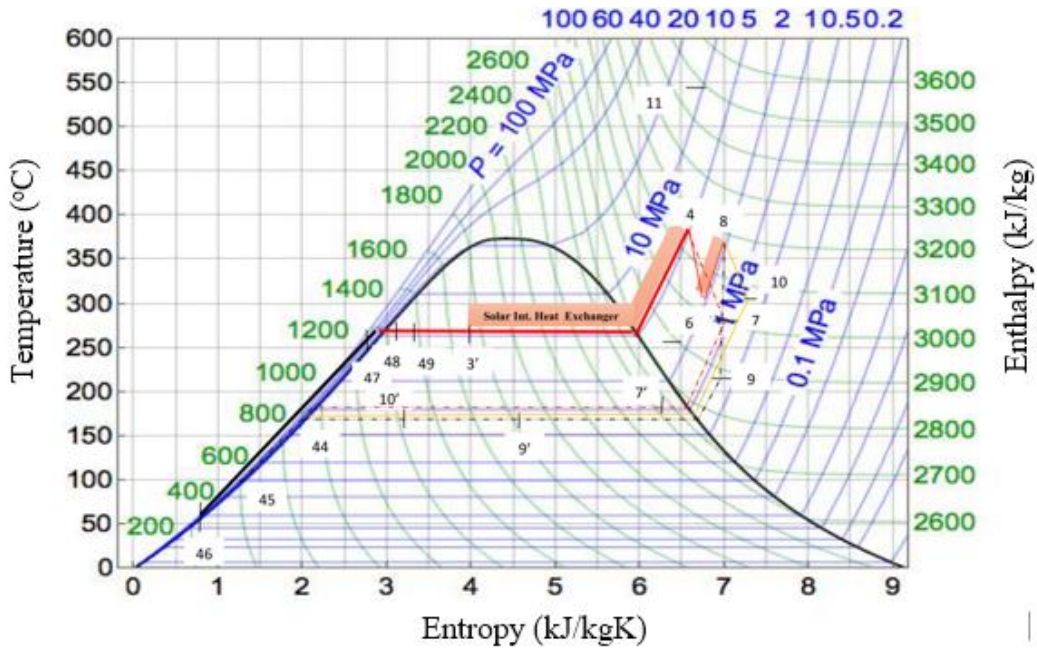
hybrid energy system using PTCs and LFRs technology are similar in more than one point, the utilization of the Therminol VP-1, the integration of intermediate heat exchanger that influences thermodynamic properties of the combined power cycles and the design of HRSG circuit. However, the major differences are in the disposal of the linear Fresnel mirrors on the field. The total land was estimated at 69679 m² where the active area covered 64.8% and consist of the arrangement of 64 lines (SCA) in 6 loops with an area of 7524 m² and length equal to 44.8 m. The thermal energy is transferred to combined power cycles by an indirect steam generation process that uses Therminol VP-1 as a heat transfer fluid operating between 230 – 400°C with a mass flow rate of 42.5 kg/s. In this study, the technical parameters of biomass-fired system do not change according to the concentrating solar power technology used for hybridization.

3.3 Thermodynamic Properties of the Hybrid Energy Systems

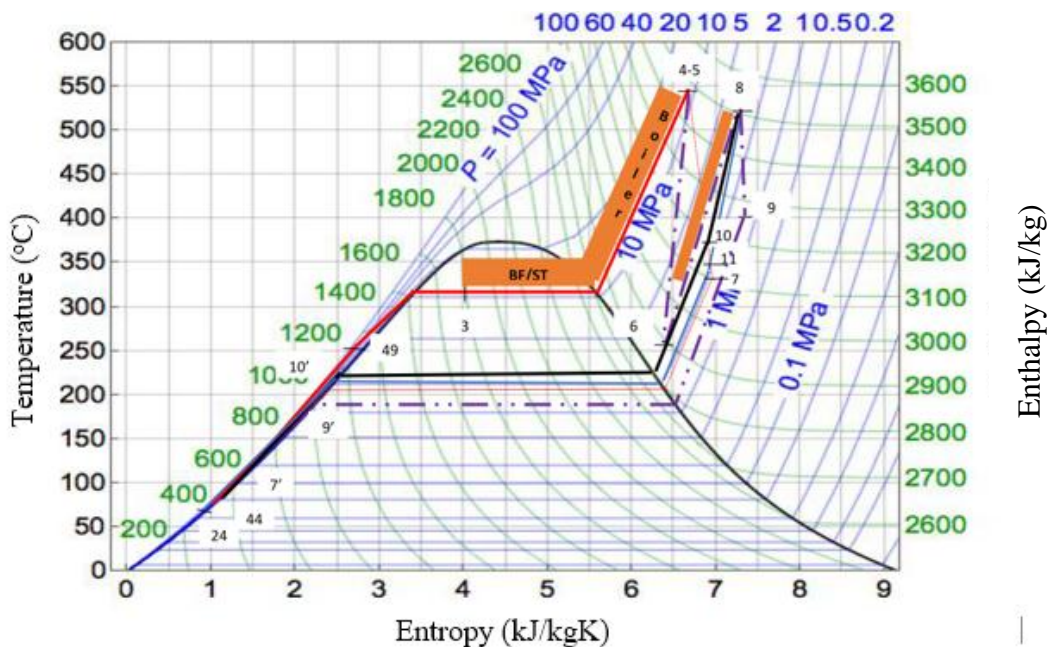
Thermodynamic properties of each point for three systems are given in Appendix A. Figure 3.5 presents T-s diagram of the steam Rankine cycle of a power system based on concentrating solar power and biomass-fired technology. The thermal energy is transferred from the Therminol VP-1 transport circuit to the power unit via the heat exchanger, thus point 4 has the thermophysical properties required to trigger the work in the HP - steam turbine. The similar process is carried out inside the boiler that triggers the work in the HP - steam turbine at point 5. The saturated steam at point 6 carries exhausting heat to be regenerated inside of the boiler or heat exchanger according to the technology used. The thermal energy carried by point 8 leads to the work of the low pressure (LP) steam turbine. This turbine discharges some of the non-transformed heat into work in the ORC's heat exchanger at point 11, to produce work using a small gas turbine. While the other part of this rejected heat is used for the steam generation process inside of the HRSG fed at points 9 and 10.

The organic fluid named as R134a used as working fluid to generate electricity, which follows a repeated state change 17 - 14 - 15 - 16 in a closed ORC system. The change of state inside of the heat exchanger leads to the absorption of thermal energy, which makes it possible to obtain the required

characteristics to trigger the work in the gas turbine. The efficiency of ORC depends essentially on the thermal efficiency of the intermediate exchanger and the thermophysical properties of the working fluid.



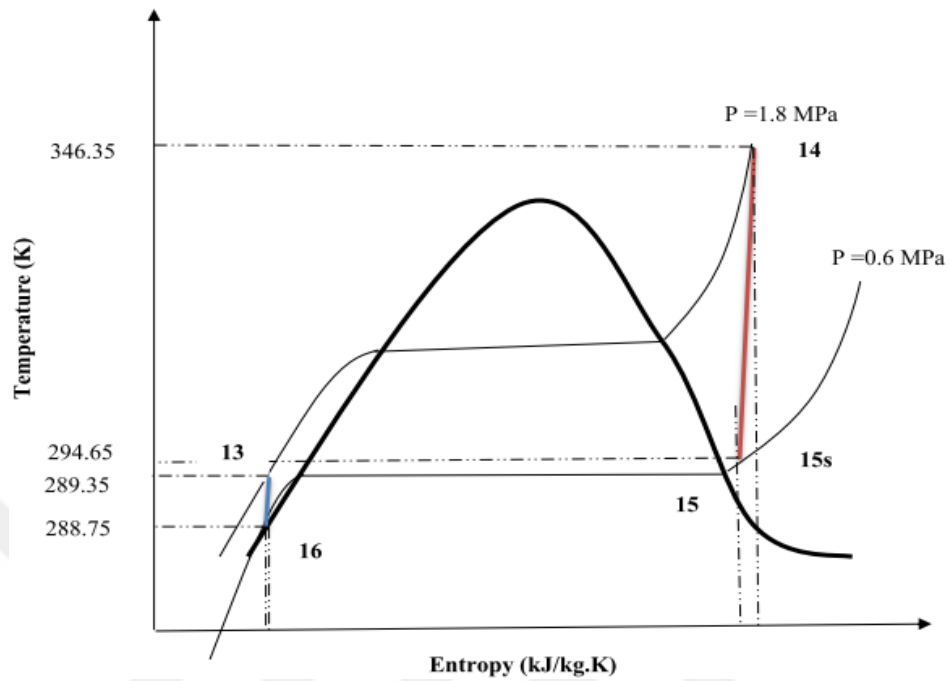
a) SRC based on PTC/LFR



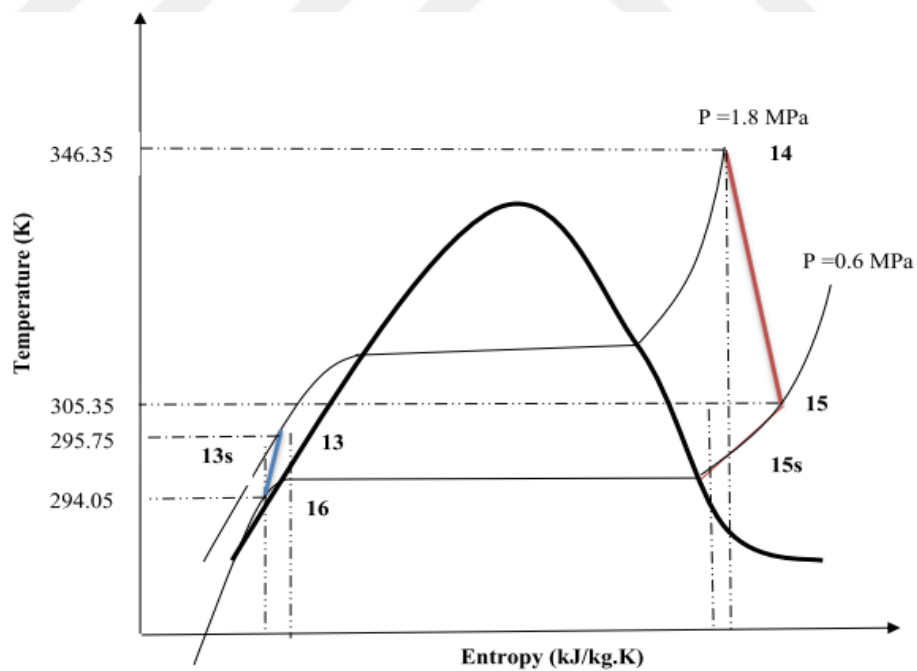
b) SRC based on ST/BF

Figure 3.5. T – s diagram of the steam Rankine cycle based on (a) PTC and LFR technologies, (b) ST and BF technologies.

Figure 3.6 presents T-s diagram of the organic Rankine cycle integrated into the power block cycle of a hybrid energy system.



a) ORC based on PTC and LFR



b) ORC based on ST and BF

Figure 3.6. T – s diagram of the organic Rankine cycle based on (a) parabolic trough collector and linear Fresnel reflector technologies. (b) solar tower and biomass-fired technologies.

Figure 3.7 presents T-s diagram of the absorption refrigeration unit integrated into the power block cycle of a hybrid energy system. The studied system uses the waste heat that could not be recovered during the steam regeneration process to produce cooling.

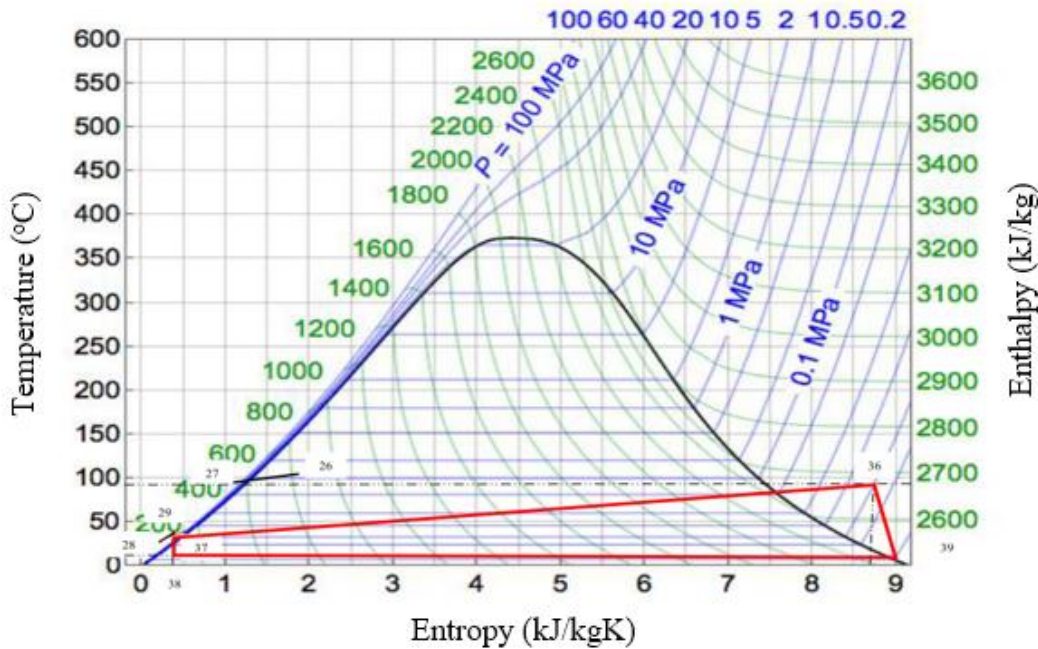


Figure 3.7. T-s diagram of lithium bromide/water of an absorption refrigeration cycle (cooling generation side).

As shown in Figure 3.7, a single-effect absorption refrigeration cycle is a commonly used technology for an absorption refrigeration system. The working fluid used during the system design determined its configuration. Then, the additive unit which produces cool and hot water for domestic use. It can be considered as a single-effect system because of the lithium bromide/water couple which is non-volatility absorbent. The heat exchanger contributes to regulating the heat input at the generator, whereas the high-temperature heat supplied to the generation helps to evaporate the refrigerant out from LiBr-water solution at point 36. The heat generated is released out at the condenser and absorber, this situation presents the irreversibility caused by the studied unit. The solution used is preheated inside of heat exchanger before entering the generator at point 32 by using heat from the weak solution leaving the generator at point 33. The drying system uses the heat released out of the HRSG system at point 9' to heat air coming from the compressor at point 22' before sending the air out of heat

exchanger at point 23. The dry air keeps the room warm at the required temperature for product preservation.

It is crucial to notice that, the design of the BF system remains unchanged even if the CSP technologies varies according to the case studies specified above. The arrangement of the combined power cycles and the regeneration system which constitutes the power block remains the same, only for the hybrid energy system using solar tower and biomass-fired technology. While the arrangement of the power block is different when the CSP technology used to operate the hybrid energy systems changes. A combined power cycles and a multi-energy generation system connected to the regeneration system are modeled to facilitate their analysis and optimization. Therefore, this section presents the advantages and disadvantages of each of the study cases for hybrid systems configuration and the benefit of using a multi-energy generation system.

4. ENERGY, EXERGY AND EXERGOECONOMIC ANALYSIS

4.1. Introduction

The formulations of mass, energy, and entropy, the exergy balance equations presented below play a key role in thermodynamic analysis of the control volume system.

- **Mass Balance**

The principle of mass conservation is a fundamental principle in the analysis of a thermodynamic system. It is defined as the time rate of accumulation of mass within the control volume equals to the difference between the total rates of mass flow entering and exiting across boundaries as shown in Figure 4.1 and it is expressed as given below in equation 1 (Bejan et al., 1996):

$$\frac{dm_{cv}}{dt} = \sum_i \dot{m}_i - \sum_e \dot{m}_e \quad \text{eq.1}$$

where \dot{m} is mass flow rate and m is mass. The subscripts i and e refer to the inlet and the exit of the control volume, respectively.

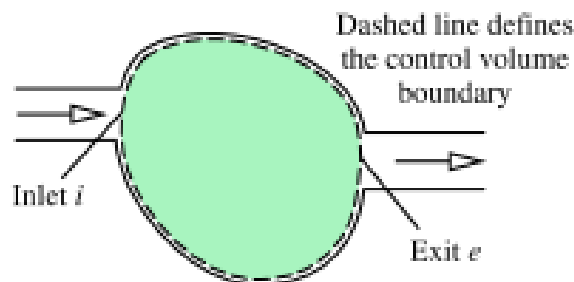


Figure 4.1. One-outlet, one-exit control volume (Moran and Shapiro, 2006).

- **Energy balance**

The energy principle of the control volume is expressed as a time rate of energy accumulation within the control volume equal to the excess of the

incoming over the outgoing energy rate. It is known as the first law of thermodynamics and defined as follows (Bejan et al., 1996):

$$\frac{d(U+KE+PE)_{cv}}{dt} = \dot{Q} - \dot{W} + \sum_i \dot{m}_i \left(h_i + \frac{1}{2} V_i^2 + g z_i \right) - \sum_e \dot{m}_e \left(h_e + \frac{1}{2} V_e^2 + g z_e \right) \quad \text{eq.2}$$

where U denote the internal energy, KE is kinetic energy, and PE is the potential energy of the control volume at time t. \dot{Q} and \dot{W} are the net rates of energy transfer by heat and work, respectively. The symbols V , h , g , and z are velocity, enthalpy, gravity, and elevation, respectively.

- **Entropy**

Entropy, like energy and mass, is an extensive property and can be transferred into or out of a control volume by streams of matter. The entropy generated within a process is called the entropy generation. The entropy change can be expressed as follows:

$$\frac{dS_{cv}}{dt} = \sum_j \frac{Q_j}{T_j} + (\sum_i \dot{m}_i s_i - \sum_e \dot{m}_e s_e) + \dot{S}_{gen} \quad \text{eq.3}$$

where $\frac{dS_{cv}}{dt}$ represents the rate of entropy change within the control volume. The terms $\dot{m}_i s_i$ and $\dot{m}_e s_e$ account for the rate of entropy transfer into and out of the control volume associated with mass flow, respectively. The ratio $\frac{Q_j}{T_j}$ accounts for the associated rate of the entropy transfer.

- **Exergy balance**

Unlike energy, exergy is not conserved. Hence, the exergy destruction is a key parameter for exergy analysis of systems. It is defined as a potential work lost due to irreversibility within the system and is related to the rate of entropy generation with the system by exergy destruction ($T_o S_{gen}$). The exergy balance leads to the second law of thermodynamic which is expressed as given below.

$$\frac{dE_{cv}}{dt} = \sum_j \left(1 - \frac{T_o}{T_j}\right) Q_j - \left(\dot{W}_{cv} - p_o \frac{dV_{cv}}{dt}\right) + (\sum_i \dot{m}_i e_i - \sum_e \dot{m}_e e_e) - T_o \dot{S}_{gen} \quad \text{eq.4}$$

where T , p , V , and e are temperature, pressure, volume and specific exergy transfer into or out of the control volume, respectively. The term $T_o \dot{S}_{gen}$ accounts for the rate of exergy destruction. The subscript j , is the property value at the state j and the subscript o is the value of a property at the surrounding.

- **Energy efficiency**

The energy efficiency depends on the useful energy of the system and the input energy transferred to the system. Therefore, energy efficiencies vary with system technology. The energy efficiencies of different subsystems are defined as illustrated below.

- Power block unit using a thermal cycle such as Brayton or Rankine

$$\eta_{cycle} = \frac{W_{cycle}}{Q_i} = \frac{\sum_j (W_T - W_P)}{Q_i} \quad \text{eq.5}$$

The isentropic thermal efficiency is related to work – producing of the devices such as turbines and is given as

$$\eta_{is} = \frac{W}{W_{is}} \quad \text{eq.6}$$

It is also related to the work–consuming of devices such as compressors, pumps and fans and is expressed as

$$\eta_{is} = \frac{W_{is}}{W} \quad \text{eq.7}$$

The value of the isentropic efficiency of work-producing and work-consuming devices are typically between 70–90% and 75–85%, respectively.

The performance of the absorption refrigeration system is evaluated as the coefficient performance (COP) and is expressed as given in equation 8 below.

$$\text{COP} = \frac{\text{desired output}}{\text{required input}} = \frac{Q_L}{(Q_H - Q_L) + W_{\text{pump}}} \quad \text{eq.8}$$

where H and L are a high and low-temperature reservoir.

- **Exergy efficiency**

The exergy analysis of multi-energy generation system introduces exergy efficiency as a key parameter for the assessment of thermodynamic performance. The exergy analysis of the system is assessed using the following equation 9 (Bejan et al., 1996):

$$\dot{E}_F = \dot{E}_P + \dot{E}_D + \dot{E}_L \quad \text{eq.9}$$

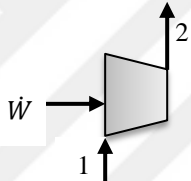
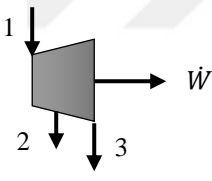
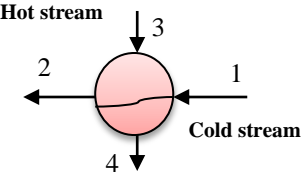
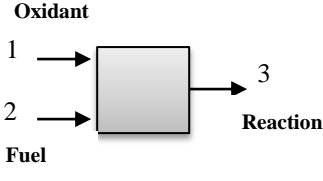
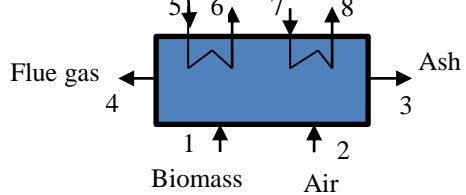
where \dot{E}_F , \dot{E}_P , \dot{E}_D , and \dot{E}_L are exergy rate of fuel, exergy rate of the product, exergy rate of destruction and exergy rate of losses, respectively.

The exergetic efficiency ε is the ratio between product and fuel exergy expressed as follows (Bejan et al., 1996):

$$\varepsilon = \frac{\dot{E}_P}{\dot{E}_F} = 1 - \frac{\dot{E}_D + \dot{E}_L}{\dot{E}_F} \quad \text{eq.10}$$

Table 4.1 presents exergy rates associated with the fuel and product for key components at steady-state and used for thermal power system design.

Table 4.1. Exergy rates associated with the fuel and product for key components at a steady-state.

Components	Schematic	Exergy rate of fuel (\dot{E}_F)	Exergy rate of product (\dot{E}_P)	Efficiency (ε)
Compressor, fan		$\dot{E}_F = \dot{W}$	$\dot{E}_P = \dot{E}_2 - \dot{E}_1$	$\varepsilon = \frac{\dot{E}_2 - \dot{E}_1}{\dot{W}}$
Turbine		$\dot{E}_F = \dot{E}_1 - (\dot{E}_2 + \dot{E}_3)$	$\dot{E}_P = \dot{W}$	$\varepsilon = \frac{\dot{W}}{\dot{E}_1 - (\dot{E}_2 + \dot{E}_3)}$
Heat exchanger		$\dot{E}_F = \dot{E}_3 - \dot{E}_4$	$\dot{E}_P = \dot{E}_2 - \dot{E}_1$	$\varepsilon = \frac{\dot{E}_2 - \dot{E}_1}{\dot{E}_3 - \dot{E}_4}$
Combustion chamber		$\dot{E}_F = \dot{E}_1 + \dot{E}_2$	$\dot{E}_P = \dot{E}_3$	$\varepsilon = \frac{\dot{E}_3}{\dot{E}_1 + \dot{E}_2}$
Boiler		$\dot{E}_F = (\dot{E}_1 + \dot{E}_2) - (\dot{E}_3 + \dot{E}_4)$	$\dot{E}_P = (\dot{E}_5 - \dot{E}_6) + (\dot{E}_7 + \dot{E}_8)$	$\varepsilon = \frac{(\dot{E}_1 + \dot{E}_2) - (\dot{E}_3 + \dot{E}_4)}{(\dot{E}_5 - \dot{E}_6) + (\dot{E}_7 + \dot{E}_8)}$

4.2 Exergoeconomic

Exergoeconomic is a branch of engineering that combines energy and economic principles to provide a better operation model of the system with information not available by using conventional energy analysis and economic evaluation. The methodology used to carry out this information makes exergoeconomic to be a crucial way for the modeling and optimizing of a cost-effective system. This consist of the determination of the best estimation of the purchased equipment costs (PEC) that can be obtained directly from vendors' quotations, purchase orders or calculations using extensive databases often maintained by engineering companies and institutions. In this research, the above approaches were combined to carry out the purchased equipment cost of components. The typical values for scaling exponent used for the effect size on equipment cost are summarized by Couper et al. (2012). Furthermore, Bejan et al. (1996) carried out various cost related to the estimation of total capital investment. The conventional economic analysis used the cost balance equation 11 as presented below to formulate the overall system cost operating at steady-state.

$$\dot{C}_{P,tot} = \dot{C}_{F,tot} + \dot{Z}_{tot}^{CI} + \dot{Z}_{tot}^{OM} \quad \text{eq.11}$$

where \dot{C}_P , \dot{C}_F , \dot{Z}^{CI} , and \dot{Z}^{OM} are the cost rate associated with the products of the system, the fuel used to generate energy, the capital investment, and the operating and maintenance, respectively. The subscript, tot, stands for the overall system. The exergoeconomic balance equation given below is defined using the heat received and the power generated by a k^{th} component.

$$\sum_e \dot{C}_{e,k} + \dot{C}_{w,k} = \dot{C}_{q,k} + \sum_i \dot{C}_{i,k} + \dot{Z}_k \quad \text{eq.12}$$

where \dot{C} is the cost rate in USDcent per second and the exergy costing is defined by the equations given below;

$$\dot{C}_q = c_q \cdot \dot{E}_q \quad \text{eq.13}$$

$$\sum_e (c_e \cdot \dot{E}_e)_k + c_{w,k} \cdot \dot{W}_k = c_{q,k} \cdot \dot{E}_{q,k} + \sum_i (c_i \cdot \dot{E}_i)_k + \dot{Z}_k \quad \text{eq.14}$$

where c is the cost per unit exergy in USD per kWh or USD per GJ, \dot{Z} is the levelized cost rate to own, maintain and operate the k^{th} component.

- **Relative cost difference**

The relative cost difference r_k for the k^{th} component is defined by equation 15:

$$r_k = \frac{c_{P,k} - c_{F,k}}{c_{F,k}} \quad \text{eq.15}$$

The interactive cost of optimization of the system is applied when the cost related to fuel changes from one component to another. The cost optimization of the component leads to a reduction in the relative cost difference rather than reducing the cost per exergy unit. To do this, equation 16 above becomes:

$$r_k = \frac{c_{F,k}(\dot{E}_{D,k} + \dot{E}_{L,k}) + (\dot{Z}_k^{CI} + \dot{Z}_k^{OM})}{c_{F,k}\dot{E}_{P,k}} \quad \text{eq.16}$$

where $c_{P,k}$ and $c_{F,k}$ are the cost per exergy unit of product and fuel the k^{th} component, respectively. $c_{F,k}\dot{E}_{D,k}$ and $c_{F,k}\dot{E}_{L,k}$ are the capital investment cost related to the exergy destruction cost and exergy loss of the k^{th} component, respectively.

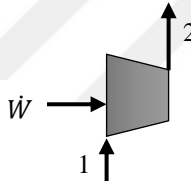
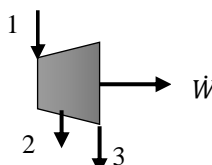
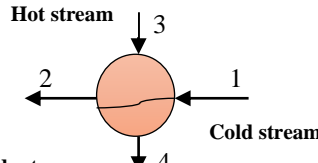
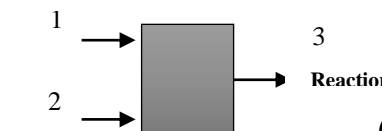
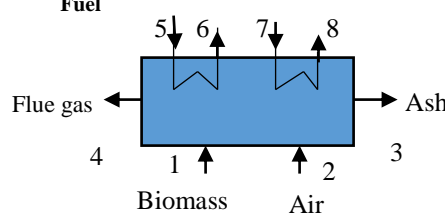
- **Exergoeconomic factor**

The exergoeconomic factor assesses the performance of the component and can be expressed as:

$$f_k = \frac{\dot{Z}_k}{\dot{Z}_k + c_{F,k}(\dot{E}_{D,k} + \dot{E}_{L,k})} \quad \text{eq.17}$$

Table 4.2 presents the calculation of associated rates with fuel and product as well as exergoeconomic relation for selected components at steady-state operation.

Table 4.2. Cost rates associated with the fuel and product as well as auxiliary exergoeconomic relations at steady-state.

Components	Schematic	Cost rate of fuel (\dot{C}_F)	Cost rate of prod. (\dot{C}_P)	Balance of component auxiliary
Compressor, fan		$\dot{C}_F = \dot{C}_w$	$\dot{C}_P = \dot{C}_2 - \dot{C}_1$	c_2 is the variable to be determined. $-\dot{C}_w + \dot{C}_2 = \dot{C}_1 + \dot{Z}$
Turbine		$\dot{C}_F = \dot{C}_1 - (\dot{C}_2 + \dot{C}_3)$	$\dot{C}_P = \dot{C}_w$	$c_2 = c_3 = c_1$, c_w is the variable to be determined. $\dot{C}_w + \dot{C}_2 + \dot{C}_3 = \dot{C}_1 + \dot{Z}$
Heat exchanger		$\dot{C}_F = \dot{C}_3 - \dot{C}_4$	$\dot{C}_P = \dot{C}_2 - \dot{C}_1$	$c_4 = c_3$, c_2 is the variable to be determined. $\dot{C}_2 + \dot{C}_4 = \dot{C}_3 + \dot{C}_1 + \dot{Z}$
Combustion chamber		$\dot{C}_F = \dot{C}_1 + \dot{C}_2$	$\dot{C}_P = \dot{C}_3$	c_3 is the variable to be determined. $\dot{C}_3 = \dot{C}_2 + \dot{C}_1 + \dot{Z}$
Boiler		$\dot{C}_F = (\dot{C}_1 + \dot{C}_2) - (\dot{C}_3 + \dot{C}_4)$	$\dot{C}_P = (\dot{C}_5 - \dot{C}_6) + (\dot{C}_7 + \dot{C}_8)$	c_8, c_6 are the variables to be determined. $\dot{C}_6 + \dot{C}_8 + \dot{C}_3 + \dot{C}_4 =$ $\dot{C}_5 + \dot{C}_7 + \dot{C}_2 + \dot{C}_1 + \dot{Z}$

4.3 Advanced Exergoeconomic Method

The advanced exergoeconomic method is a specific optimization method used in the exergoeconomic analysis that focuses on the exergy destruction of the k^{th} component to optimize its efficiency. In this respect, the total exergy destruction of the k^{th} component can be expressed as (Morosuk and Tsatsaronis, 2009):

$$\dot{E}_{D,k} = \dot{E}_{D,k}^{EN} + \dot{E}_{D,k}^{EX} \quad \text{eq.18}$$

where $\dot{E}_{D,k}^{EN}$ and $\dot{E}_{D,k}^{EX}$ are endogenous and exogenous exergy destruction of the k^{th} component, respectively. In general, endogenous exergy destruction is considered as a result of a part of the exergy destruction that depends only on the component without any external effect. While the exogenous exergy is a consequence of interactions between the under-considered component and other components. Thus, it can be expressed as

$$\dot{E}_{D,k}^{EX} = \dot{E}_{D,k} - \dot{E}_{D,k}^{EN} \quad \text{eq.19}$$

The exergy destruction of the k^{th} component is divided into an avoidable and unavoidable part and can be expressed as (Bejan and Tsatsaronis, 1996)

$$\dot{E}_{D,k} = \dot{E}_{D,k}^{UN} + \dot{E}_{D,k}^{AV} \quad \text{eq.20}$$

The avoidable and unavoidable exergy destruction of the k^{th} component are calculated using these expressions:

$$\dot{E}_{D,k}^{UN} = \dot{E}_{P,k} \left(\frac{\dot{E}_{D,k}}{\dot{E}_{P,k}} \right)^{UN} \quad \text{eq.21}$$

$$\dot{E}_{D,k}^{AV} = \dot{E}_{D,k} - \dot{E}_{D,k}^{UN} \quad \text{eq.22}$$

Figure 4.2 shows a split subdivided in 4 main parts, where left and right side expressed avoidable-exogenous or avoidable-endogenous and unavoidable-

exogenous or unavoidable-endogenous respectively, which are combination of aforementioned types of exergy destruction (endogenous, exogenous, avoidable and unavoidable).

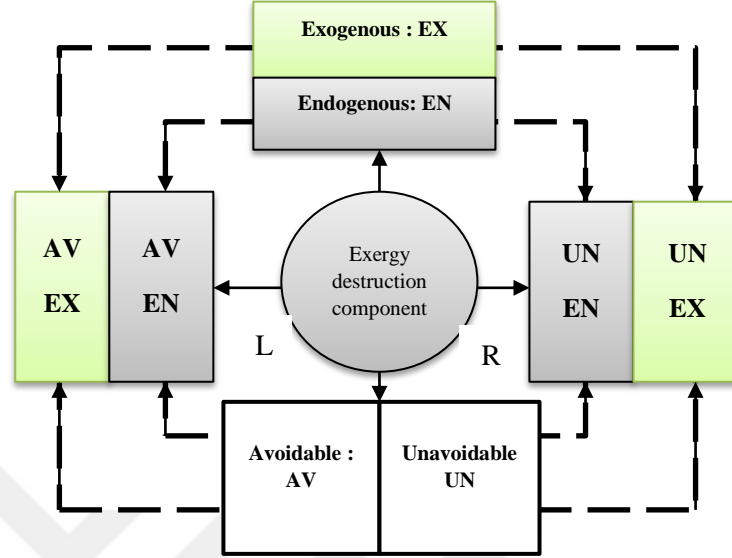


Figure 4.2. Complete splits of the exergy destruction in an advanced exergetic analysis.

As result of above equations unavoidable endogenous and exogenous exergy destruction can be written as follows (Kelly et al. 2009; Morusk and Tsatsaronis, 2008)

$$\dot{E}_{D,k}^{UN,EN} = \dot{E}_{P,k}^{EN} \left(\frac{\dot{E}_{D,k}}{\dot{E}_{P,k}} \right)^{UN} \quad \text{eq.23}$$

$$\dot{E}_{D,k}^{UN,EX} = \dot{E}_{D,k}^{UN} - \dot{E}_{D,k}^{UN,EN} \quad \text{eq.24}$$

Using the same approach, endogenous and exogenous exergy destruction can be determined using the following equations 25 and 26.

$$\dot{E}_{D,k}^{AV,EN} = \dot{E}_{D,k}^{EN} - \dot{E}_{D,k}^{UN,EN} \quad \text{eq.25}$$

$$\dot{E}_{D,k}^{AV,EX} = \dot{E}_{D,k}^{AV} - \dot{E}_{D,k}^{AV,EN} \quad \text{eq.26}$$

This approach has been extended to present parameters which cannot be found with a conventional exergoeconomic analysis

The endogenous investment cost containing capital investment and operating and maintenance cost of the k^{th} component is determined by the exergy product at the theoretical condition and the investment cost per unit exergy product at real condition given as:

$$\dot{Z}_k^{EN} = \dot{E}_k^{EN} \left(\frac{Z}{\dot{E}_P} \right)_k \quad \text{eq.27}$$

$$\dot{Z}_k^{EX} = \dot{Z}_k - \dot{Z}_k^{EN} \quad \text{eq.28}$$

The endogenous and exogenous are split into unavoidable and avoidable exergy destruction. The split right side with unavoidable-exogenous and unavoidable-endogenous parts lead to the determination of the investment cost expressed as below:

$$\dot{Z}_k^{UN,EN} = \dot{E}_k^{EN} \left(\frac{\dot{Z}_k^{UN}}{\dot{E}_P} \right)_k \quad \text{eq.29}$$

$$\dot{Z}_k^{UN,EX} = \dot{Z}_k^{EN} - \dot{Z}_k^{UN,EN} \quad \text{eq.30}$$

Subsequently, the split left with avoidable – exogenous and avoidable – endogenous part is obtained as:

$$\dot{Z}_k^{AV,EN} = \dot{Z}_k^{EN} - \dot{Z}_k^{UN,EN} \quad \text{eq.31}$$

$$\dot{Z}_k^{AV,EX} = \dot{Z}_k^{EX} - \dot{Z}_k^{UN,EX} \quad \text{eq.32}$$

The main steps of the advanced exergoeconomic analysis as summarized below:

- 1- Calculation of the entering and exiting exergy streams of each component.
- 2- Determination of the purchased equipment cost (PEC) of each component.

- 3- Calculation of fuel and product costs.
- 4- Identification of cost rate and cost per exergy unit equations.
- 5- Advanced exergy destruction analysis of entering and exiting streams of each component.
- 6- Identification of unavoidable, avoidable, endogenous and exogenous cost rate and cost per exergy destruction.
- 7- Evaluation of each component using relative cost difference and exergoeconomic factor to carry out the improvement level of the overall system.

4.4 Advanced Exergoeconomic for System Optimization

In general, a thermal system requires two conflicting objectives. The first consist of increasing the exergetic efficiency of the system and the second involves decreasing the cost rates associated with product and fuel, to satisfy the requirements of the exergoeconomic analysis. The first objective is governed by thermodynamic requirements and the second by economic constraints. Therefore, the objective function should be defined, in such a way that the optimization satisfies both requirements. For a single objective optimization, the optimization problem should be formulated as a minimization or maximization problem. The exergoeconomic analysis gives a clear picture of the costs related to the exergy destruction, exergy losses, etc. Thus, the objective function in this optimization becomes a minimization problem. Cammarata et al., (1998) used this optimization method through the genetic algorithm (GA) approach to optimize a district heating system. The objective function of the problem consisted of determination of the minimizing total cost function of the studied system, which can be modeled as:

$$\dot{C}_{sys} = \sum_k \dot{Z}_k + \sum_k \dot{C}_{D,k} + \dot{C}_{L,k} \quad \text{eq.33}$$

The multi-objective optimization focuses on the same functions as a single objective optimization which is the maximizing of total exergetic efficiency and the minimizing total cost rates of product and fuel of the studied system. The mathematical formulation of multi-objective functions can be expressed by the utilization of these following equations:

$$\varepsilon_{Tot} = \frac{\dot{E}_W}{\dot{E}_F} \quad \text{eq.34}$$

$$\dot{C}_{Tot} = \sum_k \dot{Z}_k + \sum_k \dot{C}_{D,k} + \dot{C}_{L,k} \quad \text{eq.35}$$

- **Advanced Exergoeconomic Analysis**

As summarized in Table 4.3, advanced exergoeconomic and exergoenvironmental analysis has been reviewed from 2002 to 2017 for power plant combined with various applications such as refrigeration systems (Morosuk and Tsatsaronis, 2009) and hydrogen liquefaction (H. Ansarinasab et al., 2017). The review was conducted to assess the methodology development and advantage compared to different calculation methods such exergoeconomic analysis (EEA), specific cost analysis (SPECOC), engineering functional analysis (EFA), exergetic cost theory (ETC), Modified structure productive analysis (MOPSA), and Thermo-economical functional analysis (TFA). The advanced exergy analysis methods have been applied mostly on the large power plant for various purposes, such as the hybrid molten carbonate fuel cell power plant studied by Mehrpooya et al. (2017) and the industrial plant with 1 MWe of avoidable exergy destruction located in the steam boiler (Vuckovic et al., 2012). Petrakopoulou et al. (2011b, 2011c, 2011d and 2012) evaluated the performance of various power plant with carbon capture technologies using exergoeconomic and exergoenvironmental analysis methods. Wang et al. (2012) and Yang et al. (2013) assessed the coal-fired supercritical power plant based on advanced exergy analysis combined with economic principle. Other similar studies on a large-scale using gas-fired technologies and geothermal for power generation have been summarized in Table 4.3. According to the literature, the contribution of exogenous exergy destruction varies between 10-30% (HRSG main components such as preheater or regenerators) of the overall exergy destruction. Zhu et al. (2016) established a

relation between the exogenous exergy destruction and the temperature of a component in the studied power system. The exergy destruction within heat exchangers of a power system was found to be between 35% and 50%. The range of 30-50% of exergy destruction was found within turbo-machines such as pumps, turbines, and compressors whereas 20% of exergy destruction within HRSG components was recovered. The endogenous exergy destruction of some component was found to be reaching 70% which means that, the amount of exergy destruction can be recovered during the optimization process. The usage of advanced exergoeconomic analysis leads to saving about 10% of both exergy destruction and total investment cost of the system. The boiler contributes more than other components for the avoidable investment and exergy destruction cost (Wang et al., 2019).

The exergy destruction and losses are the major thermodynamic inefficiencies in a power system which are directly related to operating cost. The exergoeconomic optimization aims at minimizing these inefficiencies and their related costs. The suitable modeling system is characterized by the obtaining of optimal values of selected criteria that lead to an efficient system. This can be done by determining an algorithm which provides the best criteria and constraints that govern the thermo-economic optimizations' behavior. Despite the results found in surveyed literature, the study cases depend on different surrounding conditions, subsystem boundaries and various criteria according to the aim of the research which impacts the selection of variables. Then, the results are generally affected not due to the accuracy of the method used but the aim of which does not match with the approach applied during analysis. The advanced exergoeconomic analysis (AEEA) has been chosen for the optimization of the case studies due to its overview of the studied system and purchase equipment costs. Figure 4.3 presents the algorithm of the exergoeconomic optimization method used for case studies. In Table 4.2 above, similar methods that have been used in other studies are shown and commented on the review of existing methods to improve the understanding of the AEEA method. The optimization modeling helps to determine an optimal design without the need to study various scenarios.

Table 4.3. Exergoeconomic methods and analysis.

Description of studied system/application	Advanced exergy-based analysis (AEA)	Exergoeconomic analysis (EEA)	Ad. exergo - economic analysis (AEEA)	Ad. exergo – environmental analysis (AEEA)	Authors, year
Solar Tower – coal-fired power generation system.	√		√		Bolatturk A. et al. (2015) Y. Zhu et al. (2016)
Existing geothermal power plant – Industrial process	√				H. Gökgedik et al. (2016)
Power plant using natural gas	√				G. Tsatsaronis and T. Morosuk (2010) E. Açıkkalp et al. (2014)
Thermal process and power plant optimization	√		√		G. Tsatsaronis et, (2006) T. Morosuk and G. Tsatsaronis (2009) G. D. Vuckovi, et al. (2012) P. Fu et al. (2016) L. Wang et al. (2017)
Combined cycles and supercritical power plant	√	√	√	√	F. Petrakopoulou et al. (2012) L. Wang, Y. Yang et al. (2012a, 2012b and 2013)
Applications: Hydrogen liquefaction plant, absorption refrigeration	√	√	√		T. Morosuk and G. Tsatsaronis, (2007, 2008 and 2009) H. Ansarinasab et al. (2017)
Power plant with CO ₂ capture technologies	√	√	√	√	F. Petrakopoulou (2011) F. Petrakopoulou, et al. (2011) F. Petrakopoulou, G. Tsatsaronis, T. Morosuk et al. (2011 and 2012) M. Mehrpooya et al. (2017)
Comprehensive analysis of exergy destruction (endogenous/exogenous, Unavoidable/avoidable)	√	√	√	√	G. Tsatsaronis and M.-H. Park (2002) G. Tsatsaronis, T. Morosuk and S. Kelly (2006) S. Kelly, G. Tsatsaronis, T. Morosuk (2009) Y. Lare, F. Petrakopoulou, et al. (2017). M. Penkuhn et al., (2019)

- **System and Subsystem Boundaries**

Considering the complexity of the overall studied system, it has been divided into three subsystems which have been modeled and optimized using the advanced exergoeconomic approach. The boundaries are imaginary surfaces that isolate each subsystem from other subsystems and their surroundings. Then, each subsystem is optimized individually using an optimization approach called sub-optimization.

- **Optimization Criteria**

The optimization criteria depend on the objective of the study and system boundaries as defined in the above subsection. Then, the optimization criteria in this study composed of obtaining data from the best economic and thermal efficiency design, to conduct suitable conditions of power plant operating parameters.

- **Variables**

The selection of the variables is influenced by the optimization boundaries and criteria. The main criterion in this study was to obtain lowest avoidable exergy destruction as possible or determine an approach for reducing avoidable exergy destruction, the lowest operating and maintenance cost, lowest cost of energy and the highest annual cash flow.

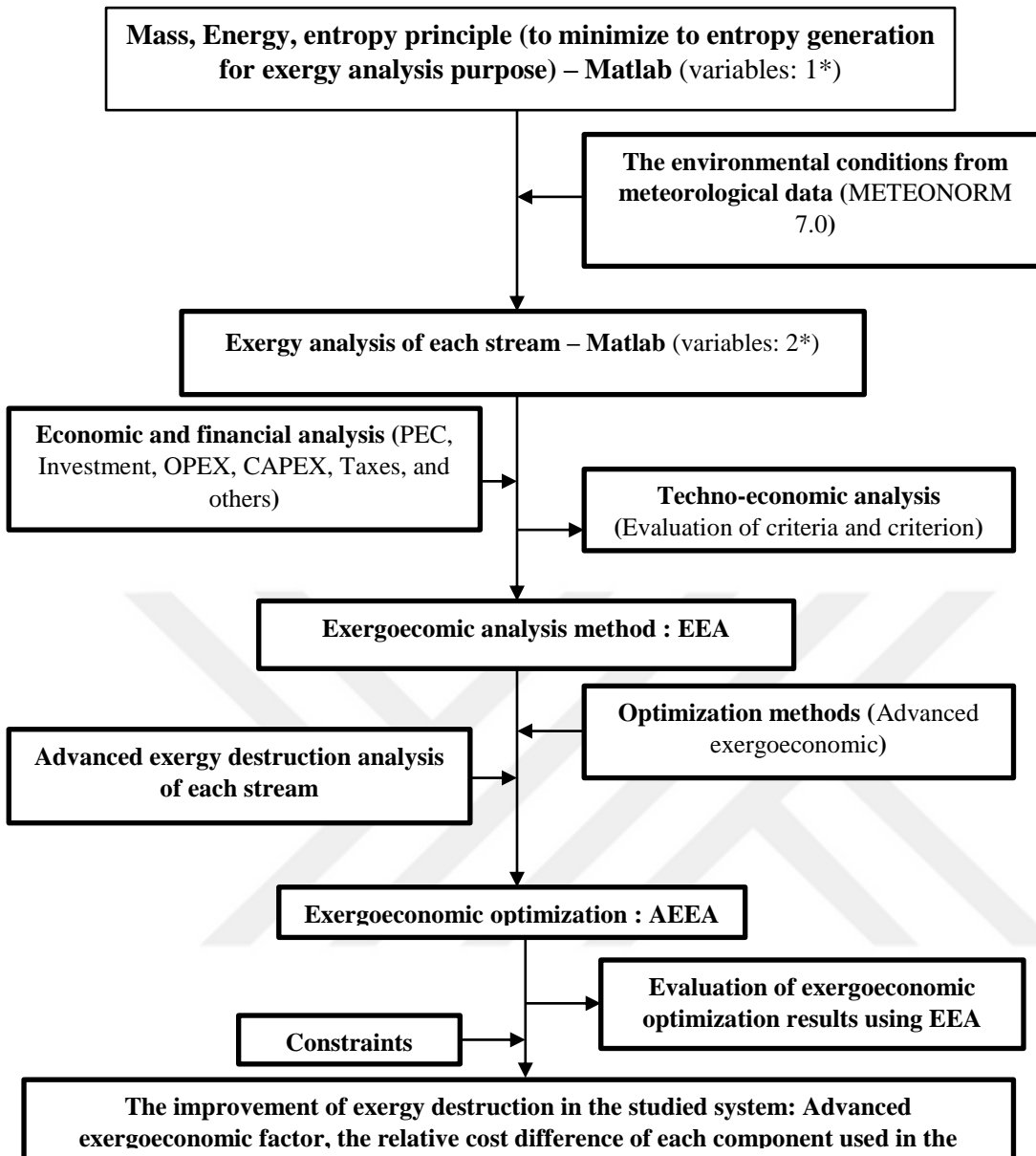


Figure 4.3. Overview of the modeling steps in advanced exergoeconomic optimization.

5. ANALYSES OF THE HYBRID ENERGY SYSTEMS

5.1 Thermodynamic Analysis of the Hybrid Energy Systems

5.1.1 Thermodynamic analysis of the prime movers

A. Solar field subsystems

This section presents the study of using solar energy resource for electricity generation using a thermal system. As explained in the literature of concentrating solar power technologies, PTCs and ST are the most mature technologies among the solar thermal technologies for power generation. These technologies have been used since the 1980s for large and commercial thermal power plant around the world. Nowadays, several solar thermal power plants are under construction in Asia, North America, Southern and North Africa, and the Middle East. The majority of these power plants are based on the PTCs and ST. However, in this study, the linear Fresnel reflectors have been also considered since it is among the promising technology due to the low installation cost. Recently, 120 MWe capacity plant has been built in India, therefore, a LFRs technology is no longer an experimental technology. Thus, this research focuses on the application of these three concentrating solar power technologies for hybridization with biomass-fired technology for electricity generation.

• Parabolic trough collector–solar field

The energy and exergy analysis of the parabolic trough collectors used for the solar field are presented in this section. The energy received by the active area of the solar field containing PTC is expressed as:

$$\dot{Q}_i = A \cdot N \cdot I = A_{act} \cdot (I_b \cdot R_b) \quad \text{eq.36}$$

where A , N , A_{act} , R_b , A_{apt} and I are the area of a collector in m^2 , the number of collectors used for the solar field, the total active area in m^2 , aperture area of

the collector in m^2 , the geometric factor and the solar intensity in W/m^2 (594 W/m^2).

$$A_{act} = A_{ap} \cdot N \quad \text{eq.37}$$

The useful power solar field is defined as:

$$\dot{Q}_u = N \cdot m_{Th} \cdot C_{Th} \cdot (T_{Th,o} - T_{Th,i}) = \dot{M}_{Th} C_{Th} \cdot (T_{Th,o} - T_{Th,i}) \quad \text{eq.38}$$

where \dot{Q}_u is the useful power and \dot{M}_{Th} is the mass flow rate of the Therminol VP – 1, outlet and inlet, respectively.

$$A_{ap} = (\omega - D_{c,o}) \cdot L \quad \text{eq.39}$$

where ω , $D_{c,o}$, and L are the collector width, the cover outer diameter and the collector length.

The absorbed radiation by the receiver can be defined as:

$$\dot{Q}_s = \eta_{opt} \cdot \dot{Q}_i \quad \text{eq.40}$$

$$\eta_{opt} = \kappa(\theta) \cdot [(\rho(\tau\alpha))_n \cdot \delta] \quad \text{eq.41}$$

where, κ , ρ , τ , α , δ and η_o incidence angle modifier, reflectivity, the transmissivity of cover, the absorptivity of absorber, the intercept factor and the optical efficiency. The energy absorbed by the absorber tube is written as follows

$$\text{The energy loss:} \quad \dot{Q}_L = \dot{Q}_s - \dot{Q}_u \quad \text{eq.42}$$

$$\text{The energy loss ratio:} \quad \eta_L = 100 \cdot [(\dot{Q}_s - \dot{Q}_u) / \dot{Q}_s] \quad \text{eq.43}$$

The first law efficiency of the studied solar – field subsystem:

$$\eta_I = \dot{Q}_u / \dot{Q}_s \quad \text{eq.45}$$

The overall efficiency of the studied solar – field subsystem:

$$\eta_{I \rightarrow O} = \dot{Q}_u / \dot{Q}_i \quad \text{eq.46}$$

The receiver absorbs solar rays and transfers a part of it to the heat transfer fluid moving through the absorber. While the remaining part of the absorbed thermal energy is dissipated to the environment by convective, conductive and reflective heat losses which depend on the receivers' characteristics. The Peleta's equation has been used to determine exergy rate received by the solar field subsystem from solar radiation using the meteorological data, and it is written as follows:

$$\dot{E}x_{sf} = I \cdot A_{act} \cdot \left(1 + \frac{1}{3} \left(\frac{T_o}{T_{sun}} \right)^4 - \frac{4}{3} \left(\frac{T_o}{T_{sun}} \right) \right) \quad \text{eq.47}$$

Using Petela's equation, the exergy destruction rate on the solar field during the transfer is given by:

$$\dot{E}x_{D,sf} = I \cdot A_{act} \cdot \left(-\frac{1}{3} \left(\frac{T_o}{T_{sun}} \right)^4 + \frac{4}{3} \left(\frac{T_o}{T_{sun}} \right) \right) \quad \text{eq.48}$$

where A_{ap} the area aperture of the solar field is, DNI is the direct normal irradiation received in the field, T_o and T_{sun} are reference and sun temperature of location in K.

The sensitive analysis in SAM 2017.9.5 software provides some parameters as the area of parabolic trough collector, the number of loops, the mass flow rate of the heat transfer fluid and many others specifications presented in table.

The exergy absorbed by collector absorber is written as presented below:

$$\dot{E}x_c = Q_s \cdot \left(1 - \frac{T_a}{T_r} \right) \quad \text{eq.49}$$

The exergy loss: $\dot{E}x_{sf} - \dot{E}x_c = \text{Irreversibility (IR)}$:

$$\% \text{ Irreversibility ratio} = 100 \left[\frac{IR}{\dot{E}x_c} \right] \quad \text{eq.50}$$

The exergy absorbed by collector $\dot{E}x_c$ is expressed as follows:

$$\dot{E}x_{c-} = Q_s \cdot \left(1 - \frac{T_a}{T_{sun}} \right) \quad \text{eq.51}$$

The exergy loss: = $\dot{E}x_{sf} - \dot{E}x_{c-}$, irreversibility (IR):

$$\% \text{ Irreversibility ratio} = 100 \left[\frac{IR}{\dot{E}x_c} \right] \quad \text{eq.52}$$

The useful exergy delivered is written as:

$$\dot{E}x_u = \dot{M}_{Th} (\dot{E}x_o - \dot{E}x_i) \quad \text{eq.53}$$

The second law efficiency is expressed as:

$$\eta_{II} = \dot{E}x_u / \dot{E}x_{c-} \quad \text{eq.54}$$

The overall second law efficiency of the collector – receiver is defined as:

$$\eta_{II \rightarrow O} = \dot{E}x_u / \dot{E}x_{sf} \quad \text{eq.55}$$

The exergy destruction rate inside of collector absorber during the heat transfer fluid is given by the following equation 56:

$$\dot{E}x_{dest} = \left(-(\dot{E}x_{out} - \dot{E}x_{int})_{solar} + \dot{E}x_{c-} \right) \cdot \left(\frac{\Delta t_{h,solar}}{24 h} \right) \quad \text{eq.56}$$

where Δt_h is the sunshine duration in hours.

The choice of the appropriate equipment is influenced by price considerations, the unavoidable inefficiency, and the life cycle assessment. The individual purchased equipment cost (PEC) used to be determined by using the

model cost of the component presented in Table 5.1. Peters et al. (2005), presented these kinds of cost evaluation models based on fluctuations in economic conditions and design studies which affects the efficiency of component.

Table 5.1. Correlation used to determine PEC and levelized costs of the main component used for the power block (Couper, et al., 2012; Dincer and Ratlamwala, 2016).

Power block	Number and specification	In k\$	Purchased equipment cost (PEC) - Correlation
Heat exchanger (Shell-and-tube)	3x	91,248	$C = 1.218 f_d f_m f_p C_b$, price in \$ $C_b = \exp [8.821 - 0.30863(\ln A) + 0.0681(\ln A)^2]$, $150 < A < 12,000$ sqft; $A=2,000$ sqft
Boiler	Q=31.14 M Btu/hr.	990,21 k\$	Cylindrical type: $C = 1.218 k (1 + f_d + f_p) Q^{0.86}$ in K\$, $20 < Q < 200$ M Btu/hr.
Power block (Combined Rankine cycles)			
Turbine			
Solar Steam turbine+generator (Vacuum discharge).	8000 HP(6MW) x2	3290	$C = 1.10(HP)^{0.81}$ in K\$, $200 < HP < 8000$
Biomass Steam turbine+generator	8000 HP (6MW) x2	3290	
HRSg system			
Solar:	Solar ($f_p=0.4$, $f_d=0$, $k=33.8$)	x3	Box type: $C = 1.218 k (1 + f_d + f_p) Q^{0.86}$, $20 < Q < 200$ M Btu/hr.
Reg1:	9788 kW	1.18	
Reg2:	1710 kW	0.27	
Reg3:	3453,2 kW	0.48	
Biomass			
	Biomass ($f_p=0.25$, $f_d=0$, $k=33.8$)	x3	
Reg1:		0.45	
Reg2:	3636,46 kW	0.36	
Reg3:	2814,77 kW	0.11	
Reg4:	704,64 kW	0.87	
Reg5:	7822,93 kW	0.63	
	375,67 kW		
Deaerator and cooling tower	1.25kgal/min x2	410	$C = 164 f. Q^{0.61}$ in K\$, $1 < Q < 60$ K gal / min [$f=2$]
Pump – SRC			
Solar Pump (Centrifugal, one-stage 1750 rpm, HSC) - 16.405kg/s Rho=997kg/m ³	300 kW (290.37) Q = 260.8 gpm	4x18,459	prices in \$: $C = F_M F_T C_b$, base cast-iron, 3550 rpm VSC $C_b = 3.00 \exp [8.833 - 0.6019(\ln QH^{1/2}) + 0.0519(\ln QH^{1/2})^2]$, Q in gpm, H in ft head.
Biomass Pump (Centrifugal, one-stage 1750 rpm, VSC) - 8.38 kg/s	65 kW (62.69) Q = 133.2gpm	4x 10,774	$F_T = \exp [b_1 + b_2(\ln QH^{1/2}) + b_3(\ln QH^{1/2})^2]$,
Pump – ORC			
(Centrifugal, Vertical mixed flow) R134a (24.75 kg/s) Rho=1206.7kg/m ³ (25C)	25kW (24.75) Q =325.28 gpm	4x 8.957	$C = 0.078(\text{gpm})^{0.82}$ in K\$, $500 < \text{gpm} < 130,000$
Biomass (Centrifugal, Vertical mixed flow) R134a (62.69 kg/s)	70kW (62.69) Q =823.19 gpm	4x 19.18	
Condenser - ORC	1.00kgal/min	2x 164 K\$	$C = 164 f. Q^{0.61}$ in K\$, $1 < Q < 60$ K gal / min [$f=1$]
Heat exchanger – ORC (Double pipe)		4x 4,87 k\$	$C = 1096 f_m f_p A^{0.18}$, in \$ $2 < A < 60$ sqft, ($A=50$ sqft) $f_m = 2.2$, (cs/316 stainless); $f_p = 1.0$, ($P < 4$ bar)

- **Solar tower– solar field**

The amount of available solar energy received by the active area of heliostat mirrors is expressed in the equation below:

$$\dot{Q}_i = A_H \cdot N \cdot N_m \cdot I = A_{act} \cdot (I_b \cdot R_b) \quad \text{eq.57}$$

where A_H is the area of an individual heliostat in m^2 and N is the number of heliostats used for the solar field construction.

Table 5.2 presents the values of the main efficiencies used for the determination of the solar field based on the heliostats – tower.

Table 5.2. Efficiencies of heliostat field (Besarati et al., 2014 and Zhu et al., 2016)

Cosine effect efficiency (η_{cos})	0.8267	Reflectivity of heliostat efficiency (η_{ref})	0.88
Atmospheric attenuation efficiency (η_{att})	0.9383	Interception efficiency (η_{int})	0.971
Shading and blocking efficiency ($\eta_{s\&b}$)	0.9698	Focused (η_{foc}) and wind (η_{win}) efficiency	1

In the case, the thermal energy received by the volumetric receiver is more than the threshold value, some of the heliostat mirrors are defocused during a period to reduce rays concentration on the receiver. The efficiency of the heliostat field depends on the availability factor, optical efficiency, wind speed, and reflection and is expressed as:

$$\eta_f = \eta_{foc} \cdot \eta_{cos} \cdot \eta_{s\&b} \cdot \eta_{int} \cdot \eta_{att} \cdot \eta_{ref} \cdot \eta_{win} \quad \text{eq.58}$$

where η_{foc} is set to be 100%, η_{ref} is the reflection efficiency of mirrors, η_{hel} is the optical efficiency of heliostat when is wholly focused onto the receiver with the mirror. The solar field depends also on the blocking and shading efficiency, cosine efficiency and atmospheric efficiency.

The thermal energy reaching the surface of the volumetric receiver and which can be absorbed is given by the equation below.

$$\dot{Q}_s = \eta_f \cdot \dot{Q}_i \quad \text{eq.59}$$

The useful power solar field is defined as:

$$\dot{Q}_u = \dot{M}_w C_{Th} \cdot (T_{w,o} - T_{w,i}) \quad \text{eq.60}$$

where \dot{Q}_u is the useful power and \dot{M}_w is the mass flow rate of the water. The subscript w, o and i indicate the water, outlet, and inlet, respectively. The aperture surface of the solar field is given.

$$A_{ap} = A_H \cdot N_m \quad \text{eq.61}$$

where N_m is the number of mirrors estimated at 16 mirrors.

- **Linear Fresnel reflector– solar field**

The energy received by the active area of the solar field containing linear Fresnel reflectors (LFRs) is estimated using equation 62:

$$\dot{Q}_i = A \cdot N \cdot I = A_{act} \cdot I \quad \text{eq. 62}$$

where A , ω , N , A_{act} , and I are the area of a Fresnel single module in m^2 , the Fresnel module width, the number of the module used for the solar field, the total active area in m^2 , and the solar intensity in W/m^2 .

$$A_{act} = \omega \cdot L \cdot N \quad \text{eq. 63}$$

The useful power solar field is defined as:

$$\dot{Q}_u = N \cdot m_{Th} \cdot C_{Th} \cdot (T_{Th,o} - T_{Th,i}) = \dot{M}_{Th} C_{Th} \cdot (T_{Th,o} - T_{Th,i}) \quad \text{eq. 64}$$

where \dot{Q}_u is the useful power and \dot{M}_{Th} is the mass flow rate of the Therminol VP – 1, subscript o is outlet and i is inlet.

The absorbed radiation by the receiver is defined as:

$$\dot{Q}_s = \eta_{opt} \cdot \dot{Q}_i \quad \text{eq. 65}$$

$$\eta_{opt} = \rho_1 \cdot \rho_2 \cdot \tau \cdot \alpha \cdot \varepsilon_c \quad \text{eq. 66}$$

where, ρ_1 , ρ_2 , τ , α , ε_c and η_{opt} primary reflectance, secondary reflectance, cover transmittance, absorber absorbance, cover and the optical efficiency of linear Fresnel collector, respectively. The energy absorbed by the absorber tube is written as given in the following equations 67 and 68.

The energy loss: $\dot{Q}_L = \dot{Q}_s - \dot{Q}_u$ eq. 67

The energy loss ratio: $\eta_L = 100 \cdot [(\dot{Q}_s - \dot{Q}_u) / \dot{Q}_s]$ eq. 68

The first law efficiency of the studied solar – field subsystem is expressed as:

$$\eta_I = \dot{Q}_u / \dot{Q}_s \quad \text{eq. 69}$$

The overall efficiency of the studied solar – field subsystem is given by:

$$\eta_{I \rightarrow 0} = \dot{Q}_u / \dot{Q}_i \quad \text{eq. 70}$$

B. Biomass-fired

The Energy Research Center of Netherlands (ERCN, 2012) suggested an equation to determine the lower heating value (LHV) of crops. This equation shows that the LHV depends on the moisture content and can be expressed as follows:

$$LHV = 15820 - X \times 181.99 \quad \text{eq. 71}$$

The expected energy generated using the available amount of biomass can be determined by using the LHV (kJ/kg) and the mass flow rate (kg/h), \dot{b} :

$$\dot{Q}_e = \dot{b} \times HHV \quad \text{eq. 72}$$

The most important efficiency losses in the studied system are dry flue gas losses, moisture in fuel, latent heat, unburned fuel, and radiation and miscellaneous. Hence, the amount of heat generated by the boiler using the mass flow rate of biomass can be determined using the following equation (Malek, et al., 2017).

$$Q_b = \dot{b} \times HHV \times (1 - (e_{moisture} + e_{manuf} + e_{rad} + e_{umb. Carb} + e_{latent heat} + e_{fuel moist})) \quad \text{eq. 73}$$

where \dot{b} is the mass flow rate of dry biomass.

In this study, the annual operating production of the biomass system was estimated at 3600 hours, the losses in the boiler were estimated at 7.13% and sustainable extraction of sorghum was assumed at 20%. Using these assumptions and the total amount of biomass available, the useful energy of the system can be expressed in another way as given below:

$$Q_u = \left(\frac{M_{dry} \times S_{ext} \times HHV}{YOP} \right) \times (1 - e_{loss}) \quad \text{eq. 74}$$

The exergy generated by the boiler is written as presented below:

$$\dot{E}x_b = Q_b \cdot \left(1 - \frac{T_a}{T_b} \right) \quad \text{eq. 75}$$

The useful exergy delivered can be expressed as in equation below:

$$\dot{E}x_u = \dot{M}_w (\dot{E}x_o - \dot{E}x_i) / \eta_b \quad \text{eq. 76}$$

The second law efficiency is given by:

$$\eta_{II} = \dot{E}x_u / \dot{E}x_b \quad \text{eq. 77}$$

5.1.2 Thermodynamic analysis of the power block subsystem

As illustrated in Figure 5.1, the combined Rankine cycle containing three turbines named HP-steam turbine and LP-steam turbine and ORC turbine to produce electricity. The mass flow rate of water can change according to the operated prime movers' technology connected with the power block system. For a control accompanying a steady-state process, energy and exergy balance equation of the power block system is expressed using these equations:

$$\dot{W}_{syst} = \sum_T(\dot{m}_i \cdot h_i - \dot{m}_o \cdot h_o)_T - \sum_P(\dot{m}_i \cdot h_i - \dot{m}_o \cdot h_o)_P \quad \text{eq. 78}$$

$$\dot{E}_{syst} = \sum_T(\dot{E}_i - \dot{E}_o)_T - \sum_P(\dot{E}_i - \dot{E}_o)_P \quad \text{eq. 79}$$

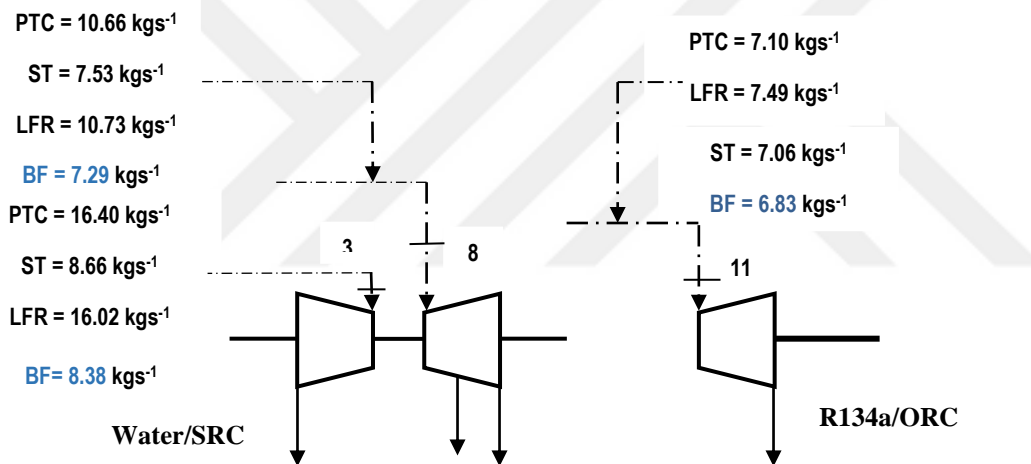


Figure 5.1. Turbines of the power block system used in the hybrid (solar-biomass) energy system.

5.1.3 Thermodynamic analysis of the absorption refrigeration subsystem

To estimate the size of the equipment and optimize single effect water - lithium bromide absorber cooler, the following assumptions, and input values were considered.

- Absorption system is operating in steady-state and refrigerant is pure water.

- There is no pressure variation, except through the flow restrictors and the pump (pump and flow restrictors are considered as isentropic and adiabatic respectively).
- Environmental heat losses are negligible. There are no jacket heat losses, and at points 26, 32, 33 and 36 there is the only saturated state.

Generator

The mass, energy and exergy balance equation of generator are presented as below:

$$\dot{m}_{32} = \dot{m}_{33} + \dot{m}_{36} \quad \text{eq. 80}$$

$$\dot{m}_{33}x_{33} = \dot{m}_{36}x_{36} \quad \text{eq. 81}$$

$$\dot{m}_{32}h_{32} - (\dot{m}_{33}h_{33} + \dot{m}_{36}h_{36}) + Q_g = 0 \quad \text{eq. 82}$$

where $Q_g = \dot{m}_{26}(h_{26} - h_{27}) = LMTD_g.U.A_g$, and $LMTD_g$ of generator is defined as follow:

$$LMTD_g = \frac{(T_{26}-T_{33}-T_{27}+T_{36})}{\ln(T_{26}-T_{33})-\ln(T_{27}-T_{36})} \quad \text{eq. 83}$$

The exergy destruction is expressed as below.

$$Ex_{d,g} = \dot{m}_{32}Ex_{32} - (\dot{m}_{33}Ex_{33} + \dot{m}_{36}Ex_{36}) + \dot{m}_{26}(Ex_{26} - Ex_{27}) \quad \text{eq. 84}$$

where the $LMTD_g$ is the log mean temperature difference, x is the concentration ratio of lithium bromide into the LiBr/Water mixture and subscript g indicates the generator.

Condenser

The mass, energy, and exergy balance equation of condenser are given below:

$$\dot{m}_{36} = \dot{m}_{37} \quad \text{eq. 85}$$

$$Q_{cond} = \dot{m}_{36}(h_{36} - h_{37}) = \dot{m}_c(h_{29} - h_{28}) = LMTD_c \cdot U \cdot A_c \quad \text{eq. 86}$$

Exergy destruction is expressed as:

$$Ex_{d,c} = \dot{m}_{36}(Ex_{36} - Ex_{37}) - \dot{m}_c(Ex_{29} - Ex_{28}) \quad \text{eq. 87}$$

where the subscript c indicates the condenser.

$$\epsilon_c = \frac{T_{28} - T_{29}}{T_{28} - T_{37}} \quad \text{eq. 88}$$

$$LMTD_c = \frac{T_{37} - T_{28} - T_{36} + T_{29}}{\ln(T_{37} - T_{28}) - \ln(T_{36} - T_{29})} \quad \text{eq. 89}$$

where the $LMTD_c$ is the log mean temperature difference and ϵ_c is the effectiveness of condenser.

Refrigeration and expansion valve

The mass, energy, and exergy balance equation of the valve are given as follows:

$$\dot{m}_{valve,1} = \dot{m}_{valve,2} \quad \text{eq. 90}$$

$$h_{valve,1} = h_{valve,2} \quad \text{eq. 91}$$

Exergy destruction is expressed as:

$$Ex_{d,c} = \dot{m}_{valve}(Ex_{valve,1} - Ex_{valve,2}) \quad \text{eq. 92}$$

The subscript Valve, 1 and Valve, 2 indicates the inlet and the outlet orifice of valve, respectively.

Evaporator

The mass, energy, and exergy balance equation of evaporator are given below:

$$\dot{m}_{39} = \dot{m}_{38} \quad \text{eq. 93}$$

$$Q_{ev} = \dot{m}_{38}(h_{39} - h_{38}) = \dot{m}_{ev}(h_{17} - h_{18}) = LMTD_{ev} \cdot U \cdot A_{ev} \quad \text{eq. 94}$$

where the $LMTD_{ev}$ is the log mean temperature difference and ϵ_{ev} is the effectiveness of condenser and ev indicates its subscript.

$$\epsilon_{ev} = \frac{T_{17} - T_{18}}{T_{17} - T_{39}} \quad \text{eq.95}$$

$$LMTD_{ev} = \frac{T_{17} - T_{39} - T_{18} + T_{38}}{\ln((T_{17} - T_{39}) / (T_{18} - T_{38}))} \quad \text{eq. 96}$$

Absorber

The mass, energy, and exergy balance equation of absorber are as given below:

$$\dot{m}_{39}h_{39} + \dot{m}_{35}h_{35} + Q_{ab} - \dot{m}_{30}h_{30} = 0 \quad \text{eq. 97}$$

where the subscript ab indicates the absorber. The energy and exergy transferred by absorber can be expressed as shown below in equation 97

$$Q_{ab} = \dot{m}_{38}(h_{39} - h_{38}) = LMTD_{ab} \cdot U \cdot A_{ab} \quad \text{eq. 98}$$

$$Ex_{d,ab} = \dot{m}_{ab}(Ex_{ab,1} - Ex_{ab,2}) - (\dot{m}_{39}Ex_{39} + \dot{m}_{35}Ex_{35} - \dot{m}_{30}Ex_{30}) \quad \text{eq. 99}$$

$$\epsilon_{ev} = \frac{T_{21} - T_{20}}{T_{21} - T_{30}} \quad \text{eq. 100}$$

$$LMTD_{ab} = \frac{T_{17}-T_{39}-T_{18}+T_{38}}{\ln((T_{17}-T_{39}) / (T_{18}-T_{38}))} \quad \text{eq. 101}$$

Solution pump

The mass, energy, and exergy balance equation of solution pump are given by:

$$\dot{m}_{31} = \dot{m}_{30} \quad \text{eq. 102}$$

$$\dot{W}_{sp} = \dot{m}_{30}(h_{31} - h_{30}) = \dot{m}_{30} \cdot v_{30}(P_{high} - P_{low}) \quad \text{eq. 103}$$

$$Ex_{d,sp} = \dot{W}_{sp} + \dot{m}_{34}(Ex_{34} - Ex_{35}) \quad \text{eq. 104}$$

where the subscript *sp* indicates the solution pump.

Heat exchanger

The mass, energy, and exergy balance equations of the heat exchanger are expressed as given below:

$$\dot{m}_{31} = \dot{m}_{32} \quad \text{eq. 105}$$

$$\dot{m}_{33} = \dot{m}_{34} \quad \text{eq. 106}$$

$$Q_{hx} = \dot{m}_{30}(h_{32} - h_{31}) = \dot{m}_{33}(h_{33} - h_{34}) = LMTD_{hx} \cdot U \cdot A_{hx} \quad \text{eq. 107}$$

where the subscript *hx* indicates the heat exchanger. The exergy of heat exchanger can be written as given in equation below.

$$Ex_{d,hx} = \dot{m}_{33}(Ex_{33} - Ex_{34}) + \dot{m}_{31}(Ex_{31} - Ex_{32}) \quad \text{eq. 108}$$

The effectiveness and the $LMTD_{hx}$ of this heat exchanger are expressed as

$$\epsilon_{hx} = \frac{T_{33}-T_{34}}{T_{33}-T_{31}} \quad \text{eq. 109}$$

$$LMTD_{hx} = \frac{T_{17}-T_{39}-T_{18}+T_{38}}{\ln((T_{33}-T_{32}) / (T_{34}-T_{31}))} \quad \text{eq. 110}$$

where $U \cdot A_{hx}$ is an overall heat transfer coefficient multiplied by the area.

The cooling COP of absorption system is defined as the ratio of the heat load outside of evaporator and the heat load inside of generator, expressed as below (Herold et al., 1996; Tozer and James, 1997):

$$COP_C = \frac{\dot{Q}_E}{\dot{Q}_G + \dot{W}_P} \quad \text{eq. 111}$$

The heating COP of absorption system is the ratio of combined heating capacity, obtained through absorber and condenser and the heat load providing from an external source, specifically inside of a generator calculated using the equation below (Herold et al., 1996; Tozer and James, 1997):

$$COP_H = \frac{\dot{Q}_A + \dot{Q}_C}{\dot{Q}_G + \dot{W}_P} = 1 + COP_C \quad \text{eq. 112}$$

The exergetic efficiency of absorption system (cooling) is an exergetic ratio between chilled water in the evaporator and the heat load in the generator, which has been calculated by using the equation expressed as given below (Talbi and Agnew, 2000; Lee and Sherif, 2001):

$$\Phi_C = \frac{\dot{E}x_E}{\dot{E}x_G + \dot{E}x_P} \quad \text{eq. 113}$$

The exergetic efficiency of absorption system (heating) is an exergetic ratio of a combination of hot water in the absorber and condenser, to a combination of heat source in the generator and pump, which is expressed as given in the equation below (Dincer and Ratlamwala, 2016).

$$\Phi_H = \frac{\dot{E}x_A + \dot{E}x_C}{\dot{E}x_G + \dot{E}x_P} \quad \text{eq. 114}$$

The exergy destruction of the absorption system is defined as the sum of destroyed exergy in each component and can be calculated using the following equation.

$$\dot{E}x_{d,ARS} = \dot{E}x_{d,g} + \dot{E}x_{d,c} + \dot{E}x_{d,abs} + \dot{E}x_{d,hx} + \dot{E}x_{d,ev} + \dot{E}x_{d,sp} + \dot{E}x_{d,valve} \quad \text{eq. 115}$$

The individual purchased equipment cost (PEC) used to be determined by using the model cost of the component presented in Table 5.3.

Table 5.3. Correlation used to determine PEC and breakdown costs of the absorption refrigeration cycle (Couper, et al., 2012; Dincer and Ratlamwala, 2016).

System and components	Specifications	PECs (k\$)	Correlation of purchased equipment cost
Absorption system			$C = 1144.3(Q)^{0.67}$ in \$
Solar:	74.87 kW		
Biomass:	511.4 kW		
Breakdown cost of ARS			
Generator /Condenser	$C_g = C - C_c$		$C = 1.218 f_d \cdot f_m \cdot f_p \cdot C_b$, price in \$
A=150 ft ²	Solar:	24,461	$C_b = \exp [8.821 - 0.30863(\ln A) + 0.0681(\ln A)^2]$,
g1 =0,8603 g2 =0,2396 (stainless steel 316)			Fixed-head:
A=1021.9 ft ²	Biomass:	111,619	$f_p = \exp [- 1.1156 + 0.0906(\ln A)]$
g1 =0,8603 g2 =0,2396 (stainless steel 316)			$f_p = 0.7771 + 0.04981(\ln A)$
			$f_m = g1 + g2 \cdot (\ln A)$
Vane1 / Water			-
Absorber/ Evaporator	$C_{abs} = C - C_{ev}$		$C = 1.218 f_d \cdot f_m \cdot f_p \cdot C_b$, price in \$
A=155 ft ²	Solar:	25,22	$C_b = \exp [8.821 - 0.30863(\ln A) + 0.0681(\ln A)^2]$,
g1 =0,8603 g2 =0,2396			Fixed-head:
A=1055.9 ft ²	Biomass:	114,68	$f_p = \exp [- 1.1156 + 0.0906(\ln A)]$
g1 =0,8603 g2 =0,2396 (stainless steel 316)			$f_p = 0.7771 + 0.04981(\ln A)$
			$f_m = g1 + g2 \cdot (\ln A)$
Condenser			$C = 1096 f_m f_p A^{0.18}$, in \$
A=3 sqft	Solar:	2,938	$2 < A < 60$ sqft, $f_m = 2.2$, (cs/316 stainless)
A=21 sqft	Biomass	4,170	$f_p = 1.0$, ($P < 4$ bar)
Strong LiBr /solution – Pump	$W_p \sim 0$		Vertical axial flow: $C = 0.0431(\text{gpm})^{0.78}$ in K\$, $1000 < \text{gpm} < 130,000$
Intermediate Heat Exchanger	Q= 2 MBtu	0,038 k\$	Box type: $C = 1.218 k (1 + f_d + f_p) Q^{0.82}$ in \$,
	Q= 3 MBtu	0,043 k\$	$2 < Q < 30$ M Btu/hr.
Evaporator			$C = 1096 f_m f_p A^{0.18}$, in \$ $2 < A < 60$ sqft, $f_m =$
A=2.084	Solar:	2,751	2.2 , (cs/316 stainless), $f_p = 1.0$, ($P < 4$ bar)
A=14.2 sqft	Biomass	3,887	

5.1.4 Thermodynamic analysis of the drying subsystem

Air compressor

The mass, energy, and exergy balance equation of the air compressor are given below:

$$\dot{m}_{22} = \dot{m}_{22'} \quad \text{eq. 116}$$

$$\dot{W}_{sp} = \dot{m}_{22}(h_{22'} - h_{22}) = \dot{m}_{22} \cdot v_{22}(P_{high} - P_{low}) \quad \text{eq. 117}$$

$$\dot{Ex}_{d,ac} = \dot{W}_{ac} + \dot{m}_{22}(Ex_{22'} - Ex_{22}) \quad \text{eq. 118}$$

where the subscript *ac* indicates the air compressor.

Heater

The mass, energy, and exergy balance equation of the heater are written in equations below:

$$\dot{m}_{22'} = \dot{m}_{23} \quad \text{eq. 119}$$

$$Q_{heater} = \dot{m}_{22'}(h_{23} - h_{22'}) = \dot{m}_h(h_{9'} - h_{45}) \quad \text{eq. 120}$$

Exergy destruction is expressed in the equation below.

$$\dot{Ex}_{d,heater} = \dot{m}_{22'}(Ex_{23} - Ex_{22'}) - \dot{m}_h(Ex_{9'} - Ex_{45}) \quad \text{eq. 121}$$

Table 5.4 presents the efficiencies of the main components used for the drying system.

Table 5.4. Input data for the drying system (DFC).

Data	System 1- PTC/LFR- Solar	System 2- Biomass- C/ ST-Solar
DFC		
Isentropic efficiency of the air compressor	80%	80%
Effectiveness of the heater	85%	85%
Electrical motor efficiency	95%	95%

5.2 Exergoeconomic Analysis of the Hybrid Energy Systems

This section presents the exergoeconomic approach of the hybrid thermal power system with the multi-energy generation. The first step of the approach consists to determine the capital investment and cost related to operation expenditure to calculate the cost rate of fuel associated to the solar field, the biomass, boiler, intermediate heat exchanger, power block system, HRSG system, Absorption refrigeration system, and drying system. It has been assumed that the lifetime of the power system will be 25 years.

5.2.1 Exergoeconomic analysis of the prime movers

Solar field

For a control volume around the solar field, the cost rate fuel equation is presented as given in the equation below:

$$\dot{C}_1 + \dot{Z}_{SF} = \dot{C}_2 \quad \text{eq. 122}$$

$$c_{fuel,SF} = c_1 = c_2 \quad \text{eq. 123}$$

where \dot{Z}_{SF} is the capital and other expenses for the solar field which is expressed as follows:

$$\dot{Z}_{SF} = \frac{[\text{initial investment on the Solar field}]}{[\text{lifetime of the system}]} \quad \text{eq. 124}$$

$$c_{fuel,SF} = \frac{\dot{Z}_{SF}}{E_2 - E_1} \quad \text{eq. 125}$$

where $c_{fuel,SF}$ is cost rate of fuel associated with the solar field per unit of Gigajoule [GJ].

Heat exchanger

For a control volume surrounding the heat exchanger, the cost rate fuel equation is presented as,

$$\dot{C}_{q,ihe} + \dot{C}_{1'} + \dot{C}_8 + \dot{C}_4 = \dot{Z}_{ihe} + \dot{C}_{2'} + \dot{C}_6 + \dot{C}_3 \quad \text{eq. 126}$$

where

$$c_{fuel,SF} = c_{1'} = c_{2'} = c_{q,ihe} \quad \text{eq. 127}$$

$$c_3 = c_4 = c_6 = c_8 \quad \text{eq. 128}$$

$$\dot{C}_{q,ihe} = c \cdot \dot{E}_{q,ihe} = c \cdot Q \left(1 - \frac{T_o}{T_s} \right) \quad \text{eq. 129}$$

where T_s is the temperature at which the heat transfer occurs in the boiler.

Biomass

The biomass fuel cost can be expressed by multiplying the annual operating biomass-fired system, the mass flow rate of feedstock, lower heating value and cost per exergy unit associated with biomass fuel cost.

$$FC = c_{fuel,bio} \cdot LHV \cdot \dot{m}_{bio} \cdot YOP \quad \text{eq. 130}$$

where $C_{fuel,bio}$, LHV , \dot{m}_{bio} and YOP are the cost per exergy unit associated with biomass fuel cost, lower heating value, mass flow rate of feedstock and yearly operating time, respectively.

Boiler

For a control volume surrounding the boiler, the cost rate fuel equation is expressed below.

$$\dot{C}_{gas} + \dot{C}_{ash} + \dot{C}_5 + \dot{C}_{8'} = \dot{Z}_b + \dot{C}_{fuel,bio} + \dot{C}_{6'} + \dot{C}_{3'} \quad \text{eq. 131}$$

$$c_{3'} = c_{6'} = c_5 = c_{8'} \quad \text{eq. 132}$$

For the effluent existing the boiler it assumes that

$$\dot{C}_{gas} = \dot{C}_{ash} = 0 \quad \text{eq. 133}$$

5.2.2 Exergoeconomic analysis of the power block and HRSG subsystem

High pressure turbine

For a control volume surrounding the high-pressure turbine, the cost rate fuel equation can be presented as:

$$\dot{C}_6 + \dot{C}_7 + \dot{C}_{W,hT} + \dot{C}_{q,hT} = \dot{Z}_{hT} + \dot{C}_4 \quad \text{eq. 134}$$

where

$$c_4 = c_6 = c_7 \quad \text{eq. 135}$$

Low pressure turbine

For a control volume surrounding the low-pressure turbine, the cost rate fuel equation is expressed as:

$$\dot{C}_{10} + \dot{C}_9 + \dot{C}_{W,lp} + \dot{C}_{q,l-T} = \dot{Z}_{lp-Turb} + \dot{C}_8 \quad \text{eq. 136}$$

where

$$c_8 = c_9 = c_{10} \quad \text{eq. 137}$$

Pump

For a control volume around the pump, the cost rate fuel equation can be presented as:

$$\dot{C}_{21} + \dot{C}_{W,P} + \dot{Z}_P = \dot{C}_{46} \quad \text{eq. 138}$$

where

$$c_{46} = c_{21} \quad \text{eq. 139}$$

ORC evaporator connected to IHE of solar field (PTC/LF)

For a control volume surrounding the evaporator, the cost rate fuel equation is given by

$$\dot{C}_{q,Ev} + \dot{C}_{1''} + \dot{C}_{14} = \dot{Z}_{Ev} + \dot{C}_{2''} + \dot{C}_{13} \quad \text{eq. 140}$$

where

$$c_{14} = c_{13} \quad \text{eq. 141}$$

$$c_{fuel,SF} = c_{1''} = c_{2''} \quad \text{eq. 142}$$

$$\dot{C}_{q,Ev} = c \cdot \dot{E}_{q,Ev} = c \cdot \dot{Q}_{Ev} \left(1 - \frac{T_o}{T_{Ev}}\right) \quad \text{eq. 143}$$

ORC evaporator

$$\dot{C}_{q,Ev} + \dot{C}_{12} + \dot{C}_{14} = \dot{Z}_{Ev} + \dot{C}_{11} + \dot{C}_{13} \quad \text{eq. 144}$$

where

$$c_{14} = c_{13} \quad \text{eq.145}$$

$$c_{12} = c_{11} \quad \text{eq. 146}$$

$$\dot{C}_{q,Ev} = c \cdot \dot{E}_{q,Ev} = c \cdot \dot{Q}_{Ev} \left(1 - \frac{T_o}{T_{Ev}}\right) \quad \text{eq. 147}$$

ORC turbine

For a control volume surrounding the ORC turbine, the cost rate fuel equation is given in equation below.

$$\dot{C}_{q,T} + \dot{C}_{W,T} + \dot{C}_{15} = \dot{Z}_T + \dot{C}_{14} \quad \text{eq. 148}$$

where

$$c_{14} = c_{15} \quad \text{eq. 149}$$

ORC condenser

For a control volume surrounding the ORC condenser, the cost rate fuel equation is expressed as:

$$\dot{C}_{43} + \dot{C}_{15} + \dot{Z}_{cond} = \dot{C}_{42} + \dot{C}_{16} \quad \text{eq. 150}$$

where

$$c_{16} = c_{15} \quad \text{eq. 151}$$

$$c_{42} = c_{43} \quad \text{eq. 152}$$

ORC pump

For a control volume surrounding the ORC pump, the cost rate fuel equation can be presented as given below.

$$\dot{C}_{16} + \dot{C}_{W,P} + \dot{Z}_P = \dot{C}_{13} \quad \text{eq. 153}$$

where

$$c_{13} = c_{16} \quad \text{eq. 154}$$

Deaerator

For a control volume surrounding the deaerator, the cost rate fuel equation is given by:

$$\dot{C}_{45} + \dot{C}_{40'} + \dot{C}_{24} + \dot{Z}_A = \dot{C}_{21} + \dot{C}_{40} \quad \text{eq. 155}$$

where

$$c_{40} = c_{40'} \quad \text{eq. 156}$$

A. HRSG system connect to ST/BF

Regenerator 1

For a control volume surrounding the Regenerator 1, the cost rate fuel equation can be presented as below.

$$\dot{C}_{12} + \dot{C}_{46} + \dot{Z}_{R1} = \dot{C}_{12'} + \dot{C}_{47} \quad \text{eq. 157}$$

where

$$c_{12} = c_{12'} \quad \text{eq. 158}$$

$$c_{46} = c_{47} \quad \text{eq. 159}$$

Regenerator 2

For a control volume surrounding the regenerator 2, the cost rate fuel equation can be presented as:

$$\dot{C}_7 + \dot{C}_{47} + \dot{Z}_{R2} = \dot{C}_{7'} + \dot{C}_{48} \quad \text{eq. 160}$$

where

$$c_7 = c_{7'} \quad \text{eq. 161}$$

$$c_{48} = c_{47} \quad \text{eq. 162}$$

Regenerator 3

For a control volume surrounding the regenerator 3, the cost rate fuel equation is given below.

$$\dot{C}_{10} + \dot{C}_{48} + \dot{Z}_{R3} = \dot{C}_{10'} + \dot{C}_{49} \quad \text{eq. 163}$$

where

$$c_{10} = c_{10'} \quad \text{eq. 164}$$

$$c_{48} = c_{49} \quad \text{eq. 165}$$

Regenerator 4

For a control volume surrounding the regenerator 4, the cost rate fuel equation is expressed as follows:

$$\dot{C}_9 + \dot{C}_{49} + \dot{Z}_{R4} = \dot{C}_{9'} + \dot{C}_3 \quad \text{eq. 166}$$

where

$$c_9 = c_{9'} \quad \text{eq. 167}$$

$$c_3 = c_{49} \quad \text{eq. 168}$$

Regenerator 5

For a control volume surrounding the regenerator 5, the cost rate fuel equation can be expressed as follows:

$$\dot{C}_{40} + \dot{C}_{12'} + \dot{Z}_{R5} = \dot{C}_{40'} + \dot{C}_{24} \quad \text{eq. 169}$$

where

$$C_{40} = C_{40'} \quad \text{eq. 170}$$

$$C_{24} = C_{12'} \quad \text{eq. 171}$$

B. HRSG system connect to PTC/LFR

Regenerator 1

For a control volume surrounding the regenerator 1, the cost rate fuel equation is given by:

$$\dot{C}_{10} + \dot{C}_{46} + \dot{Z}_{R1} = \dot{C}_{10'} + \dot{C}_{47} \quad \text{eq. 172}$$

where

$$C_{10} = C_{10'} \quad \text{eq. 173}$$

$$C_{24} = C_{12'} \quad \text{eq. 174}$$

Regenerator 2

For a control volume surrounding the regenerator 2, the cost rate fuel equation is expressed as:

$$\dot{C}_9 + \dot{C}_{47} + \dot{Z}_{R2} = \dot{C}_9 + \dot{C}_{48} \quad \text{eq. 175}$$

where

$$c_9 = c_{9'} \quad \text{eq. 176}$$

$$c_{48} = c_{47'} \quad \text{eq. 177}$$

Regenerator 3

For a control volume surrounding the regenerator 3, the cost rate fuel equation is given by:

$$\dot{C}_7 + \dot{C}_{48} + \dot{Z}_{R3} = \dot{C}_{7'} + \dot{C}_{3'} \quad \text{eq. 178}$$

where

$$c_7 = c_{7'} \quad \text{eq. 179}$$

$$c_{48} = c_{3'} \quad \text{eq. 180}$$

$$c_{48} = c_{49} \quad \text{eq. 181}$$

Regenerator 4

For a control volume around the regenerator 4, the cost rate fuel equation can be presented as below,

$$\dot{C}_{40} + \dot{C}_{12} + \dot{Z}_{R4} = \dot{C}_{40'} + \dot{C}_{24} \quad \text{eq. 182}$$

where

$$c_{40} = c_{40'} \quad \text{eq. 183}$$

$$c_{12} = c_{7'} = c_{24} \quad \text{eq. 184}$$

5.2.3 Exergoeconomic analysis of the absorption refrigeration subsystem

Generator

For a control volume surrounding the generator, the cost rate fuel equation is given as below,

$$\dot{C}_{26} + \dot{C}_{32} + \dot{Z}_G = \dot{C}_{q,G} + \dot{C}_{27} + \dot{C}_{36} + \dot{C}_{33} \quad \text{eq. 185}$$

where

$$c_{32} = c_{33} + c_{36} \quad \text{eq. 186}$$

$$c_{26} = c_{27} \quad \text{eq. 187}$$

$$\dot{C}_{q,G} = c \cdot \dot{E}_{q,G} = c \cdot \dot{Q}_G \left(1 - \frac{T_o}{T_G}\right) \quad \text{eq. 188}$$

Heat exchanger

For a control volume surrounding the heat exchanger, the cost rate fuel equation can be presented as:

$$\dot{C}_{q,G} + \dot{C}_{34} + \dot{C}_{32} = \dot{Z}_G + \dot{C}_{31} + \dot{C}_{33} \quad \text{eq. 189}$$

where

$$c_{32} = c_{31} \quad \text{eq. 190}$$

$$c_{33} = c_{34} \quad \text{eq. 191}$$

$$\dot{C}_{q,he} = c \cdot \dot{E}_{q,he} = c \cdot \dot{Q}_{he} \left(1 - \frac{T_o}{T_{he}}\right) \quad \text{eq. 192}$$

where T_{he} is the temperature at which the heat transfer from heat exchanger occurs.

Solution valve

For a control volume surrounding the solution valve, the cost rate fuel equation can be expressed as:

$$\dot{C}_{34} + \dot{Z}_{V2} = \dot{C}_{35} \quad \text{eq. 193}$$

where

$$c_{34} = c_{35} \quad \text{eq. 194}$$

Absorber

For a control volume surrounding the absorber, the cost rate fuel equation is given by:

$$\dot{C}_{39} + \dot{C}_{19} + \dot{C}_{35} + \dot{Z}_{ab} = \dot{C}_{q,ab} + \dot{C}_{20} + \dot{C}_{30} \quad \text{eq. 195}$$

where

$$c_{30} = c_{39} + c_{35} \quad \text{eq. 196}$$

$$c_{19} = c_{20} \quad \text{eq. 197}$$

$$\dot{C}_{q,ab} = c \cdot \dot{E}_{q,ab} = c \cdot \dot{Q}_{ab} \left(1 - \frac{T_o}{T_{ab}}\right) \quad \text{eq. 198}$$

Solution pump

For a control volume surrounding the solution pump, the cost rate fuel equation can be written as:

$$\dot{C}_{30} + \dot{C}_{W,SP} + \dot{Z}_{SP} = \dot{C}_{31} \quad \text{eq. 199}$$

where

$$c_{30} = c_{31} \quad \text{eq. 200}$$

Evaporator

For a control volume surrounding the evaporator, the cost rate fuel equation is written as:

$$\dot{C}_{38} + \dot{C}_{17} + \dot{Z}_{Ev} = \dot{C}_{18} + \dot{C}_{39} \quad \text{eq. 201}$$

where

$$c_{38} = c_{39} \quad \text{eq. 202}$$

$$c_{17} = c_{18} \quad \text{eq. 203}$$

Expansion valve

For a control volume surrounding the expansion valve, the cost rate fuel equation is expressed as:

$$\dot{C}_{37} + \dot{Z}_{V1} = \dot{C}_{38} \quad \text{eq. 204}$$

where

$$c_{37} = c_{38} \quad \text{eq. 205}$$

Condenser

For a control volume surrounding the condenser, the cost rate fuel equation is written below,

$$\dot{C}_{36} + \dot{C}_{28} + \dot{Z}_{Cond} = \dot{C}_{29} + \dot{C}_{37} \quad \text{eq. 206}$$

where

$$c_{37} = c_{36} \quad \text{eq. 207}$$

$$c_{28} = c_{29} \quad \text{eq. 208}$$

5.2.4 Exergoeconomic analysis of the drying subsystem

Air compressor

For a control volume surrounding the air compressor, the cost rate fuel equation is expressed in a given equation as:

$$\dot{C}_{22} + \dot{C}_{W,ac} + \dot{Z}_{ac} = \dot{C}_{22'} \quad \text{eq. 209}$$

where

$$c_{22} = c_{22'} \quad \text{eq. 210}$$

Heater

For a control volume surrounding the heater, the cost rate fuel equation can be written as:

$$\dot{C}_{22'} + \dot{C}_{9'} + \dot{Z}_H = \dot{C}_{45} + \dot{C}_{23} \quad \text{eq. 211}$$

where

$$c_{23} = c_{22'} \quad \text{eq. 212}$$

$$c_{9'} = c_{45} \quad \text{eq. 213}$$

5.3 Advanced Exergoeconomic Analysis of the Hybrid Energy Systems

This section presents the advanced exergoeconomic approach of the hybrid thermal power system for multigeneration. The approach uses a specific optimization method in the exergoeconomic analysis that focuses on the exergy destruction of the k^{th} component to optimize the effectiveness cost by identifying and reducing their impact on the overall system.

5.3.1 Advanced exergoeconomic analysis of the prime movers

A. Solar field

For a control volume surrounding the solar field, the endogenous and exogenous exergy destruction is presented in the equation as follows:

$$\dot{E}_{D,solar-field} = \dot{E}_{D,solar-field}^{EN} + \dot{E}_{D,solar-field}^{EX} \quad \text{eq. 214}$$

The endogenous exergy destruction of the solar field of the concentrating solar power technology depends only on the components used during the power system assessment (collector, receiver, piping system, tracking system, and others). While the exogenous exergy destruction of solar field is a consequence of interactions between the under-considered subsystem and other subsystems or surrounding weather. Hence, exogenous and endogenous exergy destruction can be expressed as follows:

$$\dot{E}_{D,solar-field}^{EX} = \eta_{sf} \cdot \dot{E}_{D,solar-field} \quad \text{eq. 215}$$

$$\text{where } \eta_{sf} = \frac{\dot{E}_{D,sf}}{\dot{E}_{D,T}} \quad \text{eq. 216}$$

$$\dot{E}_{D,solar-field}^{EN} = \dot{E}_{D,solar-field} - \dot{E}_{D,solar-field}^{EX} \quad \text{eq. 217}$$

Bejan and Tsatsaronis (1996) demonstrated that, the exergy destruction can be divided into two parts, avoidable and unavoidable. The solar field is considered as compact system to determine these exergy destructions:

$$\dot{E}_{D,solar-field} = \dot{E}_{D,solar-field}^{UN} + \dot{E}_{D,solar-field}^{AV} \quad \text{eq. 208}$$

The avoidable and unavoidable exergy destruction of the solar field are calculated using the expressions given below:

$$\dot{E}_{D,solar-field}^{UN} = \dot{E}_{P,solar-field} \left(\frac{\dot{E}_{D,solar-field}}{\dot{E}_{P,solar-field}} \right)^{UN} \quad \text{eq. 209}$$

$$\dot{E}_{D,solar-field}^{AV} = \dot{E}_{D,solar-field} - \dot{E}_{D,solar-field}^{UN} \quad \text{eq. 210}$$

Considering the above equations, unavoidable endogenous and exogenous exergy destruction can be expressed as follows:

$$\dot{E}_{D,solar-field}^{UN,EN} = \dot{E}_{P,solar-field}^{EN} \left(\frac{\dot{E}_{D,solar-field}}{\dot{E}_{P,solar-field}} \right)^{UN} \quad \text{eq. 211}$$

$$\dot{E}_{D,solar-field}^{UN,EX} = \dot{E}_{D,solar-field}^{UN} - \dot{E}_{D,solar-field}^{UN,EN} \quad \text{eq. 212}$$

Using the same method as above, avoidable endogenous and exogenous exergy destruction can be determined as follows:

$$\dot{E}_{D,solar-field}^{AV,EN} = \dot{E}_{D,solar-field}^{EN} - \dot{E}_{D,solar-field}^{UN,EN} \quad \text{eq. 213}$$

$$\dot{E}_{D,solar-field}^{AV,EX} = \dot{E}_{D,solar-field}^{AV} - \dot{E}_{D,solar-field}^{AV,EN} \quad \text{eq. 214}$$

The endogenous investment cost consisting of capital investment and operating and maintenance cost of the solar field subsystem are determined by using the exergy product at the theoretical condition and the investment cost per unit exergy product at real condition expressed by the following equations:

$$\dot{Z}_{solar-field}^{EN} = \dot{E}_{P,solar-field}^{EN} \left(\frac{\dot{Z}}{\dot{E}_P} \right)_{solar-field} \quad \text{eq. 215}$$

$$\dot{Z}_{solar-field}^{EX} = \dot{Z}_{solar-field} - \dot{Z}_{solar-field}^{EN} \quad \text{eq. 216}$$

The avoidable and unavoidable costs of the solar field are calculated using these expressions:

$$\dot{Z}_{solar-field}^{UN} = \dot{E}_{P,solar-field} \left(\frac{\dot{Z}}{\dot{E}_P} \right)_{solar-field}^{UN} \quad \text{eq. 217}$$

$$\dot{Z}_{solar-field}^{AV} = \dot{Z}_{solar-field} - \dot{Z}_{solar-field}^{UN} \quad \text{eq. 218}$$

Considering the endogenous and exogenous split for unavoidable exergy destruction presented in the previous chapter, the split right side with unavoidable-exogenous and unavoidable-endogenous parts lead to the determination of the investment cost of the solar field as follows:

$$\dot{Z}_{solar-field}^{UN,EN} = \dot{E}_{solar-field}^{EN} \left(\frac{\dot{Z}_{solar-field}^{UN}}{\dot{E}_P} \right)_{solar-field} \quad \text{eq. 219}$$

$$\dot{Z}_{solar-field}^{UN,EX} = \dot{Z}_{solar-field}^{UN} - \dot{Z}_{solar-field}^{UN,EN} \quad \text{eq. 220}$$

Subsequently, the split left with avoidable – exogenous and avoidable – endogenous part is obtained as:

$$\dot{Z}_{solar-field}^{AV,EN} = \dot{Z}_{solar-field}^{EN} - \dot{Z}_{solar-field}^{UN,EN} \quad \text{eq. 221}$$

$$\dot{Z}_{solar-field}^{AV,EX} = \dot{Z}_{solar-field}^{EX} - \dot{Z}_{solar-field}^{UN,EX} \quad \text{eq. 222}$$

B. Biomass

For a control volume surrounding biomass subsystem, the avoidable and unavoidable exergy destruction can be calculated using these expressions:

$$\dot{E}_{D,bio}^{UN} = \dot{E}_{P,bio} \left(\frac{\dot{E}_{D,bio}}{\dot{E}_{P,bio}} \right)^{UN} \quad \text{eq. 223}$$

$$\dot{E}_{D,bio}^{AV} = \dot{E}_{D,bio} - \dot{E}_{D,bio}^{UN} \quad \text{eq. 224}$$

The avoidable and unavoidable costs of the biomass are expressed as follows:

$$\dot{Z}_{bio}^{UN} = \dot{E}_{P,bio} \left(\frac{\dot{Z}}{\dot{E}_P} \right)_{bio}^{UN} \quad \text{eq. 225}$$

$$\dot{Z}_{bio}^{AV} = \dot{Z}_{bio} - \dot{Z}_{bio}^{UN} \quad \text{eq. 226}$$

Boiler or intermediate heat exchanger

For a control volume surrounding the boiler, the exergy destruction associated with cost can be calculated as:

$$\dot{E}_{D,boiler}^{EX} = \eta_{boiler} \cdot \dot{E}_{D,boiler} \quad \text{eq. 227}$$

and

$$\eta_{boiler} = \frac{(\dot{E}_4 - \dot{E}_3) + (\dot{E}_8 - \dot{E}_6)}{(\dot{E}_{2'} - \dot{E}_{1'})} \quad \text{eq. 228}$$

$$\dot{E}_{D,boiler}^{EN} = \dot{E}_{D,boiler} - \dot{E}_{D,boiler}^{EX} \quad \text{eq. 229}$$

The avoidable and unavoidable part of the boiler exergy destruction can be expressed as:

$$\dot{E}_{D,boiler}^{UN} = \dot{E}_{P,boiler} \left(\frac{\dot{E}_{D,boiler}}{\dot{E}_{P,boiler}} \right)^{UN} \quad \text{eq. 230}$$

Considering the normal operating conditions of the thermal power plant, Vuckovi, et al. (2012) suggested the unavoidable conditions of the steam boiler, circulation pump, and steam boiler.

$$\dot{E}_{D,boiler}^{AV} = \dot{E}_{D,boiler} - \dot{E}_{D,boiler}^{UN} \quad \text{eq. 231}$$

As result of above equations unavoidable endogenous and exogenous exergy destruction can be written as follows:

$$\dot{E}_{D,boiler}^{UN,EN} = \dot{E}_{P,boiler}^{EN} \left(\frac{\dot{E}_{D,boiler}}{\dot{E}_{P,boiler}} \right)^{UN} \quad \text{eq. 232}$$

$$\dot{E}_{D,boiler}^{UN,EX} = \dot{E}_{D,boiler}^{UN} - \dot{E}_{D,boiler}^{UN,EN} \quad \text{eq. 233}$$

Using the same approach, avoidable endogenous and exogenous exergy destruction can be expressed as:

$$\dot{E}_{D,boiler}^{AV,EN} = \dot{E}_{D,boiler}^{EN} - \dot{E}_{D,boiler}^{UN,EN} \quad \text{eq. 234}$$

$$\dot{E}_{D,boiler}^{AV,EX} = \dot{E}_{D,boiler}^{AV} - \dot{E}_{D,boiler}^{AV,EN} \quad \text{eq. 235}$$

The avoidable and unavoidable costs of the biomass are written as:

$$\dot{Z}_{boiler}^{UN} = \dot{E}_{P,boiler} \left(\frac{\dot{Z}}{\dot{E}_P} \right)_{boiler}^{UN} \quad \text{eq. 236}$$

$$\dot{Z}_{boiler}^{AV} = \dot{Z}_{boiler} - \dot{Z}_{boiler}^{UN} \quad \text{eq. 237}$$

Table 5.5 presents, unavoidable investment costs (UIC) and thermodynamic efficiencies and inefficiencies in the unavoidable conditions (UCTI) and real conditions (RCTI) of the main subsystems used in the power system design.

Table 5.5. Main parameters of prime mover subsystem used for advanced exergoeconomic analysis real conditions (RC), unavoidable thermodynamic inefficiency (UTI), unavoidable investment cost (Cziesla et al., 2006; Vuckovi et al. 2012).

Power block components	Parameters	Real conditions	Unavoidable conditions/ Un. thermodynamic ineff. (UTI)	Unavoidable investment costs (UIC)
Solar field				
PTCs	η_{S-PTC}	44.5%	75.7% (UN=24.3)	490 (124)
LFRs	η_{S-LFR}	29.73%	69.2% (UN=30.8)	652 (202)
ST	η_{S-ST}	33.7%	84.3% (UN=15.7)	216 (35)
Combustion chamber/boiler				
Excess air	$\lambda_{air}(-)$	0.2	0.15	0.31
Exit temperature	$T_5(K)$	813	1000	813
HTF circulation pump	η_P	80%	91% (UN=9)	75
Heat exchangers	$\Delta T_{min-PTC/LFR}$	181.1	50	425
	$\Delta T_{min-ST/bio}$	134.1	50	425

5.3.2 Advanced exergoeconomic analysis of the power block subsystem

Turbines

For a control volume surrounding the turbine, the endogenous and exogenous exergy destruction can be presented as follows:

$$\dot{E}_{D,Turb}^{EX} = \eta_{Turb} \cdot \dot{E}_{D,Turb} \quad \text{eq. 238}$$

$$\eta_{Turb} = \eta_{is} = 0.8$$

$$\dot{E}_{D,Turb}^{EN} = \dot{E}_{D,Turb} - \dot{E}_{D,Turb}^{EX} \quad \text{eq. 239}$$

The avoidable and unavoidable part of the boiler exergy destruction can be expressed as:

$$\dot{E}_{D,Turb}^{UN} = \dot{E}_{P,Turb} \left(\frac{\dot{E}_{D,Turb}}{\dot{E}_{P,Turb}} \right)^{UN} \quad \text{eq. 240}$$

Vuckovi, et al. (2012) suggested the unavoidable conditions of the steam turbine, circulation pump and steam boiler, expressed as:

$$\dot{E}_{D,Turb}^{AV} = \dot{E}_{D,Turb} - \dot{E}_{D,Turb}^{UN} \quad \text{eq. 241}$$

As a result of the above equations unavoidable endogenous and exogenous exergy destruction can be written as follows:

$$\dot{E}_{D,Turb}^{UN,EN} = \dot{E}_{P,Turb}^{EN} \left(\frac{\dot{E}_{D,Turb}}{\dot{E}_{P,Turb}} \right)^{UN} \quad \text{eq. 242}$$

$$\dot{E}_{D,Turb}^{UN,EX} = \dot{E}_{D,Turb}^{UN} - \dot{E}_{D,Turb}^{UN,EN} \quad \text{eq. 243}$$

Using the same approach, avoidable endogenous and exogenous exergy destruction can be shown as:

$$\dot{E}_{D,Turb}^{AV,EN} = \dot{E}_{D,Turb}^{EN} - \dot{E}_{D,Turb}^{UN,EN} \quad \text{eq. 244}$$

$$\dot{E}_{D,Turb}^{AV,EX} = \dot{E}_{D,Turb}^{AV} - \dot{E}_{D,Turb}^{AV,EN} \quad \text{eq. 245}$$

The endogenous investment cost containing capital investment and operating and maintenance cost of the turbines is determined by using the exergy product at the theoretical condition and the investment cost per unit exergy product at the real condition:

$$\dot{Z}_{Turb}^{EN} = \dot{E}_{P,Turb}^{EN} \left(\frac{\dot{Z}}{\dot{E}_P} \right)_{Turb} \quad \text{eq. 246}$$

$$\dot{Z}_{Turb}^{EX} = \dot{Z}_{Turb} - \dot{Z}_{Turb}^{EN} \quad \text{eq. 247}$$

The avoidable and unavoidable costs of the turbines are calculated using these expressions:

$$\dot{Z}_{Turb}^{UN} = \dot{E}_{P,Turb} \left(\frac{\dot{Z}}{\dot{E}_P} \right)_{Turb}^{UN} \quad \text{eq. 248}$$

$$\dot{Z}_{Turb}^{AV} = \dot{Z}_{Turb} - \dot{Z}_{Turb}^{UN} \quad \text{eq. 249}$$

Considering the endogenous and exogenous split for unavoidable exergy destruction presented in chapter 4, the right side of the split with unavoidable-exogenous and unavoidable-endogenous parts lead to the determination of the investment cost of the solar field as follows:

$$\dot{Z}_{Turb}^{UN,EN} = \dot{E}_{Turb}^{EN} \left(\frac{\dot{Z}_{Turb}^{UN}}{\dot{E}_P} \right)_{Turb} \quad \text{eq. 250}$$

$$\dot{Z}_{Turb}^{UN,EX} = \dot{Z}_{Turb}^{EN} - \dot{Z}_{Turb}^{UN,EN} \quad \text{eq. 251}$$

Subsequently, the left side of the split with avoidable – exogenous and avoidable – endogenous part is obtained as:

$$\dot{Z}_{Turb}^{AV,EN} = \dot{Z}_{Turb}^{EN} - \dot{Z}_{Turb}^{UN,EN} \quad \text{eq. 252}$$

$$\dot{Z}_{Turb}^{AV,EX} = \dot{Z}_{Turb}^{EX} - \dot{Z}_{Turb}^{UN,EX} \quad \text{eq. 253}$$

Feedwater pump

For a control volume surrounding the circulation pump, the endogenous and exogenous exergy destruction can be presented as follows:

$$\dot{E}_{D,Pump}^{EX} = \eta_{Pump} \cdot \dot{E}_{D,Pump} \quad \text{eq. 254}$$

$$\eta_{Pump} = \eta_{is} = 0.8$$

$$\dot{E}_{D,Pump}^{EN} = \dot{E}_{D,Pump} - \dot{E}_{D,Pump}^{EX} \quad \text{eq. 255}$$

The avoidable and unavoidable part of the boiler exergy destruction can be expressed as:

$$\dot{E}_{D,Pump}^{UN} = \dot{E}_{P,Pump} \left(\frac{\dot{E}_{D,Pump}}{\dot{E}_{P,Pump}} \right)^{UN} \quad \text{eq. 256}$$

Vuckovi et al. (2012) suggested the unavoidable conditions of the steam turbine, circulation pump, and steam boiler.

$$\dot{E}_{D,Pump}^{AV} = \dot{E}_{D,Pump} - \dot{E}_{D,Pump}^{UN} \quad \text{eq. 257}$$

As a result of the above equations unavoidable endogenous and exogenous exergy destruction can be written as follows:

$$\dot{E}_{D,Pump}^{UN,EN} = \dot{E}_{P,Pump}^{EN} \left(\frac{\dot{E}_{D,Pump}}{\dot{E}_{P,Pump}} \right)^{UN} \quad \text{eq. 258}$$

$$\dot{E}_{D,Pump}^{UN,EX} = \dot{E}_{D,Pump}^{UN} - \dot{E}_{D,Pump}^{UN,EN} \quad \text{eq. 259}$$

Using the same approach, avoidable endogenous and exogenous exergy destruction can be given as:

$$\dot{E}_{D,Pump}^{AV,EN} = \dot{E}_{D,Pump}^{EN} - \dot{E}_{D,Pump}^{UN,EN} \quad \text{eq. 260}$$

$$\dot{E}_{D,Pump}^{AV,EX} = \dot{E}_{D,Pump}^{AV} - \dot{E}_{D,Pump}^{AV,EN} \quad \text{eq. 261}$$

The unavoidable, avoidable, investment, endogenous and exogenous costs can be estimated by using equations presented in section 1. The specific data of advanced exergoeconomic analysis for the main component of the CRC system such as generator, absorber, evaporator, and condenser can be calculated by using the value in Table 5.3.

The endogenous investment cost containing capital investment and operating and maintenance cost of the pumps is determined by using the exergy product at the theoretical condition and the investment cost per unit exergy product at the real condition:

$$\dot{Z}_{Pump}^{EN} = \dot{E}_{P,Pump}^{EN} \left(\frac{\dot{Z}}{\dot{E}_P} \right)_{Pump} \quad \text{eq. 262}$$

$$\dot{Z}_{Pump}^{EX} = \dot{Z}_{Pump} - \dot{Z}_{Pump}^{EN} \quad \text{eq. 263}$$

The avoidable and unavoidable costs of the pumps are calculated using these expressions:

$$\dot{Z}_{Pump}^{UN} = \dot{E}_{P,Pump} \left(\frac{\dot{Z}}{\dot{E}_P} \right)_{Pump}^{UN} \quad \text{eq. 264}$$

$$\dot{Z}_{Pump}^{AV} = \dot{Z}_{Pump} - \dot{Z}_{Pump}^{UN} \quad \text{eq. 265}$$

Considering the endogenous and exogenous split for unavoidable exergy cost presented in chapter 4, the right side of the split with unavoidable-exogenous and unavoidable-endogenous parts lead to the determination of the investment cost of the solar field as follows:

$$\dot{Z}_{Pump}^{UN,EN} = \dot{E}_{P,Pump}^{EN} \left(\frac{\dot{Z}_{Pump}^{UN}}{\dot{E}_P} \right)_{Pump} \quad \text{eq. 266}$$

$$\dot{Z}_{Pump}^{UN,EX} = \dot{Z}_{Pump}^{UN} - \dot{Z}_{Pump}^{UN,EN} \quad \text{eq. 267}$$

Subsequently, the left side of the split with avoidable – exogenous and avoidable – endogenous part was determined using the following equations:

$$\dot{Z}_{Pump}^{AV,EN} = \dot{Z}_{Pump}^{EN} - \dot{Z}_{Pump}^{UN,EN} \quad \text{eq. 268}$$

$$\dot{Z}_{Pump}^{AV,EX} = \dot{Z}_{Pump}^{EX} - \dot{Z}_{Pump}^{UN,EX} \quad \text{eq. 269}$$

Table 5.6 presents unavoidable investment costs (UIC) and thermodynamic efficiencies and inefficiencies in the unavoidable conditions (UCTI) and real conditions (RCTI) of the main components used in the power block design.

Table 5.6. Main parameters of power block subsystem used for advanced exergoeconomic analysis real conditions (RC), unavoidable thermodynamic inefficiency (UTI), unavoidable investment cost (Cziesla et al., 2006; Vuckovi et al. 2012)

Power block components	Parameters	Real conditions	Unavoidable conditions/ Un. thermodynamic ineff. (UTI)	Unavoidable investment costs (UIC)
HP S. Turbine	η_T	80%	95% (UN=5)	82
LP S. Turbine	η_T	80%	95% (UN=5)	82
LP G. Turbine	η_T	80%	91% (UN=9)	75
Water Condenser	η_{wc}	82%	86 % (UN=14)	65
R134a Condenser	η_{rc}	83%	86 % (UN=14)	65
Feedwater Pump	η_P	80%	90% (UN=10)	75
Evaporator	$\Delta T_{min-PTC/LFR}$	134.1	50	425
Metallic	$\Delta T_{min-ST/bio}$	181.1	50	425

5.3.3 Advanced exergoeconomic analysis of the HRSG subsystem

The required cost for a high temperature of heat exchangers is one of the major issues which has to be considered for future thermal power plant. This can contribute to making the systems become a cost-effective alternative for commercial thermal power plant application which can be combined with various prime movers such as natural gas-fired and supercritical steam power plants. Consonni et al. (1996) presented the application of the counter-flow and parallel-flow technology during the designing of the heat exchangers to maintain the temperature of the heat transfer surface. For a control volume surrounding each regenerator used for HRSG subsystem, the endogenous and exogenous exergy destruction can be presented as follows:

$$\dot{E}_{D,regenerator}^{EX} = \eta_{Reg} \cdot \dot{E}_{D,Reg} \quad \text{eq. 270}$$

$\eta_{regenerator}$ is calculated according to real conditions

$$\dot{E}_{D,regenerator}^{EN} = \dot{E}_{D,regenerator} - \dot{E}_{D,regenerator}^{EX} \quad \text{eq. 271}$$

Assuming a minimum temperature difference of the regenerators used in the HRSG (Tsatsaronis and Park, 2002) the ratio below can be found and verified before calculating the value of the unavoidable exergy destruction.

$$\left(\frac{\dot{E}_D}{\dot{E}_P}\right)_{regenerator/HRSG}^{UN} \quad \text{eq. 272}$$

$$\dot{E}_{D,regenerator}^{UN} = \dot{E}_{P,regenerator} \left(\frac{\dot{E}_D}{\dot{E}_P}\right)_{regenerator/HRSG}^{UN} \quad \text{eq. 273}$$

Considering the normal operating conditions of the thermal power plant, Vuckovi, et al. (2012) suggested the unavoidable conditions of the steam boiler, circulation pump, and steam boiler. Avoidable exergy destruction is given as presented in the equation.

$$\dot{E}_{D,regenerator/HRSG}^{AV} = \dot{E}_{D,regenerator/HRSG} - \dot{E}_{D,regenerator/HRSG}^{UN} \quad \text{eq. 274}$$

The unavoidable investment costs can be estimated by assuming 587 K as a very high temperature exiting the HRSG subsystem. Furthermore, the unavoidable investment costs assumes a low value for the inlet temperature coming from a pump with an isentropic efficiency of about 80% and a pressure ratio of 5 for a low value of T_{46} (331 K) and a high value of T_5 (achieved for the steam turbine inlet temperature (645 -813 K) with an isentropic efficiency of 80%) according to the used prime mover. The ratio between investment cost and the exergy product can be used to verify the appropriate value of the unavoidable thermodynamic inefficiency.

$$\left(\frac{\dot{Z}}{\dot{E}_P}\right)_{regenerator/HRSG}^{UN} \quad \text{eq. 275}$$

The avoidable and unavoidable costs of the regenerator are expressed as:

$$\dot{Z}_{regenerator/HRSG}^{UN} = \dot{E}_{P,regenerator} \left(\frac{\dot{Z}}{\dot{E}_P}\right)_{regenerator/HRSG}^{UN} \quad \text{eq. 276}$$

$$\dot{Z}_{regenerator/HRSG}^{AV} = \dot{Z}_{regenerator} - \dot{Z}_{regenerator/HRSG}^{UN} \quad \text{eq. 277}$$

The endogenous investment cost containing capital investment and operating and maintenance cost of the regenerator used in the HRSG subsystem is

determined by using the exergy product at the theoretical condition and the investment cost per unit exergy product at the real condition:

$$\dot{Z}_{regenerator/HRSG}^{EN} = \dot{E}_{P,regenerator/HRSG}^{EN} \left(\frac{\dot{Z}}{\dot{E}_P} \right)_{regenerator/HRSG} \quad \text{eq. 278}$$

$$\dot{Z}_{regenerator/HRSG}^{EX} = \dot{Z}_{regenerator/HRSG} - \dot{Z}_{regenerator/HRSG}^{EN} \quad \text{eq. 279}$$

Considering the endogenous and exogenous split for unavoidable exergy cost presented in Chapter 4, the right side of the split with unavoidable-exogenous and unavoidable-endogenous parts lead to the determination of the investment cost of the regenerator used in the HRSG subsystem as:

$$\dot{Z}_{regenerator/HRSG}^{UN,EN} = \dot{E}_{regenerator/HRSG}^{EN} \left(\frac{\dot{Z}_{reg/HRSG}^{UN}}{\dot{E}_P} \right)_{regenerator/HRSG} \quad \text{eq. 280}$$

$$\dot{Z}_{regenerator/HRSG}^{UN,EX} = \dot{Z}_{regenerator/HRSG}^{EN} - \dot{Z}_{regenerator/HRSG}^{UN,EX} \quad \text{eq. 281}$$

Subsequently, the left side of the split with avoidable – exogenous and avoidable – endogenous part is determined as:

$$\dot{Z}_{regenerator/HRSG}^{AV,EN} = \dot{Z}_{regenerator/HRSG}^{EN} - \dot{Z}_{regenerator/HRSG}^{UN,EN} \quad \text{eq. 282}$$

$$\dot{Z}_{regenerator/HRSG}^{AV,EX} = \dot{Z}_{regenerator/HRSG}^{EX} - \dot{Z}_{regenerator/HRSG}^{UN,EX} \quad \text{eq. 283}$$

Table 5.7 presents unavoidable investment costs (UIC) and thermodynamic efficiencies and inefficiencies in the unavoidable conditions (UCTI) and real conditions (RCTI) of the main components used in the HRSG system design.

Table 5.7. Main parameters of HRSG subsystem used for advanced exergoeconomic analysis real conditions (RC), unavoidable thermodynamic inefficiency (UTI), unavoidable investment cost (Cziesla et al., 2006; Vuckovi et al. 2012).

ARS components	Parameters	Real conditions	Unavoidable conditions/ Un. thermodynamic ineff. (UTI)	Unavoidable investment costs (UIC)
Regenerator 1	$\Delta T_{min-PTC/LFR}$	140.8	(UN=50)	425
	$\Delta T_{min-ST/bio}$	103	(UN=50)	425
Regenerator 2	$\Delta T_{min-PTC/LFR}$	23.6	(UN=2)	150
	$\Delta T_{min-ST/bio}$	75.7	(UN=2)	150
Regenerator 3	$\Delta T_{min-PTC/LFR}$	44.9	(UN=2)	150
	$\Delta T_{min-ST/bio}$	17.8	(UN=5)	35
Regenerator 4	$\Delta T_{min-PTC/LFR}$	10.1	(UN=5)	35
	$\Delta T_{min-ST/bio}$	62	(UN=2)	150
Regenerator 5	$\Delta T_{min-PTC/LFR}$	17.6	(UN=5)	35
	$\Delta T_{min-ST/bio}$	41.7	(UN=2)	150

(50): **heat exchanger;** (5): **Evaporator,** (2): **Superheater/ economizer**

5.3.4 Advanced exergoeconomic analysis of the absorption refrigeration subsystem

The sum of heat rejected from the absorber and the condenser and the heat extracted from evaporator are the useful exergies of the studied system for heating and cooling application. This is because the advanced exergoeconomic analysis focuses on these main components to determine an effective cost analysis of the LiBr-H₂O absorption refrigeration system. The advanced exergoeconomic analysis of the intermediate heat exchanger is illustrated in this section to present the general approach of this study

For a control volume surrounding the intermediate heat exchanger of the absorption refrigeration system, the endogenous and exogenous exergy destruction are expressed as follows:

$$\dot{E}_{D,ihe}^{EX} = \eta_{ihe} \cdot \dot{E}_{D,ihe} \quad \text{eq. 284}$$

$\eta_{regenerator}$ is calculated according to real conditions

$$\dot{E}_{D,ihe}^{EN} = \dot{E}_{D,ihe} - \dot{E}_{D,ihe}^{EX} \quad \text{eq. 285}$$

A minimum temperature difference can be used to determine the ratio of the intermediate heat exchanger solution used in studied absorption refrigeration system (Tsatsaronis and Park, 2002). This ratio is expressed in equation below, can be determined and verified before calculating the value of the unavoidable exergy destruction.

$$\left(\frac{\dot{E}_D}{\dot{E}_P}\right)_{ihe}^{UN} \quad \text{eq. 286}$$

$$\dot{E}_{D,ihe}^{UN} = \dot{E}_{P,ihe} \left(\frac{\dot{E}_D}{\dot{E}_P}\right)_{ihe}^{UN} \quad \text{eq. 287}$$

Considering the normal operation conditions of thermal power plant, Cziesla, et al. (2006) has suggested the unavoidable conditions of the evaporator, superheater, heat exchanger, and economizer.

$$\dot{E}_{D,ihe}^{AV} = \dot{E}_{D,ihe} - \dot{E}_{D,ihe}^{UN} \quad \text{eq. 288}$$

The unavoidable investment costs can be estimated by assuming 337 K as a very high temperature exiting in the intermediate heat exchanger. Furthermore, the unavoidable investment costs assume a low value for the inlet temperature exiting from a pump with an isentropic efficiency of about 80% and a pressure ratio of 5 for a low value of T_{31} (307 K) and a high value of T_{33} (achieved for the intermediate heat exchanger solution, inlet temperature (362 K) with an efficiency of 93%). The ratio is between investment cost and the exergy product which can be used to verify the appropriate value of the unavoidable thermodynamic inefficiency.

$$\left(\frac{\dot{Z}}{\dot{E}_P}\right)_{ihe}^{UN} \quad \text{eq. 289}$$

The avoidable and unavoidable costs of the intermediate heat exchanger solution are expressed as follows:

$$\dot{Z}_{ihe}^{UN} = \dot{E}_{P,ihe} \left(\frac{\dot{Z}}{\dot{E}_P}\right)_{ihe}^{UN} \quad \text{eq. 290}$$

$$\dot{Z}_{ihe}^{AV} = \dot{Z}_{ihe} - \dot{Z}_{ihe}^{UN} \quad \text{eq. 291}$$

The endogenous investment cost containing capital investment and operating and maintenance cost of the intermediate heat exchanger solution used in the absorption refrigeration system was determined using the exergy product at the theoretical condition and the investment cost per unit exergy product at the real condition:

$$\dot{Z}_{ihe}^{EN} = \dot{E}_{P,ihe}^{EN} \left(\frac{\dot{Z}}{\dot{E}_P} \right)_{ihe} \quad \text{eq. 292}$$

$$\dot{Z}_{ihe}^{EX} = \dot{Z}_{ihe} - \dot{Z}_{ihe}^{EN} \quad \text{eq. 293}$$

Considering the endogenous and exogenous split for unavoidable exergy cost presented in chapter 4, the right side of the split with unavoidable-exogenous and unavoidable-endogenous parts lead to the determination of the investment cost of the intermediate heat exchanger solution used in the absorption refrigeration system as:

$$\dot{Z}_{ihe}^{UN,EN} = \dot{E}_{ihe}^{EN} \left(\frac{\dot{Z}_{ihe}^{UN}}{\dot{E}_P} \right)_{ihe} \quad \text{eq. 294}$$

$$\dot{Z}_{ihe}^{UN,EX} = \dot{Z}_{ihe}^{EN} - \dot{Z}_{ihe}^{UN,EX} \quad \text{eq. 295}$$

Subsequently, the left side of the split with avoidable – exogenous and avoidable – endogenous part can be determined using expression given below:

$$\dot{Z}_{ihe}^{AV,EN} = \dot{Z}_{ihe}^{EN} - \dot{Z}_{ihe}^{UN,EN} \quad \text{eq. 296}$$

$$\dot{Z}_{ihe}^{AV,EX} = \dot{Z}_{ihe}^{EX} - \dot{Z}_{ihe}^{UN,EX} \quad \text{eq. 297}$$

Table 5.8 presents unavoidable investment costs (UIC) and thermodynamic efficiencies and inefficiencies in the unavoidable conditions (UCTI) and real conditions (RCTI) of the main components used for the absorption refrigeration systems used in power system.

Table 5.8. Main parameters of the drying subsystem used for advanced exergoeconomic analysis real conditions (RC), unavoidable thermodynamic inefficiency (UTI), unavoidable investment cost (UIC) (Cziesla et al., 2006; Vuckovi et al. 2012).

ARS components	Real conditions	Unavoidable conditions/ un. Thermodynamic ineff. (UTI)	Unavoidable investment costs (UIC)
Absorber	$\eta = 42.64\%$	$\eta = 96\%$ (UN=4)	20
Pump	Isentropic condition (80%)	$\eta = 90\%$	-
Valve	$h_{in} = h_{out}$	$T_{in} = T_{out}$	
Heat exchanger	92.81% ($T_{34} > T_{32}$)	$\eta = 96.43\%$ (UN=3) ($T_{34} = T_{35} = 62\text{ C}$)	
Generator	$\eta = 73.22\%$	$\eta = 97\%$ (UN=3)	20
Condenser	$\eta = 83.94\%$	$\eta = 96\%$ (UN=4)	15
Evaporator	$\eta = 83.76\%$	$\eta = 97\%$ (UN=3)	5

5.3.5 Advanced exergoeconomic analysis of the drying subsystem

The useful output exergy of the drying system for industrial purposes are used for food conservation. The advanced exergoeconomic analysis of the studied subsystem focuses only on the evaluation of main components such as air compressor and heater. Table 5.10 presents, unavoidable investment costs (UIC) and thermodynamic efficiencies and inefficiencies in the unavoidable conditions (UCTI) and real conditions (RCTI) of the main components for the drying system.

Table 5.9. Main parameters of the drying subsystem used for advanced exergoeconomic analysis real conditions (RC), unavoidable thermodynamic inefficiency (UTI), unavoidable investment cost (UIC) (Tsatsaronis and Park, 2002; Cziesla et al., 2006)

ARS components	Real conditions	Unavoidable conditions/ Un. thermodynamic ineff. (UTI)	Unavoidable investment costs (UIC)
Air compressor	$\eta = 80\%$	$\eta = 85\%$ (UN=30)	75
Heater	$\eta = 87.6\%$	$\eta = 97\%$ (UN=3)	100

6. RESULTS AND DISCUSSION

In this study, hybrid energy systems based on the concentrating solar power and biomass-fired technologies are designed and analyzed to determine their overall efficiencies (energy and exergy), the costs related to the construction, initial investment, and exergy destruction. Each part of the studied hybrid energy system shown in Chapter 3 is analyzed and for each stream of the component; mass, energy, and exergy balance equations are used to calculate thermodynamic properties at different points. Engineering Equation Solver (EES) and Matlab software are used for a better understanding of fluids state and properties at these points. For the main components used in the solar field, biomass-fired, power block, heat recovery steam generation, and additional subsystems, different points of the streams are analyzed in order to carry out the mass flow of fluids at specific temperature and pressure according to data obtained from the existing processes or similar works available in literature (Appendix A). Other data such as higher heating values (HHV) or lower heating values (LHV) of sorghum straw are analyzed and chosen to be transformed as a feedstock to run the biomass-fired power system. The datasheet, technical parameters, cost of the solar field components (collector, receivers, tower, heat transfer fluid, required land and other) are presented in Table 6.1, 6.5, 6.10 and 6.15 according to the concentrating solar power technologies and the meteorological data of the location.

6.1 Conventional Exergy and Cost Analysis of the Systems

The studied hybrid energy system is based on biomass-fired technology which uses a DSG system with a generation capacity of 5 MWe. The sorghum stalk is considered as the primary energy source and transformed into feedstock. Its lower heating value is used to adjust the higher heating value of fuel under boiler conditions. The available amount of biomass is obtained from sorghum farms. Hence, this section aims to determine the breakdown cost and technical properties of the hybrid energy system based on a combination of biomass-fired and concentrating solar power technologies.

Table 6.1 presents the technical characteristics of the biomass-fired power system. The hybrid energy systems developed for electricity generation use combined Rankine cycles as a power block system. It incorporates two pressure - level for the steam Rankine cycle (SRC) connected with the HRSG system and one pressure – level for the organic Rankine cycle. The studied hybrid energy system operates with biomass during the unavailability periods of solar radiation for electricity generation. The thermodynamic properties of each stream of different components contribute to determining values such as endogenous exergy destruction, exogenous exergy destruction, unavoidable exergy destruction and avoidable exergy destruction in each component through the advanced exergy analysis. The energy efficiency and the thermal energy loss during the processes and delivered to the power block system are specified in Table 6.2.

Table 6.1. Properties of sorghum stalk and technical characteristics of the boiler - grate stoker furnace (SAM 2017.9.5).

Characteristics/ Properties	Values	Characteristics/ Properties	Values
The moisture of fuel ($e_{fuel\ moist}$) in %	3.14	HHV of sorghum (MJ/kg)	17,015
Amount of sorghum feedstock in Tons	28152	Yearly operating time (hours)	3600
Estimated (HHV) efficiency losses			
Dry flue gas losses (e_{dry-f}) in %	8.3293	Unburned fuel ($e_{unb. Carb}$) in %	3.5
Moisture in fuel ($e_{moisture}$) in %	5.6693	Radiation and miscellaneous (e_{rad}) in %	2.03
Latent heat ($e_{latent\ heat}$) in %	3.7211	Total boiler efficiency (HHV basis) η_b in %	76.75
Estimated (Boiler) efficiency losses and main parameters			
Global losses in the boiler in %	7.13	Boiler overdesign factor	10.12
Percent of excess - air	20	Steam grade and pressure	541°C - 14.4Mpa

Table 6.2. Energy analysis of the steam generation process in the grate stoker furnace (boiler) for the biomass-fired power system.

Subsystem	Energy expected (MW)	Energy delivered (MW)	Energy loss (MW)	Energy loss (%)	First law efficiency (%)
Biomass	36.96	27.21	9.75	26.4	-
Boiler	27.21	21.76	5.45	20.03	79.97
Biomass - Boiler	36.96	21.76	15.2	41.1	-

Table 6.3 and 6.4 present the results of the thermodynamic (first and second law) analysis of the steam generation process in the grate stoker furnace for the biomass-fired power system.

Table 6.3. Exergy analysis of the steam generation process in the grate stoker furnace (boiler) for the biomass-fired power system.

Subsystem	Exergy received (MW)	Exergy delivered (MW)	Exergy loss (MW)	Exergy loss (%)	Second law efficiency (%)
Biomass	-	17.29	-	-	-
Boiler	17.29	11.63	5.66	32.7	67.3
Biomass - Boiler	-	11.63	-	-	-

Table 6.4. First and second law analysis of the steam generation process in the grate stoker furnace (boiler) for the biomass-fired power system.

Subsystem	Irreversibility (MW)	Energy loss (%)	Exergy loss (%)	First law (%)	Second law efficiency (%)
Biomass	-	26.4	-	-	-
Boiler	5.66	20.03	32.7	79.97	67.3
Biomass - Boiler	-	41.1	-	-	-

- **Parabolic trough collector (PTC)– solar field**

The solar field system consists of an arrangement of collector's assemblies interconnected, piping system, intermediate heat exchanger and other control devices. The solar radiation is concentrated into a Schott PTR80's receiver by using LUZ S-3 collectors arranged in the 20 loops each containing 4 solar collector assemblies with 48 modules. Table 6.5 presents the properties and technical characteristics of the solar field based on results obtained from simulation (SAM 2017.9.5).

The Therminol VP–1 goes through each loop and heat transfer circuit to transport the thermal energy generated by the solar field that needed to be transferred to the power block system by using the intermediate heat exchanger.

Table 6.5. Properties and technical characteristics of the parabolic trough collector technology-LS3/PTR80 solar field (SAM 2017.9.5).

Total solar aperture area	43600 m ²	Loop optical efficiency	0.74
Solar Multiple (SM)	1	Total loop conv. efficiency	0.71
Single loop area	2180 m ²	Collector type	Luz LS3
Number of loops	19.987 (20)	Length of SCA	100 m
Number of SCA per loop	4	Length of module	8.33 m
Number of modules per SCA	12	Aperture width	5.75 m
Type of HTF fluid	Therminol VP-1	Receiver type	Schott PTR80
Flow velocity	0.248 – 3.744	In. diameter of glass	0.115
Operating temp. of HTF fluid	230 - 391	Out diameter of glass	0.12
Piping distance between SCA	1.2 m	In. diameter of abs. tube	0.076
Field loop pumping thermal inertia	4.5 W _{th} /K-m	Out diameter of abs. tube	0.08
IAM	1.0036	Heat loss at design	207.35W/m
Mirror washing	0.7 L/ m ²	Optical derate	0.8501
HCE Transmittance	0.96	HCE absorptivity	0.96
Mirror Reflectivity	0.94	HCE emittance	0.17

Table 6.6 presents values of energy received, energy delivered, energy loss and efficiency of the solar field based on the usage of parabolic trough collector technology.

Table 6.6. Energy analysis of the steam generation process in the PTC-solar field.

Subsystem	Energy received (MW)	Energy delivered (MW)	Energy loss (MW)	Energy loss (%)	First law efficiency (%)
Active-solar field	37.34	29.80	7.54	20.2	79.8
Receivers	29.80	22.18	7.62	25.6	74.4
Act. -solar field /Receiver	37.34	22.18	15.16	40.6	59.4

The results obtained from the thermodynamic analysis, the first and second law of the system are presented in Table 6.7 and 6.8, respectively. All the relations used to calculate exergy values consider technical specifications of equipment, thermodynamic properties of state point, heat and work interactions

during the heat transfer process and exergy for each stream of the solar field subsystem based on parabolic trough collector.

Table 6.7. Exergy analysis of the steam generation process in the PTC-solar field.

Subsystem	Exergy received (MW)	Exergy delivered (MW)	Exergy loss (MW)	Exergy loss (%)	Second law efficiency (%)
Active-solar field	35.49	20.87	14.62	41.2	58.8
Receivers (η_{opt})	20.87	15.79	5.08	24.3	75.7
Active-solar field →Receiver	35.49	15.79	19.70	55.5	44.5

Table 6.8. First and second law analysis of the steam generation process PTC-solar field.

Subsystem	Irreversibility (MW)	Energy loss (%)	Exergy loss (%)	First law (%)	Second law efficiency (%)
Active-solar field	14.62	20.2	41.2	79.8	58.8
Receivers	5.08	25.6	24.3	74.4	75.7
Active-solar field →Receiver	19.70	40.6	55.5	59.4	44.5

The overview cost estimation of the solar thermal power system without thermal energy storage and based on parabolic trough collector is presented in Table 6.9. The purchased equipment cost and data were obtained from different sources (Sargent and Lundy, 2003; Werner and Kalb, 1993) and models of cost evaluation (Couper, et al., 2012; Dincer and Ratlamwala, 2016).

Figure 6.1 shows the major cost in the breakdown of the hybrid power plant based on the combination of the parabolic trough collector and biomass-fired technology. The repartition of the key costs is presented as shown below.

Table 6.9. Major purchased equipment cost of a hybrid energy system based on PTC-BF technology (Sargent and Lundy, 2003; Werner and Kalb, 1993).

	Size	Unit cost	cost in k\$	Inst. cost	Net cost
Onsite Cost (Solar Field - Fossil backup - power block - improvement work)					
1- Solar field equipment /component costs breakdown					
Receiver and absorber		152	3479280.00	178139.14	3301140.86
Mirror		26	3305316.00	169232.18	3136083.82
Support structure		52	5044956.00	258301.75	4786654.25
Interconnection piping system			869820.00	44534.78	825285.22
Header piping			521892.00	26720.87	495171.13
Heat transfer fluid			521892.00	26720.87	495171.13
Pumps, electric auxiliaries, control and drive devices			2261532.00	115790.44	2145741.56
Pylon foundation and civil work (m ²)	43600		1391712.00	71255.65	1320456.35
			17396400.00	890695.68	16505704.3
2- Backup system					
Steam turbine/generator			3451580,00	176720.90	3274859.10
Boiler			990870,00	50732.54	940137.46
Pump, HE, Condenser, BOP, electric auxiliaries and Subsystems (cooling/dry)			1381792,00	70747.75	1311044.25
			5824242.00	298201.19	5526040,81
3- Power block and subsystem (cooling/drying)					
Steam turbine/generator			3444189.25	176342.49	3267846.76
Pump			109664	5614.80	104049.20
deaerator system + cooling tower			1148000	58777.60	1089222.40
Heat exchangers and connection system			293227	15013.22	278213.78
Electric auxiliaries and control devices			295117.3	15110.01	280007.29
BoP and drying/cooling subsystem			907269.75	46452.21	860817.54
			6197467.30	317310.33	5880156,97
Offsite cost (site improvement and contingency)					
Civil engineering and architecture work			881347.98		365138.00
Service facilities and site improvement (site preparation and steel construction)			1459122.52	-	1557922.17
4- Contingency			2353448.74		2353448.74
Total direct cost:			31171558.04		32605821,3
Land cost (USD/ m ²)	104640	2,35	245620		245620
Engineering procurement and construction works			2374629.783		2374629.78
Licensing Research and Development and Financing cost (LRDF cost)			2941810.93		
Total indirect cost:			5562060.71		
Fixed capital:			37333618.75		
Work capital			763357.6412		
Startup cost			381678.8206		
Additive subsystems and other.			-		
Outlays			1145036.462		
Total Capital invest.			38478655.21		

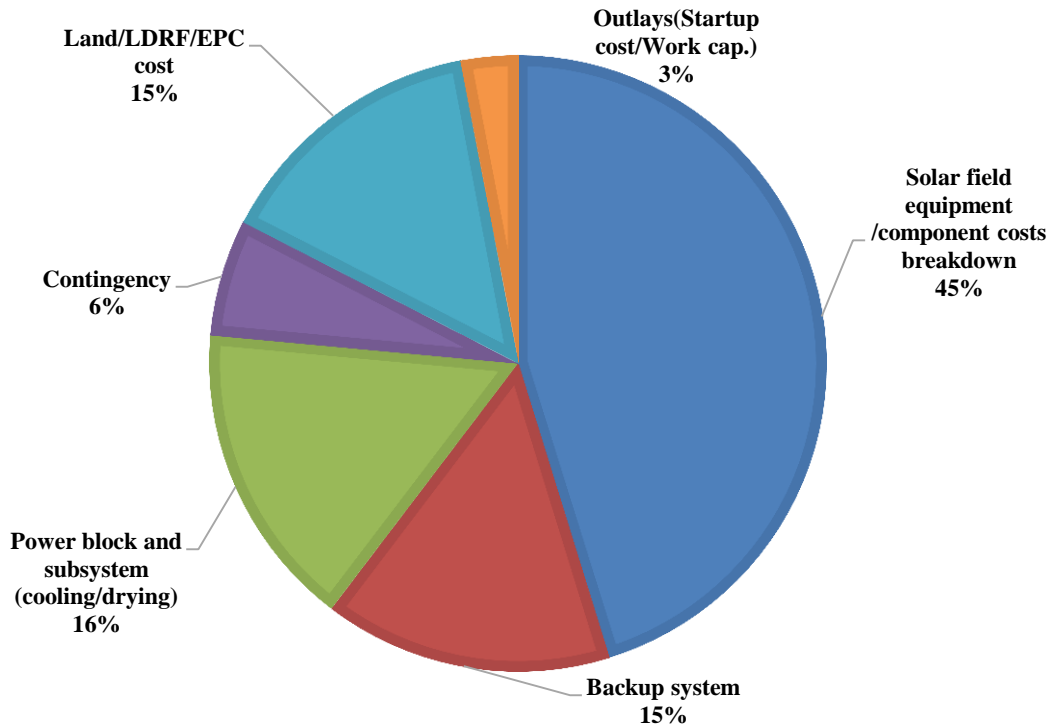


Figure 6.1. Major cost breakdown for the hybrid energy system based on PTC-BF.

- **Solar tower (ST) – solar field**

The active land of the solar field covered an area estimated at 50667.1 m^2 which contains 351 heliostats with a specific area of 144 m^2 . Table 6.5 presents the properties and technical characteristics of the solar field based on the solar tower.

The energy and exergy analysis of the solar tower technology used for the solar field sizing are presented in this section. The exergy, energy, and mass balance equations are used to find out the rate of exergy decrease, exergy destruction, the rate of irreversibility, the input energy, and exergy efficiencies are shown in Table 6.11 – 6.13.

Table 6.10. Properties and technical characteristics of the solar tower technology (SAM 2017.9.5).

Heliostat	Width	12.2 m	A= 144 m ²
	Height	12.3 m	351 Heliostats
Land	Active/Total	50667 m ²	106 acres
Solar field constraints	Hel/ Tower height		Dist from Tower
	max	8.5	max 320.11
	min	0.75	min 28.23
Tower height:	37.65 m	Nb. Panels/ Helio.	16
Receiver:			
Rec. Diameter:	4.93 m	Rec. Height:	5.39 m
Coating emittance:	0.88	Coating absorptance:	0.94
Boiler:	800 kWt/m ²	Boiler Height:	2.63 m
Material of tube	AISI316	Heat losses=	96 kW/m ²
Boiler tube ext. diam.:	0,0254 m	Thickness of tube:	0,002159 m
Superheater:	500 kWt/m ²	Superh. Height:	1.9618 m
Material of tube	AISI316	Heat losses=	80kW/m ²
Superh. tube ext. diam.:	0,01905 m	Thickness of tube:	0.001651 m
Reheater:	350 kWt/m ²	Reheater Height:	0.805 m
Material of tube	AISI316	Heat losses=	87.5 kW/m ²
Superh. tube ext. diam.:	0,0381 m	Thickness of tube:	0,002159 m
Thermal design op.		Receiver Th. Power:	19.406 MWt

Table 6.11. Energy analysis of the steam generation process of the ST-solar field.

Subsystem	Energy received (MW)	Energy delivered (MW)	Energy loss (MW)	Energy loss (%)	First law efficiency (%)
Active-solar field	43.28	27.82	15.46	35.7	64.3
Receivers	27.82	17.34	10.48	37.7	62.3
Active-solar field →Receiver	43.28	17.34	25.94	59.9	40.1

The results obtained from the thermodynamic (second law) analysis of the solar tower - solar field are presented in Table 6.12 and 6.13.

Table 6.12. Exergy analysis of the steam generation process of the ST-solar field.

Subsystem	Exergy received (MW)	Exergy delivered (MW)	Exergy loss (MW)	Exergy loss (%)	Second law efficiency (%)
Active-solar field	41.14	17.67	23.46	57.0	43.0
Receivers (η_{opt})	17.67	12.23	5.44	30.78	69.22
Active-solar field \rightarrow Receiver	41.14	12.23	28.91	70.27	29.73

Table 6.13. First and second law analysis of the steam generation process of the ST-solar field.

Subsystem	Irreversibility (MW)	Energy loss (%)	Exergy loss (%)	First law (%)	Second law efficiency (%)
Active-solar field	23.46	35.7	57.0	64.3	43.0
Receivers	5.44	37.7	30.78	62.3	69.22
Active-solar field \rightarrow Receiver	28.91	59.9	70.27	40.1	29.73

The overview cost estimation of the solar thermal power system without thermal energy storage and based on a central receiver is presented in Table 6.14. The purchased equipment cost and data were obtained from different sources (Sargent and Lundy, 2003; Werner and Kalb, 1993) and models of cost evaluation (Couper, et al., 2012; Dincer and Ratlamwala, 2016).

Figure 6.2 shows the major cost in the initial investment of the hybrid power plant based on the combination of the solar tower and biomass-fired as a backup system instead of the thermal energy storage (TES) system.

Table 6.14. Major purchased equipment cost of a hybrid energy system based on ST-BF technology (Sargent and Lundy, 2003; Werner and Kalb, 1993).

	Size	Unit cost	cost in k\$	Inst. cost	Net cost
Onsite Cost (solar field - Fossil backup - power block - improvement work)					
1- Solar field equipment /component costs breakdown					
Heliostat field	50667 m ²				
Site improvement	50667 m ²	32.61	1 652 584.25		
624 (39/16) Heliostat - Piping system- steel structure - Pylon foundation and civil work. Tower	351	50445.18	17 706 258.00		
Tower height (m)	37.65	1 400 000.00			
Receiver height (m)	5.39		1 657 989.00		
Heliostat height (m)	12.3				
Receiver system		0.694		0.00	0.00
Receiver area (m2)	74.3614	43964	7 476 222.00		
			28440496.25	1458844.33	29951897.58
2- Backup system					
Steam turbine/generator		625 \$/kWe	3451580.00		
Boiler		177 \$/kWe	990870.00		
Pump, HE, Condenser, BOP, electric auxiliaries and subsystems (cooling/dry)		193 \$/kWe	1081130.00		
			5523580.00	282807.30	5240772.70
3- Power block and subsystem (cooling/drying)					
Steam turbine/generator		624.5 \$/kWe	3444189.25		
Pump		20.01 \$/kWe	109664.00		
deaerator system + cooling tower		208.15\$/kWe	1148000.00		
Heat exchangers and connection system		53.16 \$/kWe	293227.00		
electric auxiliaries and control devices		54.02 \$/kWe	295117.30		
BoP and drying/cooling subsystem		164.51\$/kWe	907269.75		
			6197467.30	317310.33	6514777.63
Offsite cost (site improvement and contingency)					
Civil engineering and architecture work			762671.80		762671.80
Service facilities and site improvement			2058961.95	-	
4- Contingency			2821633.75		2821633.75
Total direct cost:			41383177.30		
Land cost (USD/ m ²)	81067.2	4.73	383608.72		383608.72
Engineering procurement and construction			4303573.43		4303573.43
Licensing R&D.t and Financing cost			3873216.087		3873216.09
Total indirect cost:			8560398.24		
Fixed capital:			49943575.54		
Work capital			1016443.81		1016443.81
Startup cost			515961.3254		515961.33
Outlays			1532405.13		
Total Capital investment			51475980.67		

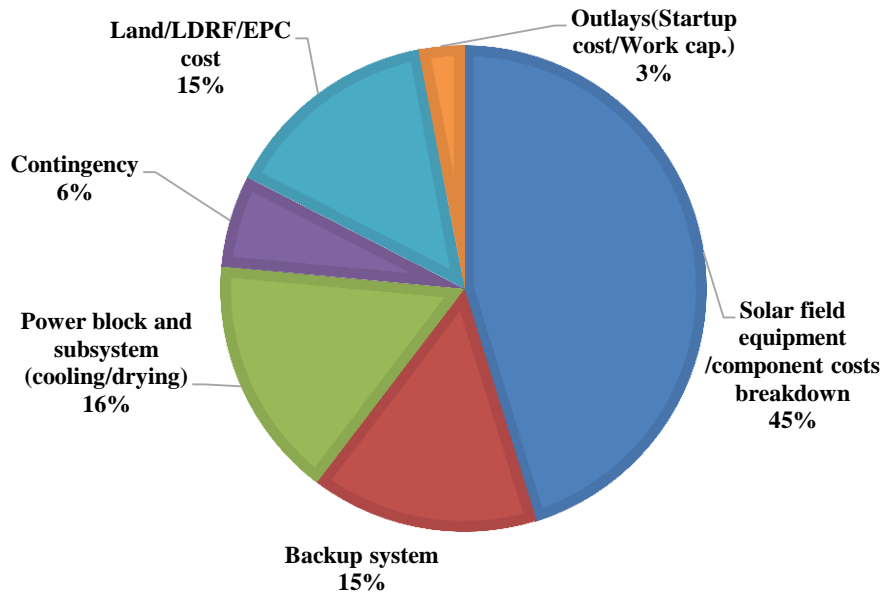


Figure 6.2. Major cost breakdown for the hybrid energy system based on ST-BF.

C. Linear Fresnel reflector (LFR) – solar field

The total land was estimated at 69679 m^2 where the active area covered 64.8% and consist of the arrangement of 64 lines (SCA) in 6 loops with an area of 7524 m^2 and length equal to 44.8m. The thermal energy is transferred to combined power cycles by an indirect steam generation process that uses Therminol VP – 1 as a heat transfer fluid operating between $230 - 400^\circ\text{C}$ with a mass flow rate of 42.5 kg/s. Table 6.15 presents the properties and technical characteristics of the solar field containing linear Fresnel reflector.

The energy and exergy analysis of the linear Fresnel reflectors used to determine the solar field efficiencies are specified in Chapter 5. For a general steady-state and steady-flow process, the balance equations, namely exergy, energy, and mass balance equations are used to determine the rate of exergy decrease, exergy destruction, and the rate of irreversibility, the input heat and efficiencies presented in Tables 6.16 - 6.18 below.

Table 6.15. Properties and technical characteristics of the linear Fresnel reflector-solar field (SAM 2017.9.5).

Linear Fresnel loop:			
Number of loops	6	Loop	7524.8 m ²
Number of lines per loop	16	Line	44.8 x10.498m ²
Efficiency:	0,6431	Thermal Eff. of loop	0,9617
Piping Thermal Efficiency	0,9989	Total loop conv. Eff.	0,6178
Cover emittance ε_c	0.88	Primary reflectance ρ_1	0.94
Cover transmittance τ	0.95	Secondary reflectance ρ_2	0.94
Absorber absorbance α	0.92		
Total area	39676 m ²	active area	45148.8 m ²
Steam receiver:	513.6 m ²	Receiver	44.8 m
Steam conditions:			
Mass flow rate (kg/s)		42.5	Therminol VP-1
SM =		1.0	

Table 6.16. Energy analysis of the steam generation process of the LFR-solar field.

Subsystem	Energy received (MW)	Energy delivered (MW)	Energy loss (MW)	Energy loss (%)	First law efficiency (%)
Active-solar field	38.66	26.27	12.39	32.0	68.0
Receivers	26.27	23.41	2.86	10.9	89.1
Active-solar field →Receiver	38.66	23.41	15.25	39.4	60.6

The efficiencies and exergies rate of the LFR - solar field are presented in Table 6.17 and 6.18.

Table 6.17. Exergy analysis of the LFR-solar field.

Subsystem	Exergy received (MW)	Exergy delivered (MW)	Exergy loss (MW)	Exergy loss (%)	Second law efficiency (%)
Active-solar field	36.75	14.68	22.07	60.0	40.0
Receivers	14.68	12.37	2.31	15.7	84.3
Active-solar field →Receiver	36.75	12.37	24.38	66.3	33.7

Table 6.18. First and second law analysis of the LFR-solar field.

Subsystem	Irreversibility (MW)	Energy loss (%)	Exergy loss (%)	First law (%)	Second law efficiency (%)
Active-solar field	22.07	32.0	60.0	68.0	40.0
Receivers	2.31	10.9	15.7	89.1	84.3
Active-solar field →Receiver	24.38	39.4	66.3	60.6	33.7

The overview cost estimation of the solar thermal power system without thermal energy storage and based on linear Fresnel reflector is presented in Table 6.18. The purchased equipment cost and data were obtained from different sources (Sargent and Lundy, 2003; Werner and Kalb, 1993) and models of cost evaluation (Couper, et al., 2012; Dincer and Ratlamwala, 2016).

Figure 6.3 shows the major cost in the investment of the hybrid power plant based on the combination of the linear Fresnel reflector and biomass-fired technology. The major categories of cost are presented below.

Table 6.19. Major purchased equipment cost of a hybrid energy system based on LFR-BF technology (Sargent and Lundy, 2003; Werner and Kalb, 1993).

	Size	Unit cost	cost in k\$	Inst. cost	Net cost
Onsite Cost (solar field - Fossil backup - power block - improvement work)					
1- Solar field equipment /component costs breakdown					
Linear Fresnel collector field (m ²)	45148				
Site improvement	45148	15.98	633 897.41		
96 (6 loops) Linear Fresnel collector - Piping system- steel structure - Pylon foundation	6	1029617.05	6 177 702.30		
Receiver and HTF system		0.694		0.00	0.00
Receiver area (m ²)	513.6	43964	1 123 218.60		
			7 934 818.3	168218.15	8103036.46
2- Backup system					
Steam turbine/generator		625 \$/kWe	3451580.00		
Boiler		177 \$/kWe	990870.00		
Pump, HE, Condenser, BOP, electric auxiliaries and subsystem (cooling/dry)		193 \$/kWe	1081130.00		
			5523580.00	282807.30	5240772.70
3- Power block and subsystem (cooling/drying)					
Steam turbine/generator		624.5\$/kWe	3444189.25		
Pump		20.01\$/kWe	109664.00		
deaerator system + cooling tower		208.15\$/kWe	1148000.00		
Heat exchangers and connection system		53.16 \$/kWe	293227.00		
electric auxiliaries and control devices		54.02 \$/kWe	295117.30		
BoP and drying/cooling subsystem		164.51\$/kWe	907269.75		
			6197467.30	131386.31	6328853.61
			19655865.30	-	18720310.01
Offsite cost (site improvement and contingency)					
Civil engineering and architecture work			353603.75		353603.75
Service facilities and site improvement (site preparation and steel construction)			582411.75	-	
4- Contingency			936015.50		936015.50
Total direct cost:			20591881.10		
Land cost	39677	9.91	393126.511		393126.511
Engineering procurement and construction			1965632.55		1965632.555
Licensing R&D. and Financing cost			1572506.04		1572506.04
Total indirect cost:			3931265.11		
Fixed capital:			24523146.21		
Work capital			471751.81		471751.81
Startup cost			235 875.91		235875.91
Outlays			707 627.72		
Total Capital investment			25230773.93		

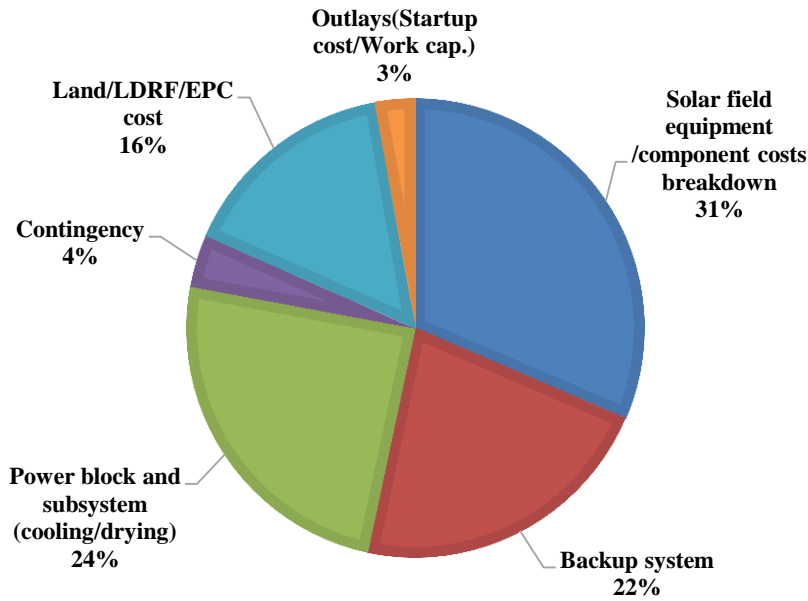


Figure 6.3. Major cost breakdown for the hybrid energy system based on LFR-BF.

As a summary of techno-economic and exergy analysis of the studied solar field. According to results presented in Figures 6.1-6.3 and Tables 6.9, 6.14, 6.19, the solar field using linear Fresnel reflector has the highest investment cost estimated at 31% of the total investment of hybrid (solar – biomass) energy system. Tables 6.6 – 6.13, 6.11 – 6.13 and 6.16 – 6.18 present the results for the solar field, they show that linear Fresnel reflector technology has the most efficient system followed by parabolic trough collector and solar tower technology. While the solar tower is the technology with the highest value of thermal energy compared to other CSP technologies. The output energy generated by the parabolic trough collector is more as compared to other CSP technologies.

- **Power block and multi-energy generation systems**

The useful exergy $(\dot{E}_1 - \dot{E}_2)_{ihe/boiler}$ represents the input power of the combined Rankine cycle. Table 6.20 presents the results of the analysis of the power block system using the first and second law of thermodynamics for $\eta_{IHE}=85\%$.

Table 6.20. Thermodynamic analysis of the power block system according to the prime movers.

Subsystem	Energy in. trans. (MW)	Exergy in. trans. (MW)	Work in (MW)	Exergy out. (MW)	First law eff. (%)	Second law eff. (%)
Biomass- combustion	16.77	11.63	5.07	5.42	30.26	46.61
PTC-Solar	18.85	15.79	5.00	5.09	26.41	32.24
ST-Solar	17.34	12.24	5.24	5.60	30.25	45.78
LFR-Solar	19.98	12.37	4.6	5.04	23.07	40.71

The pressure, the steam quality and quantity of exhaust water are important and critical parameters for HRSG designing to achieve optimal performance. The HRSG system affects the quality and volume of the steam generated during the process that needs to be transferred in the intermediate heat exchanger of the concentrating solar power technology or the boiler of the biomass-fired power technology. Furthermore, it has a direct impact on the net power output and consequently affects exergy data and total cost of the power block system. The additive systems connected to the HRSG system such as the absorption refrigeration system and the drying system were also studied to determine the thermodynamic properties at different points and lead to an advanced exergy analysis.

▪ Thermodynamic analysis of HRSG subsystems

The exhaust steam ($T=543$ K) is directly used to supply the HRSG system. The output thermal energy of the HRSG is transferred into high-temperature heat exchanger or boiler according to the used prime movers. According to the material limit conditions for the high-temperature, some recent research presents the ceramic heat exchangers as the most suitable technology to withstand high temperature close to the working fluid temperature. This helps to avoid the usage of the intermediate heat exchanger or boiler (Baum, 2001). The results from the HRSG system analysis using the first and second law of thermodynamics are presented in the table below. Table 6.21 presents the results of the thermodynamic analysis of the HRSG system of various prime movers based on the first and second law.

Table 6.21. Thermodynamic analysis of the HRSG system according to the prime movers.

System	Input (MW)		Output (MW)		Transfer (MW)		Destruction (MW)		Deaerator int. (MW)	
	En.	Ex.	En.	Ex.	En.	Ex.	En.	Ex.	En.	Ex.
Bio.	26.31	8.35	13.12	4.97	7.95	2.47	18.50	0.22	3.39	0.69
PTC	44.09	14.79	14.79	4.59	3.04	1.89	22.43	5.89	3.68	2.42
ST	27.20	8.63	8.63	5.14	6.99	2.56	4.66	0.22	1.99	0.72
LFR	43.11	14.42	14.42	4.48	5.84	3.77	18.78	5.82	3.88	0.52

Tables 6.22-6.25 present the results obtained from a thermodynamic analysis of the absorption refrigeration system using parabolic trough collector, solar tower, linear Fresnel reflector, and biomass-fired, technology, respectively. The energy flow in the studied absorption refrigeration system varies from 1834.12 to 210.6 kW.

Table 6.22. Absorption refrigeration system connected to the HRSG of the power system based on PTC technology.

ARS component	Energy flow (kW)	Exergy inp. (kW)	Exergy out. (kW)	Exergy loss (kW)
Heat exchanger	210.6	42.06		2.10
Generator	141.55	37.67	39.96	2.29
Condenser	79.82	2.16	1.04	1.12
Ext. heat exchanger	1.11	0.88	0.76	0.12
Evaporator	74.87	5.23	1.87	3.36
Absorber	135.93	9.91	2.26	7.65 (16.52)
Overall	559.89	210.41		

Table 6.23 presents energy, exergy input and output in the absorption refrigeration system using LiBr/Water as working a fluid couple and based on energy wasted from HRSG connected to the solar tower power system. Its analysis leads to a determination of an energy flow about 267.54 kW and total exergy destruction estimated at 27.95 kW.

Table 6.23. Absorption refrigeration system connected to the HRSG of the power system based on ST technology.

ARS component	Energy flow (kW)	Exergy inp. (kW)	Exergy out. (kW)	Exergy loss (kW)
Heat exchanger	267.54	53.37		2.67
Generator	141.55	37.67	50.70	13.03
Condenser	79.82	2.16	1.04	1.12
Ext. heat exchanger	1.11	0.88	0.76	0.12
Evaporator	74.87	5.23	1.87	3.36
Absorber	135.93	9.91	2.26	7.65 (27.95)
Overall	571.01	214.80		

Table 6.24 presents energy, exergy input and output in the absorption refrigeration system using LiBr/Water as a working fluid couple and based on energy wasted from HRSG connected to linear Fresnel reflector power system. Its analysis leads to determine the highest energy flow transferred about 1834.12 kW and total exergy destruction estimated at 139.46 kW.

Table 6.24. Absorption refrigeration system connected to the HRSG of the power system based on LFR technology.

ARS component	Energy flow (kW)	Exergy inp. (kW)	Exergy out. (kW)	Exergy loss (kW)
Heat exchanger	1834.12	539.11		26.60
Generator	966.38	257.26	512.51	255.25
Condenser	544.83	14.77	13.66	1.11
Ext. heat exchanger	7.58	6.01	6.00	0.01
Evaporator	511.38	35.21	15.70	19.51
Absorber	940.54	171.88	32.42	139.46 (441.94)
Overall	6493.82	2075.36		

Table 6.25 presents energy, exergy input and output in the absorption refrigeration system using LiBr/Water as a working fluid couple and based on energy wasted from HRSG connected to the biomass-fired power system. Its analysis leads to a determination total exergy destruction estimated at 229.71 kW.

Table 6.25. Absorption refrigeration system connected to the HRSG of the power system based on BF technology.

ARS components	Energy flow (kW)	Exergy inp. (kW)	Exergy out. (kW)	Exergy loss (kW)
Heat exchanger	1621.91	326.89		16.34
Generator	966.38	257.26	310.54	53.28
Condenser	544.83	14.77	13.66	1.11
Ext. heat exchanger	7.58	6.01	6.00	0.01
Evaporator	511.38	35.21	15.70	19.51
Absorber	940.54	171.88	32.42	139.46 (229.71)
Overall trans.	5084.36	2007.53		

This analysis presents both the technical and economic data, as well as the possibility of recovering the exergy destruction or decreasing of investment for the electricity, cooling and heating generation.

6.2 Conventional Exergoeconomic and Techno-economic

Since the exergoeconomic analysis provides hybrid energy systems components results, only selected data from our study are reported in Table 5.1. The products cost of each stream of main components have been calculated using expressions in Chapters 4 – 5 and presented in Tables 4.1 and 4.2. During the exergy and exergoeconomic analysis of subsystems such as solar field, biomass-fired, power block, heat recovery steam generation and additional (heating and cooling) system or units, evaluation of each study case has been done. The solar field (heliostat-receiver, parabolic/linear collector–receiver–intermediate heat exchanger) and biomass-fired scale (sorghum feedstock – combustion chamber – Boiler) own the largest cost reduction potential and can be optimized to reduce the overall effectiveness-cost of the hybrid system.

The power block system is a combination of Rankine cycles which presents similar characteristic independently of the initial investment of the studied cases. The aim of the study was a configuration of hybrid energy system able to generate output energy estimated at 5 MWe for each studied case to determine parameters of other subsystems which are connected. It is important to highlight the

particularity of the power block designed according to the concentrating solar power technology used to generate electricity. The case study based on linear Fresnel reflector and parabolic trough collector technology used a part of the thermal energy produced to supply the heat exchanger of ORC through a heat transfer fluid (Therminol VP-1) instead of recover the exhausted non – saturated steam from the steam turbines like other case studies such as the solar tower or biomass-fired technology. The HRSG system is influenced by the power block output pressures, temperatures and required input temperatures and pressures of the working fluids. Due to this and as mentioned above, two design of the HRSG system model is developed. The HRSG design specified as (Regen-1 – Regen-2-Regen-3–IHE) and (Regen-1–Regen-2–Regen-3 – Regen-4 – Regen-5 – boiler) model are appropriated to the use of the linear Fresnel reflector/parabolic trough collector technology and the solar tower/ biomass – fired technology, respectively.

The absorption refrigeration, drying and hot water subsystem connected to the outlet stream of regenerator Regen-3, Regen-2, and Regen-4 of the HRSG of the hybrid energy system based on the solar tower and the biomass-fired technology are used for food conservation and sanitary application, respectively. Their exergoeconomic analysis is related to a good knowledge of purchased equipment cost using the results of the techno-economic analysis of the hybrid energy system. The levelized cost of electricity generated, the low cost of energy, the annual energy produced, the overall plant cost, operation, and maintenance cost, operating expenditure, cost per exergy unit and other economic parameters related to the financial evaluation of the power system were analyzed. Table 6.27 – 6.29 present the financial analysis results of the studied hybrid energy system. The results of the conventional exergetic and exergoeconomic analysis of specific component which led to the determination of the average cost per exergy unit and levelized cost rate of product for each subsystem are presented in Appendix C. The usage of equations as expressed in Section 5.2 leads to the determination of the cost of each stream and working fluid. Table 6.26 presents the levelized cost rate, the exergy rate, the cost per unit exergy and the exergy costing of absorption system, organic Rankine cycle, and the standalone power system to prepare the advanced exergoeconomic analysis.

The standalone power system is based on the usage of the cited concentrating solar power and biomass-fired (sorghum straw and stalk) technology containing various subsystems such as solar field, power block, HRSG, and additional units. During the conventional exergoeconomic analysis, many data such as the exergy rate, cost rate associated with fuel (biomass and solar energy), the cost rate associated with the product and the exergy costing, have been determined and presented in Annex. That help to determine also the impact of each component in the power system. The relative cost difference and exergoeconomic factor of the solar power systems using parabolic trough collector, solar tower and linear Fresnel reflector are 0.063 and 85.2%; 0.112 and 72% and 0.086 and 90% respectively. While these values are between 0.28 and 69% in other standalone biomass power system. In another hand, the conventional exergoeconomic analysis of standalone power systems leads to the determination of the exergy rate of the product, levelized cost rate and the cost per exergy unit of the main equipment used in the subsystems that make up isolated systems. Besides, the exergy costing of the stream components has also been calculated as shown in Appendix C. This study allows the evaluation of the approximate cost per unit of the subsystems that constitute the standalone power plant.

The cost per unit exergy of the solar field system varies between 2.31 and 5.32 USD/GJ. While the value of the cost per exergy unit of the biomass-fired (combustion chamber - boiler) is equal to 3.84 USD/GJ. These results made possible the analysis of the ratio between the initial investment and the exergy rate generated by the solar field. Table 6.24 presents solar tower as the technology which owns the largest cost per exergy unit and levelized cost rate of product for a thermal energy capacity of 17.67 MWth. The biomass-fired technology using sorghum straw as feedstock has a cost per exergy unit about 3.84 USD/GJ for a thermal energy capacity of 17.29 MWth, which can be explained by low initial investment and a cost related to the daily operating expenditure which is significant compared to concentrating solar power technologies. Hence, considering these preliminary results it can be said that, the linear Fresnel reflector technology presents a better initial investment based on the cost per exergy unit. The levelized cost rate of solar field system has a positive impact due to the initial investment and their value are found to be between 3.62 USD

cents/sec and 9.40 USD cents/sec for the solar technologies. The levelized cost rate of biomass-fired technology is equal to 9.40USD cents/sec.

Table 6.26. The average cost per exergy unit and levelized cost rate of product for subsystems containing standalone power systems.

Technology	Parabolic trough collectors	Solar tower	Linear Fresnel reflectors	Biomass-fired combustion
Biomass-fired / solar field subsystem				
Cost per exergy unit (USD/GJ)	4.93	5.32	2.31	3.84
Levelized cost rate of product (USD cents/Sec)	7.78	9.40	3.62	9.40
Power block subsystem				
Cost per exergy unit (USD/GJ)	7.69	10.90	5.06	5.61
Levelized cost rate of product (USD cents/Sec)	7.20	8.36	6.72	5.01
HRSG subsystem				
Cost per exergy unit (USD/GJ)	5.02	8.41	2.41	3.96
Levelized cost rate of product (USD cents/Sec)	0.0003	0.0001	0.0003	0.0007

The results show that the cost per exergy unit of power block system connected to the CSP technologies varies between 5.06 and 10.90 USD/GJ and the levelized cost rate between 6.72 and 8.36 USD cents/sec. The biomass-fired technology has a cost per exergy unit and a levelized cost rate of product estimated at 5.61 USD/GJ and 5.01 USD cents/sec respectively. The LFR technology has the lowest value of the cost per exergy unit and the levelized cost rate of product for the power block system. The heat recovery steam generation connected with CSP technology has a cost per exergy unit between 2.41 and 8.41 USD/GJ and the solar tower technology owns the lowest levelized cost rate of product estimated at 36 USD cents/h. The cost per exergy unit and levelized cost rate of the product of the heat recovery steam generation connected with biomass-fired technology are equal to 3.96 USD/GJ and 1.18 USD/hour, respectively.

The cost per exergy unit of the equipment that constitutes the absorption refrigeration system is shown in Figure 6.4. The refrigeration system connected to the power system based LFR technology presents the best results compared to

other solar technologies. Although biomass-fired technology has a competitive cost per exergy unit compared to concentrating solar power technologies considered in the study.

Figure 6.4 shows that the exergoeconomic performances of absorption refrigeration unit connected to the heat recovery steam generation of the hybrid energy system based on parabolic trough collector and biomass-fired are low compared to others. However, it is important to note that, absorption refrigeration unit of a hybrid energy system based on LFR-BF have better cost-effectiveness.

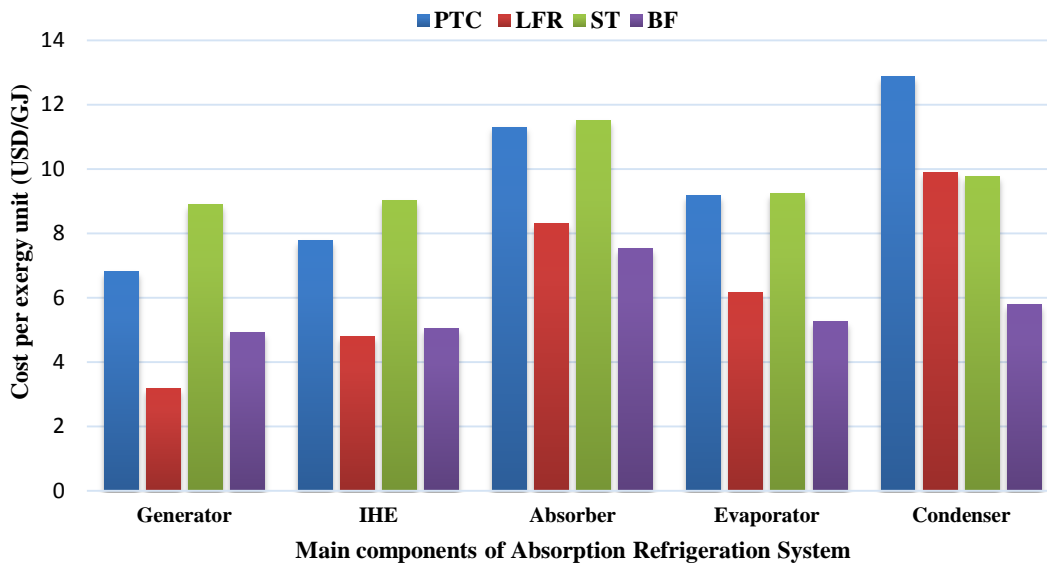


Figure 6.4. Cost per exergy unit of the absorption refrigeration unit.

Figure 6.5 shows that the cost per exergy unit of the ORC integrated into the power block system using LFR technology is significantly better than other technologies. Also, biomass-fired technology has the highest cost per exergy unit compared to other concentrating solar power technologies.

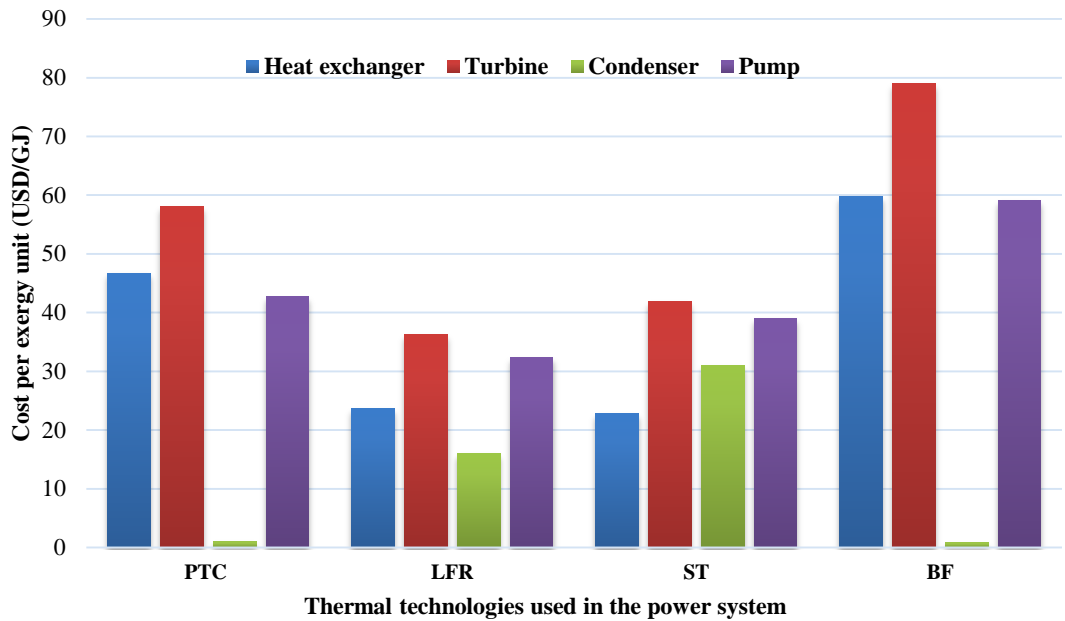


Figure 6.5. Cost per exergy unit of main components of the organic Rankine cycle.

6.3 Advanced Exergy Analysis

The in-depth study of the exergy analysis of the hybrid energy system based on concentrating solar power and biomass-fired technology has led to the evaluation of different forms of exergy destruction. Given the fact that the current study focused on the optimization of the hybrid energy system performances, special attention is given to the exergy destruction of the system. The advanced exergy analysis destruction allowed the classification of the different forms that can be resulted and their proportions according to the equipment or subsystem studied. Thus, the possibility of recovering part of this exergy destruction could be considered to increase the exergy efficiency of the studied systems. For this purpose, the exergy destruction is distributed in the following forms: unavoidable, avoidable, endogenous and exogenous. Later, it is realized that all forms of the exergy destruction which can be recovered, may come from the combination of the avoidable and the endogenous exergy destruction. This being the case, a thorough analysis of the exergy destruction forms evoked above, was conducted into the following forms: unavoidable - endogenous, unavoidable - exogenous, avoidable-endogenous and avoidable - exogenous exergy destruction.

The research consisted of optimization of the hybrid energy system using the easiest method that would help to recover the "avoidable-endogenous" exergy destruction. The exergy destruction is determined for the equipment that goes into the assembling of the subsystems connected to the hybrid energy system. The exergoeconomic tables presented in this chapter lead to the determination of the different forms of exergy destruction and show the proportions reserved for each of them according to parameters used during the analysis. The distribution of exergy destruction of the standalone power system indicates that the avoidable - endogenous exergy destruction varies between 143.25 and 570.45kW in the heat recovery steam generation which is more important than other forms of exergy destruction. Although avoidable - endogenous exergy destruction is poorly present in the studied system where it represents less than 13% of the exergy destruction. The absorption refrigeration subsystem indicates an avoidable-endogenous exergy destruction variation is between 4.6 and 33.22 kW, which represents less than 1.2% of the total exergy destruction of this system. While it varies between 5.97 kWth and 29.31 kWth in the drying unit, which is equal to 1% of total exergy destruction.

A. Hybrid energy system based on PTC

A hybrid energy system based on PTC-BF technology contains a combined Rankine cycle. The solar rays are concentrated into a Schott PTR80's receiver by using LUZ S-3 collectors arranged in 20 loops each containing 4 solar collector assemblies with 48 modules. The thermodynamic analysis conducted to evaluate the exergy production of the solar field throughout a year to determine any aspect which can create some undesirable circumstance during the exploitation of the power system. In Figure 6.6, March and August have registered the lowest and highest exergy produced production, respectively. Also, it is important to note that, during this study, an average value of the direct normal irradiation has been used instead of its monthly value which may provide a consistent difference between the compared months. Otherwise, the effects of the thermodynamic operating conditions can affect the performances of the combined Rankine cycles used for the electricity generation. Furthermore, the exergy produced capacity of

the solar power system is estimated at 15.81 MW leading to an annual exergy production of 39.64 GWh.

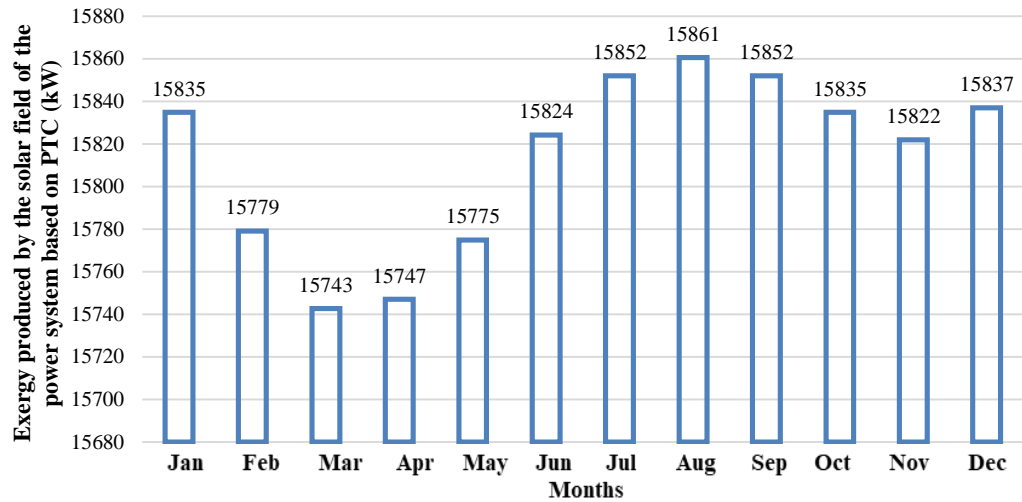


Figure 6.6. The monthly exergy production capacity of the solar field based on PTC technology.

Figure 6.7 shows that the lowest exergy produced capacity by the solar field is noticed during July for daily irradiation of 4.3 hours and the exergy generated by the solar field estimated at 4.61 GWh. The period starting from July up to September presents the highest value of exergy produced capacity. But due to short sunshine duration, the exergy generated by the solar field is the lowest throughout a year 2.11 – 2.42 GWh.

The intermediate heat exchanger is the main component of the solar field. It connects the solar field to the power block and ensures the heat transfer process between them. The exergy generated by the solar field is transferred in the combined Rankine cycles. The efficiency of the intermediate heat exchanger is one of the main parameters which needs to be analyzed for its usage in the thermal power system. To do that, the advanced exergy analysis has been done to carry out a specific exergy destruction forms which need to be considered for the decreasing of the exergy losses. Figure 6.7 presents the distribution of exergy destruction forms in the intermediate heat exchanger of the power system based on the parabolic trough collector.

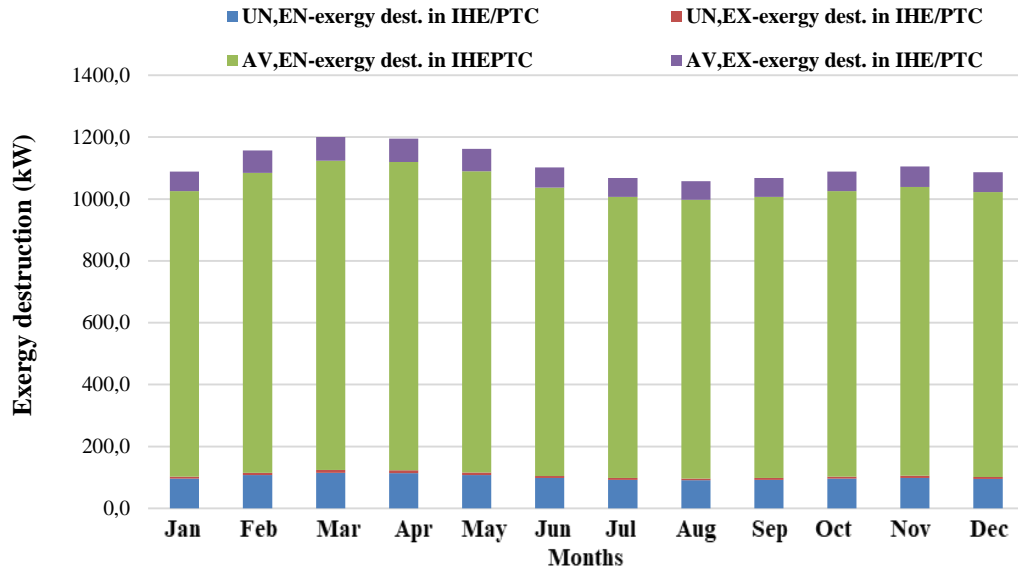


Figure 6.7. Distribution of the exergy destruction forms present in the intermediate heat exchanger of the PTC solar field.

According to the reviewed literature and the feasibility study approach adopted for this research, avoidable-endogenous exergy destruction was evaluated. This part of exergy destruction can be recovered and used to optimize the energy rate transferred independently of the type of component used. The advanced exergy analysis of the intermediate heat exchanger presents an estimated value of 3.95 GWh as the avoidable-endogenous exergy destruction per year, which is approximately 10% of the annual exergy produced by the power system. A similar analysis of unavoidable exergy destruction reveals that the unavoidable-exogenous exergy destruction has the smallest part of exergy destruction. The combination of unavoidable-endogenous exergy destruction and the-avoidable endogenous exergy destruction present more than 85% of the total exergy destroyed in the studied system.

Figure 6.8 presents the monthly exergy production and destruction in the heat recovery steam generation of the power system based on the parabolic trough collector. The exergy destruction inside of the heat recovery steam generation (HRSG) represents 29.7% of the total exergy production. The highest and lowest value of exergy destruction is found in March and September, respectively.

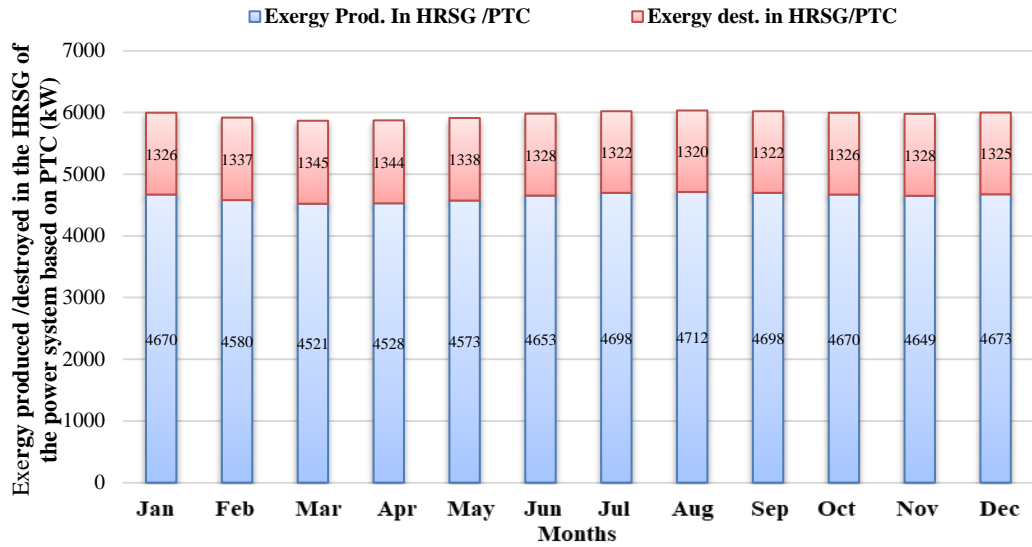


Figure 6.8. Exergy produced and destroyed in the HRSG of the power system based on PTC.

Figure 6.9 presents the monthly distribution of exergy destruction forms in the heat recovery steam generation of the power system based on the parabolic trough collector. The unavoidable/endogenous exergy destruction has the most important of exergy destruction and own more than 70% of the total exergy destruction inside of the heat recovery steam generation.

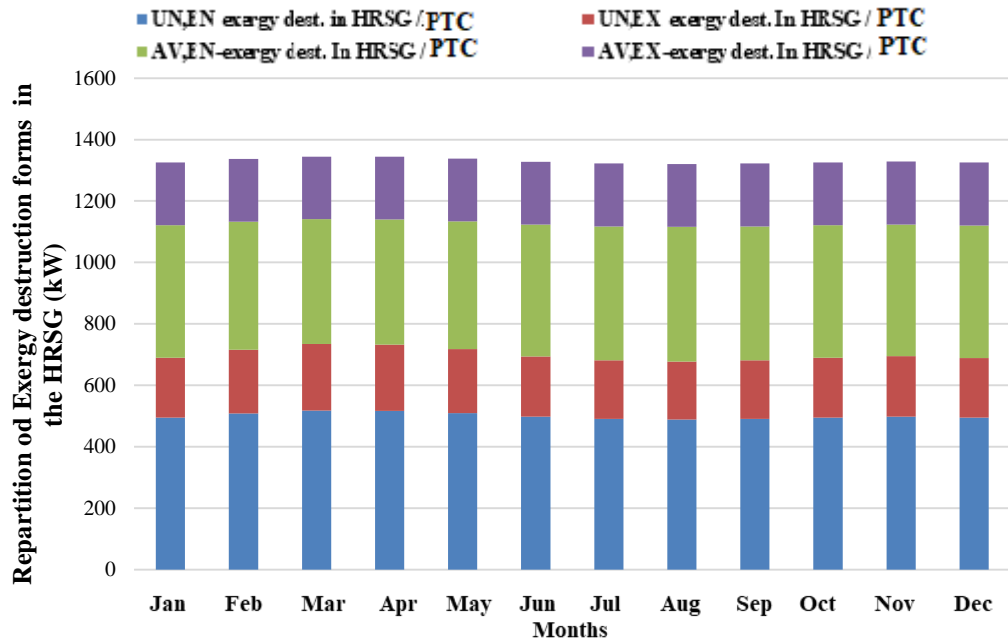


Figure 6.9. Distribution of exergy destruction forms in the HRSG of the solar power system based on PTC.

The advanced exergy analysis of the HRSG is conducted to carry out a repartition of the exergy destruction forms. The results show that the average avoidable-endogenous exergy destruction throughout a year presents less than 32.5% of the total exergy destruction. According to the monthly exergy destruction analysis, it can be observed that the unavoidable-endogenous exergy destruction is always higher than other exergy destruction forms. While the exogenous exergy destruction forms are almost equal throughout the year.

The annual thermal exergy destruction in HRSG is estimated at 3.32 GWh. As shown in Figure 6.10, the exergy destruction analysis inside of the regenerator 1 of the HRSG system of the solar power system using parabolic trough collector, the avoidable-endogenous exergy destruction is more important than the unavoidable-endogenous exergy destruction, specifically during the period between May and December. Furthermore, the endogenous exergy destruction represents more than 68% of the total exergy destruction in the regenerator. The annual avoidable-endogenous exergy destruction which can be recovered in the generator is estimated at 1.04 GWh. However, the exogenous exergy destruction of the regenerator 1 is less than the unavoidable-endogenous exergy destruction.

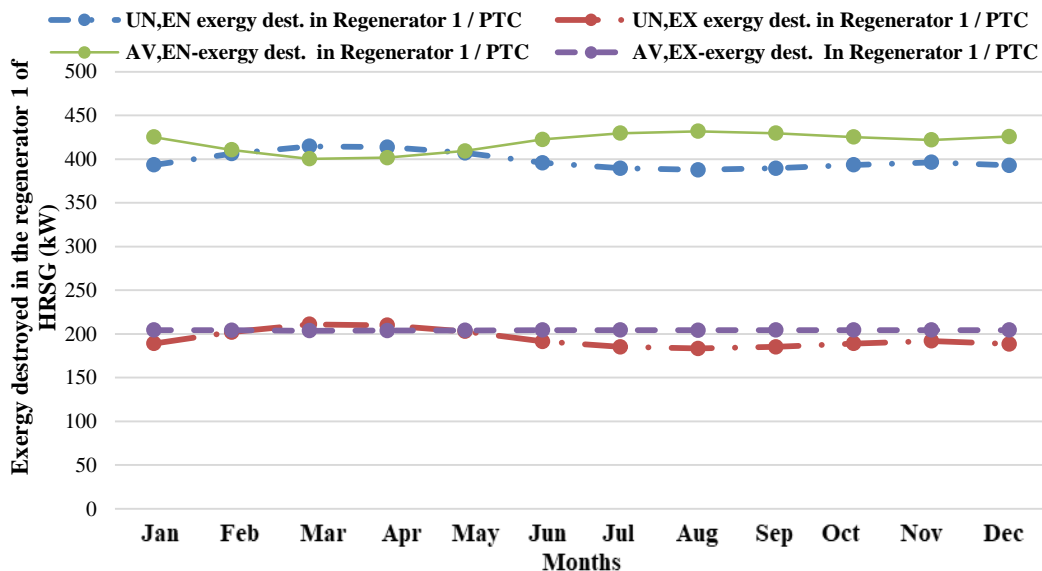


Figure 6.10. Repartition of exergy destruction forms in the regenerator 1 of the HRSG system connected to the solar power system based on PTC technology.

In Figure 6.11 it is observed that the exergy destruction of the regenerator 2 decreases considerably due to the state change occurred in the regenerator 1. During the analysis, it is observed that the unavailable-endogenous exergy destruction doesn't follow the decreasing of other exergy destruction forms. Moreover, the exogenous exergy destruction presents less than 7% of the total exergy destruction, the available-endogenous exergy destruction is almost equal to the sum of exogenous exergy destruction forms occurred inside estimated at 6.3 MWh.

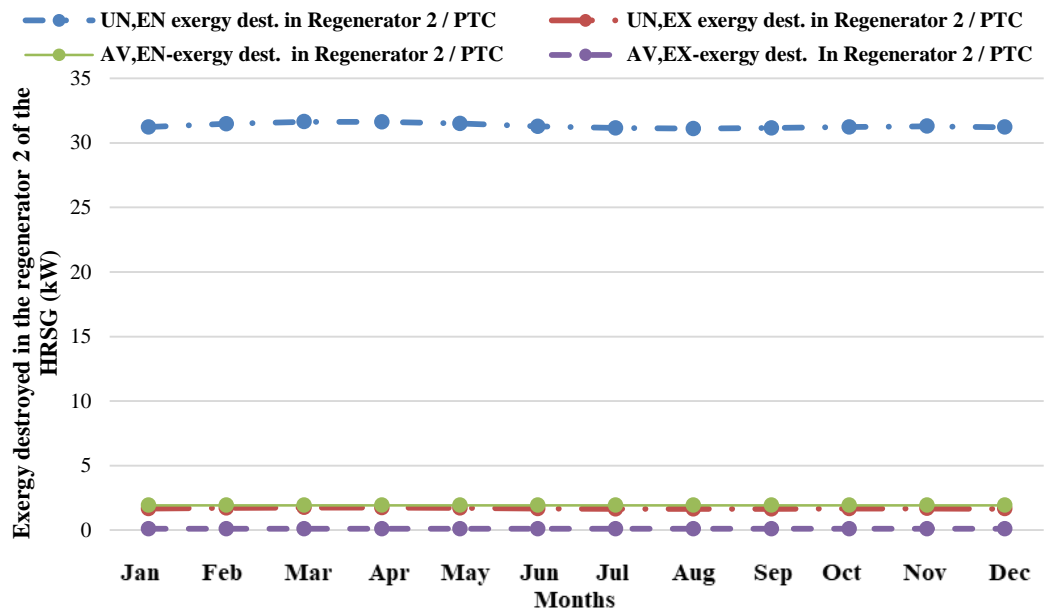


Figure 6.11. Repartition of exergy destruction forms in the regenerator 2 of the HRSG system connected to the solar power system based on PTC.

Figure 6.12 shows the exergy destruction forms occurred in the regenerator 3 throughout a year. During the analysis, it has been observed that the unavailable-endogenous exergy destruction doesn't follow the decreasing of other exergy destruction forms like in the regenerator 2.

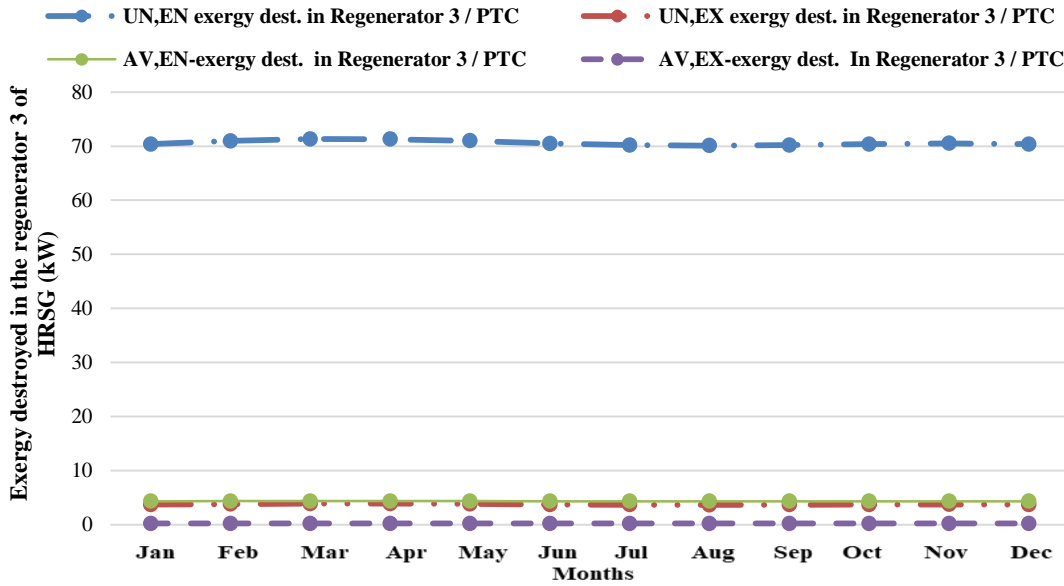


Figure 6.12. Repartition of exergy destruction in the regenerator 3 of the HRSG system of the power system based on PTC technology.

Moreover, the exogenous exergy destruction presents less than 7% of the total exergy destruction, the available-endogenous exergy destruction is almost equal to the sum of exogenous exergy destruction forms occurred inside estimated at 6.3 MWh.

B. Hybrid energy system based on ST

The solar power system based on central receiver technology presented in Figure 3.6 uses a CRC as a power block cycle. This system contains a tower and a focal point, it can produce approximately 5MWe. The active land covered by solar field was estimated at 50667.1 m² which contains 351 heliostats (16 panels/Heliostat) with a specific area of 144 m². The solar field is one of the most difficult parts of the design work due to optimization work like SCA arrangement, and land reduction through some parameters such as the distance from the tower, the height ratio of tower and heliostat that need to be determined carefully. The hybrid energy system considered has a tower with a height of 37.65 m and receiver with the following characteristic: height and diameter of 4.93 m and 5.39 m, the coating emittance and absorptance are 0.88 and 0.94, respectively. The thermodynamic analysis is done to evaluate the exergy production of the solar field throughout a year. This analysis contributes to determining any aspect which

can create some undesirable circumstance during the exploitation of the systems. The operating conditions affect the performances of a combined Rankine cycle. These results lead to the determination of the exergy produced capacity, exergy and energy efficiency of the solar power system using a central receiver. The annum exergy produced by the studied system was found to be 23.22 GWh, less than the power system using parabolic trough collector technology. Figure 6.13 presents the lowest and the highest monthly exergy generated by the solar field which corresponds to March and August, respectively. However, for the period starting from February to May, the lowest performances in term of exergy generation are registered.

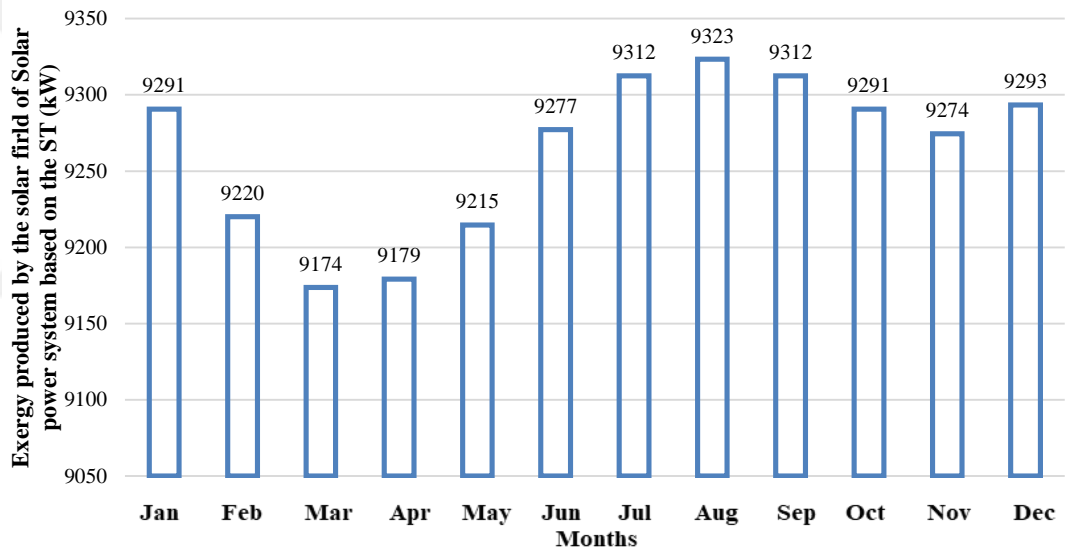


Figure 6.13. The monthly exergy production capacity of the solar field based on ST.

The analysis conducted inside of the boiler leads to the determination of various forms of the exergy destruction. In this study, the value of the avoidable-endogenous exergy destruction represents less than 40% of the total exergy destruction in the intermediate heat exchanger. Figure 6.14 presents the distribution of exergy destruction forms throughout a year in the receiver.

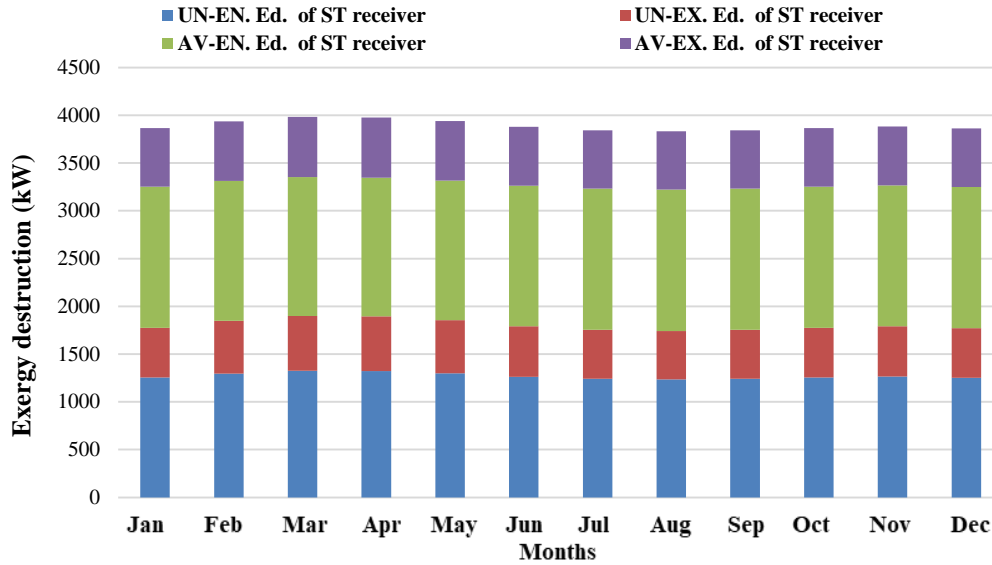


Figure 6.14. The distribution of exergy destruction forms in the intermediate heat exchanger of the ST-solar field.

The value of the unavoidable-exogenous exergy destruction increases considerably due to the high temperature operating compared to other concentrating solar power technology used in this study. Furthermore, the period from February to May has important exergy destruction compared to others. The global exergy destruction throughout a year can be estimated at 13.87 GWh. The annual avoidable-endogenous exergy destruction found in the receiver is higher than the annual exergy destruction of the heat exchanger used for the linear Fresnel reflector and parabolic trough collector.

Figure 6.15 presents the monthly exergy production and destruction in the heat recovery steam generation of the power system based on solar tower technology.

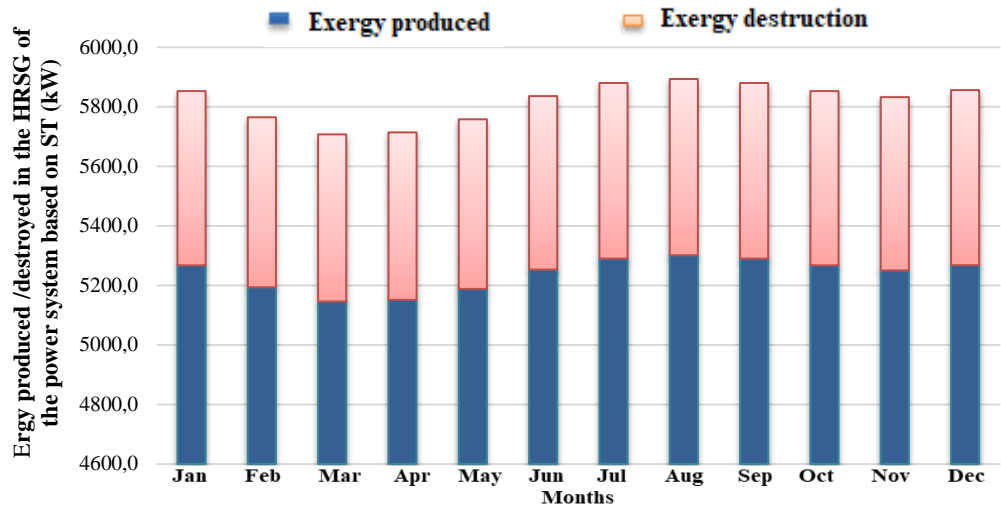


Figure 6.15. Exergy produced and destroyed in the HRSG of the power system based on ST.

The exergy destroyed inside of the heat recovery steam generation represents 11% of the total exergy produced by the solar power system using the solar tower technology. The advanced exergy destruction analysis conducted to a repartition of the different exergy destruction forms present in the HRSG.

Figure 6.16 presents the distribution of exergy destruction forms throughout a year in the HRSG. During the advanced exergy analysis of the HRSG, the average avoidable-endogenous exergy destroyed through a year represents approximately 25.6% of the total exergy destruction. According to the results of monthly exergy destruction analysis, it can be observed that the unavoidable-endogenous exergy destruction is almost equal to the half of the total exergy destruction presents in the HRSG.

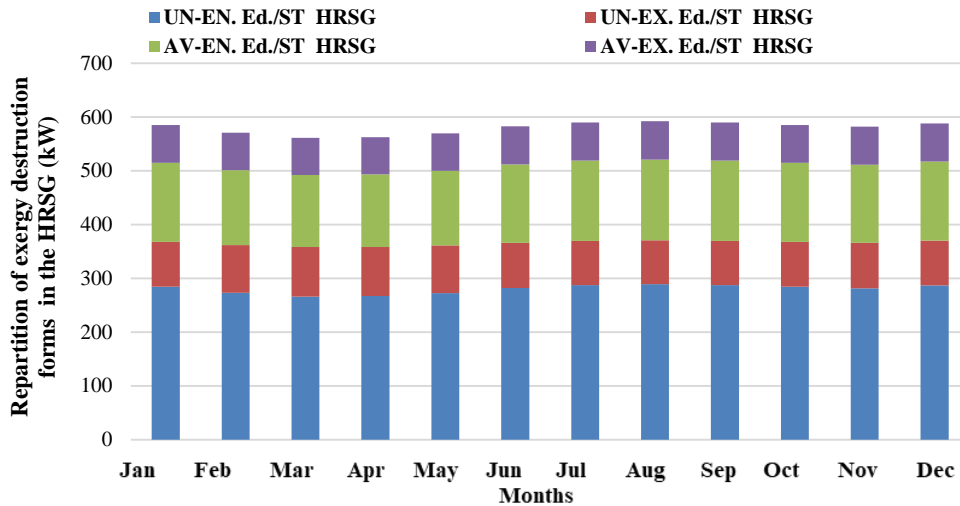


Figure 6.16. Distribution of exergy destruction forms in the HRSG of the power system based on ST technology.

The exogenous exergy destruction part is less than the avoidable-endogenous exergy destruction part, except during the periods of the year between February and May. The annual exergy destruction in the HRSG is estimated at 1.44 GWh. The regenerator 1 is considered as the most solicited generator due to the amount of heat transferred and the state change occurred inside. This process requires a substantial amount of thermal energy, more than 33% of the exergy is destroyed outside of the generator 1. This can be explained by the state change occurred during the heat transfer. The annual avoidable endogenous which can be recuperated during the optimization is estimated at 0.36 GWh for adiabatic conditions.

Figure 6.17 presents the distribution of exergy destruction forms throughout a year for the regenerator 1.

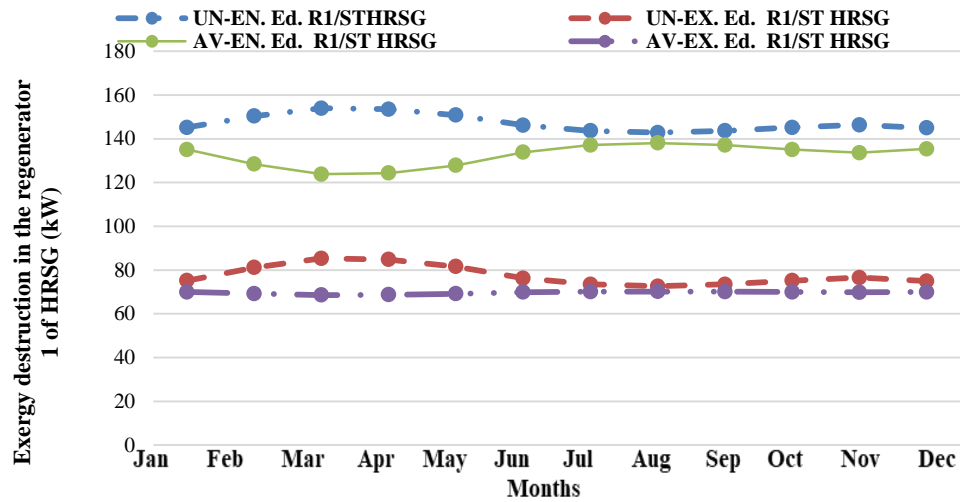


Figure 6.17. Repartition of exergy destruction forms in the regenerator 1 of the HRSG system connected to the power system based on ST.

Figure 6.18 and 6.19 present the distribution of exergy destruction forms throughout a year for the regenerator 2 and regenerator 3. These regenerators operate after the state change which explains the decreasing of the exergy destruction forms.

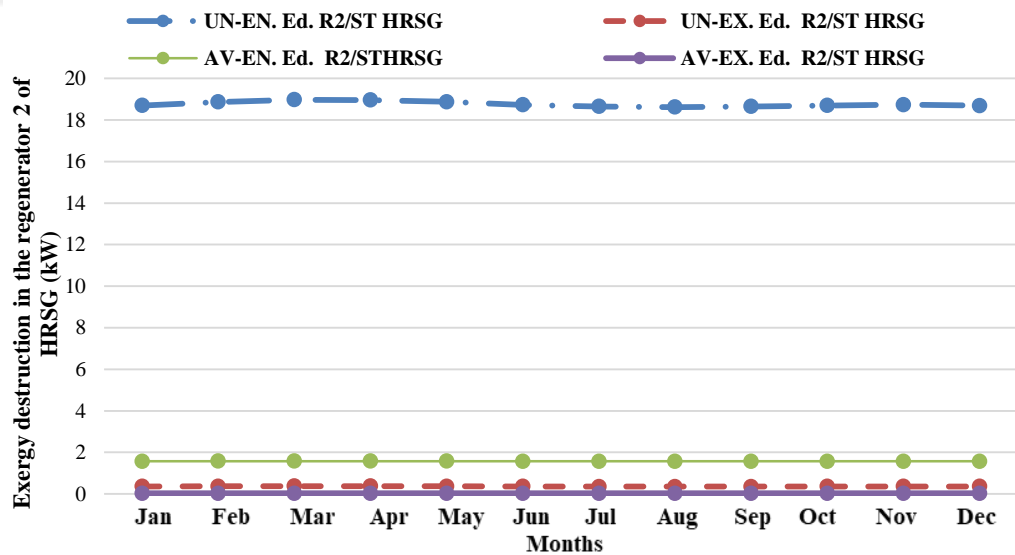


Figure 6.18. Repartition of exergy destruction forms in the regenerator 2 of the HRSG system connected to the power system based on ST.

It is observed relative stability among exogenous exergy destruction forms compared to the endogenous exergy destruction which is almost constant throughout the year.

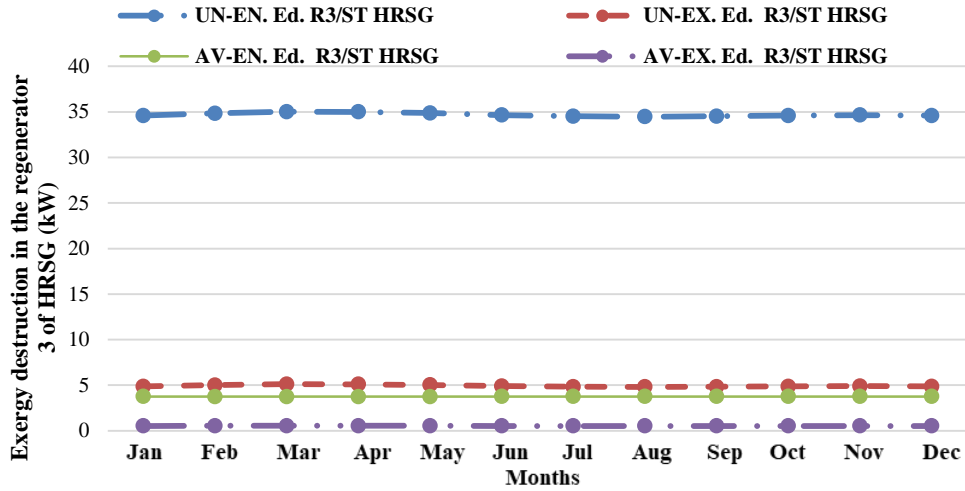


Figure 6.19. Repartition of exergy destruction forms in the regenerator 3 of the HRSG system connected to the power system based on ST.

Figure 6.20 shows an increase in the value of unavoidable-endogenous exergy destruction, while the exogenous exergy destruction forms remain constant throughout a year. The annual avoidable endogenous that can be recovered during the optimization analysis is estimated at 16.33 MWh.

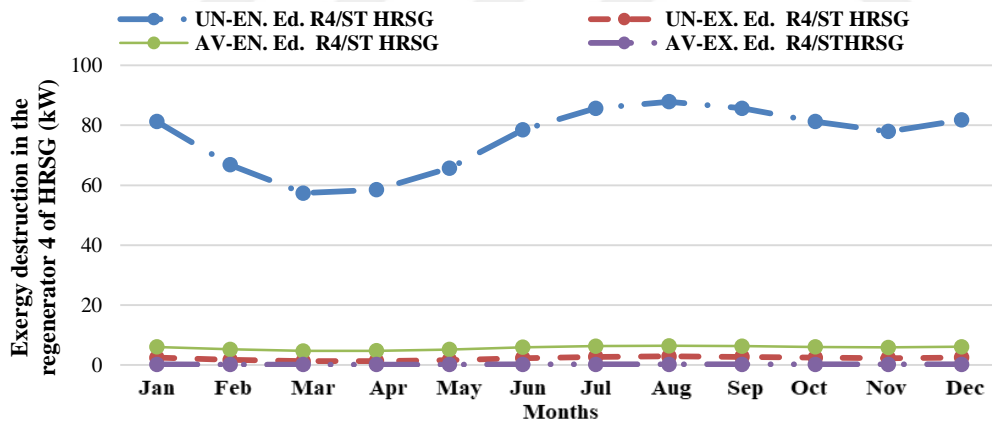


Figure 6.20. Repartition of exergy destruction forms in the regenerator 4 of the HRSG system connected to the power system based on ST.

Figure 6.21 presents a decreasing of the avoidable-endogenous exergy destruction. The periods of the year between February and June presents the most suitable conditions. The annual avoidable endogenous that can be recovered during the optimization analysis is estimated at 1.25 MWh.

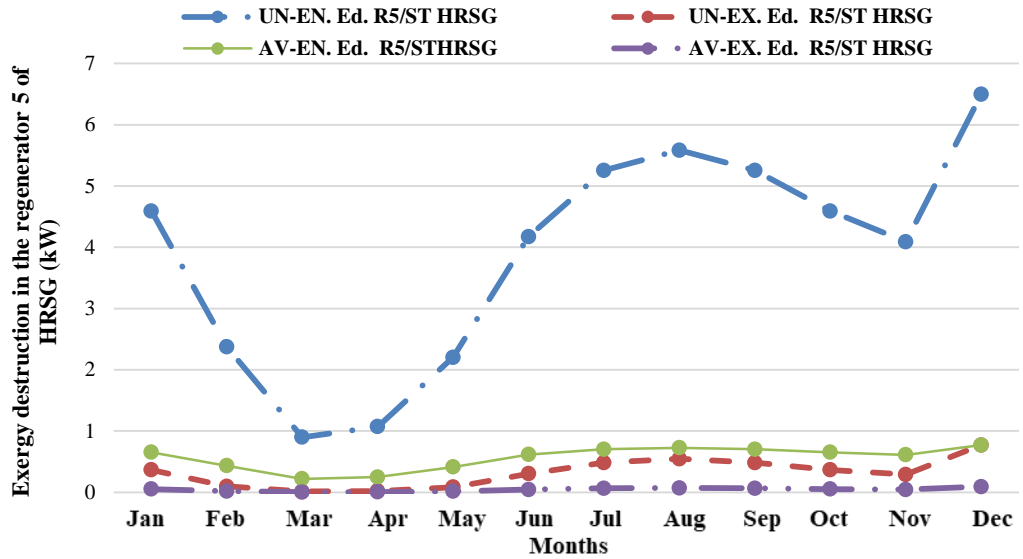


Figure 6.21. Repartition of exergy destruction forms in the regenerator 5 of the HRSG system connected to the power system based on ST.

C. Hybrid energy system based on LFR

The total land required by the system using linear Fresnel reflector technology is estimated at 69679 m² where the active area covered only 64.8% of the total land. The system consisted of the arrangement of 64 lines (SCA) in 6 loops with an area of 7524 m² and length equal to 44.8m for approximately 5 MWe output capacity.

The studied power system is similar to the power system based on parabolic trough collector in more than one case, a monthly exergy produced capacity is conducted to evaluate the exergy production of the solar field system throughout the year. The determination of the sunshine duration impact, DNI and the technology used to calculate exergy produced lead to better an understanding of results found in Figure 6.22.

Figure 6.22 shows that the lowest and the highest amount of monthly exergy produced is observed in July (2.10 GWh) and December (4.58 GWh). Furthermore, for the period from July to September has the poorest performances in term of exergy produced capacity. It is important to note that, the exergy

produced capacity of the solar power system is estimated at 15.69 MW, whereas the exergy produced capacity throughout the year was estimated at 39.34 GWh.

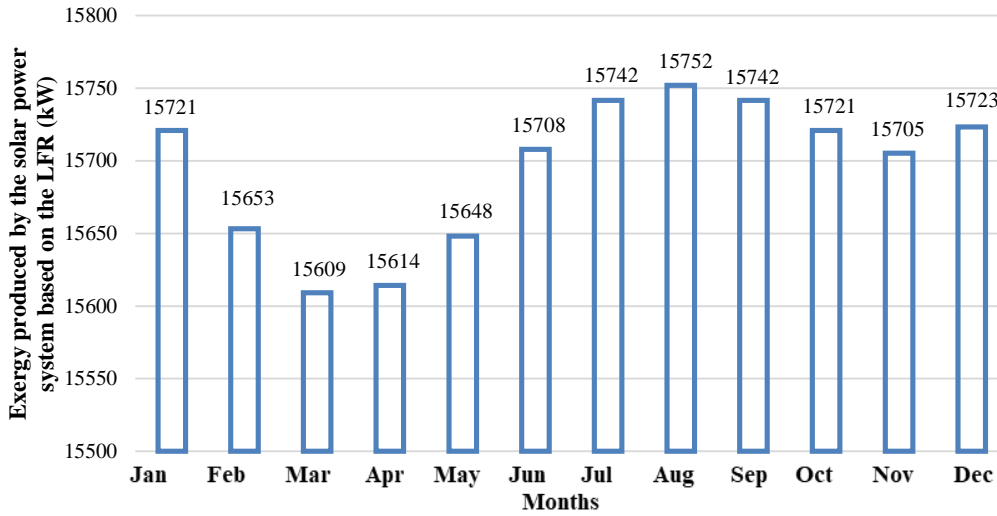


Figure 6.22. Monthly exergy production capacity of the solar field based on LFR.

Figure 6.23 presents the exergy destruction analysis of the intermediate heat exchanger used for the power system based on linear Fresnel reflector.

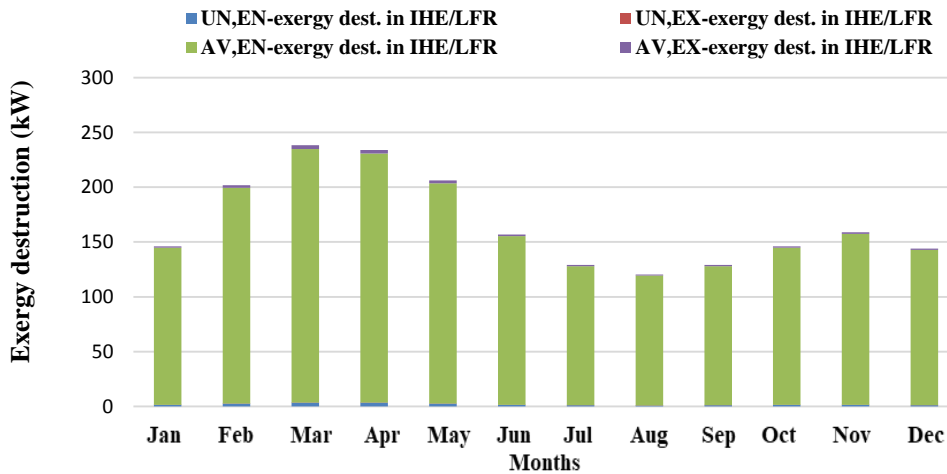


Figure 6.23. Distribution of the exergy destruction forms in the intermediate heat exchanger of the LFR - solar field.

The thermodynamic analysis consisted to determine various forms of the exergy destruction found in the heat exchanger, such as avoidable-endogenous and avoidable-exogenous exergy destruction. Out of the avoidable-endogenous exergy destruction, other exergy destruction forms present in the heat exchanger

are around 3% of the total exergy destruction. The annual exergy destruction in intermediate heat exchanger is estimated at 0.64 GWh.

Figure 6.24 presents the monthly exergy production and destruction in the heat recovery steam generation of the power system based on linear Fresnel reflector technology. The exergy destroyed inside of the heat recovery steam generation represents 26.7% of the total exergy produced by the solar power system.

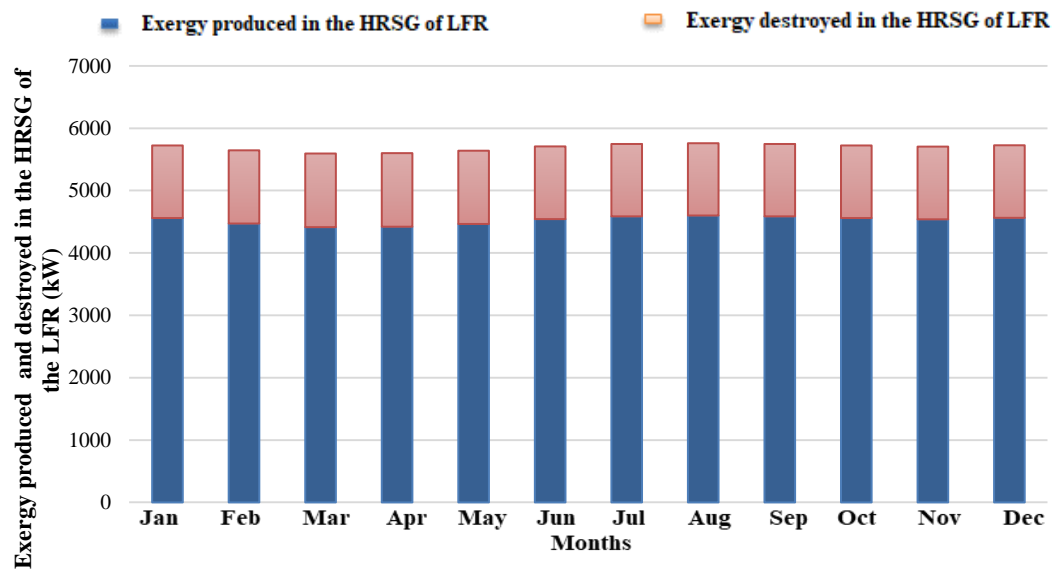


Figure 6.24. Exergy produced and destroyed in the HRSG of the power system based on LFR.

Figure 6.25 presents the distribution of exergy destruction forms throughout a year in the HRSG using the advanced exergy destruction analysis. The determination of the avoidable-endogenous and other exergy destruction forms leads to find out key data required for optimization work. The highest value of the annual exergy destruction is the avoidable-endogenous exergy destruction estimated at 1.25 GWh. The exergy destruction forms are classified as follows: avoidable-endogenous exergy destruction (43.1%), avoidable-exogenous exergy destruction (12.9%), unavoidable-exogenous exergy destruction (37.1%), and unavoidable-endogenous exergy destruction (6.9%). The annual thermal exergy destructed in the HRSG was estimated at 2.91 GWh.

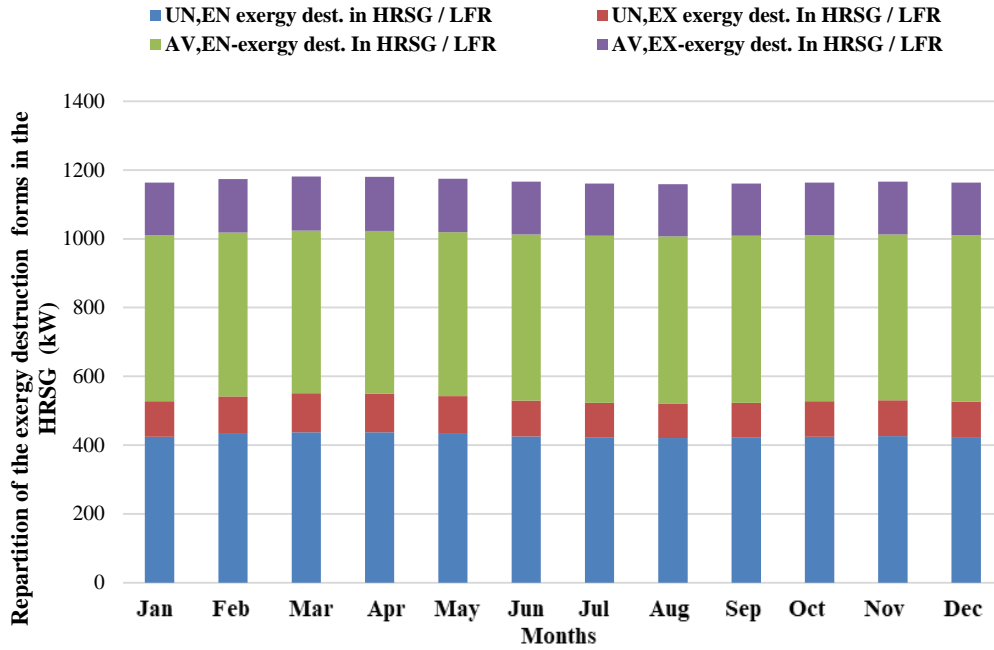


Figure 6.25. Distribution of Exergy destruction forms in the HRSG of the power system based on LFR.

Figure 6.26 presents the exergy destruction in the regenerator 1 of the HRSG connected to the power system based on LFR technology. Its analysis shows that the avoidable-endogenous exergy destruction is more important than the unavoidable-endogenous exergy destruction throughout the year.

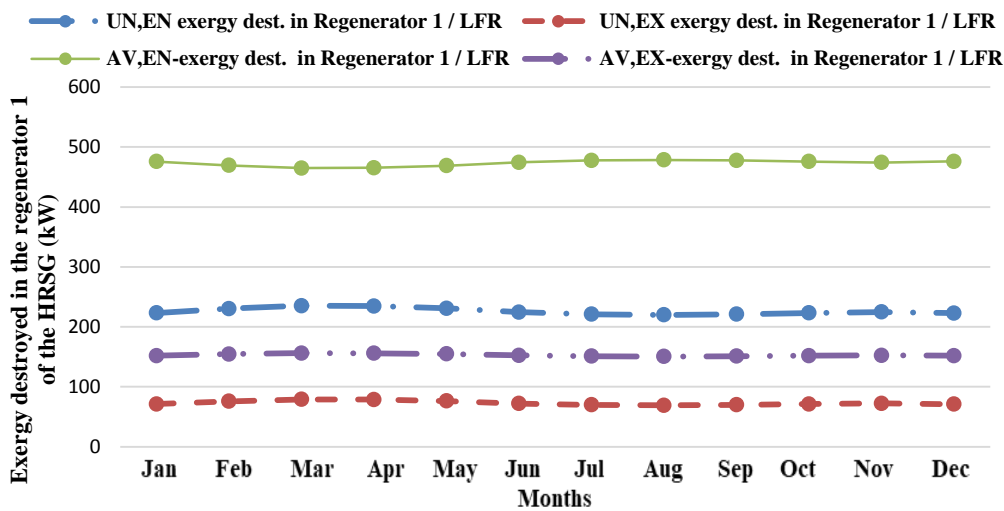


Figure 6.26. Repartition of exergy destruction forms in the regenerator 1 of the HRSG system connected to the power system based on LFR.

Furthermore, the endogenous exergy destruction represents more than 76.4% of the total exergy destruction in the regenerator. The annual avoidable-endogenous exergy destruction which can be recovered in the generator 1 is estimated at 1.79 GWh. Meanwhile, the exogenous exergy destruction of the regenerator 1 is less than the unavoidable-endogenous exergy destruction.

Figure 6.27 presents, the exergy destruction decreasing in the regenerator 2 due to the state change occurred previously in the regenerator 1. During the analysis, it is observed that the unavoidable-endogenous exergy destruction did not follow the decreasing of other exergy destruction forms.

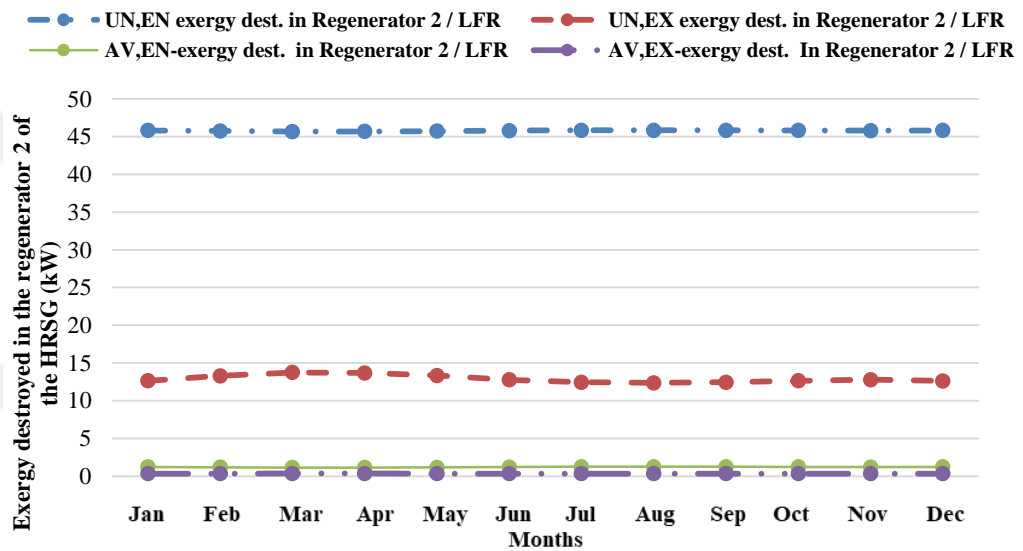


Figure 6.27. Repartition of exergy destruction forms in the regenerator 2 of the HRSG system connected to the power system based on LFR.

Moreover, the exogenous exergy destruction shows a value of less than 1% of the total exergy destruction. The avoidable endogenous exergy destruction was found to be almost equal to 20% of the total exergy destruction occurred inside which is estimated at 2.96 MWh per year.

Figure 6.28 presents, the exergy destruction increasing the regenerator 3 due to the low amount of the exergy transferred to steam water. During the analysis, it is observed that the avoidable/unavoidable-endogenous exergy destruction increase compared to other exergy destruction forms.

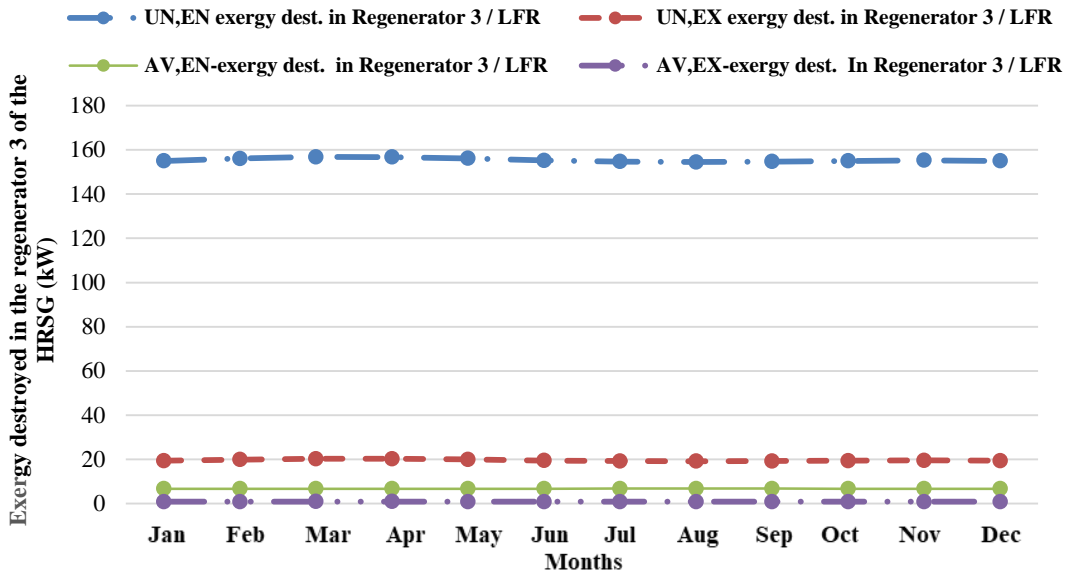


Figure 6.28. Repartition of exergy destruction forms in the regenerator 3 of the HRSG system connected to the power system based on LFR.

D. Biomass-fired system based on sorghum stalk

The capacity of the studied biomass-fired power system was estimated at 5.1 MW. The sorghum straw is used as the feedstock raw material. Its lower heating value was used to adjust the higher heating value of fuel under boiler conditions. The available biomass potential was obtained from sorghum farms. The biomass-fired power system performance is analyzed throughout the year which presented an average exergy produced capacity of 8.96 MW. Figure 6.29 presents the monthly exergy generated which has a cumulative value estimated at 32.26 GWh. The lowest exergy produced capacity of the studied power system is found for the period of the year from February to May. While the highest exergy produced a capacity of the biomass-fired system is found in August.

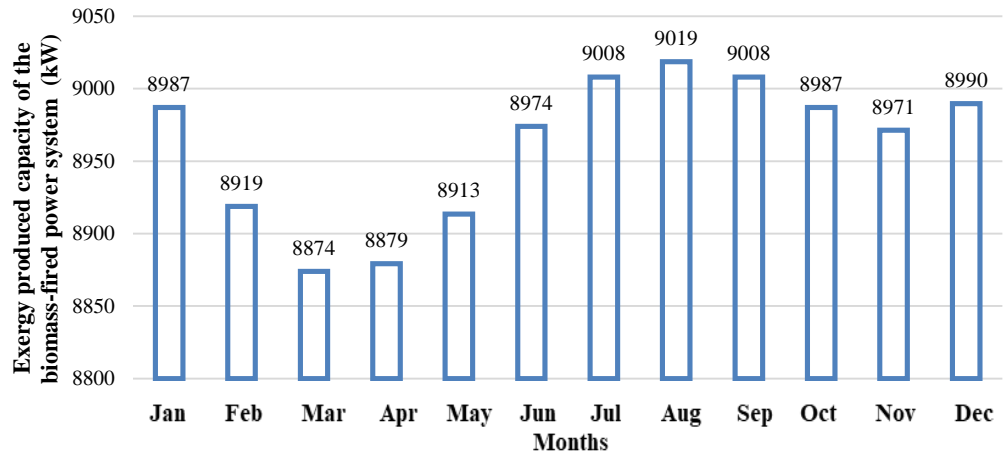


Figure 6.29. Monthly exergy produced the capacity of the power system based on BF.

Figure 6.30 presents the results of the advanced exergy analysis of the boiler based on equation 23, 24, 25 and 26. The avoidable-endogenous exergy destruction is a key parameter for the optimization work of the power system based on biomass-fired. The proportion of the various of exergy destruction forms in the boiler can be presented as follows: avoidable-exogenous exergy destruction (14–15%), avoidable endogenous exergy destruction (57.4–59%), unavoidable endogenous exergy destruction (21.3–23%), unavoidable exogenous exergy destruction (6.3–5.4%). The annual exergy destruction in the boiler is estimated at 8.46 GWh.

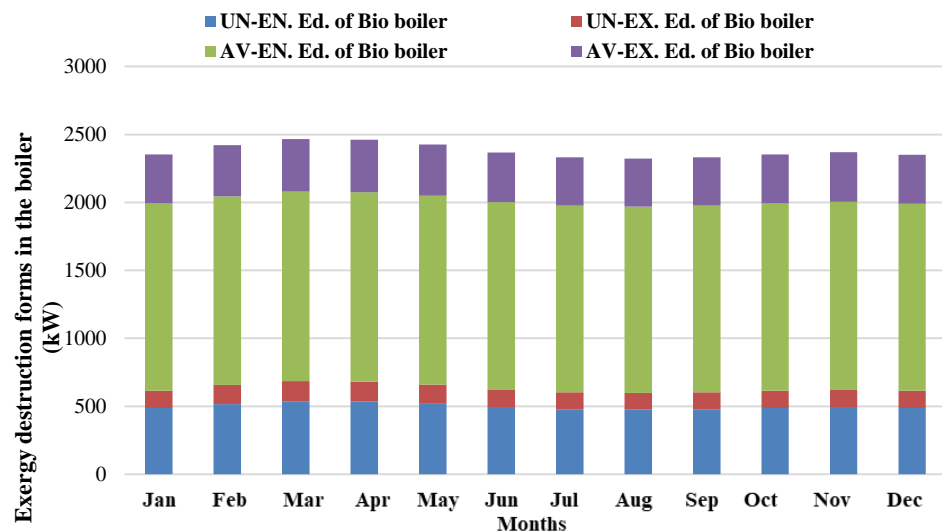


Figure 6.30. Distribution of the exergy destruction forms in the intermediate heat exchanger of BF.

Figure 6.31 presents the monthly exergy production and destruction in the heat recovery steam generation of the power system based on biomass-fired technology. The exergy destruction of the heat recovery steam generation represented more than 11.5% of the total exergy produced by the studied power system.

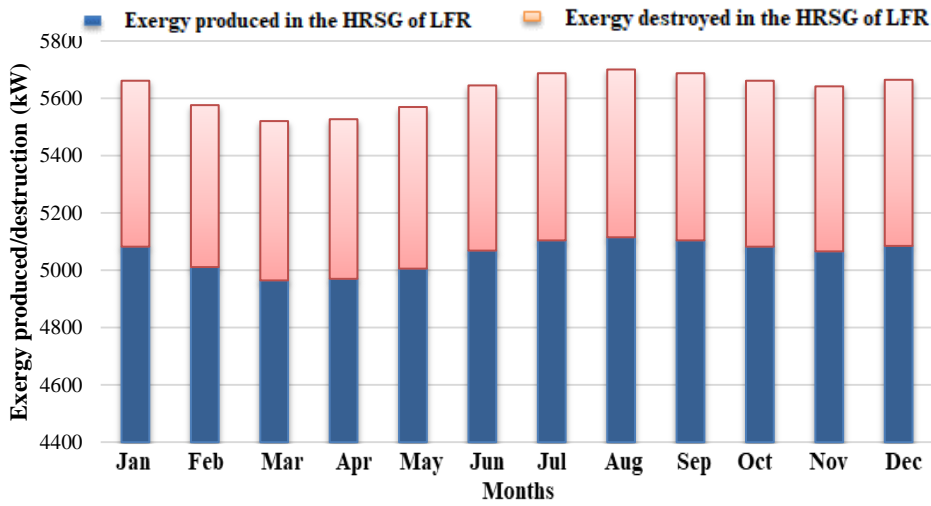


Figure 6.31. Exergy produced and destroyed in the HRSG of the power system based on BF.

The proportion of each exergy destruction forms found in the HRSG of the biomass-fired power system is specified in Figure 6.32.

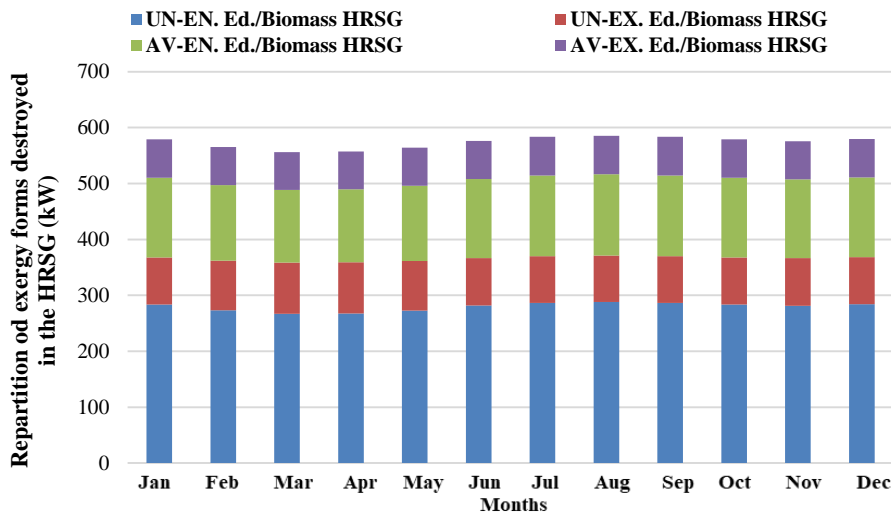


Figure 6.32. Distribution of exergy destruction forms in the HRSG of the power system based on BF technology.

This analysis has contributed to identifying the unavoidable-endogenous exergy destruction as one of the most important parts of the exergy destruction. The annual avoidable-endogenous exergy destruction inside of the HRSG is estimated at 0.35 GWh, which represents almost the quarter of the total exergy destruction. Furthermore, the unavoidable-endogenous exergy destruction represents more than half of the total thermal exergy destroyed.

Figure 6.33 presents the exergy destruction forms in the regenerator 1 of the HRSG connected to the power system based on biomass-fired technology. The regenerator 1 is the most solicited generator due to the amount of heat transferred for the state change of working fluid. This process requires a substantial amount of thermal energy. Considering adiabatic conditions, the annual amount of avoidable-endogenous exergy destruction which can be recovered during the optimization work is estimated at 60.89 MWh.

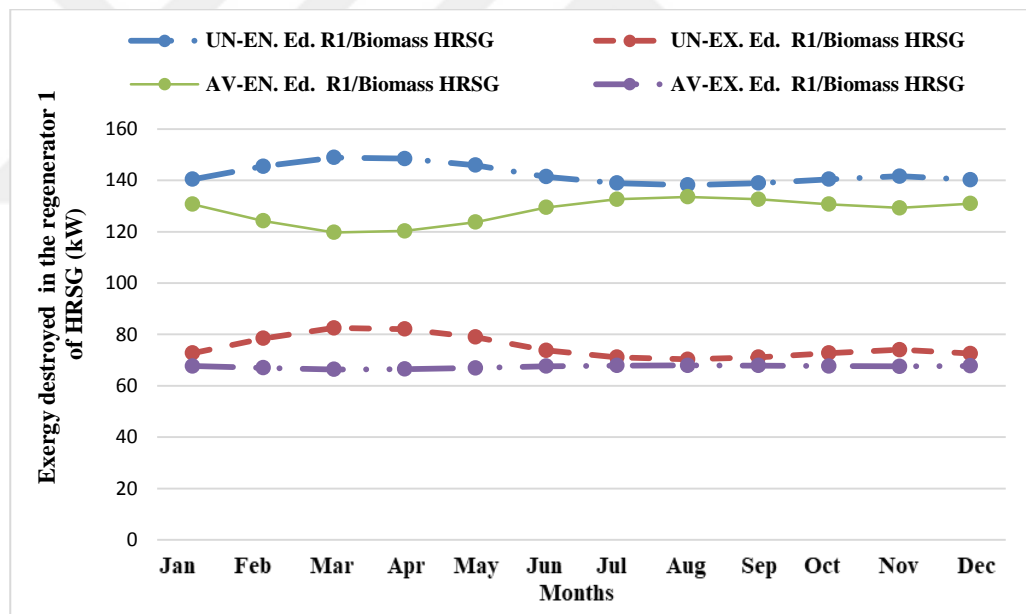


Figure 6.33. Repartition of exergy destruction forms in the regenerator 1 of the HRSG system connected to the power system based on BF.

Figure 6.34 and 6.35 present the distribution of exergy destruction forms in the regenerator 2 and regenerator 3 which operate after the state change. It observed relative stability among exogenous exergy destruction forms compared to the endogenous exergy destruction forms which are almost constant throughout the year.

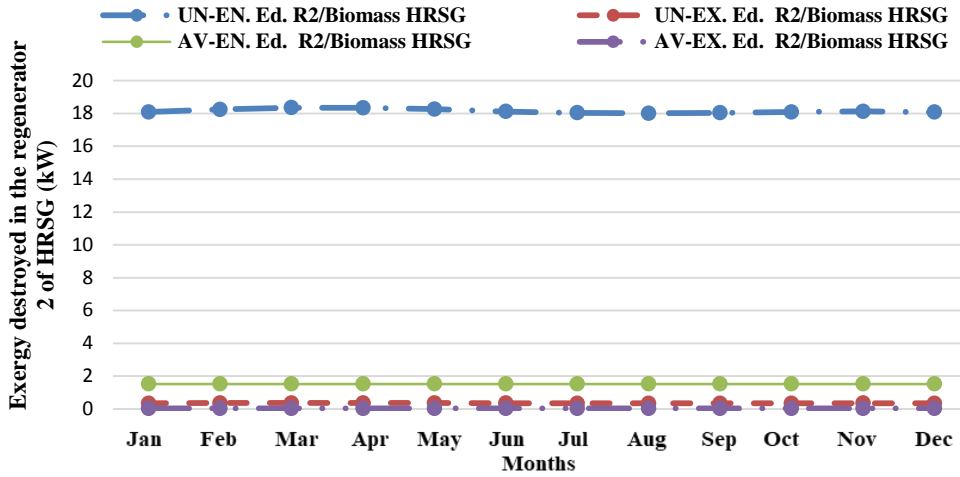


Figure 6.34. Repartition of exergy destruction forms in the regenerator 2 of the HRSG system connected to the power system based on BF.

Figure 6.35 presents the distribution of exergy destruction forms in the regenerator 3.

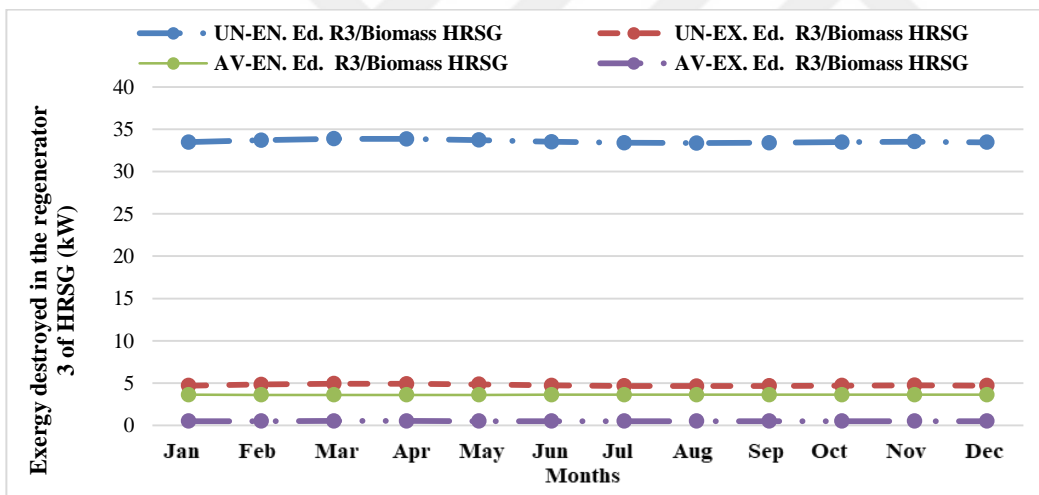


Figure 6.35. Repartition of exergy destruction forms in the regenerator 3 of the HRSG system connected to the power system based on BF.

Figure 6.36 shows the increase of the unavoidable-endogenous exergy destruction value in the regenerator 4, while the exogenous exergy destruction forms remain constant throughout a year. The annual avoidable-endogenous that can be recovered during the optimization work is estimated at 43.07 MWh.

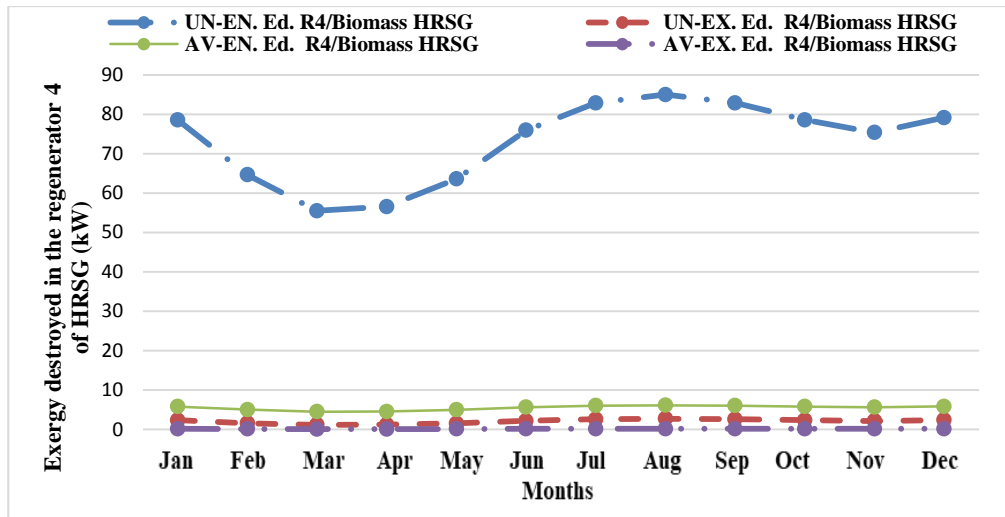


Figure 6.36. Exergy destruction in the regenerator 4 of the HRSG system of the power system based on BF.

Figure 6.37 shows a decreasing of the avoidable-endogenous exergy destruction value in the regenerator 5. The periods of the year between January and June recorded the most suitable values of avoidable-endogenous exergy destruction. The annual avoidable-endogenous that can be recovered during the optimization work is estimated below 4.38 MWh.

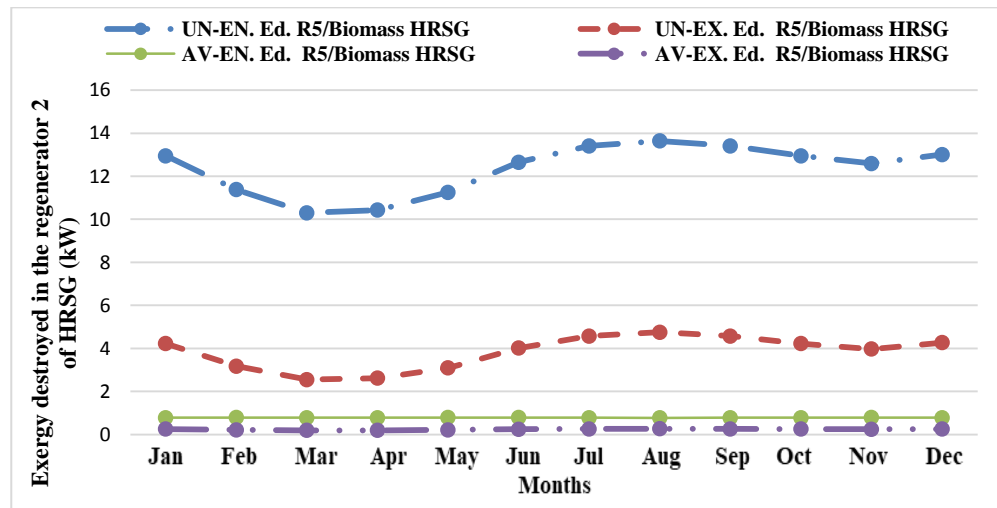


Figure 6.37. Exergy destruction in the regenerator 5 of the HRSG system of the power system based on BF.

6.4 Economic Analysis

Tables 6.27 – 6.29 present the economics parameters of the hybrid energy system using biomass- fired combined with concentrating power solar technologies. During the economic analysis, the levelized cost of electricity is found between 76.4 and 226.2 USD/MWh for the studied hybrid systems. The lowest and the highest values are found for the hybrid energy system based on the combination of the biomass–fired/linear Fresnel reflector (LFR-BF) and biomass – fired / solar tower (ST-BF) technologies, respectively. According to the following parameters, the net present value, return on investment and the internal rate of the return show that, the LFR-BF technology is the best option for hybrid energy system implementation in the sub-Saharan region. But this technology is not mature, there is need to update, train and re-evaluate the skills of workers. Furthermore, the acceptability and the well – behaviour of population living around the plant may contribute to the long-term exploitation of hybrid energy system. The main difference between this technology and others is the strength of the mechanical structure and the initial investment. The hybrid system based on biomass – fired and solar tower technology owns the highest initial investment which is estimated at 46.24 Million USD and where the solar tower technology alone represents about 89.83% of the total initial investment. The hybrid energy system based on the parabolic trough collector and biomass-fired technology has an initial investment cost of 34.38 Million USD. Meanwhile, the total initial investment cost of hybrid system based on the linear Fresnel reflector and biomass-fired is estimated at 21.78 Million USD which matched with the mechanical structure of the system and its strength. The combination of the maturity of technology and economic parameters present the hybrid energy system based on PTC-BF as the best candidate to develop power plant for commercial use in the region. The hybrid energy system based on ST-BF which is also existing in some countries like Morocco and South-Africa presents some advantages in term of O&M services and maturity. In other hand, the economic and socio-economic parameters such the initial investment and job creation does not matched with the skills of local population. Therefore, the use the aforementioned hybrid energy systems present a potential that can help to benefit some incentives from private organization, financial institution and governmental authorities for climate change which may contribute to reduce the initial investment cost for project implementation.

Table 6.27. Techno-economic analysis of hybrid energy system based on PTC and BF technology.

Calender year	2025	2026	2027	2028	2029	2030	2031	2042	2043	2044	2045	2049							
PTC solar /Biomass-fired Power	1	2	3	4	5	6	7	18	19	20	21	25							
Year from 2019	6	7	8	9	10	11	12	23	24	25	26	30							
Analysis	1	1	1	1	1	1	1	1	1	1	1	1							
Depreciation, Amortization, and Debt Service Calculations (\$ Millions)																			
Depreciation rates for 5 year	0.36	0.27	0.23	0.13	0.01	0.00	0.00	0.00	0.00	0.00	0.00	0.00							
Beginning of year values	34.38	21.86	12.62	4.76	0.34	0.00	0.00	0.00	0.00	0.00	0.00	0.00							
Tax depreciation (5 year MACRS)	12.51	9.25	7.86	4.42	0.34	0.00	0.00	0.00	0.00	0.00	0.00	0.00							
End year asset value	21.86	12.62	4.76	0.34	0.00	0.00	0.00	0.00	0.00	0.00	0.00	0.00							
Begin year amortization value	7.41	7.04	6.67	6.30	5.93	5.56	5.19	1.11	0.74	0.37	0.00	0.00							
Amortization over 20 years	0.37	0.37	0.37	0.37	0.37	0.37	0.37	0.37	0.37	0.37	0.00	0.00							
End year asset value	7.04	6.67	6.30	5.93	5.56	5.19	4.82	0.74	0.37	0.00	0.00	0.00							
Begin year debt amount	26.06	25.49	24.88	24.21	23.49	22.72	21.88	6.84	4.73	2.46	0.00	0.00							
Debt service payment	2.65	2.65	2.65	2.65	2.65	2.65	2.65	2.65	2.65	2.65	0.00	0.00							
Interest	2.08	2.04	1.99	1.94	1.88	1.82	1.75	0.55	0.38	0.20	0.00	0.00							
Debt principal repayment (mortgage)	0.57	0.62	0.66	0.72	0.77	0.84	0.90	2.11	2.28	2.46	0.00	0.00							
End year debt amount	25.49	24.88	24.21	23.49	22.72	21.88	20.98	4.73	2.46	0.00	0.00	0.00							
Energy Calculations																			
Electric energy production, GWh	32.29	31.97	31.65	31.33	31.02	30.71	30.40	27.22	26.95	26.68	26.41	25.37							
Backup unit/ Biomass fuel costs	1.47	1.47	1.47	1.47	1.47	1.47	1.47	1.47	1.47	1.47	1.47	1.47							
Income Statement and Cashflow Statement Calculations (Millions \$)																			
Plant revenue	3.52	3.52	3.52	3.52	3.52	3.52	3.52	3.52	3.52	3.52	3.52	3.52							
Rev. cover. non-fuel O&M ¹⁰	2.59	2.69	2.70	2.71	2.71	2.72	2.73	2.82	2.83	2.83	2.84	2.88							
Variable non-fuel O&M revenue	0.00	0.00	0.00	0.00	0.00	0.00	0.00	0.00	0.00	0.00	0.00	0.00							
Fuel cost revenue	0.00	0.00	0.00	0.00	0.00	0.00	0.00	0.00	0.00	0.00	0.00	0.00							
Revenue Subtotal	6.11	6.21	6.22	6.23	6.24	6.24	6.25	6.34	6.35	6.36	6.37	6.41							
O&M cost in k\$	686.67	787.95	789.25	790.56	791.87	793.20	794.54	809.92	811.38	812.85	814.34	820.38							
Fixed non-fuel O&M cost ¹¹	515.00	615.00	615.00	615.00	615.00	615.00	615.00	615.00	615.00	615.00	615.00	615.00							
Variable non-fuel O&M cost (8%)	171.67	172.95	174.25	175.56	176.87	178.20	179.54	194.92	196.38	197.85	199.34	205.38							
Insurance expense (2.42%)	214.90	220.08	225.38	230.81	236.38	242.07	247.91	322.15	329.91	337.86	346.00	380.59							
Property tax expense (0.5% of TCI)	217.24	217.24	217.24	217.24	217.24	217.24	217.24	217.24	217.24	217.24	217.24	217.24							
Tax depreciation and amortization (Million \$)	12.88	9.62	8.23	4.79	0.71	0.37	0.37	0.37	0.37	0.37	0.00	0.00							
Operating income (EBIT)	9.36	6.10	4.70	1.27	2.81	3.15	3.15	3.15	3.15	3.15	3.52	3.52							
Taxable income	11.45	8.13	6.69	3.20	0.93	1.33	1.40	2.61	2.77	2.96	3.52	3.52							
Income Tax (40,2%)	4.60	3.27	2.69	1.29	0.37	0.54	0.56	1.05	1.12	1.19	1.42	1.42							
Investment tax credit ¹²	0.00	0.00	0.00	0.00	0.00	0.00	0.00	0.00	0.00	0.00	0.00	0.00							
After Tax Income	6.84	4.86	4.00	1.91	0.56	0.80	0.84	1.56	1.66	1.77	2.11	2.11							
Add back depreciation	12.88	9.62	8.23	4.79	0.71	0.37	0.37	0.37	0.37	0.37	0.00	0.00							
Deduct repayment of debt principal	0.57	0.62	0.66	0.72	0.77	0.84	0.90	2.11	2.28	2.46	0.00	0.00							
Equity investments and dividend	5.47	4.14	3.56	2.16	0.62	1.26	1.37	3.29	3.56	3.85	2.11	2.11							
Levelized Cost of Energy in Cents/kWh (Without support)/ o/ electricity generation, nominal Cents/kWh incentives)												21.42							
Levelized and annual cost	18.92	19.44	19.66	19.88	20.10	20.33	20.56	23.29	23.56	23.83	24.11	25.26							
Carbon Tax (41.2 \$/MWh)	1.33	1.32	1.30	1.29	1.28	1.27	1.25	1.12	1.11	1.10	1.09	1.05							
Good production (25.8 \$/MWh)	0.83	0.82	0.82	0.81	0.80	0.79	0.78	0.70	0.70	0.69	0.68	0.65							
Incentives amount /year	2.16	2.14	2.12	2.10	2.08	2.06	2.04	1.82	1.81	1.79	1.77	1.70							
Levelized and annual cost of	12.22	12.74	12.96	13.18	13.40	13.63	13.86	16.59	16.86	17.13	17.41	18.56							
Levelized Cost of Energy in Cents/kWh												14.72							
Cash available for debt service	3.52	3.52	3.52	3.52	3.52	3.52	3.52	3.52	3.52	3.52	3.52	3.52							
DSCR	1.34	1.34	1.34	1.34	1.34	1.34	1.34	1.34	1.34	1.34	1.34	1.34							
Discount rate (8.0%)	1.08	1.17	1.26	1.36	1.47	1.59	1.71	4.00	4.32	4.66	5.03	6.85							
Present value	3.26	3.02	2.80	2.59	2.40	2.22	2.06	0.88	0.82	0.76	0.70	0.51							
IRR					13.79%					ROI			10.62			NPV			23.40

¹⁰ Revenue covering fixed non-fuel O&M revenue, property taxes, and insurance, fuel cost (without good sales and Credit Carbon Tax advantages "incentives")

¹¹ Fixed non-fuel O&M cost -Human Labour (25 workers)

¹² Investment tax credit (for solar investment only, when owned by taxable entity)

Table 6.28. Techno-economic analysis of hybrid energy system based on ST and BF technology.

Calender year	2025	2026	2027	2028	2029	2030	2031	2042	2043	2044	2045	2049
ST solar /Biomass-fired Power	1	2	3	4	5	6	7	18	19	20	21	25
Year from 2019	6	7	8	9	10	11	12	23	24	25	26	30
Analysis	1	1	1	1	1	1	1	1	1	1	1	1
Depreciation, Amortization, and Debt Service Calculations (\$ Millions)												
Depreciation rates for 5 year	0.36	0.27	0.23	0.13	0.01	0.00	0.00	0.00	0.00	0.00	0.00	0.00
Beginning of year values	46.24	29.41	16.97	6.40	0.46	0.00	0.00	0.00	0.00	0.00	0.00	0.00
Tax depreciation (5 year MACRS)	16.83	12.44	10.57	5.94	0.46	0.00	0.00	0.00	0.00	0.00	0.00	0.00
End year asset value	29.41	16.97	6.40	0.46	0.00	0.00	0.00	0.00	0.00	0.00	0.00	0.00
Begin year amortization value	11.37	10.80	10.23	9.66	9.09	8.53	7.96	1.71	1.14	0.57	0.00	0.00
Amortization over 20 years	0.57	0.57	0.57	0.57	0.57	0.57	0.57	0.57	0.57	0.57	0.00	0.00
End year asset value	10.80	10.23	9.66	9.09	8.53	7.96	7.39	1.14	0.57	0.00	0.00	0.00
Begin year debt amount	33.15	32.42	31.64	30.80	29.88	28.90	27.83	8.70	6.02	3.13	0.00	0.00
Debt service payment	3.38	3.38	3.38	3.38	3.38	3.38	3.38	3.38	3.38	3.38	0.00	0.00
Interest	2.65	2.59	2.53	2.46	2.39	2.31	2.23	0.70	0.48	0.25	0.00	0.00
Debt principal repayment	0.72	0.78	0.84	0.91	0.99	1.06	1.15	2.68	2.89	3.13	0.00	0.00
End year debt amount	32.42	31.64	30.80	29.88	28.90	27.83	26.68	6.02	3.13	0.00	0.00	0.00
Energy Calculations												
Electric energy production,	32.65	32.65	32.65	32.65	32.65	32.65	32.65	32.65	32.65	32.65	32.65	32.65
Backup unit/ Biomass fuel costs	1.47	1.47	1.47	1.47	1.47	1.47	1.47	1.47	1.47	1.47	1.47	1.47
Income Statement and Cashflow Statement Calculations (Millions \$)												
Plant revenue	4.48	4.48	4.48	4.48	4.48	4.48	4.48	4.48	4.48	4.48	4.48	4.48
Rev. cover. non-fuel O&M	2.73	2.83	2.84	2.85	2.86	2.87	2.88	2.99	3.00	3.01	3.02	3.07
Variable non-fuel O&M revenue	0.00	0.00	0.00	0.00	0.00	0.00	0.00	0.00	0.00	0.00	0.00	0.00
Fuel cost revenue	0.00	0.00	0.00	0.00	0.00	0.00	0.00	0.00	0.00	0.00	0.00	0.00
Revenue Subtotal	7.21	7.31	7.32	7.33	7.34	7.35	7.36	7.47	7.48	7.49	7.50	7.55
O&M cost in k\$	686.67	787.95	789.25	790.56	791.87	793.20	794.54	809.92	811.38	812.85	814.34	820.38
Fixed non-fuel O&M cost	515.00	615.00	615.00	615.00	615.00	615.00	615.00	615.00	615.00	615.00	615.00	615.00
Variable non-fuel O&M cost	171.67	172.95	174.25	175.56	176.87	178.20	179.54	194.92	196.38	197.85	199.34	205.38
Insurance expense (2.42%)	273.34	279.93	286.67	293.58	300.66	307.90	315.33	409.76	419.63	429.74	440.10	484.08
Property tax expense (0.5% of	299.17	299.17	299.17	299.17	299.17	299.17	299.17	299.17	299.17	299.17	299.17	299.17
Tax depreciation and	17.40	13.01	11.13	6.51	1.03	0.57	0.57	0.57	0.57	0.57	0.00	0.00
Operating income (EBIT)	12.92	8.53	6.65	2.03	3.45	3.91	3.91	3.91	3.91	3.91	4.48	4.48
Taxable income	15.57	11.12	9.18	4.49	1.06	1.60	1.69	3.22	3.43	3.66	4.48	4.48
Income Tax (40.2%)	6.26	4.47	3.69	1.81	0.43	0.64	0.68	1.29	1.38	1.47	1.80	1.80
Investment tax credit	0.00	0.00	0.00	0.00	0.00	0.00	0.00	0.00	0.00	0.00	0.00	0.00
After Tax Income	9.31	6.65	5.49	2.69	0.63	0.96	1.01	1.92	2.05	2.19	2.68	2.68
Add back depreciation	17.40	13.01	11.13	6.51	1.03	0.57	0.57	0.57	0.57	0.57	0.00	0.00
Deduct repayment of debt	0.72	0.78	0.84	0.91	0.99	1.06	1.15	2.68	2.89	3.13	0.00	0.00
Equity investments and dividend	7.36	5.57	4.80	2.91	0.59	1.45	1.59	4.04	4.38	4.75	2.68	2.68
Discount factor (to year of initial												
Levelized Cost of Energy in Cents/kWh (Without support)/ of electricity generation, nominal Cents/kWh (With incentives)												22.62
Levelized and annual cost	22.07	22.40	22.43	22.45	22.48	22.50	22.53	22.87	22.90	22.94	22.97	23.13
Incentives (in Millions USD)												
C. Tax carbon (41.2 \$/MWh)	1.35	1.35	1.35	1.35	1.35	1.35	1.35	1.35	1.35	1.35	1.35	1.35
Good production (25.8\$/MWh)	0.84	0.84	0.84	0.84	0.84	0.84	0.84	0.84	0.84	0.84	0.84	0.84
Incentives amount /year	2.19	2.19	2.19	2.19	2.19	2.19	2.19	2.19	2.19	2.19	2.19	2.19
Levelized and annual cost of	15.37	15.70	15.73	15.75	15.78	15.80	15.83	16.17	16.20	16.24	16.27	16.43
Levelized Cost Of Energy in Cents/kWh												15.92
Cash available for debt service	4.48	4.48	4.48	4.48	4.48	4.48	4.48	4.48	4.48	4.48	4.48	4.48
DSCR	1.34	1.34	1.34	1.34	1.34	1.34	1.34	1.34	1.34	1.34	1.34	1.34
Discount rate (8.0%)	1.08	1.17	1.26	1.36	1.47	1.59	1.71	4.00	4.32	4.66	5.03	6.85
Present value	4.15	3.84	3.56	3.29	3.05	2.82	2.61	1.12	1.04	0.96	0.89	0.65
Fixed O&M, fuel and other	2.52	2.43	2.26	2.09	1.95	1.81	1.68	0.75	0.69	0.65	0.60	0.45
Total	6.67	6.27	5.81	5.39	5.00	4.63	4.29	1.87	1.73	1.61	1.49	1.10
IRR	12.64%											
ROI	14.71											
NPV	23.45											

Table 6.29. Techno-economic analysis of hybrid energy system based on LFR and BF.

Calender year	2025	2026	2027	2028	2029	2030	2031	2042	2043	2044	2045	2049
LFR solar /Biomass-fired	1	2	3	4	5	6	7	18	19	20	21	25
Year from 2019	6	7	8	9	10	11	12	23	24	25	26	30
Analysis	1	1	1	1	1	1	1	1	1	1	1	1
Depreciation, Amortization, and Debt Service Calculations (\$ Millions)												
Depreciation rates for 5 year	0.36	0.27	0.23	0.13	0.01	0.00	0.00	0.00	0.00	0.00	0.00	0.00
Beginning of year values	21.78	13.85	7.99	3.02	0.22	0.00	0.00	0.00	0.00	0.00	0.00	0.00
Tax depreciation (5 year	7.93	5.86	4.98	2.80	0.22	0.00	0.00	0.00	0.00	0.00	0.00	0.00
End year asset value	13.85	7.99	3.02	0.22	0.00	0.00	0.00	0.00	0.00	0.00	0.00	0.00
Begin year amortization value	5.39	5.12	4.85	4.58	4.31	4.04	3.77	0.81	0.54	0.27	0.00	0.00
Amortization over 20 years	0.27	0.27	0.27	0.27	0.27	0.27	0.27	0.27	0.27	0.27	0.00	0.00
End year asset value	5.12	4.85	4.58	4.31	4.04	3.77	3.50	0.54	0.27	0.00	0.00	0.00
Begin year debt amount	15.85	15.50	15.13	14.72	14.29	13.82	13.31	4.16	2.88	1.49	0.00	0.00
Debt service payment	1.61	1.61	1.61	1.61	1.61	1.61	1.61	1.61	1.61	1.61	0.00	0.00
Interest	1.27	1.24	1.21	1.18	1.14	1.11	1.06	0.33	0.23	0.12	0.00	0.00
Debt principal repayment	0.35	0.37	0.40	0.44	0.47	0.51	0.55	1.28	1.38	1.49	0.00	0.00
End year debt amount	15.50	15.13	14.72	14.29	13.82	13.31	12.76	2.88	1.49	0.00	0.00	0.00
Energy Calculations												
Electric energy production,	31.21	31.21	31.21	31.21	31.21	31.21	31.21	31.21	31.21	31.21	31.21	31.21
Backup unit/ Biomass fuel	1.47	1.47	1.47	1.47	1.47	1.47	1.47	1.47	1.47	1.47	1.47	1.47
Income Statement and Cashflow Statement Calculations (Millions \$)												
Plant revenue	2.14	2.14	2.14	2.14	2.14	2.14	2.14	2.14	2.14	2.14	2.14	2.14
Rev. cover. non-fuel O&M	2.29	2.29	2.30	2.30	2.30	2.31	2.31	2.37	2.38	2.39	2.39	2.42
Variable non-fuel O&M	0.00	0.00	0.00	0.00	0.00	0.00	0.00	0.00	0.00	0.00	0.00	0.00
Fuel cost revenue	0.00	0.00	0.00	0.00	0.00	0.00	0.00	0.00	0.00	0.00	0.00	0.00
Revenue Subtotal	4.43	4.43	4.44	4.44	4.45	4.45	4.46	4.52	4.52	4.53	4.54	4.56
O&M cost in k\$	548.05	549.34	550.63	551.94	553.26	554.58	555.92	571.30	572.76	574.23	575.72	581.77
Fixed non-fuel O&M cost	376.38	376.38	376.38	376.38	376.38	376.38	376.38	376.38	376.38	376.38	376.38	376.38
Variable non-fuel O&M cost	171.67	172.95	174.25	175.56	176.87	178.20	179.54	194.92	196.38	197.85	199.34	205.38
Insurance expense (2.42%)	130.68	133.83	137.05	140.36	143.74	147.20	150.75	195.90	200.62	205.45	210.40	231.43
Property tax expense (0.5% of	141.07	141.07	141.07	141.07	141.07	141.07	141.07	141.07	141.07	141.07	141.07	141.07
Tax depreciation and	8.20	6.13	5.25	3.07	0.49	0.27	0.27	0.27	0.27	0.27	0.00	0.00
Operating income (EBIT)	6.05	3.99	3.10	0.93	1.66	1.87	1.87	1.87	1.87	1.87	2.14	2.14
Taxable income	7.32	5.23	4.31	2.10	0.51	0.77	0.81	1.54	1.64	1.75	2.14	2.14
Income Tax (40,2%)	2.94	2.10	1.73	0.85	0.21	0.31	0.32	0.62	0.66	0.70	0.86	0.86
Investment tax credit	0.00	0.00	0.00	0.00	0.00	0.00	0.00	0.00	0.00	0.00	0.00	0.00
After Tax Income	4.38	3.12	2.58	1.26	0.31	0.46	0.48	0.92	0.98	1.05	1.28	1.28
Add back depreciation	8.20	6.13	5.25	3.07	0.49	0.27	0.27	0.27	0.27	0.27	0.00	0.00
Deduct repayment of debt	0.35	0.37	0.40	0.44	0.47	0.51	0.55	1.28	1.38	1.49	0.00	0.00
Equity investments and	3.47	2.63	2.26	1.37	0.29	0.70	0.76	1.93	2.10	2.27	1.28	1.28
Levelized Cost Of Energy in Cents/kWh (Without support)/ of electricity generation, nominal Cents/kWh (With incentives) 14.34												
Levelized and annual cost	14.19	14.20	14.22	14.23	14.25	14.26	14.28	14.47	14.49	14.51	14.53	14.62
Incentives (in Millions USD)												
C. Tax carbon (41.2 \$/MWh)	1.29	1.29	1.29	1.29	1.29	1.29	1.29	1.29	1.29	1.29	1.29	1.29
Good production (25.8	0.81	0.81	0.81	0.81	0.81	0.81	0.81	0.81	0.81	0.81	0.81	0.81
Incentives amount /year	2.09	2.09	2.09	2.09	2.09	2.09	2.09	2.09	2.09	2.09	2.09	2.09
Levelized and annual cost of	7.49	7.50	7.52	7.53	7.55	7.56	7.58	7.77	7.79	7.81	7.83	7.92
Levelized Cost Of Energy in Cents/kWh 7.64												
Cash available for debt service	2.14	2.14	2.14	2.14	2.14	2.14	2.14	2.14	2.14	2.14	2.14	2.14
DSCR	1.34	1.34	1.34	1.34	1.34	1.34	1.34	1.34	1.34	1.34	1.34	1.34
Discount rate (8.0%)	1.08	1.17	1.26	1.36	1.47	1.59	1.71	4.00	4.32	4.66	5.03	6.85
Present value	1.98	1.84	1.70	1.57	1.46	1.35	1.25	0.54	0.50	0.46	0.43	0.31
Fixed O&M, fuel and other	2.12	1.96	1.82	1.69	1.57	1.46	1.35	0.59	0.55	0.51	0.48	0.35
Total	4.10	3.80	3.52	3.27	3.03	2.81	2.60	1.13	1.05	0.97	0.90	0.67
IRR	16.49%											
ROI	8.40											
NPV	21.30											

The economic analysis is conducted considering 25 years economic life span of the technologies used in the hybrid energy system. In the analysis, an average cost per exergy unit is determined for LFR, PTC and ST – solar field (input fuel) which were estimated at 4.93 USD/GJ, 2.31 USD/GJ and 5.32 USD/GJ, respectively. While the biomass fuel was estimated at 3.84 USD/GJ with a possible variation due to annual inflation which is considered as an operating expenditure.

To summarize, the hybrid energy system using the linear Fresnel reflector and biomass – fired technology in the sub-Saharan region presents the better economic parameters. The levelized cost of electricity is between 76.4 - 143.4 USD/MWh.

The hybrid energy system based on the parabolic trough collector and biomass–fired technology present a levelized cost of electricity estimated between 147.2 USD/MWh and 214.2 USD/MWh. The hybrid energy system using the solar tower and biomass–fired technology presents a levelized cost of electricity is estimated between 159.2 USD/MWh and 226.2 USD/MWh.

The hybrid energy systems based on the various combination of the biomass – fired and solar technologies : case 1: PTC–BF , case 2: ST–BF and case 3: LFR–BF, presented an internal rate of the return estimated at 13.79%, 12.64% and 16.49%, respectively; a return on investment (ROI) after a period of 10.62 years, 14.71 years and 8.40 years, respectively and a net present value (NPV) estimated at 23.4 Million USD, 23.45 Million USD and 21.30 Million USD dollar respectively. The levelized cost of energy is the main parameter which is highlighted in the recent studies of hybrid energy systems in order to improve the initial investment and easy development of hybrid energy system in the targeted countries.

6.5 Advanced Exergy and Exergoeconomic Analysis

6.5.1 Advanced exergy and exergoeconomic analysis of solar power system using parabolic trough collector technology

The exergy analysis of the studied hybrid energy system is achieved through the utilization of various mathematical models. Table 6.30 presents some results which have been obtained using thermodynamic properties of specific points. The exergy destruction of the solar power system using parabolic trough collector technology presented in Table 6.30 indicates, the avoidable-endogenous exergy destruction estimated at 498.81 kW in the HRSG subsystem which owns the major part of exergy destruction forms. Although, it is poorly represented in the systems where it represents less than 11.13% of the total avoidable - endogenous exergy destruction. It found an avoidable-endogenous exergy destruction of 14.13 kW in the power block. The cumulative value of the endogenous - avoidable exergy destruction of the absorption refrigeration subsystem and drying subsystem is estimated at 10.57 kW, which is equal to 0.23% of the total exergy destruction of the integrated absorption refrigeration unit.

Given the results obtained from the advanced exergetic and techno-economic analysis of the hybrid energy system, the exergy cost and capital cost associated with exergy destruction forms presented in the previous section have been determined. During this analysis the cost exergy associated with exergy destruction and capital cost associated with exergy destruction for each equipment that enters into the constitution of the hybrid energy system were found. The power block of the solar power system using parabolic trough collector is estimated at 98.27 kW. Its exergy destruction constitutes less than 2.35% of the total exergy destruction of the power system using parabolic collector. The major contribution in term of exergy destruction is the low-pressure turbine with 76.2 kW which represents 77.54% of exergy destruction. The avoidable-endogenous exergy destruction of the power block estimated at 14.37% of the exergy destruction. During the advanced exergy analysis of the power block subsystem, it was observed that there is large amount of the exergy destroyed by turbines compared to other components such as condenser or pumps. Due to these results,

a comparative analysis of different subsystems has been conducted to evaluate their impact in the studied power system. Although, it plays a key role for the electricity generation, the power system is the most efficiency subsystem, followed by absorption refrigeration and drying subsystem, heat recovery steam generation (HRSG) subsystem and solar – field (SF) subsystem with values of 599.58 kW, 1335. 98 kW and 5408.30 kW, respectively. The solar – field and HRSG constitute important parts of the power system required for optimization of the hybrid system.



Table 6.30. Advanced exergy analysis of the power system based on PTC technology.

PTC power system components	Exergy fuel (kW)	Exergy prod. and loss (kW)	Exergetic eff. η_{ex}	Exergy destruction (kW)	Exergy destruction ration Y_d (kW)	Y_d^*	Un. Conditions / Exergy eff. (UN)	$\frac{\dot{E}_d}{\dot{E}_P} \times UN$	Un. Ex. \dot{E}_d^{UN} in (kW)	Avoidable \dot{E}_d^{AV} in (kW)	$\frac{\dot{E}_d}{\dot{E}_P} \times \eta_{ex}$	Endo. \dot{E}_d^{En} in (kW)	Exo. \dot{E}_d^{Ex} in (kW)	Endo. Prod. \dot{E}_P^{En} in (kW)	Un./Endo. $\dot{E}_d^{UN,EN}$ in (kW)	Un/ Exo. $\dot{E}_d^{UN,EX}$ in (kW)	Av./ Endo. $\dot{E}_d^{AV,EN}$ in (kW)	Av./ Exo. $\dot{E}_d^{AV,EX}$ in (kW)	
Solar field	35490	20870	0.59	14620	0.41	0.73	0.62	0.43	8179.86	6440.14	0.41	8597.3	6022.7	12272.67	4810.2	3369.7	3787.1	2653.00	
Solar rec.- IHE	20870	15981	0.77	4889	0.23	0.24	0.77	0.24	92.72	4796.28	0.23	3743.70	1145.30	12237.30	71.00	21.72	3672.7	1123.58	
IHE1	15981	15790	0.99	191.1	0.01	0.01	0.50	0.01	2.31	188.79	0.01	188.82	2.29	15601.08	2.29	0.03	186.5	2.26	
Inter. HE 1	15461	15149.5	0.98	311.4	0.02	0.02	0.91	0.02	212.06	99.34	0.02	305.12	6.27	14844.43	207.79	4.27	97.3	2.00	
Inter. HE 2 Solar	36.55	19.8	0.54	16.8	0.46	0.00	0.87	0.74	16.36	0.41	0.46	9.08	7.69	10.71	8.85	7.51	0.22	0.19	
Power block System																			
HP Turbine - BP	4061.73	4048.7	1.00	12.9	0.00	0.01	0.95	0.00	9.58	3.38	0.00	12.92	0.04	4035.84	9.55	0.03	3.37	0.01	
LP Turbine- BP	1293.52	1217.3	0.94	76.2	0.06	0.05	0.95	0.06	65.84	10.34	0.06	71.69	4.49	1145.65	61.96	3.88	9.73	0.61	
Turbine ORC	31.34	25	0.80	6.35	0.20	0.00	0.91	0.23	5.54	0.80	0.20	5.06	1.29	19.92	4.42	1.12	0.64	0.16	
Condenser ORC	9.34	6.6	0.70	2.8	0.30	0.00	0.83	0.35	2.32	0.45	0.30	1.95	0.82	4.63	1.63	0.69	0.32	0.13	
Pump ORC	7.10	4.98	0.70	2.1	0.30	0.00	0.95	0.40	2.02	0.09	0.30	1.49	0.63	3.50	1.42	0.60	0.07	0.03	
HRSG System																			
Regen -1	3691.58	2470.9	0.67	1220.6	0.33	0.85	0.50	0.25	602.98	617.65	0.33	817.03	403.61	1653.92	403.61	199.38	413.42	204.23	
Regen - 2	683.95	648.8	0.95	35.2	0.05	0.02	0.98	0.05	33.13	2.03	0.05	33.36	1.81	615.43	31.43	1.70	1.93	0.10	
Regen - 3	1556.47	1477.2	0.95	79.2	0.05	0.06	0.98	0.05	74.64	4.59	0.05	75.20	4.03	1402.03	70.84	3.80	4.36	0.23	
Pump BPP	290.37	289.4	1.00	0.98	0.00	0.00	0.90	0.00	0.52	0.46	0.00	0.97	0.00	288.42	0.52	0.00	0.46	0.00	
Deaerator	2413.26	116	0.05	2297.3			0.42	8.26	661.04	1636.24	0.95	110.41	2186.87	5.57	31.77	629.27	78.64	1557.60	
Absorption refrigeration system																			
HE	210.61	92.34	0.44	118.3	0.56	0.79	0.87	1.11	95.36	22.90	0.56	51.85	66.41	40.49	53.81	41.55	1.95	24.86	
Condenser	2.16	1.40	0.65	0.7	0.35	0.01	0.96	0.52	0.75	0.02	0.35	0.49	0.27	0.91	0.48	0.26	0.01	0.01	
Absorber	25.07	2.26	0.09	22.8	0.91	0.15	0.96	9.70	2.48	20.34	0.91	2.05	20.76	0.20	0.22	2.25	1.83	18.51	
Evaporator	5.23	1.87	0.36	3.4	0.64	0.02	0.97	1.74	1.90	1.46	0.64	1.20	2.16	0.67	0.68	1.22	0.52	0.93	
Generator	42.06	37.67	0.90	4.4	0.10	0.03	0.97	0.11	4.11	0.28	0.10	3.93	0.46	33.73	3.68	0.43	0.25	0.03	
IHE	4.89	4.01	0.82	0.88	0.18	0.01	0.97	0.21	0.83	0.05	0.18	0.72	0.16	3.29	0.68	0.15	0.04	0.01	
Drying system																			
Air Compressor	80.00	59.81	0.75	20.2			0.95	0.32	19.07	1.12	0.25	15.09	5.09	44.72	14.25	4.81	0.84	0.28	
Dryer	434.28	5.34	0.01	428.9	0.99		0.82	65.92	11.75	417.19	0.99	5.27	423.68	0.07	0.14	11.61	5.13	412.07	

The heat recovery steam generation is generally utilized to recover the heat exhausted from steam turbine. It contains an economizer, an evaporator and super heater named regenerator 1, 2, and 3. The treated water enters the heat recovery steam generation system in the liquid state and exits as a steam water. During this process, the exergy balance equations of each regenerator have been established in chapter 5 to determine the exergy destruction forms and particularly the avoidable-endogenous exergy destruction.

The exergy destruction in o the PTC's receiver, regenerator 1, intermediate heat exchanger (IHE), heat exchanger (HE), regenerator 3, and Low-pressure steam turbine are estimated at 4889 kW, 1220.6 kW, 311,4 kW, 118.3 kW, 79.2 kW and 76.2 kW, respectively. The optimization analysis on these components can improved the performance of the power system by recovering more than 4.2 MW. However, it is important to notice that, the improvement of heat exchanger (HE) consist of the recovering of less than 1% of the exergy destruction. Because its avoidable-endogenous exergy destruction is equal to 1.95 kW. These components are responsible of major part of the total exergy destruction which can be recovered through optimization analysis. The results of the advanced exergy analysis, provided in table below shows the endogenous exergy destruction of each components which indicates that, the important irreversibility source in the component itself is not his interaction with others components and the environment. It has also revealed that, the heat exchanger has a large potential in the optimization work of the studied power system performance by reducing its avoidable exergy destruction through enhancing component selection.

In the section 4.4 several methodologies used to conduct the exergoeconomic analysis are presented. Therefore, for these approaches to be implemented the definition of the Fuel – Product – Loss (F – P – L) concept have been explained including the advanced exergy destruction of component. The exergoeconomic costs basically stand for monetary costs of the stream of matter and energy flows. Hence, the function of the exergoeconomic cost for incoming and outgoing stream of matter and exergy are connected with the work transfer and the exergy related to heat transfer and work. To achieve the analysis for each stream and later for each component, the capital cost of all equipment summarized

in Tables 5.1 and 5.3 have been correlated by equations (Couper, et al., 2012; Dincer and Ratlamwala, 2016). Thereafter, an individual cost associated to the specific exergy destruction for each component used in the power system was determined. To do that, auxiliaries equations based on the $(F - P - L)$ concept was used for a number of components. This led to a system of equations containing the costing equation and auxiliary equations for each component. In chapter 4, a stream analysis is conducted to evaluate, the cost of the income water streams and the cost of the exhausted non-saturated water of streams. Table 6.31 summarizes the results for the exergoeconomic analysis, which presents essential results such as the exergy cost and the capital rate cost associated to specific exergy destruction (unavoidable, avoidable, endogenous and exogenous) and others. The total cost containing cost rate related to the investment and the O&M cost associated to specific exergy destruction such as unavoidable–endogenous, avoidable– endogenous, unavoidable – exogenous and avoidable – exogenous.

As shown in Table 6.32, the regenerator 1 has the highest total capital cost associated to exergy destruction estimated at 140.11 USD. This value is the sum of Z and C_D , it is a relative high value of the exergoeconomic factor presented in Table 6.33. It is the expression of the cost rate associated to the initial investment and the O&M cost domination. The sum of the total exergy cost associated to exergy destruction depends on the purchased equipment cost (SPEC) of the solar power system using Parabolic Trough Collector technology. The main reason which increases the total cost rate is the capital investment and according to the type of the component analyzed its contribution may affect studied system significantly. The ratio between the initial investment of biomass – fired power system and solar power system depends on the type the technology used; this value varying from 11.31% to 24.01%. However, the biomass-fired technology is associated to the use of annual operating expenditure, which contribute to the increasing of the levelized cost of energy as shown in many studies. The associated cost with avoidable-endogenous exergy destruction is a main parameter for hybrid system optimization analysis.

Table 6.31. Advanced exergoeconomic analysis of the power system based on PTC.

PTC Power plant components	Exergy cost associated to Un. ex. \dot{C}^{UN} (10^{-3} USD/s)	Exergy cost associated to Av. ex. \dot{C}^{AV} (10^{-3} USD/s)	Exergy cost associated to En. ex. \dot{C}^{EN} (10^{-3} USD/s)	Exergy cost associated to Ex. ex. \dot{C}^{EX} (10^{-3} USD/s)	Exergy cost associated to Un. /En. ex $\dot{C}^{UN,EN}$ (10^{-3} USD/s)	Exergy cost associated to Un. /Ex. ex $\dot{C}^{UN,EX}$ (10^{-3} USD/s)	Exergy cost associated to AV/En. ex $\dot{C}^{AV,EN}$ (10^{-3} USD/s)	Exergy cost associated to AV/Ex. ex $\dot{C}^{AV,EX}$ (10^{-3} USD/s)	Exergy cost associated to exergy destruction \dot{C}_k (10^{-3} USD/s)	\dot{Z}_k/\dot{E}_k	Capital cost rate associated to Un. ex. \dot{Z}^{UN} (10^{-3} USD/s)	Capital cost rate associated to Av. ex. \dot{Z}^{AV} (10^{-3} USD/s)	Capital cost rate associated to En. ex. \dot{Z}^{EN} (10^{-3} USD/s)	Capital cost rate associated to Ex. ex. \dot{Z}^{EX} (10^{-3} USD/s)	Capital cost rate associated to un. En. ex. $\dot{Z}^{UN,EN}$ (10^{-3} USD/s)	Capital cost rate associated to Un. Ex. ex. $\dot{Z}^{UN,EX}$ (10^{-3} USD/s)	Capital cost rate associated to Av./En. ex. $\dot{Z}^{AV,EN}$ (10^{-3} USD/s)	Capital cost rate associated to Av./Ex. ex. $\dot{Z}^{AV,EX}$ (10^{-3} USD/s)
Solar field																		
IHE1	0.041	3.349	0.00021	3.350	0.041	276.785	0.041	0.0005	276.87	0.017	140.07	140.07	276.79	3.35	138.39	1.67	138.39	1.67
IHE1 - PB	3.827	1.793	0.00036	5.506	0.113	267.889	3.750	0.077	271.83	0.0003	4.29	0.42	4.62	0.09	4.21	0.09	0.42	0.01
IHE2Solar	2.753	0.069	0.07720	1.527	1.295	1.801	1.490	1.263	5.85	0.015	0.27	0.04	0.17	0.14	0.15	0.13	0.02	0.02
Solar subsystem																		
HP Turbine	0.266	0.094	0.00009	0.359	0.001	112.198	0.265	0.001	112.47	0.01	37.64	1.98	39.49	0.13	37.52	0.12	1.97	0.01
LP Turbine	1.794	0.282	0.00161	1.954	0.122	31.225	1.689	0.106	33.14	0.01	11.32	0.60	11.21	0.70	10.65	0.67	0.56	0.04
Turbine ORC	1.159	0.168	0.04234	1.058	0.269	4.163	0.924	0.235	5.59	0.051	1.16	0.11	1.02	0.26	0.93	0.24	0.09	0.02
Condenser ORC	0.008	0.002	0.00105	0.007	0.003	0.016	0.006	0.002	0.03	0.175	0.95	0.20	0.81	0.34	0.67	0.28	0.14	0.06
Pump ORC	0.311	0.014	0.04579	0.228	0.097	0.537	0.218	0.093	0.94	0.116	0.55	0.03	0.40	0.17	0.38	0.16	0.02	0.01
Regen -1	10.897	11.162	0.00598	14.765	7.294	29.890	7.294	3.603	48.08	0.00004	0.05	0.05	0.06	0.03	0.03	0.02	0.03	0.02
Regen - 2	0.599	0.037	0.00093	0.603	0.033	11.125	0.568	0.031	11.76	0.00003	0.02	0.0004	0.02	0.001	0.02	0.001	0.0004	0.00002
Regen - 3	1.349	0.083	0.00092	1.359	0.073	25.337	1.280	0.069	26.76	0.00003	0.04	0.0008	0.04	0.002	0.04	0.002	0.0007	0.00004
Pump BPP	0.007	0.006	0.00005	0.014	0.000	4.020	0.007	0.00002	4.03	0.004	1.07	0.12	1.18	0.004	1.07	0.004	0.12	0.00040
Deaerator	12.803	31.690	0.01844	2.138	42.354	0.108	0.615	12.187	55.26	0.11385	5.51	7.70	0.63	12.57	0.26	5.24	0.37	7.326
Absorption Refrigeration System																		
Condenser	0.035	0.001	0.01638	0.023	0.013	0.042	0.022	0.012	0.09	0.033	0.05	0.0019	0.03	0.02	0.03	0.02	0.0012	0.0007
Absorber	0.101	0.828	0.03704	0.084	0.845	0.008	0.009	0.092	0.95	0.1799	0.39	0.0162	0.04	0.37	0.04	0.35	0.0015	0.0148
Evaporator	0.063	0.048	0.02118	0.040	0.071	0.022	0.022	0.040	0.16	0.024	0.04	0.0013	0.02	0.03	0.02	0.03	0.0005	0.0009
Generator	0.101	0.007	0.00256	0.096	0.011	0.827	0.090	0.011	0.94	0.007	0.26	0.0082	0.24	0.03	0.24	0.03	0.0073	0.0009
IHE	0.023	0.001	0.00503	0.020	0.004	0.092	0.019	0.004	0.12	0.00076	0.003	0.0001	0.003	0.001	0.002	0.001	0.0001	0.0000

Power block is presented as the main subsystem which needs to be checked for any improvement, the tables show an associated cost with exergy destruction at 55.17 USD.

During the analysis of the absorption refrigeration system, the highest form of exergy destruction is found in the heat exchanger which represents more than 90% of the exergy destruction of the solar power system based on parabolic trough collector. Meanwhile the lowest exergy destruction was found in the condenser of the studied absorption refrigeration system. The exergoeconomic analysis of the absorption refrigeration system contribute to a better understanding of the relation between the exergy destruction and the initial investment. It shows the impact of the well selection of the major components such as absorber, generator, condenser and evaporator. The avoidable-endogenous exergy destruction of these components was estimated at 2,61 kW and the associated cost at 153.5 USD. For the other exergy destruction forms the cost associated can be classified as follows: unavoidable–endogenous exergy destruction (1329 USD), unavoidable– exogenous exergy destruction (1270 USD) and avoidable–exogenous exergy destruction (172.3 USD). Compared to the standalone power system, the improvement cost of the ARS unit based on the exergy destroyed was estimated at 2924.8 USD, which is an acceptable investment. The optimization cost of the main component is estimated at approximately 97.3 USD with recovery period of less than 1 year.

A joint analysis of the associated cost and capital cost associated with exergy destruction led to the determination of the total cost associated with the exergy destruction of each component put together for its exergoeconomic evaluation. Table 6.32 presents the sum of $(\dot{Z} + \dot{C}_D)$, while the sum of $(\dot{Z}_k^{AV} + \dot{C}_{D,k}^{AV})$ gives a better realistic picture of the potential to achieve cost saving in the component that need to be improved. According to the previous studies and the above assumptions. The percentage of the total cost of component, is theoretical between 45% and 80%. Considering the avoidable costs emphasizes, the cost – effectiveness of some key components used in the power block or HRSG subsystem require improvement.

Table 6.32 presents major components which need to be improved in priority according to their importance and the cost associated in the power system. According to results presented in the table below, the regenerator 1 (7.33 USD/hour), the intermediate heat exchanger connected to power block (4.17 USD/hour) and the steam turbines (4.49 USD/hour) are the components which highlighted the interest for optimization analysis. Furthermore, the total cost associated with avoidable-endogenous exergy destruction is more than 24% of the total cost required for system optimization.

Table 6.32. Advanced analysis of the total cost associated with exergy destruction of components used for power system based on PTC technology.

PTC - Power plant components	Total cost associated to Un. ex. \dot{T}^{UN} (USD/h)	Total cost associated to Av. ex. \dot{T}^{AV} (USD/h)	Total cost associated to En. ex. \dot{T}^{EN} (USD/h)	Total cost associated to Ex. ex. \dot{T}^{EX} (USD/h)	Total cost associated to Un./En. ex. $\dot{T}^{UN,EN}$ (USD/h)	Total cost associated to Un./Ex. ex. $\dot{T}^{UN,EX}$ (USD/h)	Total cost associated to Av./En. ex. $\dot{T}^{AV,EX}$ (USD/h)	Total cost associated to Av./Ex. ex. $\dot{T}^{AV,EX}$ (USD/h)
Solar field								
Solar receiver-IHE								
IHE1	140.11	143.42	276.79	6.70	138.43	278.46	138.43	1.68
Inter. HE 1	8.12	2.22	4.62	5.60	4.32	267.98	4.17	0.09
Inter. HE 2-Solar	3.03	0.11	0.25	1.67	1.44	1.93	1.51	1.28
Solar subsystem								
HP Turbine -SP	37.90	2.07	39.49	0.49	37.52	112.32	2.24	0.01
LP Turbine- SP	13.11	0.88	11.21	2.66	10.77	31.89	2.25	0.14
Turbine ORC	2.32	0.28	1.06	1.32	1.19	4.40	1.02	0.26
Condenser ORC	0.96	0.20	0.81	0.35	0.67	0.30	0.14	0.06
Pump ORC	0.86	0.04	0.45	0.40	0.48	0.70	0.24	0.10
Regen -1	10.94	11.21	0.07	14.80	7.33	29.91	7.33	3.62
Regen - 2	0.62	0.04	0.02	0.60	0.05	11.13	0.57	0.03
Regen - 3	1.39	0.08	0.04	1.36	0.11	25.34	1.28	0.07
Pump BPP	1.08	0.13	1.19	0.02	1.07	4.02	0.13	0.00
Deaerator	18.31	39.39	0.65	14.71	42.62	5.35	0.99	19.51
Absorption Refrigeration System								
Condenser	0.00	0.00	0.00	0.00	0.00	0.00	0.00	0.00
Absorber	0.08	0.0028	0.05	0.04	0.04	0.06	0.02	0.01
Evaporator	0.49	0.84	0.07	0.45	0.88	0.36	0.01	0.11
Generator	0.11	0.05	0.04	0.07	0.09	0.05	0.02	0.04
IHE	0.36	0.02	0.25	0.12	0.25	0.85	0.10	0.01

The analysis of solar field, power block, heat steam generation s and additional units such as absorption refrigeration and drying unit is carried out. The results of the total cost associated with the specific exergy destruction show that,

the solar field has the highest cost rate of exergy destruction, followed by power block, HRSG and additional units.

Table 6.32 presents this monthly shortfall of each components and this lack is determined through avoidable - endogenous exergy destruction. It is important to note that, the solar field alone accounts for 86.3% of all exergy destruction followed by the HRSG system and power block system, hence optimization will help to make the hybrid system more efficient. While the power block subsystem is one of the major sources in terms of reducing the shortfall and optimization of the hybrid system with a percentage of 7.69%. The sensitivity analysis of the studied system is based on the cost of main components presented in Table 6.33 and 6.34.

Table 6.33. Endogenous avoidable exergy cost analysis of component used for the power system based on PTC technology.

Component of studied system	Expend. Req. Jan (USD)	Expend. Req. Feb (USD)	Expend. Req. Mar (USD)	Expend. Req. Apr (USD)	Expend. Req. May (USD)	Expend. Req. June (USD)	Expend. Req. Jul (USD)	Expend. Req. Aug (USD)	Expend. Req. Sep (USD)	Expend. Req. Oct (USD)	Expend. Req. Nov (USD)	Expend. Req. Dec (USD)
IHE1 -Solar Field-Receiver	39481.16	35272.79	33044.01	28240.38	27465.15	22841.48	18453.15	18453.15	21180.29	25319.44	36961.67	40339.45
Inter. HE 1	1188.05	1061.42	994.35	849.80	826.47	687.34	555.29	555.29	637.35	761.90	1112.24	1213.88
Inter. HE 2-Solar	431.19	385.23	360.88	308.42	299.96	249.46	201.53	201.53	231.32	276.52	403.67	440.56
HP Turbine	638.86	570.77	534.70	456.97	444.43	369.61	298.60	298.60	342.73	409.71	598.09	652.75
LP Turbine	641.51	573.13	536.91	458.86	446.27	371.14	299.84	299.84	344.15	411.40	600.57	655.45
Turbine ORC	289.59	258.72	242.37	207.14	201.45	167.54	135.35	135.35	155.36	185.72	271.11	295.89
Condenser ORC	40.85	36.50	34.19	29.22	28.42	23.64	19.10	19.10	21.92	26.20	38.25	41.74
Pump ORC	67.97	60.72	56.89	48.62	47.28	39.32	31.77	31.77	36.46	43.59	63.63	69.45
Regen - 1	2089.31	1866.61	1748.66	1494.46	1453.43	1208.75	976.52	976.52	1120.84	1339.88	1955.98	2134.73
Regen - 2	162.16	144.88	135.72	115.99	112.81	93.82	75.79	75.79	86.99	104.00	151.81	165.69
Regen - 3	365.34	326.40	305.77	261.32	254.15	211.36	170.76	170.76	195.99	234.29	342.02	373.28
Pump BPP	35.86	32.03	30.01	25.65	24.94	20.74	16.76	16.76	19.24	22.99	33.57	36.63
Deaerator	280.97	251.02	235.16	200.98	195.46	162.56	131.32	131.32	150.73	180.19	263.04	287.08
Condenser	6.72	6.01	5.63	4.81	4.68	3.89	3.14	3.14	3.61	4.31	6.30	6.87
Absorber	3.01	2.69	2.52	2.15	2.09	1.74	1.41	1.41	1.61	1.93	2.81	3.07
Evaporator	6.54	5.84	5.47	4.68	4.55	3.78	3.06	3.06	3.51	4.19	6.12	6.68
Generator	27.82	24.85	23.28	19.90	19.35	16.09	13.00	13.00	14.92	17.84	26.04	28.42
IHE	5.47	4.89	4.58	3.91	3.81	3.17	2.56	2.56	2.94	3.51	5.12	5.59

In this research, advanced exergy and exergoeconomic analysis have been done for a direct steam generation power system. The maximum monthly

expenditure required to optimize the power system considering each subsystem can be presented as follows: 40339.45 USD for solar field subsystem, 1715.28 USD for power block and 2997.41 USD for heat recovery steam generation system.

Table 6.34. Data obtained from avoidable cost rates of exergy destruction in the power system based on PTC technology.

LFR SP Components	r_k	f_k	$\epsilon_{modified}$	$f_k^{AV,EN}$	f_{k-opt}	$\dot{T}_D^{AV,EN}$ (USD/s)	$\dot{C}_D^{AV,EN}$ (USD/s)	$\dot{C}_D^{AV,EX}$ (USD/s)	\dot{C}_D^{AV} (USD/s)
Solar field	0.701		0.846						
Receiver - IHE	0.306		0.813						
IHE	0.012	0.988	0.988	0.977	0.994	138.43	0.041	0.0005	3.349
Inter. HE 1	0.021	0.456	0.994	0.191	0.479	4.17	3.750	0.077	1.793
Inter. HE 2- Solar	0.848	0.100	0.989	0.372	0.052	1.51	1.490	1.263	0.069
HP Turbine -SP	0.003	0.991	0.999	0.955	0.993	2.24	0.265	0.001	0.094
LP Turbine- SP	0.063	0.852	0.992	0.679	0.876	2.25	1.689	0.106	0.282
Turbine ORC	0.254	0.490	0.975	0.406	0.801	1.02	0.924	0.235	0.168
Condenser ORC	0.421	0.992	0.954	0.992	0.848	0.14	0.006	0.002	0.002
Pump ORC	0.425	0.640	0.987	0.668	0.813	0.24	0.218	0.093	0.014
Regen -1	0.494	0.004	0.857	0.003	0.004	7.33	7.294	3.603	11.162
Regen - 2	0.054	0.032	0.997	0.011	0.036	0.57	0.568	0.031	0.037
Regen - 3	0.054	0.026	0.997	0.009	0.029	1.28	1.280	0.069	0.083
Pump BPP	0.003	0.989	0.998	0.949	0.991	0.13	0.007	0.00002	0.006
Deaerator	-	0.229	0.596	0.195	0.209	0.99	0.615	12.187	31.690
Condenser	0.546	0.572	0.991	0.682	0.590	0.00	0.022	0.012	0.001
Absorber	10.104	0.304	0.552	0.019	0.307	0.02	0.009	0.092	0.828
Evaporator	1.796	0.286	0.782	0.027	0.305	0.01	0.022	0.040	0.048
Generator	0.117	0.716	0.993	0.541	0.781	0.02	0.090	0.011	0.007
IHE	0.219	0.111	0.990	0.075	0.114	0.10	0.019	0.004	0.001

Table 6.34 presents exergoeconomic factor of each component. The avoidable-endogenous exergoeconomic factor of the intermediate heat exchanger1, Low-pressure turbine, regenerator 1 and regenerator 2 are less than the standard exergoeconomic factor. The recovered amount of the avoidable-endogenous exergy destruction led to the determination of optimized

exergoeconomic factor as shown during the analysis of the heat exchanger (IHE and IHE1), low-pressure turbine, ORC turbine water pump and regenerator. The increasing variation lays between 0.2% and 38.8%, with the highest increasing found for the ORC turbine which varies from 49% to 80.1%. The lowest variation has been found for the water pump which has an optimized exergoeconomic factor of 99.1%.

6.5.2 Advanced exergy and exergoeconomic analysis of solar power system using solar tower technology

The exergy analysis of the studied power system is achieved through the utilization of various mathematical models. Table 6.35 presents some results of state points which have obtained using thermodynamic properties (pressure, temperature, enthalpy and entropy). The mathematical models of the component helped to determine the results for the exergy destruction forms related to their usage. The exergy destruction distribution of the solar power system based on solar tower technology presented in the table below indicates that, the avoidable-endogenous is estimated at 158.5 kW in the HRSG subsystem which is less important than unavoidable-endogenous exergy destruction. Although, it is represented in the systems where it owns more than 9.2% of the total avoidable-endogenous exergy destruction. The combined Rankine cycles is considered as power block contains many components such as steam turbines, gas turbines, condenser, heat exchanger and pump which are evaluated during the analysis. The results indicated that, the endogenous-avoidable exergy destruction occurring inside the power block can be estimated at 35.25 kW. While the cumulative value of the endogenous-avoidable exergy destruction of the absorption refrigeration subsystem and drying subsystem is estimated at 62.53 kW, which represents 9.86% of total absorption refrigeration and drying subsystem exergy destruction. According to these results, the optimization analysis is required for both absorption refrigeration and drying unit in order to improve system performances.

The results obtained from the advanced exergetic and techno-economic analysis of the hybrid energy system are contributed to determination of the equipment cost and capital cost associated with different exergy destruction forms presented in Table 6.35. During this analysis, for each equipment which enters in

the hybrid energy system designing the cost and capital cost associated with exergy destruction is determined. Hence, for the power block of the solar power system using solar tower technology, exergy destruction is estimated at 332.62 kW which constitutes less than 5.45% of the total exergy destruction. The low-pressure turbine is the major contribution in term of exergy destruction with 273.71 kW which represents 82.29% of exergy destruction. The avoidable-endogenous exergy destruction of the power block is estimated at 10.6 % of the exergy destruction. During the advanced exergy analysis of the power block subsystem, an important amount of the exergy destroyed by turbines is observed compared to other components such as condenser or pumps. Due to these results, a comparative analysis of different subsystems is carried out to evaluate their impact in the studied power system. Although, it plays key role in the electricity generation, the power block is the most efficiency subsystem, followed by drying system, absorption refrigeration system, HRSG and solar – field with values of 186.93 kW, 447.91 kW, 614.86 kW and 4518.23 kW, respectively.

The solar – field and HRSG contain the most important components of the power system which need to be optimized. The heat recovery steam generator, is generally utilized to recover the heat exhausted from steam turbine. It contains an economizer, an evaporator and super heater named regenerator 1, 2, 3, 4 and 5. The treated water enters the HRSG unit in the liquid state and exits as a steam water. During this process, the exergy balance equations for each regenerator is established in order to identify the generator with the highest exergy destruction and specifically the most important part of the avoidable-endogenous exergy destruction.

The exergy destruction in the solar field-receiver, regenerator 1, generator, Low-pressure steam turbine and regenerator 4 are estimated at 4518.23 kW, 428.5 kW, 281.84 kW, 273.71 kW, and 76.94 kW, respectively. The optimization analysis on these components aims to improve the performance of power system in order to contribute in the recovery of more than 1.8 MW. But it is important to notice that, the improvement of the generator consist of the recovering of less than 4.1% of the exergy destruction. Its avoidable-endogenous exergy destruction is equal to 5.4 kW.

Table 6.35. Advanced exergy analysis of the system based on ST technology.

Component	Exergy fuel (kW)	Exergy prod. and loss (kW)	Exergetic eff. η_{ex} (%)	Exergy destruction (kW)	Exergy destruction ration Y_d (kW)	Y_d^*	Un. Conditions / Exergy eff. (UN)	$\frac{\dot{E}_d}{\dot{E}_P} \times UN$	Un. Ex. \dot{E}_d^{UN} in (kW)	Avoidable \dot{E}_d^{AV} in (kW)	$\frac{\dot{E}_d}{\dot{E}_P} \times \eta_{ex}$	Endo. \dot{E}_d^{En} in (kW)	Exo. \dot{E}_d^{Ex} in (kW)	Endo. Prod. \dot{E}_P^{En} in (kW)	Un./Endo $\dot{E}_d^{UN,EN}$ in (kW)	Un/ Exo. $\dot{E}_d^{UN,EX}$ in (kW)	Av./ Endo. $\dot{E}_d^{AV,EN}$ in (kW)	Av./ Exo. $\dot{E}_d^{AV,EX}$ in (kW)	
Solar	41140.00	17674.00	0.43	23466.00	0.57	0.7279	0.44	0.58	10653.83	12812.17	0.57	10081.14	13384.86	7592.86	4576.95	6076.88	5504.19	7307.98	
Receiver	17674.00	13155.77	0.74	4518.23	0.26	0.1401	0.63	0.22	2411.98	2106.25	0.26	3363.18	1155.05	9792.59	1795.37	616.60	1567.80	538.45	
Boiler-	13155.77	9233.59	0.70	3922.18	0.30	0.1217	0.53	0.23	1835.60	2086.57	0.30	2752.84	1169.33	6480.75	1288.35	547.26	1464.50	622.08	
Solar Field System																			
HP Turbine PB	3077.42	3040.71	0.99	36.71	0.01	0.0011	0.95	0.01	29.10	7.61	0.01	36.27	0.44	3004.43	28.75	0.35	7.52	0.09	
LP Turbine	2596.07	2322.36	0.89	273.71	0.11	0.0085	0.95	0.11	244.58	29.13	0.11	244.85	28.86	2077.50	218.79	25.79	26.06	3.07	
Turbine ORC	31.18	24.86	0.80	6.32	0.20	0.0002	0.91	0.23	5.52	0.80	0.20	5.04	1.28	19.82	4.40	1.12	0.64	0.16	
IHE 2 ORC	30.22	19.68	0.65	10.54	0.35	0.0003	0.87	0.47	9.61	0.94	0.35	6.87	3.68	12.81	6.25	3.35	0.61	0.33	
Cond. ORC	9.77	6.54	0.67	3.23	0.33	0.0001	0.83	0.41	2.79	0.43	0.33	2.16	1.07	4.38	1.87	0.92	0.29	0.14	
Pump ORC	7.06	4.96	0.70	2.11	0.30	0.0001	0.9	0.38	1.91	0.19	0.30	1.48	0.63	3.48	1.34	0.57	0.13	0.06	
Heat Recovery System																			
Regen - 1	1229.14	800.63	0.65	428.50	0.35	0.0115	0.5	0.27	229.34	199.17	0.35	279.12	149.39	521.51	149.39	79.95	129.73	69.43	
Regen - 2	1084.77	1063.96	0.98	20.81	0.02	0.0006	0.98	0.02	19.20	1.61	0.02	20.41	0.40	1043.55	18.83	0.37	1.57	0.03	
Regen - 3	351.68	307.61	0.87	44.07	0.13	0.0012	0.95	0.14	39.78	4.28	0.13	38.54	5.52	269.07	34.80	4.98	3.75	0.54	
Regen - 4	3041.64	2964.70	0.97	76.94	0.03	0.0021	0.98	0.03	71.41	5.53	0.03	74.99	1.95	2889.71	69.61	1.81	5.39	0.14	
Regen - 5	74.31	68.49	0.92	5.81	0.08	0.0002	0.95	0.08	5.11	0.71	0.08	5.36	0.45	63.13	4.71	0.40	0.65	0.06	
Pump BPP	134.22	95.49	0.71	38.73	0.29	0.0010	0.9	0.36	35.03	3.70	0.29	27.55	11.17	67.94	24.92	10.11	2.63	1.07	
Deaerator	203.73	52.27	0.26	151.46	0.74	0.0041	0.45	1.30	93.84	57.62	0.74	38.86	112.60	13.41	24.07	69.76	14.78	42.84	
Absorption refrigeration system																			
Condenser	14.77	13.66	0.92	1.11	0.08		0.96	0.08	1.00	0.11	0.08	1.03	0.08	12.63	0.93	0.08	0.10	0.01	
Evaporator	35.21	15.70	0.45	19.51	0.55		0.97	1.21	15.80	3.71	0.55	8.70	10.81	7.00	7.05	8.76	1.65	2.05	
Absorber	171.88	32.42	0.19	139.45	0.81		0.96	4.13	34.37	105.08	0.81	26.31	113.15	6.12	6.48	27.89	19.82	85.26	
IHE	33.41	27.40	0.82	6.00	0.18		0.965	0.21	5.68	0.32	0.18	4.92	1.08	22.48	4.66	1.02	0.26	0.06	
Generator	539.11	257.26	0.48	281.84	0.52		0.97	1.06	257.97	23.87	0.52	134.50	147.35	122.77	123.10	134.87	11.39	12.48	
Drying system																			
Air Comp.	1400.00	1331.11	0.95	68.89	0.05		0.91	0.05	51.40	17.49	0.05	65.50	3.39	1265.61	48.87	2.53	16.63	0.86	
Dryer	454.86	336.82	0.74	118.04	0.26		0.87	0.30	100.92	17.12	0.26	87.41	30.63	249.41	74.73	26.19	12.68	4.44	

To achieve the analysis for each stream and later for each component, the capital cost of all equipment summarized in Table 6.36 have to be correlated by equations (Sargent and Lundy, 2003; Werner and Kalb, 1993). Thereafter, an individual specific purchased equipment cost associated with the exergy destruction for each component used in the power system is determined. To do that, auxiliaries equations based on the $(F - P - L)$ concept was used for a number of components. This led to a system of equations containing the costing equation and auxiliary equations for each component. Tables below summarize the results for the exergoeconomic analysis. The table present results such as the exergy destruction and the capital rate cost associated with the exergy destruction forms (unavoidable, avoidable, endogenous and exogenous). The total cost contains, cost rate related to the investment and the O&M cost associated with the exergy destruction forms such as unavoidable–endogenous, avoidable–endogenous, unavoidable – exogenous and avoidable – exogenous.

As shown in Table 6.37, the boiler has the highest total capital cost associated with exergy destruction estimated at 120.80 USD. This value is the sum of \dot{Z} and \dot{C}_D , which is high value compared to other values of the exergoeconomic factor presented in Table 6.37. This sum is the expression of the cost rate associated to the initial investment and the O&M cost. The sum of the total exergy cost associated to exergy destruction increases according to the specific purchased equipment cost (SPEC) of the solar power system components based on the solar tower technology. The main reason for the increased total cost rate is the capital investment. According to the studied system and the type of the component analyzed, its contribution may affect it significantly. The biomass-fired technology is associated with high annual operating expenditure, which contribute to the increasing of the levelized cost of energy as observed in many studies. The associated cost with avoidable-endogenous exergy destruction is a main parameter for optimization analysis. During the study, this value has been analyzed for all the component of the studied hybrid energy system.

Table 6.36. Advanced exergoeconomic analysis of the power system based on ST technology.

Component	Exergy cost associated to Un. ex. \dot{C}^{UN} (10^{-5} USD/s)	Exergy cost associated to Av. ex. \dot{C}^{AV} (10^{-5} USD/s)	Exergy cost associated to En. ex. \dot{C}^{EN} (10^{-5} USD/s)	Exergy cost associated to Ex. ex. \dot{C}^{EX} (10^{-5} USD/s)	Exergy cost associated to Un. /En. ex $\dot{C}^{UN,EN}$ (10^{-5} USD/s)	Exergy cost associated to Un. /Ex. ex $\dot{C}^{UN,EX}$ (10^{-5} USD/s)	Exergy cost associated to AV/En. ex $\dot{C}^{AV,EN}$ (10^{-5} USD/s)	Exergy cost associated to AV/Ex. ex $\dot{C}^{AV,EX}$ (10^{-5} USD/s)	Exergy cost associated to exergy destruction \dot{C}_k (10^{-5} USD/s)	\dot{Z}_k / \dot{E}_k	Capital cost rate associated to Un. ex. \dot{Z}^{UN} (10^{-3} USD/s)	Capital cost rate associated to Av. ex. \dot{Z}^{AV} (10^{-3} USD/s)	Capital cost rate associated to En. ex. \dot{Z}^{EN} (10^{-3} USD/s)	Capital cost rate associated to Ex. ex. \dot{Z}^{EX} (10^{-3} USD/s)	Capital Cost rate associated to un. En. ex. $\dot{Z}^{UN,EN}$ (10^{-3} USD/s)	Capital cost rate associated to Un. Ex. ex. $\dot{Z}^{UN,EX}$ (10^{-3} USD/s)	Capital cost rate associated to Av./En. ex. $\dot{Z}^{AV,EN}$ (10^{-3} USD/s)	Capital cost rate associated to Av./Ex. ex. $\dot{Z}^{AV,EX}$ (10^{-3} USD/s)
Solar receiver																		
Receiver																		
Boiler-Superheater	54.49	61.94	81.72	34.71	38.25	16.25	43.47	18.47	116.43	8.25	0.01	66.31	58.80	87.81	37.30	46.54	19.77	41.27
HP Turb. PB	1.16	0.30	1.45	0.02	1.15	0.01	0.30	0.004	1.46	11.08	0.01	29.87	1.57	31.07	0.38	29.52	0.36	1.55
LP Turb. PB	9.52	1.13	9.53	1.12	8.52	1.00	1.01	0.12	10.66	10.82	0.01	22.82	1.20	21.48	2.53	20.41	2.41	1.07
Turb. ORC	1.57	0.23	1.43	0.36	1.25	0.32	0.18	0.05	1.80	78.95	0.09	1.96	0.19	1.72	0.44	1.56	0.40	0.15
IHE 2 ORC	2.07	0.20	1.48	0.79	1.35	0.72	0.13	0.07	2.27	59.78	0.01	0.19	0.03	0.15	0.08	0.13	0.07	0.02
Cond. ORC	0.01	0.001	0.01	0.003	0.01	0.003	0.001	0.0004	0.01	0.85	0.21	1.13	0.23	0.92	0.45	0.76	0.37	0.16
Pump ORC	0.41	0.04	0.31	0.13	0.29	0.12	0.03	0.01	0.45	59.03	0.18	0.79	0.09	0.62	0.26	0.56	0.24	0.06
Regen -1	6.83	5.93	8.31	4.45	4.45	2.38	3.86	2.07	12.76	8.27	0.00005	0.02	0.02	0.02	0.01	0.01177	0.00630	0.01177
Regen - 2	0.60	0.05	0.63	0.01	0.59	0.01	0.05	0.0010	0.65	8.63	0.00003	0.03	0.0006	0.03	0.0006	0.02791	0.00055	0.00057
Regen - 3	1.19	0.13	1.15	0.17	1.04	0.15	0.11	0.02	1.32	8.30	0.00003	0.01	0.0004	0.01	0.0011	0.00730	0.00105	0.00038
Regen - 4	2.18	0.17	2.29	0.06	2.13	0.06	0.16	0.0043	2.35	8.50	0.00002	0.07	0.0014	0.07	0.0018	0.06670	0.00173	0.00136
Regen - 5	0.16	0.02	0.16	0.01	0.14	0.01	0.02	0.0017	0.18	8.49	0.00007	0.00	0.0003	0.00	0.0004	0.00449	0.00038	0.00024
Pump BPP	0.86	0.09	0.68	0.28	0.61	0.25	0.06	0.0263	0.96	6.85	0.01	0.43	0.05	0.34	0.14	0.31	0.12	0.03
Deaerator	0.03	0.02	0.01	0.04	0.01	0.02	0.01	0.02	0.05	0.10	0.17	4.10	5.01	2.34	6.77	1.05	3.05	1.29
Absorption Refrigeration System																		
Condenser	0.04	0.004	0.04	0.003	0.03	0.003	0.004	0.00029	0.04	9.77	0.0034	0.04	0.0019	0.04	0.00	0.04	0.00	0.00
Evaporator	0.53	0.12	0.29	0.36	0.23	0.29	0.05	0.07	0.65	9.24	0.0028	0.04	0.0013	0.02	0.02	0.02	0.02	0.00
Absorber	1.42	4.35	1.09	4.68	0.27	1.15	0.82	3.53	5.77	11.50	0.05	1.54	0.06	0.30	1.30	0.29	1.25	0.01
IHE	0.18	0.01	0.16	0.03	0.15	0.03	0.01	0.00	0.19	9.01	0.00	0.00	0.00	0.00	0.00	0.00	0.00	0.00
Generator	8.27	0.77	4.31	4.72	3.95	4.32	0.37	0.40	9.03	8.90	0.00	1.24	0.04	0.61	0.67	0.59	0.65	0.02

Table 6.37 presents the sum of $(\dot{Z} + \dot{C}_D)$, while the sum of $(\dot{Z}_k^{AV} + \dot{C}_{D,k}^{AV})$ gives a realistic picture of the potential to achieve cost saving in the component that require improvement.

Table 6.37. Advanced analysis of the total cost associated with the exergy destruction of the components used in the power system based on ST technology.

Component	Total cost associated to Un. ex. \dot{T}_{UN} (USD\$/h)	Total cost associated to Av. ex. \dot{T}^{AV} (USD\$/h)	Total cost associated to En. ex. \dot{T}^{EN} (USD\$/h)	Total cost associated to Ex. ex. \dot{T}^{EX} (USD\$/h)	Total cost associated to Un. /En. ex. $\dot{T}_{UN,EN}$ (USD\$/h)	Total cost associated to Un. /Ex. ex. $\dot{T}_{UN,EX}$ (USD\$/h)	Total cost associated to Av./En. ex. $\dot{T}^{AV,EX}$ (USD\$/h)	Total cost associated to Av./Ex. ex. $\dot{T}^{AV,EX}$ (USD\$/h)
Solar receiver								
Receiver								
Boiler-Superheater	120.80	120.74	169.53	72.01	84.79	36.01	84.75	36.00
HP Turb. PB	31.03	1.88	32.52	0.39	30.66	0.37	1.85	0.02
LP Turb. PB	32.34	2.34	31.02	3.66	28.93	3.41	2.09	0.25
Turb. ORC	3.53	0.42	3.15	0.80	2.81	0.71	0.34	0.09
IHE 2 ORC	2.26	0.23	1.62	0.87	1.47	0.79	0.15	0.08
Cond. ORC	1.14	0.23	0.92	0.46	0.77	0.38	0.16	0.08
Pump ORC	1.20	0.13	0.93	0.40	0.84	0.36	0.09	0.04
Regen - 1	6.85	5.95	8.33	4.46	4.46	2.39	3.87	2.07
Regen - 2	0.63	0.05	0.66	0.01	0.61	0.01	0.05	0.00
Regen - 3	1.20	0.13	1.16	0.17	1.05	0.15	0.11	0.02
Regen - 4	2.25	0.17	2.36	0.06	2.20	0.06	0.17	0.00
Regen - 5	0.16	0.02	0.17	0.01	0.15	0.01	0.02	0.00
Pump BPP	1.30	0.14	1.02	0.41	0.92	0.37	0.10	0.04
Deaerator	4.13	5.03	2.35	6.81	1.06	3.07	1.29	3.74
Absorption Refrigeration System								
Condenser	0.08	0.01	0.08	0.01	0.07	0.01	0.01	0.00
Evaporator	0.57	0.12	0.31	0.38	0.25	0.31	0.06	0.07
Absorber	2.97	4.41	1.39	5.99	0.56	2.41	0.83	3.58
IHE	0.19	0.01	0.16	0.04	0.15	0.03	0.01	0.00
Generator	9.50	0.80	4.92	5.39	4.54	4.97	0.38	0.42

The above table presents major components that require improvements according to their rate of optimization in the power system. According to the results presented in Table 6.37, the regenerator 1, the volumetric receiver connected to power block and the steam turbines have an estimated total cost of 3.87 USD/hour, 84.75 USD/hour, 3.94 USD/hour, respectively. These are the components which require optimization analysis to increase hybrid system performance. Furthermore, the total cost associated with avoidable-endogenous exergy destruction is estimated at more than 26% of the total cost required for

system optimization. The analysis of solar field, power block, heat steam generation and additional unit such as absorption refrigeration and drying unit were also conducted. Table 6.37 shows that the solar field has the highest cost rate of exergy destruction, followed by power block, HRSG and additional units.

Table 6.38 presents the monthly shortfall of each components and this lack is determined through avoidable-endogenous exergy destruction. It is important to note that, the solar field alone accounts for 92.2% of all exergy destruction followed by the HRSG system with 4.8% and power block system. Hence, optimization helps to improve the hybrid energy system efficiency.

Table 6.38. Endogenous avoidable exergy cost analysis of component used for power system based on ST technology.

Component	Expend. Req. Jan (USD)	Expend. Req. Feb (USD)	Expend. Req. Mar (USD)	Expend. Req. Apr (USD)	Expend. Req. May (USD)	Expend. Req. Jun (USD)	Expend. Req. Jul (USD)	Expend. Req. Aug (USD)	Expend. Req. Sep (USD)	Expend. Req. Oct (USD)	Expend. Req. Nov (USD)	Expend. Req. Dec (USD)
SF- Rec-Boiler	24169,67	21593,38	20228,96	17288,26	16813,68	13983,15	11296,69	11296,69	12966,20	15500,11	22627,28	24695,10
HP Turbine PB	528,69	472,33	442,49	378,16	367,78	305,87	247,10	247,10	283,62	339,05	494,95	540,18
LP Turbine PB	595,78	532,28	498,64	426,15	414,46	344,68	278,46	278,46	319,62	382,08	557,76	608,73
Turbine ORC	95,77	85,56	80,15	68,50	66,62	55,40	44,76	44,76	51,38	61,42	89,66	97,85
IHE 2 ORC	42,92	38,35	35,92	30,70	29,86	24,83	20,06	20,06	23,03	27,53	40,18	43,86
Cond. ORC	44,65	39,89	37,37	31,94	31,06	25,83	20,87	20,87	23,95	28,64	41,80	45,62
Pump ORC	25,77	23,02	21,57	18,43	17,93	14,91	12,04	12,04	13,82	16,53	24,13	26,33
Regen - 1	1104,84	987,07	924,70	790,28	768,59	639,20	516,39	516,39	592,71	708,54	1034,34	1128,86
Regen - 2	14,12	12,62	11,82	10,10	9,82	8,17	6,60	6,60	7,58	9,06	13,22	14,43
Regen - 3	32,05	28,63	26,82	22,92	22,29	18,54	14,98	14,98	17,19	20,55	30,00	32,74
Regen - 4	47,38	42,33	39,65	33,89	32,96	27,41	22,14	22,14	25,42	30,38	44,35	48,41
Regen - 5	5,75	5,14	4,82	4,12	4,00	3,33	2,69	2,69	3,09	3,69	5,39	5,88
Pump BPP	28,21	25,21	23,61	20,18	19,63	16,32	13,19	13,19	15,14	18,09	26,41	28,83
Deaerator	368,16	328,92	308,14	263,34	256,11	213,00	172,08	172,08	197,51	236,10	344,67	376,17
Absorption system												
Condenser	1,51	1,35	1,27	1,08	1,05	0,88	0,71	0,71	0,81	0,97	1,42	1,55
Evaporator	15,85	14,16	13,26	11,34	11,03	9,17	7,41	7,41	8,50	10,16	14,84	16,19
Absorber	237,53	212,21	198,80	169,90	165,24	137,42	111,02	111,02	127,43	152,33	222,37	242,70
IHE	2,46	2,20	2,06	1,76	1,71	1,42	1,15	1,15	1,32	1,58	2,30	2,51
Generator	109,34	97,68	91,51	78,21	76,06	63,26	51,10	51,10	58,66	70,12	102,36	111,72

According to the high operating temperature in the power block, it becomes one of the major sources in terms of reducing the shortfall and optimize cost-effectiveness of the hybrid energy system with a percentage of 4.85%, behind the HRSG system.

The advanced exergy and exergoeconomic analysis have been conducted for a direct steam generation power system. As seen in Table 6.38, the maximum monthly expenditure required to optimize power system considering each subsystem is estimated as follows with values of 24695.1 USD for solar field, 1362.57 USD for power block, and 1230.32 USD for heat recovery steam generation, respectively. This expenditure does not take into account the equipment which may be required during the optimization analysis.

Table 6.39 presents exergoeconomic factor of each component. The optimized exergoeconomic factor (based on avoidable-endogenous exergy destruction) of the boiler, intermediate heat exchanger 2, Low-pressure turbine, regenerator 1 and regenerator 4 are less than the standard exergoeconomic factor. The recovered avoidable-endogenous exergy destruction led to the optimized exergoeconomic factor as shown during the analysis of the boiler, low-pressure turbine, ORC turbine, water pump and regenerators. The increasing variation is estimated between 8.3% and 18%, the highest increase was found for the boiler which is between 51.8% and 63.2%. The lowest variation was found for the regenerator 3, which has an optimized exergoeconomic factor of 0.7%.

Table 6.39. Data obtained from avoidable cost rates of exergy destruction analysis in the power system based on ST technology.

Component	r_k	f_k	$\varepsilon_{modified}$	$f_k^{AV,EN}$	$f_k - opt$	$\dot{T}_D^{AV,EN}$	$\dot{C}_D^{AV,EN}$ (USD/s)	$\dot{C}_D^{AV,EX}$ (USD/s)	\dot{C}_D^{AV} (USD/s)
Solar receiver	0.828								
Recevier	0.3434		0.7625						
Boiler-Superheater	0.4247	0.5180	0.8935		0.6317				
HP Turbine PB	0.01207	0.9555	0.8631	0.4870	0.9643	0.0023	0.0120763	0.0051297	0.02
LP Turbine PB	0.11786	0.6926	0.9975	0.838	0.7135	0.000514	8.34E-05	1.007E-06	0.00
Turbine ORC	0.2541	0.5451	0.9889	0.5142	0.5714	0.000508	0.0002819	3.322E-05	0.00
IHE 2 ORC	0.535	0.0898	0.9749	0.4597	0.0948	0.00009	5.039E-05	1.28E-05	6.319E-05
Cond. ORC	0.4933	0.9928	0.9698	0.1259	0.9935	0.0004180	3.654E-05	1.958E-05	0.00
Pump ORC	0.4248	0.6633	0.9573	0.9942	0.6778	0.00044	2.48E-07	1.224E-07	0.00
Regen -1	0.5352	0.0028	0.8605	0.0030	0.0040	0.0011	0.0010728	0.0005742	0.001647
Regen - 2	0.0195	0.0430	0.9985	0.0115	0.0463	0.000013	1.36E-05	2.659E-07	1.386E-05
Regen - 3	0.143	0.0066	0.9879	0.0034	0.0072	0.00003	3.111E-05	4.456E-06	0.00
Regen - 4	0.0259	0.0288	0.9981	0.0082	0.0309	0.00004	4.577E-05	1.188E-06	0.00
Regen - 5	0.0848	0.0281	0.9905	0.0117	0.0315	0.000005	5.54E-06	4.702E-07	0.00
Pump BPP	0.4055	0.3339	0.9732	0.3444	0.3497	0.00003	1.802E-05	7.306E-06	0.00
Deaerator	0.8977	0.9941	0.7795	0.9959	0.9947	0.00035	1.454E-06	4.214E-06	0.00
Absorption system									
Condenser	0.0815	0.5418	0.9925	0.3229	0.5656	1.474E-06	9.98E-07	8.138E-08	0.00
Absorber	0.2426	0.0624	0.9047	0.0104	0.0678	0.00001	1.528E-05	1.898E-05	0.00
Evaporator	0.3008	0.2178	0.6206	0.0145	0.2450	0.0002	0.000228	0.0009805	0.00
Generator	0.21901	0.0121	0.9904	0.00794	0.0127	2.397E-06	2.378E-06	5.208E-07	0.00
IHE	0.0955412	0.1236	0.957593	0.047583	0.1282	1.065E-04	0.0001014	0.0001111	0.00

6.5.3 Advanced exergy and exergoeconomic analysis of solar power system using linear Fresnel reflector technology

The exergy destruction distribution of the solar power system using Linear Fresnel Reflector technology presented in Table 6.40 indicates that the avoidable - endogenous is estimated at the value of 570.45 kW in the HRSG subsystem which is important than other forms of exergy destruction. Although, it is represented in the systems where it owns more than 13% of the total avoidable-endogenous exergy destruction.

Table 6.40. Advanced exergy analysis of the power system based on LFR technology.

Component	Exergy fuel (kW)	Exergy prod. and loss (kW)	Exergetic eff. $\eta_{ex}(\%)$	Exergy destruction (kW)	Exergy destruction ratio Y_d (kW)	Y_d^*	Un. Conditions / Exergy eff. (UN)	$\frac{\dot{E}_d}{\dot{E}_P} \times UN$	Un. Ex. \dot{E}_d^{UN} in (kW)	Avoidable \dot{E}_d^{AV} in (kW)	$\frac{\dot{E}_d}{\dot{E}_P} \times \eta_{ex}$	Endo. \dot{E}_d^{En} in (kW)	Exo. \dot{E}_d^{Ex} in (kW)	Endo. Prod. \dot{E}_P^{En} in (kW)	Un./Endo $\dot{E}_d^{UN,EN}$ in (kW)	Un/ Exo. $\dot{E}_d^{UN,EX}$ in (kW)	Av./ Endo. $\dot{E}_d^{AV,EN}$ in (kW)	Av./ Exo. $\dot{E}_d^{AV,EX}$ in (kW)	
Solar field	36750	19760	0.538	16990	0.462	0.787	0.58	0.50	13791.51	3198.5	0.46	9135.30	7 854.70	10624.70	7415.52	6375.99	1719,79	1478,70	
Receiv. -IHE	19760	16810.00	0.851	2950	0.149	0.137	0.77	0.14	8.70	2941.3	0.15	2509.59	440.41	14300.41	7.40	1.30	2502,19	439,11	
IHE 1	16810	15666.30	0.932	1144	0.068	0.053	0.53	0.04	112.29	1031.4	0.07	1065.89	77.81	14600.41	104.65	7.64	961,24	70,17	
IHE 1 -	15339.92	14843.92	0.968	496	0.032	0.023	0.90	0.03	340.00	156.0	0.03	479.96	16.04	14363.95	329.00	10.99	150,96	5,04	
IHE 2-Solar	36.26	20.88	0.576	15	0.424	0.001	0.89	0.66	14.82	0.6	0.42	8.86	6.53	12.02	8.53	6.29	0,33	0,24	
Power block System																			
HP Turbine	3992.04	3983.11	0.998	8.933	0.002	0.007	0.95	0.002	6.48	2.5	0.002	8.91	0.02	3974.20	6.47	0.01	2.45	0.01	
LP Turbine	1310.28	1233.76	0.942	76.52	0.058	0.060	0.95	0.06	66.10	10.4	0.06	72.05	4.47	1161.71	62.24	3.86	9.81	0.61	
Turbine ORC	33.07	26.37	0.797	6.70	0.203	0.005	0.91	0.23	5.85	0.8	0.20	5.34	1.36	21.03	4.67	1.19	0.68	0.17	
Condenser	10.16	6.94	0.683	3.22	0.317	0.003	0.86	0.40	2.84	0.4	0.32	2.20	1.02	4.74	1.94	0.90	0.26	0.12	
Pump ORC	7.49	5.26	0.702	2.23	0.298	0.002	0.9	0.38	2.03	0.2	0.30	1.57	0.67	3.69	1.43	0.61	0.14	0.06	
HRSG System																			
Regen -1	3765.11	2836.70	0.753	928.42	0.247	0.731	0.50	0.16	303.86	624.6	0.25	699.48	228.93	2137.21	228.93	74.93	470.55	154.01	
Regen - 2	270.67	210.22	0.777	60.45	0.223	0.048	0.98	0.28	58.93	1.5	0.22	46.95	13.50	163.27	45.77	13.16	1.18	0.34	
Regen - 3	1626.00	1442.75	0.887	183.25	0.113	0.144	0.98	0.12	175.69	7.6	0.11	162.59	20.65	1280.16	155.89	19.80	6.70	0.85	
Pump BPP	283.59	282.64	0.997	0.96	0.003	0.001	0.90	0.00	0.51	0.4	0.003	0.95	0.0032	281.68	0.51	0.00	0.45	0.00	
Deaerator	2241.53	113.28	0.051	2128.26			0.65	12.21	316.23	1812.0	0.95	107.55	2 020.71	5.72	15.98	300.25	91.57	1720.46	
Absorption refrigeration system																			
HE	214.80	80.08	0.373	134.72	0.627	0.756	0.87	1.46	85.69	49.0	0.63	50.23	84.4917	29.86	31.95	53.74	18.28	30.75	
Condenser	2.16	1.40	0.647	0.76	0.353	0.004	0.96	0.52	0.75	0.0	0.35	0.49	0.2701	0.91	0.48	0.26	0.01	0.01	
Absorber	25.07	2.26	0.090	22.81	0.910	0.128	0.96	9.70	2.48	20.3	0.91	2.05	20.7588	0.20	0.22	2.25	1.83	18.51	
Evaporator	5.23	1.87	0.358	3.36	0.642	0.019	0.97	1.74	1.90	1.5	0.64	1.20	2.1574	0.67	0.68	1.22	0.52	0.93	
Generator	53.367	37.67	0.706	15.70	0.294	0.088	0.97	0.40	15.28	0.4	0.29	11.08	4.6180	26.59	10.78	4.49	0.30	0.12	
IHE	4.891	4.01	0.820	0.88	0.180	0.005	0.97	0.21	0.83	0.0	0.18	0.72	0.1579	3.29	0.68	0.15	0.04	0.01	
Drying system																			
Air	1400	1321.73	0.944	78.27	0.056		0.95	0.06	67.45	10.82	0.06	73.90	4.38	1 247.83	63.68	3.77	10.21	0.60	
Dryer	207.19	117.91	0.569	89.27	0.431		0.87	0.66	85.64	3.64	0.43	50.81	38.47	67.11	48.74	36.90	2.07	1.57	

The power block contains components of the combined Rankine cycles such as steam turbines, gas turbines condenser, heat exchanger and pump. This subsystem has been evaluated during the analysis and the results indicated that, the endogenous-avoidable exergy destruction occurred inside of the power block is estimated at 13.34 kW. The cumulative value of the endogenous-avoidable exergy destruction of the absorption refrigeration subsystem and drying subsystem is estimated at 33.26 kW, which is equal to 9.61 % of the total exergy destruction in the absorption refrigeration subsystem. According to these results, the optimization analysis is required for both absorption refrigeration and drying subsystem in order to improve system performances. The results obtained during the advanced exergetic and techno-economic analysis of the hybrid energy system, contribute to determining the exergy cost and capital cost associated with different exergy destruction forms as presented in the previous section. During this analysis for each equipment used for of the hybrid energy system designing, its cost (specific purchased equipment cost) and capital cost associated with the exergy destruction forms are determined. The power block of the solar power system based on linear Fresnel reflector technology is estimated at 97.61 kW with its exergy destruction that constitutes less than 1.81% of the total exergy destruction. The major contribution in term of exergy destruction is found for the low-pressure turbine with 76.52 kW which represents 78.4% of exergy destruction. The avoidable-endogenous exergy destruction of the power block is estimated at 13.67% of the exergy destruction. During the advanced exergy analysis of the power block subsystem, it is observed a large amount of the avoidable -endogenous exergy destruction of steam turbines compared to other components such as condenser or pumps. Due to these results, a comparative analysis of different subsystems has been conducted to evaluate their impact in the studied power system. Although, its key role for the electricity generation, the power block remains the most efficiency subsystem, followed by drying system, absorption refrigeration, heat recovery steam generation and solar – field with values of 167.54 kW, 178.23 kW, 1172.12 kW and 4094 kW, respectively. The solar–field and HRSG constitute important parts of the power system which need to be optimized.

The exergy destroyed in the LFR's receiver, intermediate heat exchanger (IHE), regenerator 1, regenerator 3, heat exchanger (HE), and low-pressure steam turbine are estimated at 2950 kW, 1144 kW, 928.42 kW, 183.25 kW, 134.72 kW and 76.52 kW, respectively. The optimization analysis on these components consists to improve the power system performance which can contribute to recover more than 3.9 MW. But it is important to notice that the improvement of the regenerator 3 consists to recover less than 4% of the exergy destruction. Its avoidable-endogenous exergy destruction equal to 6.7 kW.

The capital cost requested for optimization of all equipment are summarized in Table 6.41 based on correlated equations (Couper, et al., 2012; Dincer and Ratlamwala, 2016). Then, an individual cost associated to the specific exergy destruction for each component used in the power system is determined. To do that, auxiliaries equations based on the $(F - P - L)$ concept are used for a number of components. This leads to a system of equations containing the costing equation and auxiliary equations for each component. Tables below summarize the results for the exergoeconomic analysis. It presents essential results such as the exergy cost and the capital rate cost associated to specific exergy destruction (unavoidable, avoidable, endogenous and exogenous) and others. The total cost (containing cost rate related to the investment and the O&M cost) associated with specific exergy destruction such as unavoidable–endogenous, avoidable–endogenous, unavoidable–exogenous and avoidable–exogenous.

As shown in Table 6.42, the intermediate heat exchanger has the highest total capital cost associated to exergy destruction estimated at 70.09 USD. This value is the sum of Z and C_D , it is a relative high value of the exergoeconomic factor presented in Table 6.36. It is the expression of the cost rate associated to the initial investment and the O&M cost domination. The sum of the total exergy cost associated with exergy destruction increases because of the specific purchased equipment cost (SPEC) of the solar power system based on linear Fresnel reflector technology. The main reason which increases the total cost rate is the capital investment. According to studied system and the type of the component analyzed its contribution may affect it significantly. The biomass-fired technology usage is associated to the annual operating expenditure, which contributes to increase the levelized cost of energy in many studies. The associated cost with avoidable - endogenous exergy destruction is a main parameter for optimization analysis.

Table 6.41. Advanced exergoeconomic analysis of the power system based on LFR technology.

Component	Exergy cost associated to Un. ex. \dot{C}^{UN} (10^{-3} USD/s)	Exergy cost associated to Av. ex. \dot{C}^{AV} (10^{-3} USD/s)	Exergy cost associated to En. ex. \dot{C}^{EN} (10^{-3} USD/s)	Exergy cost associated to Ex. ex. \dot{C}^{EX} (10^{-3} USD/s)	Exergy cost associated to Un. /En. ex $\dot{C}^{UN,EN}$ (10^{-3} USD/s)	Exergy cost associated to Un. /Ex. ex $\dot{C}^{UN,EX}$ (10^{-3} USD/s)	Exergy cost associated to AV/En. ex $\dot{C}^{AV,EN}$ (10^{-3} USD/s)	Exergy cost associated to AV/Ex. ex $\dot{C}^{AV,EX}$ (10^{-3} USD/s)	Exergy cost associated to exergy destruction \dot{C}_k (10^{-3} USD/s)	\dot{Z}_k/\dot{E}_k	Capital cost rate associated to Un. ex. \dot{Z}^{UN} (10^{-3} USD/s)	Capital cost rate associated to Av. ex. \dot{Z}^{AV} (10^{-3} USD/s)	Capital cost rate associated to En. ex. \dot{Z}^{EN} (10^{-3} USD/s)	Capital cost rate associated to Ex. ex. \dot{Z}^{EX} (10^{-3} USD/s)	Capital cost rate associated to un. En. ex. $\dot{Z}^{UN,EN}$ (10^{-3} USD/s)	Capital cost rate associated to Un. Ex. ex. $\dot{Z}^{UN,EX}$ (10^{-3} USD/s)	Capital cost rate associated to Av./En. ex. $\dot{Z}^{AV,EX}$ (10^{-3} USD/s)	Capital cost rate associated to Av./Ex. ex. $\dot{Z}^{AV,EX}$ (10^{-3} USD/s)	
Solar field																			
rec.-IHE																			
IHE1	0.94	8.59	8.88	0.65	0.87	0.06	8.01	0.58	9.53	0.01	69.16	61.33	121.61	8.88	64.45	4.71	57.15	4.17	
Inter. HE 1	2.94	1.35	4.15	0.14	2.84	0.09	1.30	0.04	4.28	0.0003	4.25	0.47	4.57	0.15	4.11	0.14	0.46	0.02	
Inter. HE 2-	1.26	0.05	0.75	0.56	0.73	0.54	0.03	0.02	1.31	0.02	0.33	0.04	0.21	0.16	0.19	0.14	0.02	0.02	
Solar subsystem																			
HP Turbine	0.12	0.05	0.17	0.0004	0.12	0.00	0.05	0.0001	0.17	0.01	38.51	366.90	40.45	0.09	38.43	0.09	2.02	0.00	
LP Turbine	1.20	0.19	1.31	0.08	1.13	0.07	0.18	0.01	1.39	0.01	11.93	0.63	11.82	0.73	11.23	0.70	0.59	0.04	
ORC Turbine	0.77	0.11	0.70	0.18	0.61	0.16	0.09	0.02	0.88	0.06	1.37	0.14	1.20	0.31	1.09	0.28	0.11	0.03	
Condenser	0.16	0.02	0.13	0.06	0.11	0.05	0.01	0.01	0.18	0.20	1.17	0.19	0.93	0.43	0.80	0.37	0.13	0.06	
Pump ORC	0.24	0.02	0.18	0.08	0.17	0.07	0.02	0.01	0.26	0.13	0.61	0.07	0.48	0.20	0.43	0.18	0.05	0.02	
Regen -1	2.63	5.41	6.06	1.98	1.98	0.65	4.08	1.33	8.04	0.00003	0.05	0.05	0.07	0.02	0.04	0.01	0.04	0.01	
Regen - 2	0.51	0.01	0.41	0.12	0.40	0.11	0.01	0.003	0.53	0.00010	0.02	0.0004	0.02	0.005	0.02	0.0047	0.0003	0.0001	
Regen - 3	1.52	0.07	1.41	0.18	1.35	0.17	0.06	0.01	1.59	0.00003	0.04	0.0008	0.03	0.004	0.03	0.0043	0.0007	0.0001	
Pump BPP	0.002	0.002	0.004	0.00001	0.002	0.00001	0.002	0.00001	0.0042	0.0042	1.07	0.12	1.18	0.004	1.07	0.00	0.12	0.00	
Deaerator	11.70	67.06	3.98	74.79	0.59	11.11	3.39	63.68	78.77	0.12	8.58	4.62	0.67	12.54	0.43	8.15	0.23	4.39	
Absorption Refrigeration System																			
Condenser	0.03	0.001	0.02	0.01	0.02	0.01	0.0004	0.0002	0.03	0.03	0.05	0.0019	0.03	0.02	0.03	0.02	0.0012	0.0007	
Absorber	0.07	0.61	0.06	0.62	0.01	0.07	0.05	0.55	0.68	0.18	0.39	0.02	0.04	0.37	0.04	0.35	0.0015	0.0148	
Evaporator	0.04	0.03	0.03	0.05	0.02	0.03	0.01	0.02	0.07	0.02	0.04	0.00	0.02	0.03	0.02	0.03	0.0005	0.0009	
Generator	0.21	0.01	0.15	0.06	0.15	0.06	0.0041	0.00	0.22	0.01	0.26	0.01	0.19	0.08	0.19	0.08	0.0058	0.0024	
IHE	0.01	0.001	0.01	0.0027	0.01	0.0026	0.0007	0.00	0.02	0.0008	0.003	0.0001	0.0025	0.0005	0.002	0.0005	0.0001	0.0000	

The domestic hot and chilled water cannot be recovered or re-used for cooling or heating in the absorption refrigeration system (ARS). During the analysis of the absorption refrigeration system, the highest exergy destruction form was the unavoidable-exogenous exergy destruction which represents more than 30% of the total exergy destruction in the ARS. While the lowest associated cost of exergy destruction for the studied system was also found in the ARS. The exergoeconomic analysis of the absorption refrigeration system contributes to a better understanding of the relation between the exergy destruction and the initial investment. It shows, the impact of the specific purchased equipment cost of their major components such as absorber, generator, condenser and evaporator. The avoidable-endogenous exergy destruction of these components is estimated at 21.52 kW.

To complete the analysis of the equipment cost and capital cost associated with exergy destruction, the total cost associated with the exergy destruction of each component put together for its exergoeconomic evaluation has been determined. Table 6.42 presents the sum of $(\dot{Z} + \dot{C}_D)$, while the sum of $(\dot{Z}_k^{AV} + \dot{C}_{D,k}^{AV})$ gives a realistic picture of the potential to achieve cost saving in the component that requires improvement. According to the previous studies and the aforementioned assumptions, the percentage of the total cost of component varies between 45% and 80%. Considering the available costs emphasizes, the cost – effectiveness of some components used in the power block and HRSG require an improvement. Table 6.42 presents results of major components which require improvements according to their rate of optimization in the power system. The results presented in the table show that total cost associated with avoidable-endogenous exergy destruction in the regenerator 1, the intermediate heat exchanger connected to power block and the steam turbines are estimated at 4.11 USD/hour 1.76 USD/hour and 2.84 USD/hour respectively. These values highlighted the interest of the optimization analysis which needs to be conducted in the studied system. Furthermore, the total associated cost with avoidable-endogenous exergy destruction represents more than 24.5% of the total cost associated with the exergy destruction of the system that cannot be considered as negligible. The solar field, power block, heat recovery steam generation and additive multi-energy generation unit have been analyzed to meet the target of the

study. According to the results presented in tables above, the solar field has the highest total cost associated with of exergy destruction followed by power block, HRSG and additive multi-energy generation unit.

Table 6.42. Advanced analysis of the total cost associated with exergy destruction of components used for the power system based on LFR technology.

Component	Total cost associated to Un. ex. \dot{T}^{UN} (USD\$/h)	Total cost associated to Av. ex. \dot{T}^{AV} (USD\$/h)	Total cost associated to En. ex. \dot{T}^{EN} (USD\$/h)	Total cost associated to Ex. ex. \dot{T}^{EX} (USD\$/h)	Total cost associated to Un. /En. ex. $\dot{T}^{UN,EN}$ (USD\$/h)	Total cost associated to Un. /Ex. ex. $\dot{T}^{UN,EX}$ (USD\$/h)	Total cost associated to Av./En. ex. $\dot{T}^{AV,EX}$ (USD\$/h)	Total cost associated to Av./Ex. ex. $\dot{T}^{AV,EX}$ (USD\$/h)
Solar field								
Solar receiver-IHE								
IHE1	70.09	69.92	130.48	9.53	65.32	4.77	65.16	4.76
Inter. HE 1 PB	7.19	1.82	8.71	0.29	6.95	0.23	1.76	0.06
Inter. HE 2-Solar	1.59	0.09	0.97	0.71	0.92	0.68	0.05	0.04
Solar subsystem								
HP Turbine -SP	38.64	366.95	40.62	0.09	38.55	0.09	2.07	0.00
LP Turbine- SP	13.13	0.82	13.14	0.81	12.37	0.77	0.77	0.05
Turbine ORC	2.14	0.25	1.90	0.48	1.70	0.43	0.20	0.05
Condenser ORC	1.33	0.21	1.05	0.49	0.91	0.42	0.14	0.07
Pump ORC	0.85	0.09	0.66	0.28	0.60	0.25	0.06	0.03
Regen - 1	2.68	5.46	6.13	2.01	2.02	0.66	4.11	1.35
Regen - 2	0.53	0.01	0.43	0.12	0.42	0.12	0.01	0.0031
Regen - 3	1.56	0.07	1.44	0.18	1.38	0.18	0.06	0.01
Pump BPP	1.07	0.12	1.19	0.004	1.07	0.004	0.12	0.0004
Deaerator	20.29	71.69	4.65	87.32	1.03	19.26	3.62	68.06
Absorption Refrigeration System								
Condenser	0.07	0.003	0.05	0.03	0.05	0.03	0.002	0.001
Absorber	0.46	0.62	0.10	0.99	0.04	0.42	0.056	0.57
Evaporator	0.09	0.03	0.04	0.08	0.03	0.05	0.012	0.02
Generator	0.47	0.01	0.34	0.14	0.33	0.14	0.010	0.0041
IHE	0.02	0.001	0.01	0.003	0.01	0.003	0.001	0.0002

The sensitivity analysis of the studied system is based on the costs of main components presented in Table 6.43 and 6.44. Table 6.43 presents both monthly and annual shortfall of each components and this shortfall is determined through avoidable-endogenous exergy destruction. It is important to note that, the solar field alone accounts for 85.4% of all exergy destruction followed by the HRSG with 13.48% and power block. Hence optimization analysis helped to improve the efficiency of the hybrid system. The power block subsystem is one of the major sources in terms of reducing the shortfall and optimization of the hybrid energy system due to the high operating temperature.

Table 6.43. Endogenous avoidable exergy cost analysis of component used for power system based on LFR technology.

Component	Expend. Req. Jan (USD)	Expend. Req. Feb (USD)	Expend. Req. Mar (USD)	Expend. Req. Apr (USD)	Expend. Req. May (USD)	Expend. Req. Jun (USD)	Expend. Req. Jul (USD)	Expend. Req. Aug (USD)	Expend. Req. Sep (USD)	Expend. Req. Oct (USD)	Expend. Req. Nov (USD)	Expend. Req. Dec (USD)
IHE1 -Solar Field-Receiver	18583.89	16603.00	15553.91	13292.82	12927.92	10751.55	8685.95	8685.95	9969.62	11917.93	17397.96	18987.89
Inter. HE 1 - PB	502.16	448.63	420.28	359.19	349.33	290.52	234.70	234.70	269.39	322.04	470.11	513.07
Inter. HE 2-Solar	14.66	13.10	12.27	10.49	10.20	8.48	6.85	6.85	7.87	9.40	13.73	14.98
HP Turbine -SP	589.95	527.06	493.76	421.98	410.40	341.31	275.74	275.74	316.49	378.34	552.30	602.77
LP Turbine- SP	219.58	196.18	183.78	157.07	152.75	127.04	102.63	102.63	117.80	140.82	205.57	224.36
Turbine ORC	56.11	50.13	46.96	40.14	39.03	32.46	26.23	26.23	30.10	35.98	52.53	57.33
Condenser ORC	41.27	36.87	34.54	29.52	28.71	23.87	19.29	19.29	22.14	26.46	38.63	42.16
Pump ORC	18.36	16.41	15.37	13.14	12.77	10.62	8.58	8.58	9.85	11.78	17.19	18.76
Regen -1	1172.63	1047.64	981.44	838.77	815.74	678.42	548.08	548.08	629.08	752.01	1097.80	1198.13
Regen - 2	3.03	2.70	2.53	2.16	2.10	1.75	1.41	1.41	1.62	1.94	2.83	3.09
Regen - 3	16.76	14.97	14.03	11.99	11.66	9.69	7.83	7.83	8.99	10.75	15.69	17.12
Pump BPP	34.36	30.70	28.76	24.58	23.90	19.88	16.06	16.06	18.43	22.03	32.17	35.11
Deaerator	1033.18	923.05	864.72	739.02	718.73	597.74	482.90	482.90	554.26	662.58	967.24	1055.64
Absorption system												
Condenser	0.47	0.42	0.40	0.34	0.33	0.27	0.22	0.22	0.25	0.30	0.44	0.48
Absorber	16.05	14.34	13.43	11.48	11.17	9.29	7.50	7.50	8.61	10.29	15.03	16.40
Evaporator	3.43	3.07	2.87	2.45	2.39	1.99	1.60	1.60	1.84	2.20	3.21	3.51
Generator	2.80	2.50	2.34	2.00	1.95	1.62	1.31	1.31	1.50	1.80	2.62	2.86
IHE	0.21	0.19	0.18	0.15	0.15	0.12	0.10	0.10	0.12	0.14	0.20	0.22

In this work, advanced exergy and exergoeconomic analysis are conducted for a direct steam generation power system. The maximum monthly expenditure required to optimize the power system considering each subsystem is estimated as follow: 18987.9 USD for solar field, 926.6 USD for power block, and 1218.34 USD for HRSG system. This expenditure does not take into account all the equipment costs required to improve the system and achieve optimal performance. Table 6.44 presents exergoeconomic factor of each component. The optimized exergoeconomic factor (based on avoidable-endogenous exergy destruction values) of the intermediate heat exchanger 1, low-pressure turbine, regenerator 1 and regenerator 2 are less than the standard exergoeconomic factor. The recovery of the avoidable-endogenous exergy destruction leads to the optimized exergoeconomic factor as shown during the analysis of the heat exchanger (IHE 1 and IHE 2), low-pressure turbine, ORC turbine, water pump and regenerator. The increasing variation was estimated between 0.2% and 49.5%. The highest increasing is found for the regenerator 1 which varies from 1.2% to 2.3%. The lowest variation is found for the water pump which has an optimized exergoeconomic factor of 99.8%.

Table 6.44. Data obtained from avoidable cost rates of exergy destruction analysis in the power system based on LFR technology.

Component	r_k	f_k	$\epsilon_{modified}$	$f_k^{AV,EN}$	f_{k-opt}	$\dot{T}_D^{AV,EN}$ (USD/s)	$\dot{C}_D^{AV,EN}$ (USD/s)	$\dot{C}_D^{AV,EX}$ (USD/s)	\dot{C}_D^{AV} (USD/s)
Solar field	0.859818		0.919935						
Solar receiver - IHE	0.175491		0.870435						
IHE	0.092	0.932	0.942	0.877	0.9885	65.16	8.01	0.58	8.59
Inter. HE 1	0.034	0.524	0.990	0.260	0.6131	1.76	1.30	0.04	1.35
Inter. HE 2-Solar	0.778	0.221	0.985	0.457	0.2242	0.05	0.03	0.02	0.05
HP Turbine -SP	0.026	0.996	0.999	0.978	0.9970	2.07	0.05	0.0001	0.05
LP Turbine- SP	0.086	0.900	0.992	0.768	0.9117	0.77	0.18	0.01	0.19
Turbine ORC	0.386	0.632	0.975	0.550	0.6568	0.20	0.09	0.02	0.11
Condenser ORC	0.917	0.880	0.964	0.898	0.8889	0.14	0.01	0.01	0.02
Pump ORC	0.725	0.724	0.974	0.743	0.7373	0.06	0.02	0.01	0.02
Regen -1	0.327	0.012	0.858	0.009	0.0234	4.11	4.08	1.33	5.41
Regen - 2	0.288	0.039	0.994	0.031	0.0396	0.01	0.01	0.003	0.01
Regen - 3	0.127	0.024	0.995	0.012	0.0247	0.06	0.06	0.01	0.07
Pump BPP	0.013	0.996	0.998	0.984	0.9981	0.12	0.002	0.00001	0.002
Deaerator	19.058	0.144	0.553	0.064	0.1491	3.62	3.39	63.68	67.06
Absorption system									
Condenser	0.624	0.635	0.991	0.737	0.6386	0.002	0.0004	0.0002	0.001
Absorber	10.520	0.373	0.552	0.026	0.3927	0.056	0.05	0.55	0.61
Evaporator	1.850	0.373	0.782	0.040	0.4128	0.012	0.01	0.02	0.03
Generator	0.433	0.558	0.992	0.586	0.5624	0.010	0.0041	0.0017	0.01
IHE	0.221	0.168	0.990	0.117	0.1746	0.001	0.0007	0.0001	0.001

6.5.4 Advanced exergy and exergoeconomic analysis of biomass - fired technology

The results of exergy destruction distribution of the power system based biomass-fired technology presented in Table 6.45 shows the avoidable - endogenous estimated at 143.25 kW in the HRSG subsystem which is less important than unavoidable-endogenous exergy destruction. Although, it is represented in the systems where it represents more than 9.2% of the total avoidable-endogenous exergy destruction, the power block subsystem indicates an endogenous- avoidable exergy destruction of 32.91 kW. The cumulative value of the avoidable-endogenous exergy destruction of the absorption refrigeration

subsystem and drying subsystem was estimated at 42.17 kW, which is equal to 9.17% of total the absorption refrigeration and drying subsystem exergy destruction. According to these results, the optimization analysis was required for both absorption refrigeration and drying subsystem in order to improve system performances.

The advanced exergetic and techno-economic analysis of the power system, contributes to determine the exergy cost and capital cost associated with different exergy destruction forms presented in Table 6.45. During this analysis, the costs associated with the exergy destruction of each equipment used for the designing of the hybrid energy system has been determined. The power block of the studied power system based on the biomass-fired technology is estimated at 327.05 kW which owns an exergy destruction less than 8.65% of the total cost associated with the exergy destruction. The major contribution in term of exergy destruction is found for the low-pressure turbine and estimated at 264.77 kW which represents 80.96% of exergy destruction. The avoidable-endogenous exergy destruction of the power block was equal to 10.1% of the exergy destruction. Due to these results, a comparative analysis of different subsystems has been done to evaluate their impact in the studied power system. Although, it plays a key role in the electricity generation and was the most efficiency subsystem, followed by drying system, absorption refrigeration system, Heat recovery steam generation (HRSG) and biomass-fired subsystem with values estimated at 224 kW, 235.7 kW, 605.22 kW and 2408.15 kW, respectively.

The exergy destruction in the biomass-fired boiler, regenerator 1, low-pressure steam turbine and regenerator 4 are estimated at 2408.15 kW, 414.05 kW, 264.77 kW, and 74.42 kW, respectively. The optimization analysis on these components aims to improve the performance of power system that can contribute to recover of more than 1.6 MW. However, it is important to notice that, the improvement of the generator consists of the recovering of less than 8% of the exergy destruction with its avoidable-endogenous exergy destruction which was equal to 5.21 kW.

Table 6.45. Advanced exergy analysis of the power system based on BF technology.

Component	Exergy fuel (kW)	Exergy prod. and loss (kW)	Exergetic eff. $\eta_{ex}(\%)$	Exergy destruction (kW)	Exergy destruction ratio Y_d	Y_d^*	Un. Conditions / Exergy eff. (UN)	$\frac{\dot{E}_d}{\dot{E}_P} \times UN$	Un. Ex. \dot{E}_d^{UN} in (kW)	Avoidable \dot{E}_d^{AV} in (kW)	$\frac{\dot{E}_d}{\dot{E}_P} \times \eta_{ex}$	Endo. \dot{E}_d^{En} in (kW)	Exo. \dot{E}_d^{Ex} in (kW)	Endo. Prod. \dot{E}_P^{En} in (kW)	Un./Endo. $\dot{E}_d^{UN,EN}$ in (kW)	Un/ Exo. $\dot{E}_d^{UN,EX}$ in (kW)	Av./ Endo. $\dot{E}_d^{AV,EN}$ in (kW)	Av./ Exo. $\dot{E}_d^{AV,EX}$ in (kW)	
Biomass	17290.0	11630.00	0.673	5660	0.3274	0.6110	0.800	0.39	317.51	5342.49	0.33	3807.16	1852.84	7822.84	213.57	103.94	3593.59	1748.90	
Combustion	11630.00	11340.0	0.975	290	0.0249	0.0313	0.87	0.02	167.68	122.32	0.02	282.77	7.23	11057.23	163.50	4.18	119.27	3.05	
Biomass	11340.0	8931.84	0.788	2408.15	0.2124	0.2600	0.500	0.13	649.28	1758.88	0.21	1896.76	511.40	7035.08	511.40	137.88	1385.37	373.52	
Biomass Fired system																			
HP Turbine PB	2976.85	2941.34	0.988	35.51	0.0119	0.0038	0.95	0.01	28.15	7.37	0.01	35.09	0.42	2906.25	27.81	0.34	7.28	0.09	
LP Turbine	2511.23	2246.46	0.895	264.77	0.1054	0.0286	0.95	0.11	236.59	28.18	0.11	236.85	27.92	2009.61	211.64	24.94	25.21	2.97	
Turbine ORC	30.16	24.05	0.797	6.11	0.2026	0.0007	0.95	0.24	5.69	0.43	0.20	4.87	1.24	19.17	4.53	1.15	0.34	0.09	
IHE 2 ORC	37.21	19.04	0.512	18.17	0.4884	0.0021	0.87	0.83	18.05	0.13	0.49	9.30	8.88	9.74	9.23	8.81	0.06	0.06	
Cond. ORC	6.77	6.33	0.934	0.45	0.0658	0.0001	0.83	0.06	0.26	0.19	0.07	0.42	0.03	5.91	0.24	0.02	0.17	0.01	
Pump ORC	6.83	4.79	0.702	2.04	0.2981	0.0002	0.91	0.39	1.87	0.17	0.30	1.43	0.61	3.37	1.31	0.56	0.12	0.05	
Power block system																			
Regen - 1	1188.97	774.47	0.651	414.50	0.3486	0.0447	0.5	0.27	221.84	192.66	0.35	270.00	144.50	504.47	144.50	77.34	125.49	67.16	
Regen - 2	1049.32	1029.19	0.981	20.13	0.0192	0.0022	0.98	0.02	18.58	1.55	0.02	19.74	0.39	1009.45	18.22	0.36	1.52	0.03	
Regen - 3	340.19	297.56	0.875	42.63	0.1253	0.0046	0.95	0.14	38.48	4.14	0.13	37.28	5.34	260.28	33.66	4.82	3.62	0.52	
Regen - 4	2942.24	2867.81	0.975	74.42	0.0253	0.0080	0.98	0.03	69.08	5.34	0.03	72.54	1.88	2795.27	67.33	1.75	5.21	0.14	
Regen - 5	71.88	55.80	0.776	16.08	0.2237	0.0017	0.95	0.27	15.06	1.02	0.22	12.48	3.60	43.32	11.69	3.37	0.79	0.23	
Pump BPP	129.83	92.37	0.711	37.46	0.2885	0.0040	0.9	0.36	33.89	3.57	0.29	26.65	10.81	65.72	24.11	9.78	2.54	1.03	
Deaerator	88.34	50.56	0.572	37.78			0.58	0.43	30.64	7.13	0.43	21.62	16.15	28.94	17.54	13.10	4.08	3.05	
Absorption refrigeration system																			
Condenser	14.77	13.66	0.925	1.11	0.0754		0.96	0.08	1.00	0.11	0.08	1.03	0.08	12.63	0.93	0.08	0.10	0.01	
Evaporator	35.21	15.70	0.446	19.51	0.5541		0.97	1.21	15.80	3.71	0.55	8.70	10.81	7.00	7.05	8.76	1.65	2.05	
Absorber	171.88	32.42	0.189	139.45	0.8114		0.96	4.13	34.37	105.08	0.81	26.31	113.15	6.12	6.48	27.89	19.82	85.26	
IHE	33.41	27.40	0.820	6.00	0.1797		0.97	0.21	5.68	0.32	0.18	4.92	1.08	22.48	4.66	1.02	0.26	0.06	
Generator	326.89	257.26	0.787	69.63	0.2130		0.97	0.26	66.87	2.76	0.21	54.80	14.83	202.47	52.63	14.24	2.17	0.59	
Drying system																			
Air Comp.	1400	1331.11	0.95	68.89			0.95	0.05	58.95	9.94	0.05	65.50	3.39	1265.61	56.05	2.90	9.45	0.49	
Dryer	439.99	284.89	0.647	155.10	0.3525		0.87	0.47	141.63	13.47	0.35	100.43	54.67	184.47	91.70	49.92	8.72	4.75	

The function of the exergoeconomic cost for incoming and outgoing stream of components and exergy connected with the work transfer and the exergy related to heat transfer and work have been determined. To achieve the analysis for each stream and each component, the specific purchased equipment cost is summarized in Table 5.1 and correlated by equations (Sargent and Lundy, 2003; Werner and Kalb, 1993).

As shown in Table 6.47, the boiler has the highest total cost associated with exergy destruction and estimated at 44.32 USD. This value is the sum of \dot{Z} and \dot{C}_D , which are relative high values of the exergoeconomic factor presented in Table 6.49. The total cost associated with exergy destruction value is the expression of the cost rate associated with the initial investment and the O&M cost. The main component which increases the total cost is the capital investment. According to studied system and the type of the component used for the capital investment contribution may affect total cost significantly. The power block required an improvement work estimated at 43.12 USD in terms of cost associated with exergy destruction. During the analysis of the absorption refrigeration unit, the highest value of the cost associated with the exergy destruction form is found to be more than 37% of the exergy destruction in the ARS. The lowest cost associated of exergy destruction is found in the ARS connected to biomass-fired power system. The exergoeconomic analysis of the absorption refrigeration system, contribute to a better understanding of the relation between the exergy destruction and the initial investment.

Table 6.47 presents the sum of $(\dot{Z} + \dot{C}_D)$, while the sum of $(\dot{Z}_k^{AV} + \dot{C}_{D,k}^{AV})$ gives a realistic picture of a potential which need to be achieve in the component that require improvements. According to the previous studies and the above considered assumptions, the cost – effectiveness of some key components used, the power block and HRSG required improvement works.

Table 6.46. Advanced exergoeconomic analysis of the power system based on BF.

Component	Exergy cost associated to Un. ex. \dot{C}^{UN} (10^{-5} USD/s)	Exergy cost associated to Av. ex. \dot{C}^{AV} (10^{-5} USD/s)	Exergy cost associated to En. ex. \dot{C}^{EN} (10^{-5} USD/s)	Exergy cost associated to Ex. ex. \dot{C}^{EX} (10^{-5} USD/s)	Exergy cost associated to Un. /En. ex $\dot{C}^{UN,EN}$ (10^{-5} USD/s)	Exergy cost associated to Un. /Ex. ex $\dot{C}^{UN,EX}$ (10^{-5} USD/s)	Exergy cost associated to AV/En. ex $\dot{C}^{AV,EN}$ (10^{-5} USD/s)	Exergy cost associated to AV/Ex. ex $\dot{C}^{AV,EX}$ (10^{-5} USD/s)	Exergy cost associated to exergy destruction \dot{C}_k (10^{-5} USD/s)	\dot{Z}_k/\dot{E}_k	Capital cost rate associated to Un. ex. \dot{Z}^{UN} (10^{-3} USD/s)	Capital cost rate associated to Av. ex. \dot{Z}^{AV} (10^{-3} USD/s)	Capital cost rate associated to En. ex. \dot{Z}^{EN} (10^{-3} USD/s)	Capital cost rate associated to Ex. ex. \dot{Z}^{EX} (10^{-3} USD/s)	Capital cost rate associated to un. En. ex. $\dot{Z}^{UN,EN}$ (10^{-3} USD/s)	Capital cost rate associated to Un. Ex. ex. $\dot{Z}^{UN,EX}$ (10^{-3} USD/s)	Capital cost rate associated to Av./En. ex. $\dot{Z}^{AV,EN}$ (10^{-3} USD/s)	Capital cost rate associated to Av./Ex. ex. $\dot{Z}^{AV,EX}$ (10^{-3} USD/s)
Biomass comb Chamber	4.39	73.90	52.66	25.63	2.95	1.44	49.71	24.19	78.29	0.00	0.00	2.44	0.61	2.06	1.00	1.65	0.80	0.41
Biomass Boiler	8.98	24.33	26.24	7.07	7.07	1.91	19.16	5.17	33.31	3.84	0.00	5.50	5.50	8.67	2.34	4.33	1.17	4.33
HP Turb. PB	0.73	0.19	0.92	0.01	0.73	0.01	0.19	0.0023	0.93	7.25	0.01	34.73	1.83	36.12	0.44	34.31	0.41	1.81
LP Turb. PB	3.44	0.41	3.45	0.41	3.08	0.36	0.37	0.04	3.85	4.04	0.001	1.71	0.09	1.61	0.19	1.53	0.18	0.08
Turb. ORC	0.86	0.06	0.74	0.19	0.68	0.17	0.05	0.01	0.92	41.91	0.09	1.98	0.10	1.66	0.42	1.58	0.40	0.08
IHE 2 ORC	1.48	0.01	0.76	0.73	0.76	0.72	0.01	0.01	1.49	22.75	0.01	0.19	0.03	0.11	0.11	0.10	0.09	0.01
Cond. ORC	0.03	0.02	0.05	0.0033	0.03	0.0019	0.02	0.0014	0.05	30.96	0.21	1.10	0.22	1.24	0.09	1.03	0.07	0.21
Pump ORC	0.26	0.02	0.20	0.09	0.18	0.08	0.02	0.01	0.29	39.00	0.18	0.78	0.08	0.60	0.25	0.54	0.23	0.05
Regen - 1	3.08	2.68	3.75	2.01	2.01	1.07	1.74	0.93	5.76	3.86	0.00003	0.01	0.01	0.02	0.01	0.01	0.00	0.01
Regen - 2	0.28	0.02	0.29	0.01	0.27	0.01	0.02	0.0004	0.30	4.12	0.00002	0.02	0.0004	0.02	0.00	0.02	0.00	0.00
Regen - 3	0.54	0.06	0.52	0.07	0.47	0.07	0.05	0.01	0.60	3.88	0.00002	0.01	0.0003	0.01	0.00	0.01	0.00	0.00
Regen - 4	1.00	0.08	1.05	0.03	0.97	0.03	0.08	0.0020	1.08	4.02	0.00002	0.05	0.0010	0.05	0.00	0.05	0.00	0.00
Regen - 5	0.21	0.01	0.18	0.05	0.16	0.05	0.01	0.0032	0.23	3.90	0.00006	0.0034	0.0002	0.00	0.00	0.00	0.00	0.00
Pump BPP	0.29	0.03	0.23	0.09	0.21	0.08	0.02	0.01	0.32	2.40	0.00518	0.43	0.05	0.34	0.14	0.31	0.12	0.03
Deaerator	8.77	2.04	6.19	4.62	5.02	3.75	1.17	0.87	10.81	79.47	0.18	5.30	3.81	5.21	3.90	3.04	2.27	2.18
Absorption Refrigeration System																		
Condenser	0.02	0.00	0.02	0.0018	0.02	0.0016	0.0021	0.0002	0.02	5.80	0.0034	0.04	0.0019	0.04	0.00	0.04	0.00	0.00
Evaporator	0.30	0.07	0.16	0.20	0.13	0.17	0.03	0.04	0.37	5.27	0.0028	0.04	0.0013	0.02	0.02	0.02	0.02	0.00
Absorber	0.93	2.85	0.71	3.06	0.18	0.76	0.54	2.31	3.78	7.52	0.0496	1.54	0.0643	0.30	1.30	0.29	1.25	0.01
IHE	0.10	0.01	0.09	0.02	0.08	0.02	0.0048	0.0010	0.11	5.04	0.0001	0.0023	0.0001	0.00	0.00	0.00	0.00	0.00
Generator	1.19	0.05	0.97	0.26	0.93	0.25	0.04	0.01	1.23	4.93	0.0050	1.24	0.0382	1.00	0.27	0.97	0.26	0.03

Table 6.47. Advanced analysis of the total cost associated with the exergy destruction of the components used in the power system based on BF.

Component	Total cost associated to Un. ex. \dot{T}^{UN} (USD/h)	Total cost associated to Av. ex. \dot{T}^{AV} (USD/h)	Total cost associated to En. ex. \dot{T}^{EN} (USD/h)	Total cost associated to Ex. ex. \dot{T}^{EX} (USD/h)	Total cost associated to Un. /En. ex. $\dot{T}^{UN,EN}$ (USD/h)	Total cost associated to Un. /Ex. ex. $\dot{T}^{UN,EX}$ (USD/h)	Total cost associated to Av./En. ex. $\dot{T}^{AV,EX}$ (USD/h)	Total cost associated to Av./Ex. ex. $\dot{T}^{AV,EX}$ (USD/h)
Biomass comb	6.84	74.51	54.72	26.63	4.60	2.24	50.12	24.39
Combustion chamber								
Bio-Boiler	14.48	29.83	34.90	9.41	11.41	3.08	23.50	6.33
HP Turbine	35.46	2.02	37.04	0.45	35.04	0.42	2.00	0.02
LP Turbine	5.15	0.50	5.05	0.60	4.60	0.54	0.45	0.05
OR-Turbine	2.83	0.17	2.39	0.61	2.26	0.57	0.13	0.03
IHE 2 ORC	1.67	0.04	0.87	0.83	0.85	0.81	0.02	0.02
Cond. ORC	1.13	0.25	1.28	0.09	1.05	0.07	0.23	0.02
Pump ORC	1.04	0.10	0.80	0.34	0.73	0.31	0.07	0.03
Regen -1	3.09	2.69	3.77	2.02	2.02	1.08	1.75	0.94
Regen - 2	0.30	0.02	0.31	0.01	0.29	0.01	0.02	0.0004
Regen - 3	0.54	0.06	0.53	0.08	0.48	0.07	0.05	0.01
Regen - 4	1.05	0.08	1.10	0.03	1.02	0.03	0.08	0.0020
Regen - 5	0.21	0.01	0.18	0.05	0.17	0.05	0.01	0.0032
Pump BPP	0.72	0.08	0.57	0.23	0.52	0.21	0.06	0.02
Deaerator	14.07	5.85	11.40	8.52	8.05	6.02	3.35	2.50
Absorption Refrigeration System								
Condenser	0.07	0.0042	0.06	0.01	0.06	0.0049	0.0038	0.0003
Evaporator	0.34	0.07	0.18	0.23	0.15	0.19	0.03	0.04
Absorber	2.47	2.91	1.02	4.37	0.47	2.01	0.55	2.36
IHE	0.11	0.01	0.09	0.02	0.09	0.02	0.0049	0.0011
Generator	2.42	0.09	1.97	0.53	1.91	0.52	0.07	0.02

The results exergoeconomic analysis in Table 6.47 above presents major components which required improvements according to their costs associated to optimization work in the power system. According to the results presented in Table 6.47, the regenerator 1, the boiler connected to power block and the steam turbines had an estimated value of 1.75 USD/hour, 23.5 USD/hour, and 2.45 USD/hour and are the major components which required the optimization work. Furthermore, the total cost associated with avoidable-endogenous exergy destruction is found more than 26% of the total cost required for system optimization. The analysis of solar field, power block, heat steam generation subsystem and additional units such as absorption refrigeration and drying unit has been carried out. The results of the total cost associated with the exergy destruction show that, the solar field has the highest cost rate of exergy destruction, followed by power block, HRSG and additional unit. Table 6.48

presents the monthly shortfall of each components which is determined through avoidable- endogenous exergy destruction.

Table 6.48. Endogenous avoidable exergy cost analysis of component used for power system based on BF.

Component	Expend. Req. Jan (USD)	Expend. Req. Feb (USD)	Expend. Req. Mar (USD)	Expend. Req. Apr (USD)	Expend. Req. May (USD)	Expend. Req. Jun (USD)	Expend. Req. Jul (USD)	Expend. Req. Aug (USD)	Expend. Req. Sep (USD)	Expend. Req. Oct (USD)	Expend. Req. Nov (USD)	Expend. Req. Dec (USD)
Bio- comb	14294.18	12770.54	11963.61	10224.45	9943.78	8269.78	6680.98	6680.98	7668.34	9166.92	13382.00	14604.92
Bio-Boiler												
HP Turb. PB	6701.03	5986.75	5608.47	4793.16	4661.58	3876.82	3132.00	3132.00	3594.87	4297.40	6273.40	6846.70
LP Turb. PB	569.26	508.59	476.45	407.19	396.01	329.34	266.07	266.07	305.39	365.07	532.94	581.64
Turbine ORC	127.50	113.91	106.71	91.20	88.69	73.76	59.59	59.59	68.40	81.76	119.36	130.27
IHE 2 ORC	38.24	34.17	32.01	27.35	26.60	22.13	17.87	17.87	20.52	24.53	35.80	39.07
Cond. ORC	5.61	5.01	4.69	4.01	3.90	3.24	2.62	2.62	3.01	3.60	5.25	5.73
Regen - 1	65.45	58.47	54.78	46.81	45.53	37.86	30.59	30.59	35.11	41.97	61.27	66.87
Regen - 2	499.54	446.29	418.09	357.31	347.50	289.00	233.48	233.48	267.98	320.35	467.66	510.40
Regen - 3	6.55	5.85	5.48	4.69	4.56	3.79	3.06	3.06	3.52	4.20	6.13	6.70
Regen - 4	14.52	12.97	12.15	10.39	10.10	8.40	6.79	6.79	7.79	9.31	13.60	14.84
Regen - 5	21.78	19.46	18.23	15.58	15.15	12.60	10.18	10.18	11.68	13.97	20.39	22.25
Pump BPP	3.21	2.87	2.69	2.30	2.23	1.86	1.50	1.50	1.72	2.06	3.01	3.28
Deaerator	15.99	14.28	13.38	11.44	11.12	9.25	7.47	7.47	8.58	10.25	14.97	16.34
Condenser	1.10	0.98	0.92	0.78	0.76	0.63	0.51	0.51	0.59	0.70	1.03	1.12
Evaporator	9.10	8.13	7.62	6.51	6.33	5.26	4.25	4.25	4.88	5.84	8.52	9.30
Absorber	156.58	139.89	131.05	112.00	108.92	90.59	73.18	73.18	84.00	100.41	146.59	159.98
IHE	1.38	1.24	1.16	0.99	0.96	0.80	0.65	0.65	0.74	0.89	1.30	1.41
Generator	19.56	17.47	16.37	13.99	13.61	11.31	9.14	9.14	10.49	12.54	18.31	19.98

It is important to note that, the biomass-fired system alone accounts for 63.53% of all avoidable endogenous exergy destruction followed by the power block with 8.62% and HRSG being the least. For each subsystem, the maximum monthly expenditure required for the optimization of the power system has been estimated as follows, 14604.92 USD for biomass-fired scale, 7698.27 USD for power block and 589.72 USD for Heat recovery steam generation subsystem.

Table 6.49 presents optimized exergoeconomic factor of components used for power system designing.

Table 6.49. Data to choose the corresponding approach for reducing avoidable cost rates of exergy destruction in the power system based on BF.

Component	τ_k	f_k	$\varepsilon_{modified}$	$f_k^{AV,EN}$	f_{k-opt}	$\dot{T}_D^{AV,EN}$	$\dot{C}_D^{AV,EN}$ (USD/s)	$\dot{C}_D^{AV,EX}$ (USD/s)	\dot{C}_D^{AV} (USD/s)
Biomass comb	0.27		0.87	0.18		50.12	49.71	24.19	73.90
Biomass Boiler	0.02	0.5180	1.00	0.90	0.6517				
HP Turbine PB	0.12	0.9555	0.99	0.18	0.9643	23.50	19.16	5.17	24.33
LP Turbine PB	0.28	0.6926	0.99	0.62	0.7135	2.00	0.19	0.0023	0.19
Turbine ORC	0.96	0.5451	1.00	0.73	0.5714	0.45	0.37	0.04	0.41
IHE 2 ORC	0.14	0.0898	0.97	0.92	0.0948	0.13	0.05	0.01	0.06
Cond. ORC	0.48	0.9928	0.98	0.77	0.9935	0.02	0.01	0.01	0.01
Pump ORC	0.27	0.6633	0.87	0.18	0.6778	0.23	0.02	0.0014	0.02
Regen - 1	0.54	0.0028	0.86	0.00	0.0040	1.75	1.07	1.74	2.68
Regen - 2	0.02	0.0430	0.997	0.02	0.0463	0.02	0.01	0.02	0.02
Regen - 3	0.14	0.0066	0.99	0.01	0.0072	0.05	0.07	0.05	0.06
Regen - 4	0.03	0.0288	0.996	0.01	0.0309	0.08	0.03	0.08	0.08
Regen - 5	0.29	0.0281	0.99	0.01	0.0315	0.01	0.05	0.01	0.01
Pump BPP	0.41	0.3339	0.97	0.61	0.3497	0.06	0.08	0.02	0.03
Deaerator	0.81	0.9941	0.93	0.65	0.9947	3.35	1.17	0.87	2.04
Absorption System									
Condenser	0.08	0.5418	0.99	0.45	0.5656	0.0038	0.0021	0.0002	0.002
Evaporator	1.24	0.0624	0.90	0.02	0.0678	0.03	0.03	0.04	0.07
Absorber	4.32	0.2178	0.62	0.02	0.2450	0.55	0.54	2.31	2.85
IHE	0.22	0.0121	0.99	0.01	0.0127	0.0049	0.0048	0.0010	0.01
Generator	0.27	0.1236	0.99	0.44	0.1282	0.07	0.04	0.01	0.05

Table 6.49 presents exergoeconomic factor of each component. The calculation of the optimized exergoeconomic factor is based on avoidable-endogenous exergy destruction. So, the optimized exergoeconomic factor value of the boiler, intermediate heat exchanger 2, Low-pressure turbine, regenerator 1 and regenerator 4 are less than the standard exergoeconomic factor. The recovered avoidable-endogenous exergy destruction led to the determination of the optimized exergoeconomic factor as shown during the analysis of the biomass-boiler, low-pressure turbine, ORC turbine, water pump and regenerators mentioned in Table 6.48. The increasing variation is estimated between 8.3% and 13.3%, and the highest increasing variation was found for the biomass boiler which varied from 51.8% to 65.1% and the lowest value is for the regenerator 4 which had an optimized exergoeconomic factor of 3.1%.

7. CONCLUSION

In this research, a comprehensive economic and thermodynamic analysis of the proposed hybrid energy systems based on concentrating solar-biomass technologies is conducted. Their results are used in advanced exergy and exergoeconomic analyses. The exergoeconomic analysis aims to minimize the cost per exergy unit of the proposed hybrid energy systems. The results obtained from the various analysis are used for the comparison of three hybrid energy systems based on various concentrating solar technologies namely; parabolic trough collector, solar tower and linear Fresnel reflector. The key parameters to be found are the levelized cost of energy, , return on investment, internal rate of return, net present value, cost per exergy unit, levelized cost rate of product, avoidable-endogenous exergy destruction, ratio between the avoidable-endogenous exergy destruction and exergy destruction of the overall power system, costs associated with avoidable-endogenous exergy destruction, exergoeconomic factors and expenditure required for optimization work. Also, the environmental impact of the proposed systems is considered for the overall system technical performance coupled with the lowest CO₂ emissions. The results of the exergoeconomic and techno-economic analysis are summarized in Section 7.1 as below to highlight the potential of hybrid energy systems using concentrating solar power and biomass-fired technologies, and Section 7.2 presents recommendations for future studies.

7.1 Summary of the Results

Nowadays a few numbers of a commercial thermal power plant based on the concentrating solar power technologies and biomass-fired system have been implemented due to many reasons such as the existing contrast between their levelized cost of energy, thermodynamic properties of working fluid which lead to the use of a particular design of power block and others. Their combination can be presented as a suitable solution in the Sub-Saharan region due to the abundance of these energy sources and especially for the biomass-fired and solar tower technology. Furthermore, this combination does not need two different design of

the steam regeneration system which led to a very short period to change the technology used.

Because of the water conflicts in these areas, the deployment of the thermal power plant can be seen as a non-acceptable technology for electricity production and food conservation if there is no direct advantage for the population living around and end-users. The use of advanced exergy and exergoeconomic approach for this study can be seen as a valuable and an appropriated way to reduce the final cost of the power system, increase the amount of the energy produced to reduce levelized cost of energy and the amount of the CO₂ generated per MWh. The advanced exergy analysis is a key analysis which helps for a gradual analysis from techno-economic analysis to advanced exergoeconomic analysis, to perform the cost-efficiency analysis of the hybrid energy system by determining avoidable-endogenous exergy destruction and giving the way to reduce exergy destruction and the cost per exergy unit.

The studies consist to determine the better concentrating solar power technology that matched with biomass-fired technology for a selected hybrid energy system which owns an optimal design, levelized cost of energy, payback period, return on investment, internal rate of return, net present value, cost per exergy unit, levelized cost rate of product, and other characteristics related to the techno-economic and exergoeconomic analysis. Because the thermodynamic performance of the biomass-fired system and annual operation duration remain constant for any combination and are used to determine the amount of biomass feedstock required to run the proposed system throughout the year. The determination of system design consists of evaluation different subsystems (solar field, power block, and HRSG) of the studied power system based on the ratio between the avoidable-endogenous exergy destruction and exergy destruction of the overall power system ($\dot{E}_{\text{syst}}^{\text{AV,EN}}/\dot{E}_{\text{d-syst}}$). The determination of the best power system based on techno-economic parameters has been done based on the cost evaluation, cost per exergy unit, levelized cost rate of the product of the subsystems, levelized cost of energy, return on investment, internal rate of return of the concentrating solar technology. From the cost evaluation of the 5 MWe hybrid energy system based on parabolic trough collector, solar tower and linear

Fresnel reflector, initial investment costs are 38.47 Million USD, 51.47 Million USD and 25.23 million USD, respectively. The annual operating expenses related to operation and maintenance costs, feedstock acquisition, labor costs, and others are the major parameters influencing the levelized cost of energy of the proposed hybrid system.

The hybrid energy system based on the parabolic trough collector and biomass-fired technology considering Cameroon's local climate and technology characteristics, including CAPEX and OPEX for a levelized cost of electricity which is estimated between 214.2 USD/MWh and 147.2 USD/MWh. The return on investment, net present value and the internal rate of return are around 10.62 years, 23.40 Million USD and 13.79%. According to results obtained from exergoeconomic analysis, the value of the total cost associated with the avoidable – endogenous exergy destruction of the regenerator 1, the intermediate heat exchanger connected to power block and the steam turbines are 7.33 USD/hour, 4.17 USD/hour and 4.49 USD/hour, respectively. It is also important to note that, the solar field alone accounts for 86.3% of all exergy destruction followed by the HRSG system and power block system. While the power block subsystem is one of the major parts of the hybrid energy system for optimization work due to its capacity to increase the current production up to 7.69%. The maximum monthly expenditure required to optimize the hybrid energy system is distributed as follows: 41553.3 USD for the solar field subsystem, 1715.28 USD for the power block and 2997.41 USD for the heat recovery steam generation. It should be noted that the exergoeconomic factor of each component can be optimized by recovering the avoidable-endogenous exergy destruction which leads to the optimized exergoeconomic factor. The current study has illustrated that the increasing variation is found between 0.2% and 38.8%, with the highest increasing noticed for the ORC turbine which varies from 49% to 80.1% and the lowest variation was observed for the water pump which has an optimized exergoeconomic factor of 99.1%.

The hybrid energy system based on solar tower and biomass-fired technology has a levelized cost of electricity which varies from 159.2 USD/MWh to 226.2 USD/MWh. The return on investment, net present value and the internal

rate of return are estimated at 14.71 years, 22.1 Million USD and 12.64%, respectively. According to the results obtained from exergoeconomic analysis, the value of cost associated with the avoidable–endogenous exergy destruction of the regenerator 1, the volumetric receiver connected to power block and the steam turbines are estimated at 3.87 USD/hour, 84.75 USD/hour and 3.94 USD/hour, respectively. The total cost associated with avoidable-endogenous exergy destruction represents more than 26% of the total cost required for system optimization. The boiler has the highest total capital cost associated with exergy destruction estimated at 120.81 USD/hour. It is also important to notice that, the solar field alone accounts for 92.2% of all exergy destruction followed by the HRSG system with 4.8% and power block system. Due to the high operating temperature in the power block subsystem, hence this component is not one of the major parts for losses with a percentage of 4.85%, less than the HRSG system. The solar field has the highest cost rate of exergy destruction, followed by HRSG and additional units. The maximum monthly expenditure required to optimize the hybrid energy system is distributed as follows: 24695.1 USD for the solar field, 1362.57 USD for the power block and 1230.32 USD for the HRSG system. The current study has illustrated that the increasing variation is between 8.3% and 11.4%, with the highest increase observed for the boiler which varies from 51.8% to 63.2%. Whereas, the lowest variation was obtained for the regenerator 3 which has an optimized exergoeconomic factor of 0.7%.

The hybrid energy system based on linear Fresnel reflector and biomass-fired technology has a levelized cost of electricity between 76.4 USD/MWh and 143.4 USD/MWh. The return on investment, net present value and the internal rate of return are estimated at 8.4 years, 21.3 205 Million USD and 16.49%, respectively. According to the results obtained from exergoeconomic analysis, the value of cost associated with the avoidable–endogenous exergy destruction of regenerator 1, the intermediate heat exchanger connected to power block and the steam turbines are estimated at 4.11 USD/hour, 1.76 USD/hour and 2.84 USD/hour, respectively. The total cost associated with the avoidable-endogenous exergy destruction is around 24.5% of the total cost required for system optimization. It is therefore important to note that, the solar field alone accounts for 85.4% of all exergy destruction followed by the HRSG with 13.48% and

power block system. The power block is one of the main subsystems that require to pay attention to the optimization of the hybrid system which is estimated 4.15%, less than the HRSG system. The maximum monthly expenditure required to optimize the hybrid energy system is distributed as follows: 18987.9 USD for the solar field, 926.6 USD for power block and 1218.34 USD for a heat recovery steam generation system. As seen from the exergoeconomic factor of each component can be optimized by recovering the avoidable-endogenous exergy destruction which conducts to the optimized exergoeconomic factor. The current study has illustrated that the increasing variation is found to lay between 0.2% and 49.5%, with the highest increasing found for the regenerator 1 which varies from 1.2% to 2.3% and the lowest variation is observed for water pump with optimized exergoeconomic factor of 99.8%.

From the researching findings, it can be concluded that the hybrid energy system based concentrating solar power and biomass-fired are classified as follows: The linear Fresnel reflector technology is the suites combination, followed by parabolic trough collector technology which is the most mature concentrating solar power technology and least being the solar tower technology. This is mainly due to the lower cost per exergy unit, initial investment cost and better economic parameters such as levelized cost of energy, return on investment and the net present value.

7.2 Future Works and Recommendations

The research focuses on the economic and exergoeconomic aspects of the hybrid energy systems for the sub-Saharan region. Therefore, the framework of the study is to use of concentrating solar power and biomass-fired technologies for developing hybrid energy systems in the arid region. This research provides answers to some unanswered questions concerning implementation and cost reduction of a thermal hybrid (solar-biomass) power system to achieve a levelized cost of energy close to solar PV in the regions with high solar irradiation potential. For further studies, the followings should be considered for investigations:

- *To replace conventional combined Rankine cycle by a Joule cycle using a gas-turbine combined with organic Rankine Cycle. This may increase the power block efficiency and reduce water consumption.*
- *To use combined gas-turbine in the power cycle. It may be one of the most potentially interesting configurations due to the high conversion efficiency and a reduction in social impact. Furthermore, this may allow the deployment of the hybrid energy system in completed arid locations.*
- *To perform an analysis of the hybrid (solar – biomass) energy systems by considering socio-environmental and political aspects. It should take into account acceptability, employment level and environmental effect of the systems.*

REFERENCES

- Abanda, F.**, 2012, Renewable energy sources in Cameroon: potentials, benefits and enabling environment, *Renewable Sustainable Energy Review*; 16:4557–62.
- Abdelhady, S., Borello D. and Shaban, A.**, 2018, Techno-economic assessment of biomass power plant fed with rice straw: Sensitivity and parametric analysis of the performance and the LCOE, *Renewable Energy*, 115 () 1026-1034 pp.
- Abdelhady, S., Borello, D., Shaban A. and Rispoli, F.**, 2014, Viability Study of Biomass Power Plant Fired with Rice Straw in Egypt, *ICAE2014, Energy Procedia*, 61: 211 – 215 pp.
- Açikkalp, E., Aras, H. and Hepbasli, A.**, 2014, Advanced exergy analysis of an electricity-generating facility using natural gas, *Energy Conversion and Management* 82:146–153 pp.
- Ackom, E., Alemagi, D., Ackom, B. N., Minang, A. P. and Tchoundjeu Z.**, 2013, Modern bioenergy from agricultural and forestry residues in Cameroon: potential, challenges and the way forward, *Energy Policy*, 63: 101-113 pp.
- Adibhatla, S. and Kaushik, S.C.**, Exergy and thermoeconomic analyses of 500 MWe sub critical thermal power plant with solar aided feed water heating, *Applied Thermal Engineering*, 123 pp.
- Africa-EU Energy Partnership**, 2014, Country Power Market Brief: Cameroon, Workshop Report, Yaounde Cameroon. https://www.ruralelec.org/sites/default/files/aEEP_cameroon_power_sector_market_brief_en.pdf (Accessed on 15 April 2019)
- Ahmadi, M. H., Ghazvini, M., Sadeghzadeh, M. Nazari, M., Kumar, R., Naeimi, A. and Mingh, T.**, 2018, Solar power technology for electricity generation: A critical review, *Energy Science and Engineering*, 2018:1-22 pp.

REFERENCES (continued)

- Ahmadi, P., Dincer I. and Rosen, M. A.,** 2011, Exergy, exergoeconomic and environmental analyses and evolutionary algorithm based multi-objective optimization of combined cycle power plants, *Energy* 36: 5886-5898 pp.
- Ahmadi, Pouria,** 2013, Modeling, Analysis and Optimization of Integrated Energy Systems for Multigeneration Purposes, PhD Thesis, University of Ontario Institute of Technology.
- Ahmadzadeh, A., Salimpour, M.R. and Sedaghat, A.,** 2017, Thermal and exergoeconomic analysis of a novel solar driven combined power and ejector refrigeration (CPER) system. *International Journal of Refrigeration* 83, 143–156 pp.
- Alexopoulos, S. and Hoffschmidt, B.,** 2010, Solar tower power plant in Germany and future perspectives of the development of the technology in Greece and Cyprus. *Renewable Energy*, 35:1352–6.
- Al-Sulaiman, F. A., Dincer I. and Hamdullahpur, F.,** 2012, Energy and exergy analyses of a biomass trigeneration system using an organic Rankine cycle, *Energy* 45: 975-985 pp.
- Amin, A., Alibakhsh K., Fatollah, P. and Ahmadi, M.,** 2017, Thermodynamic analysis of a combined gas turbine, ORC cycle and absorption refrigeration for a CCHP system, *Applied Thermal Engineering*, 111: 397–406 pp.
- Ansarinassab, H., Mehrpooya, M. and Mohammadi, A.,** 2017, advanced exergy and exergoeconomic analyses of a hydrogen liquefaction plant equipped with mixed refrigerant system, *Journal of cleaner production* 144: 248-259 pp.
- Badami, M., Mauro, G.F. and Portoraro, A.,** 2015, Dynamic parsimonious model and experimental validation of a gas microturbine at part-load conditions, *Applied Thermal Engineering*, 75:14-23 pp.
- Bahadori, A. and Vuthaluru, H.B.,** 2010, Estimation of performance of steam turbines using a simple predictive tool. *Applied Thermal Engineering*, 30:1832-1838 pp.

REFERENCES (continued)

- Bakir, A.**, 2017, Techno-economic optimization for the design of solar chimney power plants, *Energy Conversion and Management* 138: 461–473 pp.
- BAUD, Germain**, 2011, Conception de récepteurs solaires à lit fluidisé sous flux radiatif concentré, PhD Thesis, INP Toulouse.
- Baum J.**, 2001, Investigation of an externally-fired gas turbine system with a high-temperature heat exchanger, *Fortschritt-Berichte*, Düsseldorf: VDI Verlag.
- Baumeister, T., Sadegh, A.M. and E.A. Avallone**, 2007, Marks' standard handbook for mechanical engineers, McGraw-Hill, New York p.
- Becker, M.**, 1980, Comparison of Heat Transfer Fluids for Use in Solar Thermal Power Stations, *Electric Power Systems Research*, 3:139 -150 pp.
- Bejan, A., Tsatsaronis G., and Moran, M.**, 1996, Thermal Design and Optimization, USA, John WILEY and sons inc.
- Bellos, E., Vellios, L., Ioannis-Christos, T. and Tzivanidis, C.**, 2018, Investigation of a solar-biomass polygeneration system, *Energy Conversion and Management*, 173: 283–295 pp.
- Bellos, V., Tzivanidis, C. and Papadopoulos, A.**, 2018, Optical and thermal analysis of a linear Fresnel reflector operating with thermal oil, molten salt and liquid sodium, *Applied Thermal Engineering*, S1359-4311(17):36968-75 pp.
- Benoit, H., Spreafico, L., Gauthier, D. and Flamant, G.**, 2016, Review of heat transfer fluids in tube-receivers used in concentrating solar thermal systems: Properties and heat transfer coefficients, *Renewable and Sustainable Energy Reviews*, 55: 298–315 pp.
- Berit, R.A. and Ertesvåg, I.S.**, 2011, Exergy analysis of a steam production and distribution system including alternatives to throttling and the single pressure steam production, *Energy Conversion and Management*, 52: 703–712 pp.

REFERENCES (continued)

- Besarati S. M. and Yogi Goswami D.**, 2014, A computationally efficient method for the design of the heliostat field for solar power tower plant, *Renew Energy*, 69:226–32 pp.
- Bolatturk, A., Coskun, A. and Geredelioglu, C.**, 2015, Thermodynamic and exergoeconomic analysis of Çayırhan thermal power plant. *Energy Convers. Manag.* 101:371–378 pp.
- Bonyadi, N., Johnson, E., and Baker, D.**, 2018, Technoeconomic and exergy analysis of a solar geothermal hybrid electric power plant using a novel combined cycle, *Energy Conversion and Management*, 156: 542–554 pp.
- Booth M., and Miller, E.**, 2014, Trees, trash, and toxics: How biomass energy has become the new coal, Partnership for Policy Integrity’s report.
- Braimakas, K., Preibinger, M., Brüggemann, D., Karellas, S. and Panopoulos, K.**, 2015, Low grade waste heat recovery with subcritical and supercritical Organic Rankine Cycle based on natural refrigerents and their binary mixtures, *Energy* 88, 80-92.
- Brakmann, G., Aringhoff, R. and ESTIA, G. M.**, 2005, Concentrated solar thermal power, IEA SolarPACES report, Brussels.
- Braun, F.G., Hooper, E., Wand R. and Zloczysti P.**, 2011, Holding a candle to innovation in concentrating solar power technologies: a study drawing on patent data, *Energy Policy*, 39:2441–56 pp.
- Cammarata, G., Fichera, A. and Marletta, I.**, 1998, using genetic algorithms and the exergoeconomic approach to optimize heating district networks, *ASME: Journals of Energy Resource Technology*, 120 (3): 241-246.
- Cao, J.-C., Liu, F.-Q., Qin, Z.-H., Cao, S.-H. and Zhang, S.-F.**, 2004, Energy and exergy analysis, and thermoeconomic performance of a BCHP system, *Journal of Dong Hua University*, 2: 36-42 pp.
- Casten, T.R.**, 1994, District energy with trigenerated ammonia cooling. *ASHRAE Transactions*, 100(1): 1136–1143 pp.

REFERENCES (continued)

- Cavallaro, F.**, 2009, Multi-criteria decision aid to assess concentrated solar thermal technologies. *Renewable Energy*; 34:1678–85 pp.
- CEIP**, 2013a. Clean Energy Information Portal. <http://www.reegle.info/countries/Cameroon-energy-profile/CM> (Accessed on 15th April 2019)
- Cheng, S., Li, Z., Gao, R., Wang X. and Mang, H.-P.**, 2014, Methodology development of evaluating agricultural biomass potential for biomass power plant in China, *ICAE2014, Energy Procedia*, 61:13 – 16 pp.
- Chua, N.S.**, 1991, Optimal utilisation of energy sources in a palm oil processing complex. In: Proceedings of the Seminar on Developments in Palm Oil Milling Technology and Environmental Management by the Palm Oil Research Institute of Malaysia.
- Chuah, T.G., Wan Azlina, A.G.K., Robiah, Y., & Omar, R.**, 2006, Biomass as the renewable energy sources in Malaysia: An overview. *International Journal of Green Energy*, 3(3), 323-346.
- Chunhui, Liao, Ertesvåg, I.S. and Jianing, Zhao**, 2013, Energetic and exergetic efficiencies of coal-fired CHP (combined heat and power) plants used in district heating systems of China, *Energy*, 57: 671-681 pp.
- Cihan, A., Hacıhafızoglu, O. and Kahveci, K.**, 2005, Energy–exergy analysis and modernization suggestions for a combined-cycle power plant, *international journal of energy research*, 30:115–126 pp.
- Consonni, S., Macchi, E., and Farina, F.**, 1996, Externally fired combined cycles (EFCC), Part A: Thermodynamics and technological, *issues Proceedings of the International Gas Turbine and Aeroengine Congress and Exhibition*, Birmingham- UK, ASME: 96-GT-92.
- Corona, B. and San Miguel, G.**, 2015, Environmental analysis of a concentrated solar power (CSP) plant hybridised with different fossil and renewable fuels, *Fuel*, 145:63–69 pp.

REFERENCES (continued)

- Coscia, K., Nelle, S., Elliott, T., Mohapatra, S., Oztekin, A. and Neti, S.,** 2013, Thermophysical properties of LiNO₃ –NaNO₃ –NO₃ mixtures for use in concentrated solar power. *Journal of Solar Energy*, 135:034506.
- Couper, J. R., Penney, W. R., Fair J. R. and Walas, S. M.,** 2012 *Chemical Process Equipment Selection and Design, Butterworth-Heinemann is an imprint of Elsevier*, 801p.
- Cui N.,** 2008, Study and application on real-time dynamic simulation model for heavy-duty gas turbine combined cycle power unit, *PhD thesis, North China Electric Power University, Baoding, China.*
- Cziesla, F., Tsatsaronis, G. and Gao, Z.,** 2006, Avoidable thermodynamic inefficiencies and costs in an externally fired combined cycle power plant, *Energy* 31: 1472–1489.
- Da Fonseca, M. B., Poganietz, W.-R. and Gehrman, H.-J.,** 2014, Environmental and economic analysis of SolComBio concept for sustainable energy supply in remote regions, *Applied Energy*, 135: 666–674 pp.
- Daolin, L. and Shifei, Z.,** 1999, Tri-generation (electrical power, heated and chilled water) system and their application in shanghai. In American Society of Mechanical Engineers, 34-2: 265 – 270 pp.
- Deepak, B. and Sudhakar, K.,** Modeling and performance simulation of 100 MW LFR based solar thermal power plant in Udaipur India, *Resource-Efficient Technologies* 3(4) pp.
- Dincer, Ibrahim and Ratlamwala, T. A. H. ,** 2016, Integrated absorption refrigeration systems -Comparative energy and exergy analyses, *Green energy and technology*, Springer International Publishing Switzerland 1-280 pp.
- Donatien NJOMO,** 1989, Modélisation des variations mensuelles de l'irradiation solaire reçue au Cameroun. *Model, AMSE Simulation Control*, 18: 39–64 pp.

REFERENCES (continued)

- Du, B., He, Y., Zheng, Z., and Cheng, Z.,** 2016, Analysis of thermal stress and fatigue fracture for the solar tower molten salt receiver, *Applied Thermal Energy*, 99:741–50.
- Ehtiwesh, I.A.S., Coelho, C. et Al.,** 2016, Exergetic and environmental life cycle assessment analysis of concentrated solar power plants, *Renewable and Sustainable Energy Reviews*, 56: 145–155 pp.
- Eisentraut, A.,** 2010, Sustainable production of second-generation biofuels: potential and perspectives in major economies and developing countries, International Energy Agency.
- Energy Research Center of Netherlands (ERCN),** 2012. Phyllis2; Database for Biomass and Waste. Energy Research Centre of the Netherlands, Netherlands, <http://www.ecn.nl/phyllis2/> . (Consulted on 21 July 2018)
- Engelken Maximilian, et al.,** 2016, Comparing drivers, barriers, and opportunities of business models for renewable energies: a review, *Renewable and Sustainable Energy Reviews*, 60:795–809 pp.
- Eshoul, N., Agnew, B., Al-Wesahi, M. and Mathkor, R.,** 2015, Validation and Thermal Analysis of Combined Cycle Power Plant (CCPP) Standalone and with Multi Effect Desalination with Thermal Vapour Desalination (MED-TVC), 2015 5th Int. Conf. on Environ. Sc. and Eng. V83. 4: 20-27 pp.
- Evangelos, B., Christos T., Kimon, A. and Antonopoulos,** 2017, A detailed working fluid investigation for solar parabolic trough collectors. *Applied Thermal Engineering*, 114:374–86 pp.
- FAO,** 2018, FAO agriculture statistic and climate. < <http://www.fao.org/countryprofiles/index/en/?iso3=CMR>> (Accessed on 19th April 2019)
- Fei, CaoC., Tian YangY., and Liu, Q., et Al,** 2017, Design and simulation of a solar double-chimney power plant, *Renewable Energy*, 113 pp.
- Fernández-García, A., Zarza, E., Valenzuela, L. and Pérez, M.,** 2010, Parabolic-trough solar collectors and their applications, *Renewable and Sustainable Energy Reviews*, 14:1695–721pp.

REFERENCES (continued)

- Fotsing, T.C., Njomo, D., Cornet, C., Dubuisson, P. and Nsouandele, J.L.,** 2015, Acquisition and study of global solar radiation in Maroua-Cameroon: potential, *International Journal of Renewable Energy Research* 5: pp.
- Fu, P., Wang, N., Wang, L., Morosuk, T., Yang Y. and Tsatsaronis, G.,** 2016, Performance degradation diagnosis of thermal power plants: A method based on advanced exergy analysis. *Energy Conversion and Management* 130:219–229 pp.
- Ganapathy, V.,** 1990, Simplify heat recovery steam generator evaluation, *Hydrocarbon Processing*, 77 p.
- Gebreegziabher, T., Oyedun, O., Luk, H.T., Lam, Y.G., Zhang Y. and Hui, C.W.,** 2014, Design and optimization of biomass power plant, *chemical engineering research and design*, 92:1412-1427 pp.
- Giglio, A., Lazini, A., Pierluigi, L., Margarita, M. and Zarza, M.E.,** 2017, Direct steam generation in parabolic-trough collectors: a review about the technology and a thermo-economic analysis of a hybrid system, *Renewable and Sustainable Energy Reviews*, 74:453–73.
- Gökgedik, H., Yürüsoy, M. and Keçeba, A.,** 2016, Improvement potential of a real geothermal power plant using advanced exergy analysis. *Energy* 112: 254–263 pp.
- Guo, J., Huai, X. and Liu Z.,** 2016, Performance investigation of parabolic trough solar receiver. *Applied Thermal Energy*, 95: 357–64.
- Guoqiang, Zhang, Jiongzhi, Z., Angjun, X., Yongping, Y. and Wenyi, L.,** 2016, Thermodynamic analysis of combined cycle under design/off-design conditions for its efficient design and operation, *Energy Conversion and Management*, 126: 76–88 pp.
- Hasan, H., Erdem, Ali, V. A. and Burhanettin C.,** 2009, Comparative energetic and exergetic performance analyses for coal-fired thermal power plants in Turkey, *International Journal of Thermal Sciences* 48: 2179–2186 pp.

REFERENCES (continued)

- Heinz, P.B. and Singh, M. P.**, xxxx, Steam Turbines; design, applications and Re-rating, 2nd Edition; McGraw-Hill, London p.
- Heller, Lukas**, 2013, Literature Review on Heat Transfer Fluids and Thermal Energy Storage Systems in CSP Plants, Solar Thermal Energy Research Group (STERG) Report, Stellenbosch University.
- Herold, K. E., Radermacher R. and Klein, S. A.**, 1996, Absorption chillers and heat pumps, *Boca Raton, FL: CRC Press.*
- Hiloidhari, M., and Burah, D.C.**, 2011, Rice straw residue biomass potential for decentralized electricity generation: a GIS based study Ladhimpur district of Assam, India, *Energy Sustain. Dev.* 15 (3), 214 – 22.
- Hinrichs, D.**, 2004, Cogeneration. *In Encyclopedia of Energy Elsevier*, 1: 581–594 pp.
- Hoffmann, A., Hirsch, T. and Robert P.P.**, 2016, Numerical investigation of severe slugging under conditions of a parabolic trough power plant with direct steam generation. 133:567-85 pp.
- Husain, Z., Zainal, A.Z. and Abdullah, M.Z.**, 2003, Analysis of biomass – residues based cogeneration system in palm oil mills, *Biomass and Bioenergy*, 24, 117 -124.
- IEA Statistics**, 2009, IEA statistical database. <https://www.iea.org/countries/Cameroon/> (Accessed on 15 April 2019)
- IEA**, 2008, Combined heat and power: evaluating the benefits of greater global investment.
https://www.iea.org/publications/freepublications/publication/chp_report.pdf (Accessed on 15 April 2019)
- IEA**, 2010, Technology Roadmap – concentrating solar power. Accessed on 15 April 2019:
<https://www.iea.org/publications/freepublications/publication/csp_roadmap.pdf> (Accessed on: 5 May 2019)

REFERENCES (continued)

- IEA, 2016,** <https://www.iea.org/statistics/?country=CAMEROON&year=2016&category=Energy%20supply&indicator=TPESbySource&mode=chart&dataTable=BALANCES>
- IEA, 2018,** <https://www.eia.gov/beta/international/country.php?iso=CMR>
- IFC and WB, 2012,** Lighting Africa Policy Report, Yaounde Cameroon. https://sun-connect-news.org/fileadmin/DATEIEN/Dateien/New/LA-Africa_Market_Report_2012.pdf (Accessed on: 15 April 2019)
- Iftekhar, C.M., Norton, B. and Duffy, A., 2017,** Technological assessment of different solar-biomass systems for hybrid power generation in Europe, *Renewable and Sustainable Energy Reviews* 68: 1115-1129 pp.
- IRENA, 2012,** Renewable Energy Technologies: Cost analysis series, Concentrating Solar Power. https://www.irena.org/documentdownloads/publications/re_technologies_cost_analysis-csp.pdf (Accessed on 15 April 2019)
- IRENA, 2018,** Renewable Capacity Statistics 2018. < https://www.irena.org/-/media/Files/IRENA/Agency/Publication/2018/Mar/IRENA_RE_Capacity_Statistics_2018.pdf> (Accessed on 15 April 2019)
- IRENA, 2018,** Renewable Power Generation Costs in 2017. < https://www.euractiv.com/wp-content/uploads/sites/2/2018/01/IRENA_Renewable_Power_Generation_Costs_embargo_light.pdf> (Accessed on 15 April 2019)
- Jacek, Kalina, 2017,** Analysis of alternative configurations of heat recovery process in small and medium scale combined cycle power plants, *Energy Conversion and Management* 152:13–21 pp.
- Jacek, Kalina, 2017,** Techno-economic assessment of small-scale integrated biomass gasification dual fuel combined cycle power plant, *Energy xxx* 1-9 pp.

REFERENCES (continued)

- Karellas, S. and Braimakis, K.,** 2015, Energy–exergy analysis and economic investigation of a cogeneration and trigeneration ORC–VCC hybrid system utilizing biomass fuel and solar power, *Energy Conversion and Management*.
- Kelly, S., Tsatsaronis, G. and Morosuk, T.,** 2009, Advanced exergetic analysis: approaches for splitting the exergy destruction into endogenous and exogenous parts, *Energy* 34: 384 – 391pp.
- Kerr, T.,** 2008, Combined heating and power and emissions trading: options for policy makers. International Energy Agency (In press).
- Khalid, F., Dincer, I. and Rosen, M.A.,** 2015, Energy and exergy analyses of a solar-biomass integrated cycle for multigeneration, *Solar Energy* 112: 290–299 pp.
- Khaliq, A. and Kumar, R.,** 2008, Thermodynamic performance assessment of gas turbine trigeneration system for combined heat cold and power production, *Journal of Engineering for Gas Turbines and Power, Transactions of the ASME*, 130(2).
- Khaliq, A.,** 2009, Exergy analysis of gas turbine trigeneration system for combined production of power heat and refrigeration, *international journal of refrigeration*, 32: 534-545 pp.
- Krzywik, A. and Szwaja, S.,** 2017, Putrid Potatoes as Biomass Charge to an Agricultural Biomass-to-Biogas Power Plant, ICACER 2017, *Energy Procedia*, 118: 40–45 pp.
- Lare, Y., Petrakopoulou, F., Morosuk, T., Boyano, A. and Tsatsaronis, G.,** 2017, An exergy-based study on the relationship between costs and environment impacts in power plants, *Energy* 138: 920-928 pp.
- Lee, S.F. and Sherif, A.,** 2001, Thermodynamic analysis of a lithium bromide/water absorption system for cooling and heating applications. *International Journal of Energy Research*, 25:1019–1031.

REFERENCES (continued)

- Li, J., Wu, Z., Zeng, K., Flamant, G., Ding, A.S. and Wang, J.Z.**, 2017, Safety and efficiency assessment of a solar-aided coal-fired, *Energy Conversion and Management*, 150:714–724 pp.
- Lim, J.S., Maman, Z.A., Alwi, S.R.W., and Hashim, H.**, 2012, A review on utilization of biomass from rice industry as a source of renewable energy, *Renew. Sustain. Energy Rev.* 16, 84 – 94.
- Liu, Q., Bai, Z., Wang, X., Lei, J. and Jin, H.**, 2016, Investigation of thermodynamic performances for two solar-biomass hybrid combined cycle power generation systems, *Energy Conversion Management*, 122: 252–262 pp.
- Lüpfert, E., Riffelmann, K., Price, H. and Moss, T.**, 2006, Experimental analysis of overall thermal properties of parabolic trough receivers. In: *Proceedings of the 13th international symposium on concentrated solar power and chemical energy technologies*.
- Malek, A., Hasanuzzaman, M., Rahim, N.A. and Al Turki, Y.A.**, 2017, Techno-economic analysis and environmental impact assessment of a 10 MW biomass-based power plant in Malaysia, *Journal of Cleaner Production*, 141: 502- 513 pp.
- Malik, M., Dincer, I. and Rosen, M. A.**, 2015, Development and analysis of a new renewable energy-based multi-generation system, *Energy* 79: 90-99 pp.
- Malika, O., Abdallah, K. and Larbi, L.**, 2013, Estimation of the temperature, heat gain and heat loss by solar parabolic trough collector under Algerian climate using different thermal oils. *Energy Conversion Management*, 75 :191–201 pp.
- Malinowski, L. and Lewandowska, M.**, 2013, Analytical model-based energy and exergy analysis of a gas microturbine at part-load operation, *Applied Thermal Engineering*, 57:125-132 pp.

REFERENCES (continued)

- Masood, E., Keshavarz, A. and Arash, J.**, 2012, Energy and exergy analyses of micro-steam CCHP Cycle for a residential building, *Energy and Buildings* 45: 202–210 pp.
- Mehrpooya, M., Ansarinasab, H., Mofkatklari M.M. and Rosen, M.A.**, 2017, process development and exergy cost sensitivity analysis of hybrid molten carbonate fuel cell power plant and carbon dioxide capturing process, *Journal of power sources* 364: 299 – 315 pp.
- Milani, R., Szklo A. and Hoffmann, B.S.**, 2017, Hybridization of concentrated solar power with biomass gasification in Brazil's semiarid region, *Energy Conversion and Management* 143:522–537pp.
- MINEE**, 1990, Plan énergétique national, diagnostic sectoriel : les énergies nouvelles et renouvelables, Yaoundé République of Cameroon.
- MINEE**, 2005, Plan d'Action National Energie pour la Réduction de la Pauvreté, Yaoundé République of Cameroon.
- MINEE**, 2011, Loi N° 2011/022 du 14 Décembre 2011 régissant le secteur de l'électricité au Cameroun, Yaounde Cameroon.
- Mohammadi, M., Noorollahi, V., Mohammadi– Ivatoo, B., Yousefi, H. and Jalilinasrabady, S.**, 2017, Optimal scheduling of energy hubs in the presence of uncertainty – A review. *Journal of energy management technology* 1 (1): 1 – 17.
- Moran, J. and Shapiro, N.M.**, 2006, Fundamentals of engineering thermodynamic, 5th Edition, John Wiley and sons inc.
- Morosuk T. and Tsatsaronis, G.**, 2007, Exergoeconomic evaluation of refrigeration machines based on avoidable endogenous and exogenous costs. In proceedings of the 20th international conference, 1459–1467 pp.
- Morosuk T. and Tsatsaronis, G.**, 2008, A new approach to the exergy analysis of absorption refrigeration machines, *Energy* 33: 890 – 907 pp.

REFERENCES (continued)

- Morosuk T. and Tsatsaronis, G.,** 2009, Advanced exergetic evaluation of refrigeration machines using different working fluids, *Energy* 34: 2248–2258 pp.
- Morosuk T. and Tsatsaronis, G.,** 2009, Advanced exergy analysis for chemically reacting systems—Application to a simple open gas-turbine system, *Int. J. Thermophys.* 12: 105–111 pp.
- Müller-Steinhagen, H. and Trieb F.,** 2004, Concentrating solar power: a review of the technology.
https://www.dlr.de/Portaldata/41/Resources/dokumente/institut/system/publications/Concentrating_Solar_Power_Part_1.Pdf (Accessed on 15 April 2019)
- Munoz, M., Rovira, A., Sanchez, C. and Montes, M.J.,** 2017, Off-design analysis of a Hybrid Rankine-Brayton cycle used as the power block of a solar thermal power plant, *Energy*, 134: 369-381 pp.
- Nathan, G.J., Jafarian, M., Dally, B.B., W.L. Saw, Ashman, P.J., Hu, E. and Steinfeld, A.,** 2018, Solar thermal hybrids for combustion power plant: A growing opportunity, *Progress in Energy and Combustion Science* 64: 4-28 pp.
- Nfah, E. M. and Ngundam, J. M.,** 2008, Feasibility of pico-hydro and photovoltaic hybrid power systems for remote villages in Cameroon. *Renewable Energy* 33 (5), 1064–1072.
- Nfah, E. M., Ngundam, J. M., Vandenberg, M. and Schmid, J.,** 2009, Simulation of off-grid generation options for remote electrification in Cameroon, *Renewable Energy* 34 (5): 1445–1450.
- Nfah, E.M., Ngundam, J.M. and Tchinda, R.,** 2007, Modelling of solar/diesel/battery hybrid power systems for far-north Cameroon, *Renewable Energy*, 32: 832–844 pp.
- Ngnikam, Emmanuel,** 2009, Renewable Energies in West Africa: Cameroon country, gtz regional report (in press).

REFERENCES (continued)

- Nixon, J.D., Dey, P.K. and Davies, P.A.,** 2012, The feasibility of hybrid solar-biomass power plants in India, *Energy*, 46: 541–554 pp.
- NREL,** 2019, <https://www.nrel.gov/csp/> (accessed on 23th June 2019)
- Nunes, L.J. R., Matias, J.C.O. and Catalao, J.P.S.,** 2017, Biomass in the generation of electricity in Portugal: A review, *Renewable and Sustainable Energy Reviews* 71: 373–378 pp.
- Nunes, V., Queirós, C., Lourenço, M., Santos, F. and Castro C.,** 2016, Molten salts as engineering fluids – a review: Part I. Molten alkali nitrates. *Applied Energy*, 183: 603–11.
- Omendra, Kumar Singh,** 2016, Performance enhancement of combined cycle power plant using inlet air cooling by exhaust heat operated ammonia-water absorption refrigeration system, *Applied Energy*, 180: 867–879 pp.
- Onovwiona, H.I. and Ugursal, V.I.,** 2006, Residential cogeneration systems: Review of the current technology, *Renewable and Sustainable Energy Reviews*, 10(5):389–431 pp.
- Ozturk, M., and Dincer, I.,** 2013, Thermodynamic assessment of an integrated solar power tower and coal gasification system for multi-generation purposes, *Energy Conversion and Management* 76: 1061–1072 pp.
- Pacheco, J.,** 2002, Final test and evaluation results from the solar two project. Sandia Report SAND 2002–0120.
- Pantaleo, A.M., Camporeale, S.M., Miliozzi, A., Russo, V., Shah, N. and Markides, C.N.,** 2017, Novel hybrid CSP-biomass CHP for flexible generation: Thermo-economic analysis and profitability assessment, *Applied Energy*, 204: 994–1006 pp.
- Pavlović, T.M., Radonjić, I.S., Milosavljević D.D. and Pantić, L.S.,** 2012, A review of concentrating solar power plants in the world and their potential use in Serbia. *Renewable and Sustainable Energy Reviews*, 16:3891–902 pp.

REFERENCES (continued)

- Penkuhn, M. and Tsatsaronis, G.,** 2017, A decomposition method for the evaluation of component interactions in energy conversion systems for application to advanced exergy-based analyses. *Energy* 133: 388–403 pp.
- Permit Exempt and Trivial Activities,** Subchapter 201-3.2 Exempt Activities. [https://govt.westlaw.com/nycrr/Browse/Home/NewYork/NewYorkCodesRulesandRegulations?guid=Iaffb9c00b5a011dda0a4e17826ebc834&originatio nContext=documenttoc&transitionType=Default&contextData=\(sc.Default\)](https://govt.westlaw.com/nycrr/Browse/Home/NewYork/NewYorkCodesRulesandRegulations?guid=Iaffb9c00b5a011dda0a4e17826ebc834&originatio nContext=documenttoc&transitionType=Default&contextData=(sc.Default)) (Accessed August 2019)
- Perna, A., Minutillo, M., Cicconardi, S.P., Jannelli, E. and Scarfogliero, S.,** 2015, Conventional and advanced biomass gasification power plants designed for cogeneration purpose, *Energy Procedia*, 82: 687 – 694 pp.
- Peterseim, J.H., Hellwig, U., Tadros, A. and White, S.,** 2014a, Hybridisation optimization of concentrating solar thermal and biomass power generation facilities, *Sol. Energy* 99: 203–214 pp.
- Peterseim, J.H., Herr, A., Miller, S. and White, S., D.A. O’Connell,** 2014c, Concentrating solar power/alternative fuel hybrid plants: annual electricity potential and ideal areas in Australia, *Energy*, 68:698–711 pp.
- Peterseim, J.H., Tadros A., White, S., Hellwig, U., Landler, J. and Galang, K.,** 2014b, Solar tower-biomass hybrid plants – maximizing plant performance, SolarPACES 2013, *Energy Procedia*, 49: 1197 – 1206 pp.
- Petrakopoulou, F.,** 2011, Comparative Evaluation of Power Plants with CO₂ Capture: Thermodynamic, Economic and Environmental Performance; Technical University of Berlin: Berlin/Heidelberg, Germany.
- Petrakopoulou, F., Boyano, A., Cabrera, M. and Tsatsaronis, G.,** 2011, Exergoeconomic and exergoenvironmental analyses of a combined cycle power plant with chemical looping technology, *International Journal of Greenhouse Gas Control*, 5: 475–482 pp.

REFERENCES (continued)

- Petrakopoulou, F., Tsatsaronis, G. and Morosuk, T.,** 2012 Conventional exergetic and exergoeconomic analyses of a power plant with chemical looping combustion for CO₂ capture, *International Journal of Thermodynamics*, 13: 77 - 86 pp.
- Petrakopoulou, F., Tsatsaronis, G., Morosuk, T. and Carassai, A.,** 2011, Advanced Exergoeconomic Analysis Applied to a Complex Energy Conversion System. *ASME J. Eng. Gas Turbine. Power* 134, 243–250 pp.
- Petrakopoulou, F., Tsatsaronis, G., Morosuk, T. and Carassai, A.,** 2012, A. Conventional and advanced exergetic analyses applied to a combined cycle power plant. *Energy* 41: 146–152 pp.
- Philibert, C.,** 2010, Technology roadmap: concentrating solar power.
- Pramod, K., Nagaraj, B., Priyanka, S., Jitalaxmi, B., Peddy, V., Nettem, V. and Kanaparthi, R.,** 2016, Preparation and characterization of molten salt based nanothermic fluids with enhanced thermal properties for solar thermal applications, *Applied Thermal Energy*, 109:901–5.
- Prasertsan, S. and Prasertsan, P.,** 1996, Biomass residues from palm – oil mills in Thailand: An overview on quality and potential usage, *Biomass and Bioenergy*, 11, 387 – 395.
- Rathore, M.M.,** 2010, Thermal engineering, Tata McGraw-Hill Education, New Delhi p.
- Ren, Y., Qi, H., He, M., Ruan, S., Ruan, L. and Tan H.,** 2016, Application of an improved firework algorithm for simultaneous estimation of temperature–dependent thermal and optical properties of molten salt. *International Communication Heat Mass*, 77:33–42.
- Richert, T., Riffelmann, K. and Nava, P.,** 2015, The influence of solar field inlet and outlet temperature on the cost of electricity in a molten salt parabolic trough power plant. *Energy Procedia*, 69:1143–51.

REFERENCES (continued)

- Sahoo, U., Kumar, R., Pant, P.C. and Chaudhary, R.,** 2016, Resource assessment for hybrid solar-biomass power plant and its thermodynamic evaluation in India, *Solar Energy*, 139:47–57 pp.
- Sahoo, U., Kumar, R., Singh, S.K. and Tripathi, A.K.,** 2018, Energy, exergy, economic analysis and optimization of polygeneration, hybrid solar-biomass system, *Applied Thermal Engineering*, 145:685–692 pp.
- Sampim, T., Kokkaew, N. and Parnphumeesup, P.,** 2017, Risk Management in Biomass Power Plants Using Fuel Switching Flexibility, *AEDCEE- Energy Procedia*, 138: 1099–1104 pp.
- Sargent and Lundy LLC Consulting Group,** 2013, Executive summary: assessment of parabolic trough and Power Tower Solar Technologies cost and performances Forecasts, report, NREL/SR – 550 – 35060.
- Schofield, Peter,** Steam turbines sustained efficiency, *GE Power systems Schenectady (GER-3750C)*, New York.
- Seif, E.T., Qoaide L. and Guizani, A.,** 2018, Investigation of using molten salt as heat transfer fluid for dry cooled solar parabolic trough power plants under desert conditions, *Energy Conversion and Management*, 156: 253–263 pp.
- Shahnazari, M.R. and Lari, H.R.,** 2017, Modeling of a solar power plant in Iran, *Energy Strategy Reviews* 18: 24-37 pp.
- Sharma, A.,** 2011, A comprehensive study of solar power in India and World. *Renewable and Sustainable Energy Reviews*, 15:1767–76 pp.
- Sharma, C., Sharma, A.K., Mullick, S.C. and Kandpal, T.C.,** 2015, Assessment of solar thermal power generation potential in India, *Renewable and Sustainable Energy Reviews*, 42:902–12 pp.
- Shouman, E. and Khattab N.,** 2015, Future economic of concentrating solar power (CSP) for electricity generation in Egypt, *Renewable and Sustainable Energy Reviews*, 41:1119–27.
- SIE-Cameroun,** 2011, Système d'Information Energétique du Cameroun rapport.

REFERENCES (continued)

- Simin, A., Sharam, K. and Zare, V.,** 2018, Exergoeconomic and environmental analysis of a novel configuration of solar-biomass hybrid power generation system, *Energy*, 165:776-789 pp.
- Soares, J. and Oliveira, A.C.,** 2017, Numerical simulation of a hybrid concentrated solar power/biomass mini power plant, *Applied Thermal Engineering*, 111: 1378–1386 pp.
- Soria, R., Portugal-Pereira, J., Szklo, A., Milani, R. and Schaeffer, R.,** 2015, Hybrid concentrated solar power (CSP)-biomass plants in a semiarid region: a strategy for CSP deployment in Brazil, *Energy Policy* 86:57–72 pp.
- Srinivas, T. and Reddy, B.V.,** 2014, Hybrid solar–biomass power plant without energy storage, *Case Studies in Thermal Engineering*, 2: 75–81 pp.
- Svein, J., Nesheim and Ertesvag, I.S.,** 2007, Efficiencies and indicators defined to promote combined heat and power, *Energy Conversion and Management* 48: 1004–1015 pp.
- Talbi, M. M. and Agnew, B.,** 2000, Exergy analysis: an absorption refrigerator using lithium bromide and water as working fluids. *Appl Therm Eng.*, 20: 619–30.
- Tamo, T., Kemajou, A. and Diboma B.,** 2010, Electricity self-generation costs for industrial companies in Cameroon. *Energies*, 3: 1353–68 pp.
- Tanaka, Y., Mesfun, S., Umeki, K., Toffolo, A., Tanaura, Y. and Yoshikawa, K.,** 2015, Thermodynamic performance of a hybrid power generation system using biomass gasification and concentrated solar thermal processes, *Applied Energy*, 160: 664–672.
- Taylor, R., Phelan, P., Otanicar, T., Walker, C., Nguyen, M., Trimble, S. and Prasher R.,** 2011, Applicability of nanofluids in high flux solar collectors. *Renewable and Sustainable Energy Reviews*, 3,023104:1-15.
- Tchatat, G.,** 2014, Seforall rapport. https://www.seforall.org/sites/default/files/Cameroon_RAGA_FR_Released.pdf (Accessed on 2nd January 2018)

REFERENCES (continued)

- Tony, Ennis**, 2009, Safety in Design of Thermal Fluid Heat Transfer Systems, *ICHEM-Symposium*, 155, Hazards XXI: 162-169 pp.
- Tozer R.M. and James, R.W.** 1997, Fundamental thermodynamics of ideal absorption cycles, *International Journal of Refrigeration*, 20(2):120–135.
- Tsatsaronis G. and Morosuk, T.**, 2010, Advanced exergetic analysis of a novel system for generating electricity and vaporizing liquefied natural gas. *Energy* 35: 820–829 pp.
- Tsatsaronis G. and Park, M.-H.**, 2002, On avoidable and unavoidable exergy destructions and investment costs in thermal systems. *Energy Conversion and Management* 43: 1259–1270 pp.
- Tsatsaronis, G., Kelly, S. and Morosuk, T.**, 2006, Endogenous and exogenous exergy destruction in thermal systems. In Proceedings of the ASME International Mechanical Engineering Congress and Exposition, Chicago, IL, USA, 311–317 pp.
- Tsatsaronis, G., Morosuk, T. and Kelly, S.**, 2006, Approaches for Splitting the Exergy Destruction into Endogenous and Exogenous Parts. In Proceedings of the 5th Workshop Advances in Energy Studies, Porto Venere, Italy, 12–16 pp.
- U.S. Environmental Protection Agency**, 1997, EPA's Revised Particulate Matter standards, Fact Sheet, Washington, DC: U.S. Government Printing Office.
- U.S. Environmental Protection Agency**, 2018, Particulate Matter, Accessed 2018. <https://www.epa.gov/pm-pollution> (Accessed August 2019).
- Ummadisingu, A. and Soni, M.**, 2011, Concentrating solar power–technology, potential and policy in India, *Renewable and Sustainable Energy Reviews*, 15:5169–75 pp.
- Viswanathan, R. and Bakker, W.**, 2001, Materials for ultrasupercritical coal power plants—Turbine materials: Part II. *Journal of Materials Engineering and Performance*, 10:96-101 pp.

REFERENCES (continued)

- Vuckovi, G.D., Vukic, M.V., Stojiljkovic M.M. and Vuckovic, D.D.,** 2012, Avoidable and unavoidable exergy destruction and exergoeconomic evaluation of the thermal processes in a real industrial plant, *Thermal Science*, 16: 433-446 pp.
- Wang, L., Fu, P., Wang, N., Morosuk, T., Yang Y. and Tsatsaronis, G.,** 2017, Malfunction diagnosis of thermal power plants based on advanced exergy analysis: The case with multiple malfunctions occurring simultaneously, *Energy Conversion and Management* 148: 1453–1467 pp.
- Wang, L., Yang, Y., Morosuk T. and Tsatsaronis, G.,** 2012, Advanced thermodynamic analysis and evaluation of a supercritical Power Plant. *Energies* 5: 1850–1863 pp.
- Wang, L., Yang, Z., Sharma, S., Mian, A., Tzu-En, L. et al.,** 2019, A review of evaluation, optimization and synthesis of energy systems: Methodology and application to thermal power Plants, *Energies* 12 (73): 1-53 pp.
- Werner, V. and Henry, K.,** 2010, Large – Scale Solar Thermal Power Technologies, cost and development, *WILEY – VCH Verlag GmbH&Co. KGaA*, ISBN:978-3-527-40515-2.
- WHO, 2016,** Accelerating Nutrition Improvements (ANI): mapping of stakeholders and nutrition actions in three scaling-up countries in sub-Saharan Africa, Report of the second meeting. https://www.who.int/nutrition/publications/ANI_2nd_meeting_report/en/ (accessed on 23th June 2019)
- Woodward,** 2011, Industrial Steam Turbine Control, in Application Note, 83403.
- Woudstra, N., Woudstra, T., Pirone, A. and van der Stelt, T.,** 2010, Thermodynamic evaluation of combined cycle plants, *Energy Conversion and Management* 51:1099–1110 pp.

REFERENCES (continued)

- Xu, X., Vignarooban, K., Xu, B., Hsu, K. and Kannan, A.**, 2016, Prospects and problems of concentrating solar power technologies for power generation in the desert regions, *Renewable and Sustainable Energy Reviews*, 53:1106–31 pp.
- Yang, Y., Wang, L., Dong, C., Xu, G., Morosuk, T. and Tsatsaronis, G.**, 2013, Comprehensive exergy-based evaluation and parametric study of a coal-fired ultra-supercritical power plant. *Applied Energy* 112, 1087–1099 pp.
- Yilmazoğlu, M.Z. and Amirabedin, E.**, 2011, Second Law and Sensitivity Analysis Of A Combined Cycle Power Plant in Turkey, *Isı Bilimi ve Tekniği Dergisi*, 31(2): 41-50 pp.
- Yusoff, S.**, 2006, Renewable energy form palm – oil innovation and effective utilization of wastes, *Journal of clean production* 14, 87 – 93.
- Yu-Ting, W., Chen, C., Liu, B. and Ma, C.-F.**, 2012, Investigation on forced convective heat transfer of molten salts in circular tubes, *International Communications in Heat and Mass Transfer*, 39: 1550–55 pp.
- Zachary, J., Kochis, P. and Narula, R.**, 2007, Steam Turbine Design Considerations for Supercritical Cycles, in *Coal Gen.*
- Zare, V. and Hasanzadeh, M.**, 2016, Energy and exergy analysis of a closed Brayton cycle-based combined cycle for solar power tower plants, *Energy Conversion and Management*, 128: 227–237 pp.
- Zarza, E., Valenzuela, L., Leon, J., Hennecke, K., Eck, M., Weyers, H. and Eickhoff, M.**, 2004, Direct steam generation in parabolic troughs final results and conclusions of the DISS Project, *Energy*, 29:635–44 pp.
- Zhang, G., Zheng, J., Yang, Y., Liu, W.**, 2016, Thermodynamic performance simulation and concise formulas for triple-pressure reheat HRSG of gas–steam combined cycle under off-design condition. *Energy Conversion Management*, 122: 372–85 pp.

REFERENCES (continued)

- Zhu, Y., Zhai, R., Peng, H. and Yang, Y.,** 2016, Exergy destruction analysis of solar tower aided coal-fired power generation system using exergy and advanced exergetic methods. *Appl. Therm. Eng.* 108: 339–346 pp.
- Ziher, D. and Poredos, A.,** 2006, Economics of a trigeneration system in a hospital. *Applied Thermal Engineering*, 26(7): 680 – 687pp.



APPENDIX

A - THERMODYNAMIC PROPERTIES

Table A.1: Thermodynamic properties of the power system using PTC technology.

Table A.2: Thermodynamic properties of the power system using ST technology.

Table A.3: Thermodynamic properties of the power system using LFR technology.

Table A.4: Thermodynamic properties of the power system using BF technology.

B - EXERGY ANALYSIS

Table B.1: Exergy analysis of the power system using PTC technology.

Table B.2: Exergy analysis of the power system using ST technology.

Table B.3: Exergy analysis of the power system using LFR technology.

Table B.4: Exergy analysis of the power system using BF technology.

C - CONVENTIONAL EXERGO-ECONOMIC ANALYSIS OF THE POWER SYSTEM USING BIOMASS-FIRED TECHNOLOGY

Table C.1: Conventional exergo-economic analysis of the power system using PTC technology (Power block and HRSG).

Table C.2: Conventional exergo-economic analysis of the power system using PTC technology (ORC).

- Table C.3: Conventional exergo-economic analysis of the power system using PTC technology (ARS).
- Table C.4: Conventional exergo-economic analysis of the power system using ST technology (Power block and HRSG).
- Table C.5: Conventional exergo-economic analysis of the power system using ST technology (ORC).
- Table C.6: Conventional exergo-economic analysis of the power system using ST technology (ARS).
- Table C.7: Conventional exergo-economic analysis of the power system using LFR technology (Power block and HRSG).
- Table C.8: Conventional exergo-economic analysis of the power system using LFR technology (ORC).
- Table C.9: Conventional exergo-economic analysis of the power system using LFR technology (ARS).
- Table C.10: Conventional exergo-economic analysis of the power system using BF technology (Power block and HRSG).
- Table C.11: Conventional exergo-economic analysis of the power system using BF technology (ORC).
- Table C.12: Conventional exergo-economic analysis of the power system using BF technology (ARS).

A - THERMODYNAMIC PROPERTIES

Table A.1: Thermodynamic properties of the power system using PTC technology.

	T	P	h	s	m	Ex	Fluid	state
	°C	kPa	kJ/kg	kJ/kgK	kg/s	kW		
0a	25	101,3	298	6,86		-		
0	25	101,3	104,8	0,367		-	Water	Death state
0t	25	101,3	20,14	0,685		-	Therminol	Death state
0r	25	101,3	275,39	0,982		-	R134a	Death state
0s	25	101,3	58,27	0,127		-	LiBr-Water	Death state
1	210	850	357,1	1,331	52,800	7621,95	Therminol	Liquid
1'	210	850	357,1	1,331	51,700	7463,16	Therminol	Liquid
1"	210	850	357,1	1,331	1,100	158,79	Therminol	Liquid
2	391,1	1200	777,2	1,737	52,800	23411,85	Therminol	Liquid
2'	391,1	1200	777,2	1,737	51,700	22924,10	Therminol	Liquid
2"	391,1	1200	777,2	1,737	1,100	487,75	Therminol	Liquid
12'	230	850	399,1	1,372	52,800	9192,54	Therminol	Liquid
3	264,02	5010	1734,4	4,000	16,405	8964,06	Water	Comp. Liquid
4	373,2	5070	3126,8	6,535	16,405	19407,34	Water	Superheated
6s	248,8	2010	2898,1	6,535	10,663	10176,08	Water	Saturated (x=0,81)
6	309,4	2010	3044,1	6,800	10,663	10890,42	Water	Saturated(x=0,82)
7s	181,6	1040	2762,1	6,535	5,742	4698,55	Water	saturated (x=0,84)
7	273,5	1040	2992,2	7,000	5,742	5223,69	Water	saturated (x=0,87)
7'	181,6	1040	2664,3	6,320	5,742	4505,06	Water	saturated (x=0,57)
41	67,2	1040	1817,0	4,140	5,742	3372,02	Water	saturated (x=0,39)
8	361	2010	3160,4	6,992	10,663	11520,14	Water	Superheated
9s	231,5	750	2911,2	6,992	2,050	1703,87	Water	Saturated
9	224	750	2894,9	6,959	2,050	1690,63	Water	Saturated (x=1,00)
9'	167	750	1836,9	4,577	2,050	977,62	Water	Saturated (x=0,45)
45	100	750	419,6	1,306	7,792	271,44	Water	Saturated (x=0,14)
10s	239,5	800	2925,9	6,992	8,613	7285,59	Water	Saturated
10	310	800	3077	7,268	8,613	7878,28	Water	Saturated (x=0,97)
10'	170,4	800	1232,0	3,200	8,613	2433,60	Water	Saturated (x=0,37)
44	170,4	800	1050,0	2,788	8,613	1924,02	Water	Saturated (x=0,33)
13	16,2	1800	74,2	0,280	2,112	17,26	R134a	Comp. Liquid
14	73,2	1800	293	0,946	2,112	59,99	R134a	Superheated
15s	28,8	600	269,2	0,946	2,112	9,72	R134a	Saturated
15	32,2	600	273	0,957	2,112	10,82	R134a	Saturated (x=0,30)
16	15,6	600	73,2	0,287	2,112	10,74	R134a	Liquid
13s	17,8	1800	76,3	0,287	2,112	17,28	R134a	Comp. Liquid
46	58,1	5014		0,805	16,405	198,67	Water	Comp. Liquid

Table (Continued)

47	264	5014	1186,9	2,981	16,405	4966,40	Water	Comp. Liquid
48	246	5014	1250,0	3,100	16,405	5419,51	Water	Comp. Liquid
49	264,02	5014	1369,0	3,320	16,405	6295,65	Water	Comp. Liquid
21	57,9	101,3	242,4	0,805	16,405	115,98	Water	Liquid
22	25	101,3	298	6,86	0,5	0,00	Air	gas
22'	25,9	400	299	6,47	0,5	59,81	Air	Comp. Gas
23	66,2	400	384	6,72	0,5	65,15	Air	Comp. Gas
25	25	101,3	104,8	0,367	1,1	0,00	Water	Liquid
26	100	101,3	657,00	1,945	1,1	92,34	Water	Saturated (x=0,11)
27	100	101,3	471,00	1,446	1,1	50,28	Water	Saturated (x=0,02)
28	25	101,3	104,8	0,367	1,9	0,00	Water	Liquid
29	34,9	101,3	146,4	0,504	1,9	1,40	Water	Liquid
30	35	0,93	87,61	0,2024	0,697	4,68	Sol.Li-Br	Liquid
31	35	4,82	87,61	0,2224	0,697	0,52	Sol.Li-Br	Comp. Liq.
32	58,2	4,82	133,2	0,356	0,697	4,53	Sol.Li-Br	Liquid
33	90	4,82	225,9	0,487	0,665	40,02	Sol.Li-Br	Liquid
34	65	4,82	179,82	0,3571	0,665	35,13	Sol.Li-Br	Liquid
35	65	0,93	179,82	0,3571	0,665	35,13	Sol.Li-Br	Liquid
36	90	4,82	2668,6	8,734	0,032	2,18	Water	Superh. Steam
37	32,1	4,82	134,5	0,465	0,032	0,02	Water	Sat. Liquid
38	5,9	0,93	134,5	0,483	0,032	-0,15	Water	Sat. Liquid
39	5,9	0,93	2511,4	9,012	0,032	-5,38	Water	Sat. Liquid
17	25	101,3	104,8	0,367	1,32	0,00	Water	Liquid
18	11,4	101,3	48,08	0,172	1,32	1,87	Water	Liquid
19	25	101,3	104,8	0,367	8,26	0,00	Water	Liquid
20	29	101,3	121,5	0,422	8,26	2,26	Water	Liquid
42	25	101,3	104,8	0,367	7,80	0,00	Water	Liquid
43	39,2	101,3	158,90	0,548	7,80	1,05	Water	Liquid

Table A.2: Thermodynamic properties of the power system using ST technology.

	T	P	h	s	m	Ex	Fluid	state
	°C	kPa	kJ/kg	kJ/kgK	kg/s	kW		
0	25	101,3	104,8	0,367		-	Water	Death state
0t	25	101,3	20,14	0,685		-	Therminol	Death state
0r	25	101,3	275,39	0,9822		-	R134a	Death state
0s	25	101,3	58,27	0,1265		-	LiBr-Water	Death state
3	314,9	10542	1812,0	4,046	8,66	5284,66	Water	Comp. Liquid (x=0,3)
4	541	10429	3473,8	6,705	8,66	12809,53	Water	Superheated
6"	245,8	3567	3132	6,694	7,53	8594,09	Water	sturated (x=0,97)
7s	287,8	1750	3001,9	6,787	1,13	1106,51	Water	sturated
7	313,3	1750	3060	6,888	1,13	1138,02	Water	sturated
7'	113	1750	475	1,45	1,13	53,25	Water	Liquid
8	532	3523	3523,4	7,246	7,53	10302,82	Water	Superheated
9s	373,5	1222	3203,2	7,282	3,39	3514,40	Water	Saturated
9	394,6	1222	3248,6	7,351	3,39	3598,57	Water	Saturated
9'	188,6	1217	863	2,359	3,39	556,93	Water	Two-phase(x=0,03)
45	93,9	1217	394,3	1,237	3,39	102,07	Water	Liquid
10s	335,6	1010	3126,5	7,246	2,54	2468,08	Water	Saturated
10	372,8	2800	3172	6,862	2,54	2874,86	Water	Saturated
10'	240	1010	2919,2	6,875	2,54	2222,25	Water	Saturated
44	87	1007	365,1	1,157	5,93	146,90	Water	Liquid
11s	306,1	814	3068,6	7,246	1,60	1461,29	Water	Saturated
11	349,1	2000	3134,5	6,952	1,60	1707,11	Water	Saturated
12	215	814	2872	6,877	1,60	1322,68		Saturated
12'	124,6	814	523,7	1,576	1,60	93,55	Water	Liquid
24	67	814	281,1	0,918	1,60	19,24		Liquid
13	22,6	1800	83,1	0,310	2,00	16,27	R134a	Comp. Liquid
14	73,2	1800	293	0,946	2,00	56,86	R134a	Superheated
15s	28,8	600	269,2	0,946	2,00	9,22	R134a	Saturated
15	21,59	600	262,4	0,922	2,00	9,93	R134a	Saturated (x=0,30)
16	20,9	600	80,6	0,305	2,00	14,25	R134a	Liquid
13s	21,6	1800	81,6	0,305	2,00	16,25	R134a	Comp. Liquid
46	56,4	10600	245,0	0,780	8,66	147,76	Water	Comp. Liquid
47	159,4	10587	679,1	1,926	8,66	948,39	Water	Comp. Liquid
48	235,1	10587	1015,2	2,641	8,66	2012,35	Water	Comp. Liquid
49	252,9	10572	1089,4	2,804	8,66	2234,28	Water	Comp. Liquid
46s	79,8	10600	344,9	1,073	8,66	256,36	Water	Comp. Liquid
21	55,4	101,3	229,5	0,765	8,66	52,27	Water	Liquid
22	25	101,3	298	6,86	11,4	0,00	Air	gas
22'	25,9	400	299	6,47	11,4	1331,11	Air	Comp. Gas
23	159	400	439	6,84	11,4	1667,93	Air	Comp. Gas

Table (Continued)

25	25	101,3	104,8	0,367	8,5	0,00	Water	Liquid
26	100	101,3	868,78	2,445	8,5	1227,60	Water	Saturated (x=0,19)
27	100	101,3	653,00	1,934	8,5	688,49	Water	Saturated (x=0,10)
28	25	101,3	104,8	0,367	8,2	0,00	Water	Liquid
29	40,9	101,3	171,2	0,584	8,2	13,66	Water	Liquid
30	35	0,93	87,61	0,2024	4,760	31,94	Sol.Li-Br	Liquid
31	35	4,82	87,61	0,2224	4,760	3,56	Sol.Li-Br	Comp. Liq.
32	58,2	4,82	133,2	0,356	4,760	30,96	Sol.Li-Br	Liquid
33	90	4,82	225,9	0,487	4,545	273,35	Sol.Li-Br	Liquid
34	65	4,82	179,82	0,3571	4,545	239,95	Sol.Li-Br	Liquid
35	65	0,93	179,82	0,3571	4,545	239,95	Sol.Li-Br	Liquid
36	90	4,82	2668,6	8,734	0,215	14,87	Water	Superh. Steam
37	32,1	4,82	134,5	0,465	0,215	0,10	Water	Sat. Liquid
38	5,9	0,93	134,5	0,481	0,215	-0,92	Water	Sat. Liquid
39	5,9	0,93	2511,4	9,002	0,215	-36,13	Water	Sat. Liquid
17	25	101,3	104,8	0,367	7,62	0,00	Water	Liquid
18	9,0	101,3	37,69	0,135	7,62	15,70	Water	Liquid
19	25	101,3	104,8	0,367	10,36	0,00	Water	Liquid
20	46,7	101,3	195,6	0,661	10,36	32,42	Water	Liquid
40	56,4	101,3	236,2	0,786	2,15	13,92	Water	Liquid
40'	98,1	101,3	416,83	1,285	2,15	82,41	Water	Liquid
42	25	101,3	104,8	0,367	9,60	0,00	Water	Liquid
43	36	101,3	142,71	0,518	9,60	-68,23	Water	Liquid

Table A.3: Thermodynamic properties of the power system using LFR technology.

	T	P	h	s	m	Ex	Fluid	state
	°C	kPa	kJ/kg	kJ/kgK	kg/s	kW		
0a	25	101,3	298	6,86		-		
0	25	101,3	104,8	0,367		-	Water	Death state
0t	25	101,3	20,14	0,685		-	Therminol	Death state
0r	25	101,3	275,39	0,982		-	R134a	Death state
0s	25	101,3	58,27	0,127		-	LiBr-Water	Death state
1	210	850	357,1	1,331	52,800	7621,95	Therminol	Liquid
1'	210	850	357,1	1,331	51,700	7463,16	Therminol	Liquid
1"	250	850	357,1	1,331	1,100	158,79	Therminol	Liquid
2	400	1200	800,5	1,823	52,800	23288,25	Therminol	Liquid
2'	400	1200	800,5	1,823	51,700	22803,08	Therminol	Liquid
2"	400	1200	800,5	1,823	1,100	485,17	Therminol	Liquid
12'	230	850	399,1	1,372	52,800	9192,54	Therminol	Liquid
3	264,02	5010	1734,4	4,000	16,022	8754,85	water	Comp. Liquid
4	373,2	5070	3126,8	6,535	16,022	18954,39	water	Superheated
6s	248,8	2010	2898,1	6,535	10,735	10244,38	Water	(x=0,81)
6	309,4	2010	3044,1	6,800	10,735	10963,51	Water	Saturated
7s	181,6	1040	2762,1	6,535	5,287	4326,67	Water	(x=0,99)
7	273,5	1040	2992,2	7,000	5,287	4810,24	Water	saturated
7'	181,6	1040	2664,3	6,320	5,287	4148,49	Water	(x=0,57)
41	67,2	1040	1817,0	4,140	5,287	3105,13	Water	Comp. liquid
8	361	2010	3160,4	6,992	10,735	11597,46	Water	Superheated
9s	231,5	750	2911,2	6,992	1,950	1620,75	Water	Saturated
9	224	750	2894,9	6,959	1,950	1608,16	Water	Saturated
9'	167	750	1836,9	4,577	1,950	929,93	Water	(x=0,45)
45	100	750	419,6	1,306	7,237	252,13	Water	liquid
10s	239,5	800	2925,9	6,992	8,785	7430,72	Water	Saturated
10	310	800	3077	7,268	8,785	8035,21	Water	Saturated
10'	170,4	800	1232,0	3,200	8,785	2482,08	Water	(x=0,37)
44	170,4	800	1050,0	2,788	8,785	1962,35	Water	(x=0,16)
13	16,2	1800	74,2	0,280	2,229	18,21	R134a	Comp. Liquid
14	73,2	1800	293	0,946	2,229	63,31	R134a	Superheated
15s	28,8	600	269,2	0,946	2,229	10,26	R134a	Saturated
15	32,2	600	273	0,957	2,229	11,42	R134a	(x=0,30)
16	15,6	600	73,2	0,287	2,229	11,33	R134a	Liquid
13s	17,8	1800	76,3	0,287	2,229	18,24	R134a	Comp. Liquid
46	58,1	5014	247,5	0,805	16,022	194,03	Water	Comp. Liquid
47	264	5014	1186,9	2,981	16,022	4850,48	Water	(x=0,02)
48	246	5014	1250,0	3,100	16,022	5293,02	Water	(x=0,16)
49	264,02	5014	1369,0	3,320	16,022	6148,71	Water	Comp. Liquid

Table (Continued)

21	57,9	101,3	242,4	0,805	16,022	113,28	Water	Liquid
22	25	101,3	298	6,86	11,3	0,00	Air	gas
22'	25,9	400	299	6,47	11,3	1321,73	Air	Comp. Gas
23	66,2	400	384	6,72	11,3	1439,64	Air	Comp. Gas
25	25	101,3	104,8	0,367	1,0	0,00	Water	Liquid
26	100	101,3	657,00	1,945	1,0	80,08	Water	(x=0,11)
27	91,7	101,3	384,00	1,212	1,0	26,72	Water	Liquid
28	25	101,3	104,8	0,367	1,9	0,00	Water	Liquid
29	34,9	101,3	146,4	0,504	1,9	1,40	Water	Liquid
30	35	0,93	87,61	0,2024	0,697	4,68	Sol.Li-Br	Liquid
31	35	4,82	87,61	0,2224	0,697	0,52	Sol.Li-Br	Comp. Liq.
32	58,2	4,82	133,2	0,356	0,697	4,53	Sol.Li-Br	Liquid
33	90	4,82	225,9	0,487	0,665	40,02	Sol.Li-Br	Liquid
34	65	4,82	179,82	0,3571	0,665	35,13	Sol.Li-Br	Liquid
35	65	0,93	179,82	0,3571	0,665	35,13	Sol.Li-Br	Liquid
36	90	4,82	2668,6	8,734	0,032	2,18	Water	Superh. Steam
37	32,1	4,82	134,5	0,465	0,032	0,02	Water	Comp. Liquid
38	5,9	0,93	134,5	0,483	0,032	-0,15	Water	(x=0,04)
39	5,9	0,93	2511,4	9,012	0,032	-5,38	Water	Sat steam
17	25	101,3	104,8	0,367	1,32	0,00	Water	Liquid
18	11,4	101,3	48,08	0,172	1,32	1,87	Water	Liquid
19	25	101,3	104,8	0,367	8,26	0,00	Water	Liquid
20	29	101,3	121,5	0,422	8,26	2,26	Water	Liquid
42	25	101,3	104,8	0,367	8,50	0,00	Water	Liquid
43	39,2	101,3	157,20	0,548	8,50	-13,32	Water	Liquid

Table A.4: Thermodynamic properties of the power system using BF technology.

	T	P	h	s	m	Ex	Fluid	State
	°C	kPa	kJ/kg	kJ/kgK	kg/s	kW		
0	25	101,3	104,8	0,367		-	Water	Death state
0t	25	101,3	20,14	0,685		-	Therminol	Death state
0r	25	101,3	275,39	0,9822		-	R134a	Death state
0s	25	101,3	58,27	0,1265		-	LiBr-Water	Death state
3	314,9	10542	1812,0	4,046	8,66	5284,66	Water	Comp. Liquid (x=0,3)
4	541	10429	3473,8	6,705	8,66	12809,53	Water	Superheated
6"	245,8	3567	3132	6,694	7,53	8594,09	Water	sturated (x=0,97)
7s	287,8	1750	3001,9	6,787	1,13	1106,51	Water	sturated
7	313,3	1750	3060	6,888	1,13	1138,02	Water	sturated
7'	113	1750	475	1,45	1,13	53,25	Water	Liquid
8	532	3523	3523,4	7,246	7,53	10302,82	Water	Superheated
9s	373,5	1222	3203,2	7,282	3,39	3514,40	Water	Saturated
9	394,6	1222	3248,6	7,351	3,39	3598,57	Water	Saturated
9'	188,6	1217	863	2,359	3,39	556,93	Water	Two-phase(x=0,03)
45	93,9	1217	394,3	1,237	3,39	102,07	Water	Liquid
10s	335,6	1010	3126,5	7,246	2,54	2468,08	Water	Saturated
10	372,8	2800	3172	6,862	2,54	2874,86	Water	Saturated
10'	240	1010	2919,2	6,875	2,54	2222,25	Water	Saturated
44	87	1007	365,1	1,157	5,93	146,90	Water	Liquid
11s	306,1	814	3068,6	7,246	1,60	1461,29	Water	Saturated
11	349,1	2000	3134,5	6,952	1,60	1707,11	Water	Saturated
12	215	814	2872	6,877	1,60	1322,68		Saturated
12'	124,6	814	523,7	1,576	1,60	93,55	Water	Liquid
24	67	814	281,1	0,918	1,60	19,24		Liquid
13	22,6	1800	83,1	0,310	2,00	16,27	R134a	Comp. Liquid
14	73,2	1800	293	0,946	2,00	56,86	R134a	Superheated
15s	28,8	600	269,2	0,946	2,00	9,22	R134a	Saturated
15	21,59	600	262,4	0,922	2,00	9,93	R134a	Saturated (x=0,30)
16	20,9	600	80,6	0,305	2,00	14,25	R134a	Liquid
13s	21,6	1800	81,6	0,305	2,00	16,25	R134a	Comp. Liquid
46	56,4	10600	245,0	0,780	8,66	147,76	Water	Comp. Liquid
47	159,4	10587	679,1	1,926	8,66	948,39	Water	Comp. Liquid
48	235,1	10587	1015,2	2,641	8,66	2012,35	Water	Comp. Liquid
49	252,9	10572	1089,4	2,804	8,66	2234,28	Water	Comp. Liquid
46s	79,8	10600	344,9	1,073	8,66	256,36	Water	Comp. Liquid
21	55,4	101,3	229,5	0,765	8,66	52,27	Water	Liquid
22	25	101,3	298	6,86	11,4	0,00	Air	gas
22'	25,9	400	299	6,47	11,4	1331,11	Air	Comp. Gas
23	159	400	439	6,84	11,4	1667,93	Air	Comp. Gas

Table (Continued)

25	25	101,3	104,8	0,367	8,5	0,00	Water	Liquid
26	100	101,3	868,78	2,445	8,5	1227,60	Water	Saturated (x=0,19)
27	100	101,3	653,00	1,934	8,5	688,49	Water	Saturated (x=0,10)
28	25	101,3	104,8	0,367	8,2	0,00	Water	Liquid
29	40,9	101,3	171,2	0,584	8,2	13,66	Water	Liquid
30	35	0,93	87,61	0,2024	4,760	31,94	Sol.Li-Br	Liquid
31	35	4,82	87,61	0,2224	4,760	3,56	Sol.Li-Br	Comp. Liq.
32	58,2	4,82	133,2	0,356	4,760	30,96	Sol.Li-Br	Liquid
33	90	4,82	225,9	0,487	4,545	273,35	Sol.Li-Br	Liquid
34	65	4,82	179,82	0,3571	4,545	239,95	Sol.Li-Br	Liquid
35	65	0,93	179,82	0,3571	4,545	239,95	Sol.Li-Br	Liquid
36	90	4,82	2668,6	8,734	0,215	14,87	Water	Superh. Steam
37	32,1	4,82	134,5	0,465	0,215	0,10	Water	Sat. Liquid
38	5,9	0,93	134,5	0,481	0,215	-0,92	Water	Sat. Liquid
39	5,9	0,93	2511,4	9,002	0,215	-36,13	Water	Sat. Liquid
17	25	101,3	104,8	0,367	7,62	0,00	Water	Liquid
18	9,0	101,3	37,69	0,135	7,62	15,70	Water	Liquid
19	25	101,3	104,8	0,367	10,36	0,00	Water	Liquid
20	46,7	101,3	195,6	0,661	10,36	32,42	Water	Liquid
40	56,4	101,3	236,2	0,786	2,15	13,92	Water	Liquid
40'	98,1	101,3	416,83	1,285	2,15	82,41	Water	Liquid
42	25	101,3	104,8	0,367	9,60	0,00	Water	Liquid
43	36	101,3	142,71	0,518	9,60	-68,23	Water	Liquid

B - EXERGY ANALYSIS**Table B.1: Exergy analysis of the power system using PTC technology.**

Component	Exergy fuel Ef (kW)	Exergy produced and loss Ep+El (kW)	Exergetic eff. Ed/Ep (kW)	Exergy destruction Ed (kW)	Exergy destruction ration (Yd) (kW)
Solar field	15981	15789,90	0,9880	191,1	0,0120
Inter. HE 1	15460,94	15149,55	0,9799	311,4	0,0201
Inter. HE 2-Solar	137,63	68,97	0,5011	68,7	0,4989
Solar subsystem			Ed tot-solsub	571,1	
HP Turbine -SP	4061,73	4048,76	0,997	12,96	0,0032
LP Turbine- SP	1293,52	1217,34	0,941	76,18	0,0589
Turbine ORC	109,26	87,12	0,797	22,14	0,2026
Condenser ORC	37,83	22,92	0,606	14,91	0,3942
Pump ORC	24,75	17,37	0,702	7,38	0,2981
Regen - 1	3691,58	2470,95	0,669	1220,63	0,3307
Regen - 2	683,95	648,78	0,949	35,17	0,0514
Regen - 3	1556,47	1477,23	0,949	79,24	0,0509
Pump BP	290,37	289,39	0,997	0,98	0,0034
			Edtot BPPsys	1469,58	
Deaerator	2413,26	115,98	0,048060548	2297,28	
HE	210,61	92,34	0,4385	118,27	0,5615
Condenser	2,16	1,40	0,6467	0,76	0,3533
Absorber	25,07	2,26	0,0901	22,81	0,9099
Evaporator	5,23	1,87	0,3577	3,36	0,6423
Generator	42,062	37,67	0,8955	4,39	0,1045
IHE	4,891	4,01	0,8203	0,88	0,1797
Pump	-	-			
Fan	-	-			
Fan	-	-			
			Ed-tot	150,47	
Air Compressor	23,27	2729,07			
Dryer	434,28	243,46	0,561	190,82	0,439391417

Table B.2: Exergy analysis of the power system using ST technology.

Component	Exergy fuel Ef (kW)	Exergy produced and loss Ep+El (kW)	Exergetic eff. Ed/Ep (kW)	Exergy destruction Ed (kW)	Exergy destruction ration (Yd) (kW)
Solar field	28657,36888	18417,16749	0,642667775	10240,20138	0,3573
Recevier	18417,167	13155,770	0,714	5261,397048	0,2857
Boiler-Superheater	13155,8	9233,59	0,702	3922,177353	0,2981
HP Turbine PB	3077,42	3040,71	0,988	36,71	0,0119
LP Turbine PB	2596,07	2322,36	0,895	273,71	0,1054
Turbine ORC	286,09	228,12	0,797	57,97	0,2026
IHE 2 ORC	211,57	180,60	0,854	30,97	0,1464
Cond. ORC	191,67	60,01	0,313	131,66	0,6869
Pump ORC	64,81	45,49	0,702	19,32	0,2981
Reheater block (Exergy destruction)				550.34	
Regen - 1	1229,14	800,63	0,651	428,50	0,3486
Regen - 2	1084,77	1063,96	0,981	20,81	0,0192
Regen - 3	351,68	307,61	0,875	44,07	0,1253
Regen - 4	3041,64	2964,70	0,975	76,94	0,0253
Regen - 5	74,31	68,49	0,922	5,81	0,0782
Pump BPP	134,22	95,49	0,711	38,73	0,2885
Deaerator	203,73	52,27	0,257	151,46	0,7434
Heat Recovery Steam Generator (HRSG)				766.42	
Condensor	14,77	13,66	0,925	1,11	0,0754
Evaporator	35,21	15,70	0,446	19,51	0,5541
Absorber	171,88	32,42	0,189	139,45	0,8114
IHE	33,41	27,40	0,820	6,00	0,1797
Generator	539,11	257,26	0,477	281,84	0,5228
Fan1	239,95	239,95			
Fan2	-	-			
Pump	-	-			
Refrigeration system				447,92	
Air Compressor	11,35	-			
Dryer	454,86	336,82	0,740	118,04	0,2595

Table B.3: Exergy analysis of the power system using LFR technology.

	Exergy fuel E_f (kW)	Exergy produced and loss E_p+E_l (kW)	Exergetic eff. E_d/E_p (kW)	Exergy destruction E_d (kW)	Exergy destruction ration (Y_d) (kW)
Solar field	16211,47323	15666,30	0,9664	545,2	0,0336
Inter. HE 1	15339,92	14843,92	0,9677	496,0	0,0323
Inter. HE 2-Solar	135,05	81,51	0,6035	53,5	0,3965
Solar subsystem (exergy destruction)					1094,7
HP Turbine -SP	3992,04	3983,11	0,998	8,93	0,0022
LP Turbine- SP	1310,28	1233,76	0,942	76,52	0,0584
Turbine ORC	129,12	102,96	0,797	26,16	0,2026
Condenser ORC	319,44	27,08	0,085	292,36	0,9152
Pump ORC	29,25	20,53	0,702	8,72	0,2981
Regen-1	3765,11	2836,70	0,753	928,42	0,2466
Regen-2	270,67	210,22	0,777	60,45	0,2233
Regen-3	1626,00	1442,75	0,887	183,25	0,1127
Pump BPP	283,59	282,64	0,997	0,96	0,0034
Power Block and Heat Recovery Steam Generation (exergy destruction)					1585,76
Deaerator	2241,53	113,28	0,050534842	2128,26	
HE	214,80	92,34	0,4299	122,46	0,5701
Condenser	2,16	1,40	0,6467	0,76	0,3533
Absorber	25,07	2,26	0,0901	22,81	0,9099
Evaporator	5,23	1,87	0,3577	3,36	0,6423
Generator	42,062	37,67	0,8955	4,39	0,1045
IHE	4,891	4,01	0,8203	0,88	0,1797
Pump	-	-			
Fan	-	-			
Fan	-	-			
Absorption refrigeration system (exergy destruction)					154,67
Air Compressor	23,27	2729,07			
Dryer	207,19	243,46	1,175	-36,28	-0,175092021

Table B.4: Exergy analysis of the power system using BF technology.

	Exergy fuel E _f (kW)	Exergy produced and loss E _p +E _l (kW)	Exergetic eff. E _d /E _p	Exergy destruction E _d (kW)	Exergy destruction ration (Y _d) (kW)
Biomass Boiler	9126,6	8931,84	0,979	194,7833154	0,0213
HP Turbine PB	2976,85	2941,34	0,988	35,51	0,0119
LP Turbine PB	2511,23	2246,46	0,895	264,77	0,1054
Turbine ORC	276,74	220,67	0,797	56,07	0,2026
IHE 2 ORC	204,66	174,70	0,854	29,96	0,1464
Cond. ORC	59,13	58,05	0,982	1,08	0,0183
Pump ORC	62,69	44,00	0,702	18,69	0,2981
Power block			Ed-tot	105,81	
Regen - 1	1188,97	774,47	0,651	414,50	0,3486
Regen - 2	1049,32	1029,19	0,981	20,13	0,0192
Regen - 3	340,19	297,56	0,875	42,63	0,1253
Regen - 4	2942,24	2867,81	0,975	74,42	0,0253
Regen - 5	71,88	55,80	0,776	16,08	0,2237
Pump BPP	129,83	92,37	0,711	37,46	0,2885
				1100,28	
Deaerator	187,07	50,56	0,270	136,51	
Condensor	14,77	13,66	0,925	1,11	0,0754
Evaporator	35,21	15,70	0,446	19,51	0,5541
Absorber	171,88	32,42	0,189	139,45	0,8114
IHE	33,41	27,40	0,820	6,00	0,1797
Generator	326,89	257,26	0,787	69,63	0,2130
Fan1	239,95	239,95			
Fan2	-	-			
Pump	-	-			
Refrigeration system				235,70	
Air Compressor	11,35	-			
Dryer	439,99	284,89	0,647	155,10	0,352505085

C - CONVENTIONAL EXERGO-ECONOMIC ANALYSIS OF THE POWER SYSTEM USING CSP AND BIOMASS-FIRED TECHNOLOGY.

- PTC Technology

Table C.1: Conventional exergo-economic analysis of the power system using PTC technology (Power block and HRSG).

Solar field						
	Zsf=	0,077815352	\$/s	C2=	0,115377637	\$/s
	E2-E1=	15789,90	kJ/s	C1=	0,037562286	\$/s
	c_sf=	4,928173139	\$/GJ			
Heat exchanger						
	Zihe=	0,00131	\$/s	C2' =	0,112973937	\$/s
	E2'-E1'=	15460,94	kJ/s	C1'=	0,036779738	\$/s
	c_ihe=	5,012902776	\$/GJ	C3=	0,025035107	\$/s
				C4=	0,092980499	\$/s
				C6=	0,045736393	\$/s
	Zihe+C3+C6+C2'			C8=	0,053734225	\$/s
	Cq_ihe+C1'+C8+C4=	0,1850554		Cq_ihe=	0,001560975	\$/s
Steam -Turbine HP (76,88%)		0,768834692				
	Zturbine=	0,011005001	\$/s	C7=	0,026883067	\$/s
	E4-(E7+E6)=	4061,73	kJ/s	C6=	0,045736393	\$/s
	Whp-turb. =	4048,764489	kJ/s	Cw_hp=	0,031265946	\$/s
	c_hp-urbine=	7,722342376	\$/GJ	Cq_hp=	0,000100094	\$/s
	C7+C6+Cw_hp+Cq_hp			Zt_hp+C4=	0,1039855	
Steam -Turbine LP		0,231165308	23,12%			
	Zturbine_LP=	0,003308871	\$/s	C9=	0,009673168	\$/s
	E8-(E9+E10)=	1293,52	kJ/s	C10=	0,037576768	\$/s
	Wlp-turb=	1217,340864	kJ/s	Cw_lp=	0,009216414	\$/s
	c_hp-urbine=	7,570939124	\$/GJ	Cq_lp=	0,000576746	\$/s
				C9+C10+Cw_lp+Cq_lp=	0,057043096	\$/s
				Zt_lp+C8=	0,057043096	\$/s
	Zsteam_turbine=	0,0143139	\$/s			
	Wsteam_turbine=	5266,1054	kJ/s			
	(E4+E8)-(E7+E6+E9+E10)=	5342,28	kJ/s			
	C_turbine=	7,6873432	\$/GJ			
Regenerator 1						
	Zreg1 =	0,00002634	\$/s	C10'=	0,019071231	\$/s
	E10-E10'=	3691,58	kJ/s	C46=	0,002032098	\$/s
	c_reg1=	5,020039057	\$/GJ	C47=	0,014418721	\$/s
				Cq_reg1	0,006127624	\$/s

Table (Continued)

Table (Continued)						
	C10+C46+Zreg1			C47+C10+Cq_reg1=	0,039617577	
Regenerator 2						
	Zreg2=	0,000005918	\$/s	C9'=	0,006244602	\$/s
	E9-E9'=	683,95	kJ/s	C48=	0,017671008	\$/s
	c_reg2=	5,021555295	\$/GJ	Cq_reg2=	0,000176583	\$/s
				C9'+C48+Cq_reg2=	0,024092194	\$/s
				C9+C47+Zreg2=	0,024097807	\$/s
Regenerator 3						
	Zreg3=	0,00001075	\$/s	C7'=	0,019080643	\$/s
	E7-E7'=	1556,47	kJ/s	C49=	0,025076225	\$/s
	c_reg3=	5,019811536	\$/GJ	Cq_reg3=	0,000397754	\$/s
				C7'+C49+Cq_reg3=	0,044554623	\$/s
				C48+C7+Zreg3=	0,04456483	\$/s
Pump						
	Zpump=	0,000330274		C21=	0,000581409	\$/s
	E46-E21=	289,39		Cq_pump=	0,000003787	\$/s
	c_pump=	3,871631176		Cw_pump=	0,001124203	\$/s
	Wpump=	290,3692523		C21+Cw_pump+Zpump=	0,002035885	\$/s
				C46+Cq_pump=	0,002035885	\$/s
Condenser						
	Zcond.=	0,003667919		C44=	0,018015472	\$/s
	c_cond.=	5,635523632		C45=	0,012097428	\$/s

Table C.2: Conventional exergo-economic analysis of the power system using PTC technology (ORC).

	Zhe=	0,00008714	\$/s	E14-E13=	68,97	kJ/s
	c_he=	5,561305514	\$/GJ	C2''=	0,002403701	\$/s
				C1''=	0,001725456	\$/s
				C14=	0,001508227	\$/s
				C13=	0,001124666	\$/s
				Cq_he=	0,000381819	\$/s
				C2' '+ C16 + Zhe =	0,00361550	\$/s
				C1''+C14+Cq_he=	0,003615502	\$/s
Turbine:						
	Zorc_turb=	0,000354312	\$/s	C15=	0,000900612	\$/s
	c_orc-turb=	8,804209622	\$/GJ	Cq_turb=	0,000194904	\$/s
	E_orc-turb=	109,26	kJ/s	Cw_orc-turb=	0,000767023	\$/s
	W_orc-turb=	87,12	kJ/s	C15+Cw_orc-turb+Cq_turb=	0,001862539	\$/s
				C14+Zturb=	0,001862539	\$/s
Condenser:						
	Zcondenser =	0,000319154	\$/s	C16=	0,001028061	\$/s
	c_cond=	3,634585351	\$/GJ	E43-E42=	37,83	kJ/s
	Cq_cond=	0,000054205	\$/s	C43=	0,000189642	\$/s
	C42+C16+Cq_cond=	0,001082266	\$/s	C42=	0	\$/s
Pump:				Zcond+C15=	0,001219765	
	Zpump=	0,000160261	\$/s	Cw_orc-pump=	0,00019787	\$/s
	c_pump=	7,994764382	\$/GJ	Cq-pump=	0,000059	\$/s
	W_orc-Pump=	24,75	kJ/s	Zpump+C13=	0,001284927	\$/s
				C16+Cw_orc_pump+Cq_pump=	0,001285	\$/s

Table C.3: Conventional exergo-economic analysis of the power system using PTC technology (ARS).

Generator:	Zgenerator=	0,00007550	\$/s	C26=	0,00046291	\$/s
	c_generator=	6,807791923	\$/GJ	C27=	0,00025205	\$/s
				C33=	0,00027246	\$/s
				C32=	0,00003086	\$/s
				C36=	0,00001484	\$/s
				Cq_gen=	0,00002991	\$/s
				Zgen. +C32+C26=	0,00056926	\$/s
				C33+C36+C27+Cq_ge.=	0,00056926	\$/s
Intermediate Heat exchanger:	Zihe=	0,0000008499	\$/s	C31=	0,00000355	\$/s
	c_ihe=	7,774947255	\$/GJ	C34=	0,00023917	\$/s
				Cq_ihe=	0,00000683	\$/s
				C31+C33+Zihe=	0,00027686	\$/s
				C34+C32 +Cq_ihe=	0,00027686	\$/s
Pump:	Zpump=	0,000003221	\$/s	C30=	0,00003184	\$/s
	c_pump=	0	\$/GJ	CW_pump=	0,00000000	\$/s
	W_pump=	0	kJ/s	E31-E30=	4,15566419	kJ/s
				C30+Zpump=	0,00003506	\$/s
				C31+CW_pump=	0,00000355	\$/s
Absorber:	Zabsorber=	0,00011282	\$/s	C35=	0,00023917	\$/s
	c_abs=	11,30778174	\$/GJ	C39=	-0,00003665	\$/s
				C19=	0,00000000	\$/s
				C20=	0,00002553	\$/s
				C_abs=	0,00025797	\$/s
				C19+C39+C35+Zabs=	0,00031534	\$/s
				C20+C30+Cq_abs=	0,00031534	\$/s
Evaporator:	Zevap=	0,000012305	\$/s	C38=	-0,00000105	\$/s
	c_evap=	9,16076988	\$/GJ	C17=	0,00000000	\$/s
				C18=	0,00001714	\$/s
				Cq_evap=	0,00003077	\$/s
				C17 + C38 +Zevap=	0,00001126	\$/s
				C18 + C39 + Cq_eva=	0,00001126	\$/s
Condenser:	Zcond.=	0,000013142	\$/s	C37=	0,00000010	\$/s
	c_cond.=	12,8807617	\$/GJ	C28=	0,00000000	\$/s
				C29=	0,00001803	\$/s
				Cq_condenser=	0,00000985	\$/s
				C28+C36+Zcond=	0,00002798	\$/s
				C37+C29+Cq_cond=	0,00002798	\$/s

- **ST Technology****Table C.4: Conventional exergo-economic analysis of the power system using ST technology (Power block and HRSG).**

Solar Field						
	Zsf=	0,094009802	\$			
	E2-E1=	18417,16749	kJ/s			
	c_sf=	5,104465801	\$/GJ			
Receiver and boiler						
	Zboiler=	0,034753306	\$/s	E=	13,8614	MJ/s
	c_boiler=	8,019929223	\$/GJ	C_fuel=	0,070755042	\$/s
	Cq_boiler=	0,031455585	\$/s	C3'=	0,042382618	\$/s
				C6'=	0,068924033	\$/s
				C5=	0,10273152	\$/s
				C8=	0,082627893	\$/s
	C5 + C8 + Cq_boiler=	0,216814998		C3' + C6' + Zboiler + Cfuel + Zboiler =	0,216814998	
Steam turbine:						
	Zsteam_turbine=	0,010630214	\$/s	Wsteam_turbine=	5363,06284	kJ/s
				(E5+E8)- (E7+E6+E9+E10+E11)=	5673,49	kJ/s
				c_turbine=	10,74198043	\$/GJ
steam turbine HP: 56,70%					C7=0,009126	
	Zhp_turbine=	0,008734832	\$/s	Cq_hp/turbine=	0,000398626	\$/s
	E5-(E6+E7)=	3077,42	kJ/s	C6=	0,068924033	\$/s
	Whp_turbine=	3040,706731	kJ/s	C5=	0,10273152	\$/s
	c_hp-turbine=	10,85829272	\$/GJ			
Steam turbine LP: 43,30%						
	Zlp_turbine=	0,006671275	\$/s	C9=	0,028860254	\$/s
	E8-(E9+E10+E11)=	2596,07	kJ/s	C10=	0,020642758	\$/s
	Wlp_turb.=	2322,356109	kJ/s	C11=	0,0123046	\$/s
	c_lp-turbine=	10,58969046	\$/GJ	Cw_lp-turb=	0,024593032	\$/s
				Cq_lp-turbine=	0,002898524	\$/s
	Zlp_turbine + C8=	0,089299168	\$/s	C9+C10+C11+Cw_lp- turb+Cq_lp-turb.=	0,089299168	\$/s
Regenerator 1					C12=0,01060	
	Zreg.1=	0,000010035	\$/s	C12'=	0,000750246	\$/s
	E12-E12'=	1229,14	kJ/s	C46=	0,00118501	\$/s
	c_reg.1=	8,04334875	\$/GJ	C47=	0,007606024	\$/s
				Cq_reg.1=	0,003446599	\$/s
				Zreg.1 + C12 + C46 =	0,011802869	\$/s
				C47 + C12' + Cq_reg.1=	0,011802869	\$/s
Regenerator 2						
	Zreg.2=	0,000008066	\$/s	C7'=	0,000427048	\$/s
	E7-E7'=	1084,77	kJ/s	C48=	0,016138904	\$/s
	c_reg.2=	8,40757453	\$/GJ	Cq_reg.2=	0,000174948	\$/s
				Zreg.2 + C7 + C47 =	0,016740901	\$/s

Table (Continued)						
				C48 + C7' + Cq_reg.2=	0,016740901	\$/s
Regenerator 3						
	Zreg.3=	0,000002441	\$/s	C10'=	0,017822321	\$/s
	E10-E10'=	351,68	kJ/s	C49=	0,01860594	\$/s
	c_reg.3=	8,07532838	\$/GJ	Cq_reg.3=	0,000355842	\$/s
				Zreg.3 + C10 + C48 =	0,036784103	\$/s
				C49 + C10' + Cq_reg.3=	0,036784103	\$/s
Regenerator 4						
	Zreg.4=	0,00001940	\$/s	C9'=	0,00446653	\$/s
	E9-E9'=	3041,64	kJ/s	C3=	0,042382618	\$/s
	c_reg.4=	8,272044108	\$/GJ	Cq_reg.4=	0,000636443	\$/s
				C9 + C49 + Zreg.4=	0,04748559	\$/s
				C3 + C9' + Cq_reg.4=	0,047485591	\$/s
Regenerator 5						
	Zreg.5=	0,000001425	\$/s	C40=	0,00011165	\$/s
	E12'-E24 =	74,31	kJ/s	C40'=	0,00066096	\$/s
	C_reg.5=	8,265077911	\$/s	C24=	0,00015431	\$/s
				Cq_reg.5=	0,0000480	\$/s
				C40+C12'+Zreg.5=	0,000863321	\$/s
				C40'+C24+Cq_reg.5=	0,00086332	\$/s
Pump-SRC						
	Zpump2=	0,00013301	\$/s	C21=	0,00041919	\$/s
	E46-E21=	95,49	kJ/s	cq_pump=	0,000256632	\$/s
	c_pump=	6,62697917	\$/GJ	cw_pump=	0,00088944	\$/s
	Wpump=	134,215043	kJ/s	C12+Cw_pump+Zpump=	0,001441643	\$/s
				C46+Cq_pump=	0,001441643	\$/s
Deaerator						
	Zdear =	0,002531	\$/s	C45=	0,000818607	\$/s
	E40'+E24+E45 - E21=	5478,76	kJ/s	Cq_deaer=	0,003633905	\$/s
	c_deaerator=	0,663271	\$/GJ	Cq_deaer+C21+C40=	0,00416474	\$/s
				Z_deaer + C45+C40' + C24=	0,00416474	\$/s
	Zdear=	0,003668	\$/s	C45=	0,017976941	\$/s
	E45 - E21=	2128,26	kJ/s	Cq_deaer=	0,021373101	\$/s
	c_deaerator=	10,04253	\$/GJ	Cq_deaer+C21=	0,02164486	\$/s
				Z_deaer + C45=	0,02164486	\$/s

Table C.5: Conventional exergo-economic analysis of the power system using ST technology (ORC).

Heat Exchanger:					
Zhe=	0,000062168	\$/s	E14-E13=	180,60	kJ/s
c_he=	8,313768737	\$/GJ	C14=	0,005903945	\$/s
			C13=	0,004402498	\$/s
			Cq_he=	0,000257498	\$/s
			C11+ C13 +Zhe=	0,016769266	\$/s
			C12+ C14 +Cq_he=	0,016769266	\$/s
Turbine:					
Zturbine=	0,000597575	\$/s	C15=	0,003525439	\$/s
W_orc-turbine=	228,1247351	kJ/s	Cw_orc-turbine=	0,002373072	\$/s
E14-E14=	286,09	kJ/s	Cq_turbine=	0,00060301	\$/s
c_turbine=	10,40251841	\$/GJ	Zturbine + C14 =	0,00650152	\$/s
			C15 + Cw_orc-turbine+ Cq_turbine=	0,00650152	\$/s
Condenser:					
Zcondenser=	0,000379851	\$/s	C16=	0,004024341	\$/s
c_cond=	0,368198393	\$/GJ	E43-E42=	191,67	kJ/s
Cq_cond=	0,000048478	\$/s	E15-E16=	60,01	kJ/s
			C43=	0,00007057	\$/s
			C42=	0	\$/s
			Zcondenser + C15 +C43 =	0,00397586	\$/s
			Cq_cond + C16 + C42 =	0,004072819	\$/s
Pump:					
Zpump=	0,000244841	\$/s	Cw_orc-turbine=	0,000479912	\$/s
c_pump=	7,405117247	\$/GJ	Cq_orc-turbine=	0,000143086	\$/s
Wpump=	64,80816339	kJ/s	Zpump + C13 =	0,004647339	\$/s
			Cw_orc-turbine +Cq_orc- turbine +C16 =	0,004647339	\$/s

Table C.6: Conventional exergo-economic analysis of the power system using ST technology (ARS).

Generator:					
Zgenerator=	0,00035396	\$/s	C26=	0,009845258	\$/s
c_regenerator=	8,676494904	\$/GJ	C27=	0,00552165	\$/s
			C33=	0,002371737	\$/s
			C32=	0,000268633	\$/s
			C36=	0,000129050	\$/s
			Cq_gen=	0,002445416	\$/s
			Zgen. + C32 + C26 =	0,01046785	\$/s
			C33 + C36 + C27 + Cq_gen=	0,010467852	\$/s
Zihe=	0,0000006636	\$/s	C31=	0,000030868	\$/s
c_ihe=	8,787057818	\$/GJ	C34=	0,002081896	\$/s
			Cq_ihe=	0,00005274	\$/s
			Cq_ihe + C32 + C34=	0,00240327	\$/s
			Zihe + C31 + C33=	0,0024032678	\$/s
Zpump=	0,000004059	\$/s	C30=	0,000277134	\$/s
c_pump=	0	\$/s	Cw_ars-pump=	0	\$/s
W_pump=	0	kJ/s	E31-E30=	28,38	kJ/s
			Cq_pump=	0,000250325	\$/s
Absorber:					
Zabsorber=	0,00044655	\$/s	C35=	0,002081896	\$/s
c_abs =	11,27458403	\$/GJ	C39=	0,00031347	\$/s
			C19=	0	\$/s
			C20=	0,00036557	\$/s
			Cq_abs=	0,001572275	\$/s
			C19 + C39 + C35 +Zabs=	0,00221498	\$/s
			C20 + C30 + Cq_bas.=	0,002214979	\$/s
Zevap=	0,00001200	\$/s	C38=	-0,000008007	\$/s
c_evaporator=	9,017259827	\$/GJ	C17=	0	\$/s
			C18=	0,000141557	\$/s
			Cq_eva=	0,000175903	\$/s
			C17 + C38 +Zevap=	0,000003990	\$/s
			C18 + C39 + Cq_eva=	0,000003990	\$/s
Zcond=	0,00001287	\$/s	C37=	0,0000008978	\$/s
c_cond=	9,547881156	\$/GJ	C28=	0	\$/s
			C29=	0,000130390	\$/s
			Cq_condenser=	0,000010632	\$/s
			C28+C36+Zcond=	0,000141920	\$/s
			C37+C29+Cq_cond=	0,0001419200	\$/s

- LFR Technology

Table C.7: Conventional exergo-economic analysis of the power system using LFR technology (Power block and HRSG).

Solar field					
	Zsf=	0,036245466	\$/s	C2=	0,053879568 \$/s
	E2-E1=	15666,30	kJ/s	C1=	0,017634102 \$/s
	c_sf=	2,313594767	\$/GJ		
Heat exchanger					
	Zihe=	0,001311626	\$/s	C2' =	0,052757077 \$/s
	E2'-E1'=	15339,92	kJ/s	C1' =	0,017266725 \$/s
	c_ihe=	2,399098846	\$/GJ	C3=	0,011701782 \$/s
				C4=	0,043460472 \$/s
				C6=	0,022035653 \$/s
				C8=	0,025888984 \$/s
	Cq_ihe+C1'+C8+C4=	0,087806138		Cq_ihe=	0,001189958 \$/s
Steam - Turbine HP (76,88%)		0,763505814			
	Zturbine=	0,011261563	\$/s	C7=	0,011847515 \$/s
	E4-(E7+E6)=	3992,04	kJ/s	C6=	0,022035653 \$/s
	Whp-turb.=	3983,108976	kJ/s	Cw_hp=	0,020792235 \$/s
	c_hp-urbine=	5,220102044	\$/GJ	Cq_hp=	4,66312E-05 \$/s
	C7+C6+Cw_hp+Cq_hp			Zt_hp+C4=	0,054722035
Steam - Turbine LP (23,12%)		0,236494186			
	Zturbine_LP=	0,003488244	\$/s	C9=	0,004403605 \$/s
	E8-(E9+E10)=	1310,28	kJ/s	C10=	0,018341889 \$/s
	Wlp-turb=	1233,758926	kJ/s	Cw_lp=	0,006244439 \$/s
	c_hp-urbine=	5,061312024	\$/GJ	Cq_lp=	0,000387295 \$/s
				C9+C10+Cw_lp+Cq_lp=	0,029377227 \$/s
Steam Turbine					
	Zsteam_turbine=	0,0143139	\$/s		
	Wsteam_turbine=	5216,8679	kJ/s		
	(E4+E8)-(E7+E6+E9+E10)=	5293,39	kJ/s		
	C_turbine=	5,1825491	\$/GJ	Zt_lp+C8=	0,029377227 \$/s
Regenerator 1					
	Zreg1 =	0,00002634	\$/s	C10'=	0,009309007 \$/s
	E10-E10'=	3765,11	kJ/s	C46=	0,000949833 \$/s
	c_reg1=	2,406095754	\$/GJ	C47=	0,007755352 \$/s
				Cq_reg1	0,002233859 \$/s
				C47+C10'+Cq_reg1=	0,019298218
				C10+C46+Zreg1	0,01931807

Table (Continued)

Regenerator 2						
	Zreg2=	0,000005918	\$/s	C9'=	0,003754232	\$/s
	E9-E9'=	270,67	kJ/s	C48=	0,008259693	\$/s
	c_reg2=	2,420962356	\$/GJ	Cq_reg2=	0,000146353	\$/s
				C9'+C48+Cq_reg2=	0,012160278	\$/s
				C9+C47+Zreg2=	0,012164874	\$/s
Regenerator 3						
	Zreg3=	0,00001075	\$/s	C7'=	0,007946581	\$/s
	E7-E7'=	1626,00	kJ/s	C49=	0,011721002	\$/s
	c_reg3=	2,405712171	\$/GJ	Cq_reg3=	0,000440837	\$/s
				C7'+C49+Cq_reg3=	0,02010842	\$/s
				C48+C7+Zreg3=	0,02011796	\$/s
Pump						
	Zpump=	0,000330274		C21=	0,000271759	\$/s
	E46-E21=	282,64		Cq_pump=	0,000001176	\$/s
	c_pump=	1,230554212		Cw_pump=	0,000348976	\$/s
	Wpump=	283,592232		C21+Cw_pump+Zpump=	0,000951009	\$/s
				C46+Cq_pump=	0,000951009	\$/s
Condenser						
	Zcond.=	0,003667919		C44=	0,008793672	\$/s
	c_cond.=	3,032190246		C45=	0,005377661	\$/s

Table C.8: Conventional exergo-economic analysis of the power system using LFR technology (ORC).

Heat Exchanger:					
	Zhe=	0,00010299	\$/s	E14-E13=	81,51 kJ/s
	c_he=	3,076226114	\$/GJ	C2"=	0,001122491 \$/s
				C1"=	0,000810038 \$/s
				C14=	0,000985959 \$/s
				C13=	0,000735217 \$/s
				Cq_he=	0,000164706 \$/s
				C2' + C16 + Zhe =	0,00196070 \$/s
				C1"+C14+Cq_he=	0,001960702 \$/s
Turbine:					
	Zorc_turb=	0,000418797	\$/s	C15=	0,000588748 \$/s
	c_orc-turb=	6,31962913	\$/GJ	Cq_turb=	0,000165338 \$/s
	E_orc-turb=	129,12	kJ/s	Cw_orc-turb=	0,000650669 \$/s
	W_orc-turb=	102,96	kJ/s	C15+Cw_orc-turb+Cq_turb=	0,001404756 \$/s
				C14+Zturb=	0,001404756 \$/s
Condenser:					
	Zcondenser =	0,00037724	\$/s	C16=	0,000672065 \$/s
	c_cond=	0,480425327	\$/GJ	E43-E42=	319,44 kJ/s
	Cq_cond=	0,000140456		C43=	0,00076637 \$/s
				C42=	0 \$/s
				C42+C16+Cq_cond=	0,000812521 \$/s
Pump:					
	Zpump=	0,000189429	\$/s	Zcond+C15=	0,000965988 \$/s
	c_pump=	6,651963633	\$/GJ	Cw_orc-pump=	0,00019457 \$/s
	W_orc-Pump=	29,25	kJ/s	Cq_pump=	0,000058 \$/s
				Zpump+C13=	0,000924646 \$/s
				C16+Cw_orc_pump+Cq_pump=	0,000925 \$/s

Table C.9: Conventional exergo-economic analysis of the power system using LFR technology (ARS).

Generator:				
	Zgenerator=	0,00007550 \$/s	C26=	0,00022154 \$/s
	c_generator=	4,193987993 \$/GJ	C27=	0,00012063 \$/s
			C33=	0,00016785 \$/s
			C32=	0,00001901 \$/s
			C36=	0,00000914 \$/s
			Cq_gen=	0,00001843 \$/s
			Zgen. +C32+C26=	0,00031605 \$/s
			C33+C36+C27+Cq_ge. =	0,00031605 \$/s
Intermediate Heat exchanger:				
	Zihe=	0,000008499 \$/s	C31=	0,00000218 \$/s
	c_ihe=	5,161143325 \$/GJ	C34=	0,00014734 \$/s
			Cq_ihe=	0,00000454 \$/s
			C31+C33+Zihe=	0,00017089 \$/s
			C34+C32 +Cq_ihe=	0,00017089 \$/s
Pump:				
	Zpump=	0,000003221 \$/s	C30=	0,00001961 \$/s
	c_pump=	0 \$/GJ	CW_pump=	0,00000000 \$/s
	W_pump=	0 kJ/s	E31-E30=	4,15566419 kJ/s
			C30+Zpump=	0,00002283 \$/s
Absorber:				
			C31+CW_pump=	0,00000218 \$/s
	Zabsorber=	0,00011282 \$/s	C35=	0,00014734 \$/s
	c_abs=	8,693977814 \$/GJ	C39=	-0,00002258 \$/s
			C19=	0,00000000 \$/s
			C20=	0,00001963 \$/s
			C_abs=	0,00019834 \$/s
			C19+C39+C35+Zabs=	0,00023758 \$/s
			C20+C30+Cq_abs=	0,00023758 \$/s
Evaporator:				
	Zevap=	0,000012305 \$/s	C38=	0,00000065 \$/s
	c_evap=	6,54696595 \$/GJ	C17=	0,00000000 \$/s
			C18=	0,00001225 \$/s
			Cq_evap=	0,00002199 \$/s
			C17 + C38 +Zevap=	0,00001166 \$/s
			C18 + C39 + Cq_eva=	0,00001166 \$/s
Condenser:				
	Zcond. =	0,000013142 \$/s	C37=	0,00000006 \$/s
	c_cond.=	10,26695777 \$/GJ	C28=	0,00000000 \$/s
			C29=	0,00001437 \$/s
			Cq_condenser=	0,00000785 \$/s
			C28+C36+Zcond=	0,00002228 \$/s
			C37+C29+Cq_cond=	0,00002228 \$/s

- **BF Technology****Table C.10: Conventional exergo-economic analysis of the power system using BF technology (Power block and HRSG).**

Biomass					
YOP=	3600	hr			
Available amount of resource=	28152	Tons			
Annual expenditure cost=	1466719,2	\$			
HHV of sorghum=	17,015	MJ/kg			
Biomass fuel cost =	3,062004114	\$/GJ			
Boiler					
Zboiler=	0,003056204	\$/s	E=	13,23180928	MJ/s
c_boiler=	4,774169876	\$/GJ	C_fuel=	0,040515854	\$/s
Cq_boiler=	0,000929929	\$/s	C3'=	0,02440537	\$/s
C5 + C8 + Cq_boiler =	0,107666258		C6'=	0,03968883	\$/s
			C5=	0,059156345	\$/s
			C8=	0,047579985	\$/s
			C3' + C6' + Zboiler + Cfuel + Zboiler =	0,107666258	
Steam turbine:					
Zsteam_turbine=	0,010653025	\$/s	Wsteam_turbine=	5187,799349	kJ/s
			(E5+E8)- (E7+E6+E9+E10+E11)=	5488,08	kJ/s
			c_turbine=	6,794161288	\$/GJ
steam turbine HP (56,70%):			C7=	0,005255531	\$/s
Zhp_turbine=	0,010154321	\$/s	Cq_hp/turbine=	0,000290675	\$/s
E5-(E6+E7)=	2976,85	kJ/s	C6=	0,03968883	\$/s
Whp_turbine=	2941,33723	kJ/s	C5=	0,059156345	\$/s
c_hp-turbine=	8,1852668	\$/GJ			
Steam turbine LP (43,30%):	0,43302795				
Zlp_turbine=	0,000498704	\$/s	C9=	0,016618727	\$/s
E8-(E9+E10+E11)=	2511,23	kJ/s	C10=	0,01188681	\$/s
Wlp_turb.=	2246,462119	kJ/s	C11=	0,007085412	\$/s
c_lp-turbine=	4,97275936	\$/GJ	Cw_lp-turb=	0,011171116	\$/s
			Cq_lp-turbine=	0,001316623	\$/s
Zlp_turbine + C8=	0,048078688	\$/s	C9+C10+C11+Cw_lp- turb+Cq_lp-turb. =	0,048078688	\$/s
Regenerator 1			C12=	0,00610835	\$/s
Zreg.1=	0,000006924	\$/s	C12'=	0,000432017	\$/s
E12-E12'=	1188,97	kJ/s	C46=	0,00068237	\$/s
c_reg.1=	4,790875278	\$/GJ	C47=	0,004379811	\$/s
			Cq_reg.1=	0,001985816	\$/s
			Zreg.1 + C12 + C46 =	0,006797644	\$/s
			C47 + C12' + Cq_reg.1=	0,006797644	\$/s
Regenerator 2					
Zreg.2=	0,000005556	\$/s	C7'=	0,000245909	\$/s
E7-E7'=	1049,32	kJ/s	C48=	0,009293336	\$/s

Table (Continued)					
c_reg.2=	5,050221456	\$/GJ	Cq_reg.2=	0,000101653	\$/s
			Zreg.2 + C7 + C47 =	0,009640898	\$/s
			C48 + C7' + Cq_reg.2=	0,009640898	\$/s
Regenerator 3					
Zreg.3=	0,000001684	\$/s	C10'=	0,010262706	\$/s
E10-E10'=	340,19	kJ/s	C49=	0,01071394	\$/s
c_reg.3=	4,813686694	\$/GJ	Cq_reg.3=	0,000205185	\$/s
			Zreg.3 + C10 + C48 =	0,021181831	\$/s
			C49 + C10' + Cq_reg.3=	0,021181831	\$/s
Regenerator 4					
Zreg.4=	0,00001338	\$/s	C9'=	0,002571982	\$/s
E9-E9'=	2942,24	kJ/s	C3=	0,02440537	\$/s
c_reg.4=	4,95400615	\$/GJ	Cq_reg.4=	0,0003687	\$/s
			C9 + C49 + Zreg.4=	0,02734605	\$/s
			C3 + C9' + Cq_reg.4=	0,027346052	\$/s
Regenerator 5					
Zreg.5=	0,000000983	\$/s	C40=	0,00006646	\$/s
E12'-E24 =	71,88	kJ/s	C40'=	0,00033287	\$/s
C_reg.5=	4,835335418	\$/GJ	C24=	0,00008886	\$/s
			Cq_reg.5=	0,0000777	\$/s
			C40+C12'+Zreg.5=	0,000499465	\$/s
			C40'+C24+Cq_reg.5=	0,00049946	\$/s

Table C.11: Conventional exergo-economic analysis of the power system using BF technology (ORC).

Heat exchanger:						
Zhe=	0,000060123	\$/s	E14-E13=	174,70	kJ/s	
c_he=	5,067947946	\$/GJ	C14=	0,003481343	\$/s	
			C13=	0,002595994	\$/s	
			Cq_he=	0,000151837	\$/s	
			C11+ C13 +Zhe=	0,009741530	\$/s	
			C12+ C14 +Cq_he=	0,00974153	\$/s	
Turbine:						
Zturbine=	0,000577926	\$/s	C15=	0,002078824	\$/s	
W_orc-turbine=	220,6696784	kJ/s	Cw_orc-turbine=	0,00157917	\$/s	
E14-E14=	276,74	kJ/s	Cq_turbine=	0,000401275	\$/s	
c_turbine=	7,156260873		Zturbine + C14 =	0,004059269	\$/s	
			C15 + Cw_orc-turbine+ Cq_turbine=	0,004059269	\$/s	
Condenser:						
Zcondenser=	0,000367361	\$/s	C16=	0,002373008	\$/s	
c_cond=	1,215244666	\$/GJ	E43-E42=	59,13	kJ/s	
Cq_cond=	0,000001317	\$/s	E15-E16=	58,05	kJ/s	
			C43=	0,00007186	\$/s	
			C42=	0	\$/s	
			Zcondenser + C15 +C43 =	0,00251804	\$/s	
			Cq_cond + C16 + C42 =	0,002374325	\$/s	
Zpump=	0,00023679		Cw_orc-turbine=	0,000354178		
c_pump=	5,649642677		Cq_orc-turbine=	0,000105598		
Wpump=	62,69024955		Zpump + C13 =	0,002832784		
			Cw_orc-turbine +Cq_orc-turbine +C16 =	0,002832784		
Zpump2=	0,00013301	\$/s	C21=	0,000241384	\$/s	
E46-E21=	92,37	kJ/s	cq_pump=	0,000124897	\$/s	
c_pump=	3,3341607	\$/GJ	cw_pump=	0,000432871	\$/s	
Wpump=	129,82893	kJ/s	C12+Cw_pump+Zpump=	0,000807267	\$/s	
Deaerator - BPP				C46+Cq_pump=	0,000807267	\$/s
Zdear =	0,002531	\$/s	C45=	0,000471382	\$/s	
E40'+E24+E45 - E21=	136,51	kJ/s	Cq_deaer=	0,003116127	\$/s	
c_deaerator=	22,82693	\$/GJ	Cq_deaer+C21+C40=	0,00342398	\$/s	
Deaerator - SPP				Z_deaer + C45+C40' + C24=	0,00342398	\$/s
Zdeaer=	0,003668		C45=	0,011521304	\$/s	
E45 - E21=	2297,28		Cq_deaer=	0,014607814	\$/s	
c_deaerator=	6,358756		Cq_deaer+C21=	0,015189223	\$/s	
			Z_deaer + C45=	0,015189223	\$/s	

Table C.12: Conventional exergo-economic analysis of the power system using BF technology (ARS).

Generator					
Zgenerator=	0,00035396	\$/s	C26=	0,00484761	\$/s
c_regenerator=	5,856974685	\$/GJ	C27=	0,003286973	\$/s
			C33=	0,001601015	\$/s
			C32=	0,000181338	\$/s
			C36=	0,000087114	\$/s
			Cq_gen=	0,000407805	\$/s
			Zgen. + C32 + C26 =	0,00538291	\$/s
			C33 + C36 + C27 + Cq_gen=	0,005382908	\$/s
Intermediate heat exchanger					
Zihe=	0,0000006636	\$/s	C31=	0,000020837	\$/s
c_ihe=	5,967537599	\$/GJ	C34=	0,001405362	\$/s
			Cq_ihe=	0,00003582	\$/s
			Cq_ihe + C32 + C34=	0,00162252	\$/s
			Zihe + C31 + C33=	0,0016225158	\$/s
Pump					
Zpump=	0,000004059		C30=	0,000187076	
c_pump=	0		Cw_ars-pump=	0	
W_pump=	0		E31-E30=	28,38	
			Cq_pump=	0,000170298	
Absorber					
Zabsorber=	0,00044655	\$/s	C35=	0,001405362	\$/s
c_abs =	8,455063812	\$/GJ	C39=	-0,000211604	\$/s
			C19=	0	\$/s
			C20=	0,000274149	\$/s
			Cq_abs=	0,001179084	\$/s
			C19 + C39 + C35 +Zabs=	0,00164031	\$/s
			C20 + C30 + Cq_abs.=	0,00164031	\$/s
Evaporator					
Zevap=	0,00001200	\$/s	C38=	-0,000005405	\$/s
c_evaporator=	6,197739608	\$/GJ	C17=	0	\$/s
			C18=	0,000097295	\$/s
			Cq_eva=	0,000120902	\$/s
			C17 + C38 +Zevap=	0,000006592	\$/s
			C18 + C39 + Cq_eva=	0,000006592	\$/s
Condenser					
Zcond=	0,00001287	\$/s	C37=	0,0000006061	\$/s
c_cond=	6,728360937	\$/GJ	C28=	0	\$/s
			C29=	0,000091885	\$/s
			Cq_condenser=	0,000007493	\$/s
			C28+C36+Zcond=	0,000099984	\$/s
			C37+C29+Cq_cond=	0,0000999839	\$/s

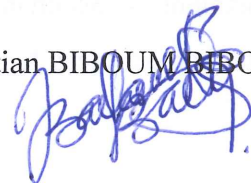
ACKNOWLEDGEMENT

This PhD thesis is the result of a four-year study at Ege University Solar Energy Institute. During this period, I have received support from a wide range of colleagues. First and foremost, I would like to thank all professors in the thesis supervising committee which supervised the progress of this work and particularly Asst. Prof. Dr. Ahmet YILANCI, for their advice and guidance throughout the writing of this thesis. I also would like to give my appreciation to Prof. Dr. Mustafa GÜNEŞ who has encouraged me to study on this subject.

Special thanks go to the women of my life, Julienne, Jacqueline, Nadine, Dany, Clara, Pathy and Madame who provided their support, inspiration, encouragement and motivation during this work and helped to finalize this PhD Thesis. To my dear friends in Turkey, thank for the tea and lunch discussion. To my distant friends in Cameroon, Senegal, Mali and all around the world, thank you for your positive wishes and support. Lastly, I would like to thank my parents who have given me love and support throughout my entire career, without whom this thesis would definitely not have been possible.

19 / 08 / 2019

Alain Christian BIBOUM BIBOUM



CURRICULUM VITAE

Personal Information

Name: Biboum Biboum

Surname: Alain Christian

Date and Place of Birth: 16/03/1987 - À Ngaoundere, Cameroon

e-mail: biboumalain@gmail.com

Research Fields

Heat Transfer, Thermodynamic, Techno-economic and Exergo-economic Analyses, Solar Thermal Applications, Biomass Technologies.

Education

M.Sc.: Cheickh Anta Diop University, Laboratory of Applied Energy, Thermal Energetic System and Environment, “Study of a solar volumetric receiver with fluidized bed (Direct Steam Generation / Brayton Joule Cycle)”.

B.Sc.: A.B.T. – National School of Engineering, Industrial Engineering Department - Mechanical Engineering, “Design and technical analysis of hydraulic machinery for urban electrification works based on MMT”.

Publications from this Thesis

Biboum A.C., and Yilanci A., (2019). “Feasibility study of biomass power plants fired with maize and sorghum stalk in the Sub-Saharan region: a case for the northern part of Cameroon”. European Mechanical Science, ISSN: 2587-1110, DOI Prefix: 10.26701/ems.

Biboum A.C., and Yilanci A., (2018). “Techno-economic analysis of 1 MWe Solar Power Plant using a combined Rankine Cycle in Izmir, Turkey”.

International Journal of Energy and Smart Grid 3 (2), 40 – 59. DOI: 10.23884/IJESG.2018.3.2.01.

Biboum A., Yılanıcı A., “Comparative techno-economic study of a solar thermal power plants using different technology of various capacities in the northern region of Cameroon”, 3rd International Mediterranean Science and Engineering Congress (IMSEC 2018), Adana, Türkiye, pp.1648-1658.

Biboum A., Yılanıcı A., “Techno economic analysis of 5 MWe hybrid power plant using a combined Rankine cycle in Faro Bouki Cameroon”, International Conference on Engineering Technologies (ICENTE'18), Konya, Türkiye, 26-28 September 2018, pp.610-620

Biboum A.C., Mwanza M., Yılanıcı A., (2017). “Performances Analysis of Combined Rankine and Absorption Refrigeration Cycles for a Small Size Solar Power Plant”, IEA SHC International Conference on Solar Heating and Cooling for Buildings and Industry, ISES Solar World Congress 2017.